FiPo FDTD: A Method to Calculate Both Electromagnetic Fields and Potentials from First-Order Equations with Convolutional Perfectly Matched Layer Boundary Conditions

By
Michelle L. King

A dissertation submitted in partial fulfillment of
the requirements for the degree of

Doctor of Philosophy
(Materials Science and Engineering)

at the
UNIVERSITY OF WISCONSIN–MADISON
2021

Date of final oral examination: 08/26/2021

The dissertation is approved by the following members of the Final Oral Committee:

Knezevic I. Faculty, Professor, Electrical and Computer Engineering
Hagness, S. Faculty, Professor, Electrical and Computer Engineering
Kats, M. Faculty, Associate Professor, Electrical and Computer Engineering
Booske, J. Faculty, Professor, Electrical and Computer Engineering
Evans, P. Faculty, Professor, Materials Science and Engineering

To my dad, the person I most wish could read this.

ACKNOWLEDGMENTS

I would like to thank my advisor, Irena Knezevic. You have taught me a great deal, and not just about the math and physics. You are intuitive, tough, brilliant, caring, and a powerful force to be reckoned with. We all talk about how much we look up to you, and your strong leadership has carried us mostly unscathed through unprecendented times. Thank you for your time, mentorship, and support throughout my five years at UW-Madison.

I also want to thank my undergraduate research advisor, Sylke Boyd. Our work in halo detection algorithms began my love for developing methods, and look at me now! Thank you for teaching me the science involved in the complicated atmosphere. Every time I look at the sky, I am amazed by both the beauty and the science.

I want to thank all of the group members in my time of study, Laleh Avazpour, Kübra Eryilmaz, Sam Belling, Sina Soleimanikahnoj, Yichen Li, Shuva Mitra, Farhad Karimi, Stefan Schmidt, Jason Hsu, Song Mei, Olafur Jonasson, and Amirhossein Davoody. Laleh, being able to work with you directly during my Ph.D. has been a pleasure. As well as your expertise, you have brought a lot of fun into our project — I look forward to more in the future! I'd also like to thank group members from before my time who left legacy notes and code for future graduate students; you are the real heroes.

Additionally, I would like to thank my family and friends. Mom, thank you for always being there for me. Your support means more than you know. Morton, we made it through undergraduate together at UMM and graduate school together in spirit. We will always be the dream team. Thank you to both my real life and internet friends for your encouragement and support.

Lastly, I would like to thank my cat, Ada King, named after the first computer programmer, Ada King, Countess of Lovelace (Ada Lovelace). You have helped me through a global pandemic,

getting stuck in my research, frustrating computer bugs, and writing my thesis. Thank you for telling me when I need a break to pet you, you always know.

DISCARD THIS PAGE

TABLE OF CONTENTS

Page

Appendix

Page

DISCARD THIS PAGE

LIST OF TABLES

DISCARD THIS PAGE

LIST OF FIGURES

Figure Page

Appendix
Figure Page

DISCARD THIS PAGE

NOMENCLATURE

ϕ	electric potential
$\mathbf{A}$	magnetic vector potential
$\mathbf{E}$	electric field
$\mathbf{D}$	electric displacement field
$\mathbf{H}$	magnetic field
$\mathbf{B}$	magnetic flux density
$\mathbf{J}$	current density
ρ	charge density
ϵ	permittivity
ϵ_0	permittivity of free space
μ	permeability
μ_0	permeability of free space

σ^E	conductivity
σ^H	magnetic loss
σ^A	magnetic vector potential loss
σ^ϕ	electric potential loss
κ^E	relative dielectric permittivity
κ^H	relative magnetic permeability
κ^A	material property that slows the propagation of $\mathbf{A}$
κ^ϕ	material property that slows the propagation of ϕ

FIPO FDTD: A METHOD TO CALCULATE BOTH ELECTROMAGNETIC FIELDS AND POTENTIALS FROM FIRST-ORDER EQUATIONS WITH CONVOLUTIONAL PERFECTLY MATCHED LAYER BOUNDARY CONDITIONS

Michelle L. King

Under the supervision of Professor Irena Knezevic

At the University of Wisconsin-Madison

Modeling light–matter interaction at the nanoscale requires careful and accurate handling of both the quantum and electromagnetic systems. We have developed and implemented the electromagnetics piece of the puzzle in a way that is suitable for coupling with quantum-transport solvers, a field–potential finite-difference time-domain (FiPo FDTD) algorithm, which solves a set of first-order equations for the electric and magnetic fields, $\mathbf{E}$ and $\mathbf{H}$, as well as the magnetic vector potential $\mathbf{A}$ and scalar electric potential ϕ.

FiPo FDTD has two algorithms, FiPo Basic and FiPo Hybrid. FiPo Basic is similar to conventional FDTD with additional updates for the potentials. FiPo Hybrid is a self-consistent method to update both field and potentials. We were able to derive and implement a convolutional perfectly matched layer (CPML) absorbing boundary condition for FiPo equations in order to minimize reflections in the simulation due the reflective boundary. We show simulation examples for two versions of the algorithm and analyze the effectiveness of their respective CPMLs.

Potentials $\mathbf{A}$ and ϕ can be used as input for the single-particle electron Hamiltonian in a quantum transport solver. An efficient and accurate quantum-transport solver is needed to characterize nonlinear optical effects and other quantum behavior in nanostructures. In order to couple these systems, the current and charge density can be obtained from the quantum solver and input back into the electromagnetics solver. FiPo FDTD uses current density as an input, but can be sourced with charge density with the addition of a Poisson solver.

Irena Knezevic

ABSTRACT

Modeling light–matter interaction at the nanoscale requires careful and accurate handling of both the quantum and electromagnetic systems. We have developed and implemented the electromagnetics piece of the puzzle in a way that is suitable for coupling with quantum-transport solvers, a field–potential finite-difference time-domain (FiPo FDTD) algorithm, which solves a set of first-order equations for the electric and magnetic fields, $\mathbf{E}$ and $\mathbf{H}$, as well as the magnetic vector potential $\mathbf{A}$ and scalar electric potential ϕ.

FiPo FDTD has two algorithms, FiPo Basic and FiPo Hybrid. FiPo Basic is similar to conventional FDTD with additional updates for the potentials. FiPo Hybrid is a self-consistent method to update both field and potentials. We were able to derive and implement a convolutional perfectly matched layer (CPML) absorbing boundary condition for FiPo equations in order to minimize reflections in the simulation due the reflective boundary. We show simulation examples for two versions of the algorithm and analyze the effectiveness of their respective CPMLs.

Potentials $\mathbf{A}$ and ϕ can be used as input for the single-particle electron Hamiltonian in a quantum transport solver. An efficient and accurate quantum-transport solver is needed to characterize nonlinear optical effects and other quantum behavior in nanostructures. In order to couple these systems, the current and charge density can be obtained from the quantum solver and input back into the electromagnetics solver. FiPo FDTD uses current density as an input, but can be sourced with charge density with the addition of a Poisson solver.

Chapter 1

Introduction

Devices continue to get smaller, on the order of nanometers, and at these scales, quantum behavior becomes prevalent for device operation [1, 2, 3, 4, 5, 6]. Emerging technology from these devices will be in electronic and biosensors, communications, and energy harvesting. The quantum response of these devices to electromagnetic waves is more complex than at larger scales and needs to be understood [7]. Modeling light–matter interaction at the nanoscale requires methods that can accurately and efficiently calculate the electromagnetic fields, as well as the quantum response.

Quantum modeling is needed to capture nonlinear optical response from materials and devices [8]. In modeling radio-frequency bowtie antennas, the metallic patches are assumed to behave as perfect electrical conductors (PECs); however, in optical nanoantennas, the PEC assumption no longer holds because optical frequencies of light excite free electrons on the surface of the metal [9]. This is only one possible source of electronic excitations, called surface plasmons, which cause the material to exhibit a nonlinear optical response. Additionally, in bowtie nanoantennas, a plasmon-enhanced field is present in the nanogap [1, 2, 9]. Tunneling of electrons in the nanogap is enhanced by these plasmonic fields, which is another source of nonlinearity [10]. The nonlinear optical response from tunneling needs to be calculated by a quantum model. Tunneling in nanostructures has been shown experimentally below 0.3 nm [11], and quantum effects begin to affect optical response below 1 nm [12].

Two-dimensional (2D) van der Waals (vdW) materials also require electronic-structure calculation and time-dependent quantum transport. 2D vdW materials also exhibit tunable nonlinearities, such as in transition metal dichalcoginide (TMD) nanotriangles, where nonlinearities stem from geometry and number of layers [3]. Other 2D materials have strong light–matter interaction and

nonlinear susceptibilities and can be used in all-optical signal processing [13]. To accurately model devices with tunneling or nonlinear optical properties exposed to electromagnetic fields, we need to couple quantum transport with electromagnetics.

Choosing a quantum transport solver necessitates balancing computational expense and accuracy; the choice requires enough accuracy to capture the nonlinear optical response from materials and devices but must be fast enough to be updated at timesteps like the electromagnetics solver. Ryu *et al.* [14] coupled a second-order FDTD to a simple quantum solver, which demonstrates the concept of coupling, but solving the Schrödinger equation alone is not sufficient for modeling devices. Time-domain density functional theory (TDDFT) is an atomistic modeling method that has been used to capture nonlinearities [15, 16, 17, 18, 19]. Although accurate, TDDFT is expensive for many-atom devices, and a multiscale approach to solving quantum and electrodynamics problems is needed [20]. Nonequilibrium Green's function (NEGF) also has a high computational expense and accuracy but is generally not used for time-dependent systems [21, 22, 23]. In larger structures, modeling can be accurately and efficientely handled by using density matrix (DM) or Wigner functions techniques [24]. However, these techniques have heretofore not been fully coupled with electrodynamics solvers.

In order to couple quantum transport with electromagnetics, information must be passed between the two systems. Electromagnetics is governed by Maxwell's equations, which, in their common form, describe the relationship between electric field $\mathbf{E}$ and magnetic field $\mathbf{H}$ [25, 26, 27]. Maxwell's equations can also be written in terms of magnetic vector potential $\mathbf{A}$ and electric scalar potential ϕ [26]. The ability to couple electromagnetics with quantum transport is through $\mathbf{A}$ and ϕ [28, 14, 29, 30, 31, 32, 33]. $\mathbf{A}$ and ϕ enter in the Hamiltonian for a single electron in an electromagnetic field, and the Hamiltonian is a key part in any quantum-transport solver. After $\mathbf{A}$ and ϕ are given to the quantum transport solver, the electromagnetic response from charge carriers in the system can be modeled in order to find the current density $\mathbf{J}$ and charge density ρ. In turn, $\mathbf{J}$ and ρ can be fed back into the electromagnetics solver as sources [14, 34, 35].

In quantum mechanics, the Hamiltonian for a particle in an electromagnetic field is written as

$$H = \frac{1}{2m}(\mathbf{p} - q\mathbf{A})^2 + q\phi, \tag{1.1}$$

where m is the mass of the particle, $\mathbf{p}$ is the momentum of the particle, and q is the charge of the particle [36, 37, 38, 39, 40, 41]. This electromagnetic Hamiltonian is derived from the Lagrangian of a classical particle in an electromagnetic field [38, 41]. Solving for charge transport using this Hamiltonian will allow for the coupling of electromagnetics with quantum transport. Since $\mathbf{p}$ is an operator, $\mathbf{A}$ and ϕ are the quantities that need to be defined in order to use this Hamiltonian. $\mathbf{A}$ and ϕ are ways of expressing electromagnetic fields, so the electromagnetic solver needs to calculate $\mathbf{A}$ and ϕ in order to provide an input for the quantum solver. One challenge in coupling these systems is that $\mathbf{A}$ and ϕ require a choice of gauge, which will be discussed in 2.2.2, as these quantities are gauge dependent [42]. Ensuring that gauge dependence is taken into consideration will be important when coupling a quantum-mechanical solver to an electromagnetics solver.

The finite-difference time-domain (FDTD) method is an intuitive method commonly used to solve Maxwell's equations for the electric and magnetic fields for problems with dispersive media, photonics, and devices [43, 44, 45]. FDTD software ranges from commercial solvers such as Lumerical [46] to free, editable software such as Meep [47]. Previously, semiclassical transport methods coupled to FDTD electromagnetics solver have been implemented in [48, 49, 50]. Semiclassical transport solvers, such as those based on the Boltzman transport equation (BTE), are valid at low enough frequencies where electronic transport remains intraband. When light reaches higher frequenies, the increased energy induces interband or intersubband transitions, and a quantum-transport picture becomes necessary.

In order to model light–matter interaction at the nanoscale, tunneling and other quantum effects need to be addressed by modeling and coupled to FDTD [51, 52]. A second-order FDTD for potentials has been formulated by Ryu *et al.* [14, 29, 35], which obtains $\mathbf{A}$ and ϕ from $\mathbf{J}$ and ρ. Due to the second-order of these equations, implementation of a perfectly matched layer (PML) absorbing boundary layer is difficult. The PML calculation presented involves five timesteps of a single field as well as numerous operations to compute various field values [14]. ***For this reason, we aimed to develop a set of first-order equations for FDTD to calculate*** $\mathbf{A}$ ***and*** ϕ ***and implement a PML.***

In order to address the electromagnetic aspect of coupling, we developed a field–potential (FiPo) FDTD algorithm based on a set of first-order update equations. We developed absorbing boundary layer for potentials in the form of convolutional PML (CPML), a method commonly used to minimize reflections in FDTD simulations. We test our method in simple examples that show the FDTD algorithm is working and the PML absorbs well.

1.1 Summary of Results

The development of the FiPo algorithm, as well as the CPML formulation for the method, are the main contributions of this work. The FiPo algorithm is a new, first-order algorithm to solve for both fields and potentials. Two versions of the algorithm have been developed: FiPo Basic and FiPo Hybrid. FiPo Basic is an extension of conventional FDTD that also allows for calculation of the potentials. FiPo Hybrid is a self-consistent method to solve for fields and potentials. The absorbing boundary layer developed for FiPo FDTD extends the formalism for CPML for conventional FDTD to now absorb potentials. This means advancements in the CPML formalism for conventional FDTD should be able to applied to FiPo FDTD's CPML. The development of FiPo FDTD with CPML has laid a groundwork for solving for the potentials using first-order equations, as well as giving us an intuitive electromagnetic solver that can be coupled to a quantum transport solver.

1.2 Organization of Thesis

Chapter 2 addresses necessary background information in electromagnetics. Maxwell's equations (Section 2.1) give the relationship between electromagnetic waves and how they interact with materials. Electromagnetic waves can be expressed in terms of the vector and scalar potentials (Section 2.2), and Maxwell's equations can be expressed in terms of these potentials (Section 2.2.1). The potentials have a degree of freedom that is limited by a choice of gauge (Section 2.2.2). Common examples of gauges are the Coulomb (Section 2.2.2.1) and Lorenz (Section 2.2.2.2) gauges. Potentials can be written in a different gauge by undergoing gauge transformations

(Section 2.3). A simple analytical example for current density on a square wire loop is analyzed (Section 2.4).

Chapter 3 covers how to solve for equations on a discrete grid using the FDTD method. Section 3.1 covers how to use finite differences. Section 3.2 discusses discretization of Maxwell's equations for FDTD. The Yee grid is explained in Section 3.3 as is how it is used for both fields and potentials. Lastly, Section 3.4 goes over discretization of more complicated equations using vector calculus operations, which is needed for discretizing second-order equations.

Chapter 4 introduces the second-order $\mathbf{A}$-ϕ FDTD from Ryu *et al.* [14]. The second-order wave equations (Section 4.1) are written as time-stepping equations (Section 4.2) and discretized for FDTD (Section 4.3). The equations are also formulated for FDTD on a graded mesh (Section 4.4). Results generated from these equations are presented in Section 4.5. The PML for the second-order FDTD method is examined in Section 4.6.

Chapter 5 introduces the FiPo FDTD method. Section 5.1 introduces first-order equations for the algorithm. The equations are discretized in Section 5.2. Simulations for FiPo with reflecting boundary conditions are shown in Section 5.3.

Chapter 6 explains the development and implementation of the CPML for FiPo FDTD. A formalism for stretched coordinates for potentials is developed in Section 6.1. Section 6.2 contains the derivation for the CPML for the FiPo algorithm. We prove that PML parameters are equal for fields and potentials (Section 6.3), and we define values for CPML paramters used in simulations (Section 6.4). Simulations for the FiPo algorithm with a CPML are shown in Section 6.5.

Chapter 2

Electromagnetic Fields and Potentials

In order to solve for electromagnetic fields, we need a formalism to describe them. Maxwell's equations give us this formalism, and we can solve them for the electric and magnetic fields in a system. In order to handle electromagnetics in quantum transport, using a potential formalism is useful, so this chapter will cover how to formulate Maxwell's equations for the potentials. Additionally, the vector and scalar potentials require a choice of gauge, so the Coulomb and Lorenz gauges are discussed, as well as how to transform between them. Finally, an analytical steady-state example of solving for a vector potential from a current density is presented.

2.1 Maxwell's Equations for Electromagnetic Fields

Maxwell's equations are a set of coupled first-order partial differential equations that, together, describe the physics of electromagnetic waves. The equations describe the relationship between electromagnetic fields and their sources with the quantities of electric field $\mathbf{E}$, electric displacement field $\mathbf{D}$, magnetic field $\mathbf{H}$, magnetic flux density $\mathbf{B}$, current density $\mathbf{J}$, and charge density ρ.

The following equations are the differential form of Maxwell's Equations:

$$\nabla \cdot \mathbf{D} = \rho, \tag{2.1a}$$

$$\nabla \cdot \mathbf{B} = 0, \tag{2.1b}$$

$$\nabla \times \mathbf{E} = -\frac{\partial}{\partial t}\mathbf{B}, \tag{2.1c}$$

$$\nabla \times \mathbf{H} = \frac{\partial}{\partial t}\mathbf{D} + \mathbf{J}. \tag{2.1d}$$

Equation (2.1a) is Gauss's law, Equation (2.1b) is Gauss's law of magnetism, Equation (2.1c) is Faraday's law, and Equation (2.1d) is Ampere's law.

Information about how materials respond to eletromagnetic waves is reflected in the relationships between $\mathbf{D}$ and $\mathbf{E}$ and between $\mathbf{B}$ and $\mathbf{H}$. We can rewrite Maxwell's Equations in terms of only $\mathbf{E}$ and $\mathbf{H}$ using the constitutive relations

$$\mathbf{D} = \epsilon \mathbf{E} \tag{2.2a}$$

and

$$\mathbf{B} = \mu \mathbf{H}, \tag{2.2b}$$

where the ϵ is the electric permittivity, and μ is the magnetic permeability is the magnetic permeability of the material. Equations (2.2a) and (2.2b) are valid for isotropic, nondispersive, inhomogeneous media. An isotropic medium is one in which ϵ and μ are the same in every direction light travels in a material. If the medium is anisotropic, ϵ and μ can be described by tensors. A non-dispersive medium is one in which ϵ and μ are both entirely real, changing the propagation characteristics but not attenuating the wave. An inhomogeneous medium is one in which ϵ and μ vary with respect to position, and inhomogeneity needs to be considered for modeling Maxwell's equations, where vector operations act on both the fields and materials properties. It is common to see Maxwell's equations in free space with $\epsilon = \epsilon_0$ and $\mu = \mu_0$ pulled out of the vector operations because the values are constant, which is accurate in free space, but this is not the most general form of Maxwell's equations.

Maxwell's equations rewritten in terms of $\mathbf{E}$ and $\mathbf{H}$ are as follows:

$$\nabla \cdot \epsilon \mathbf{E} = \rho, \tag{2.3a}$$

$$\nabla \cdot \frac{1}{\mu} \mathbf{H} = 0, \tag{2.3b}$$

$$\nabla \times \mathbf{E} = -\mu \frac{\partial}{\partial t} \mathbf{H}, \tag{2.3c}$$

$$\nabla \times \mathbf{H} = \epsilon \frac{\partial}{\partial t} \mathbf{E} + \mathbf{J}. \tag{2.3d}$$

In these equations, ϵ and μ cannot be taken out of Equations (2.3c) and (2.3d) due to inhomogeneity but can be pulled in front of the time derivative in Equations (2.3a) and (2.3b) since the material properties are not changing over time.

2.2 Vector and Scalar Potentials

As explained in Section 2.1, electromagnetic waves can be described by Maxwell's equations for electromagnetic fields by using $\mathbf{E}$, $\mathbf{D}$, $\mathbf{H}$, and $\mathbf{B}$. Electromagnetic waves can also be described by potentials.

From the vector identity

$$\nabla \cdot (\nabla \times \mathbf{A}) = 0, \tag{2.4}$$

we can define solenoidal vector field $\mathbf{B}$ in terms of the magnetic vector potential $\mathbf{A}$ such that the vector identity matches Equation (2.1b)

$$\mathbf{B} = \nabla \times \mathbf{A}. \tag{2.5}$$

Using Equation (2.2b) also means $\mathbf{H}$ can be calculated using $\mathbf{A}$ and μ

$$\mathbf{H} = \frac{1}{\mu}(\nabla \times \mathbf{A}). \tag{2.6}$$

Equation (2.6) is the definition of the magnetic field in terms of potentials. By substituting Equation (2.5) into Equation (2.1c), we can find a relation between $\mathbf{E}$ and $\mathbf{A}$

$$\nabla \times \mathbf{E} = -\frac{\partial}{\partial t}(\nabla \times \mathbf{A}). \tag{2.7}$$

Since time and position are independent variables, their derivative operators commute, so we can exchange the order of the time and position variables

$$\nabla \times \mathbf{E} + (\nabla \times \frac{\partial}{\partial t}\mathbf{A}) = 0. \tag{2.8}$$

We can further simplify to

$$\nabla \times (\mathbf{E} + \frac{\partial}{\partial t}\mathbf{A}) = 0. \tag{2.9}$$

Using the vector identity

$$\nabla \times (-\nabla\phi) = 0, \tag{2.10}$$

we can introduce the scalar potential ϕ into Equation (2.9)

$$\nabla \times (\mathbf{E} + \frac{\partial}{\partial t}\mathbf{A}) = \nabla \times (-\nabla\phi). \tag{2.11}$$

And we can solve for an equation for $\mathbf{E}$ in terms of $\mathbf{A}$ and ϕ

$$\mathbf{E} = -\frac{\partial}{\partial t}\mathbf{A} - \nabla\phi. \tag{2.12}$$

Equation (2.12) is the definition for the electric field in terms of potentials. The addition of ϕ to Equation (2.12) is important because, in electrostatics,

$$\mathbf{E} = -\nabla\phi \tag{2.13}$$

must hold.

2.2.1 Potential Formulation of Maxwell's Equations

We substitute Equations (2.6) and (2.12) into Equations (2.3a) and (2.3d) to obtain

$$\nabla \times \frac{1}{\mu}(\nabla \times \mathbf{A}) = \epsilon\frac{\partial}{\partial t}(-\frac{\partial}{\partial t}\mathbf{A} - \nabla\phi) + \mathbf{J}, \tag{2.14a}$$

$$\nabla \cdot (-\epsilon\frac{\partial}{\partial t}\mathbf{A} - \epsilon\nabla\phi) = \rho. \tag{2.14b}$$

We simplify to obtain an $\mathbf{A}$-ϕ formulation of Maxwell's equations:

$$\nabla \times \frac{1}{\mu}(\nabla \times \mathbf{A}) = -\epsilon\frac{\partial^2}{\partial t^2}\mathbf{A} - \epsilon\frac{\partial}{\partial t}\nabla\phi + \mathbf{J}, \tag{2.15a}$$

$$-\frac{\partial}{\partial t}\nabla \cdot \epsilon\mathbf{A} - \nabla \cdot \epsilon\nabla\phi = \rho. \tag{2.15b}$$

Maxwell's equations in terms of $\mathbf{E}$ and $\mathbf{H}$ are four first-order equations. In both of the curl equations, Equations (2.3c) and (2.3d), the electric and magnetic fields are coupled. In both of the second-order equations, Equations (2.15a) and (2.15b), $\mathbf{A}$ and ϕ are coupled.

2.2.2 Gauge

In order to specify $\mathbf{A}$ and ϕ for the second-order $\mathbf{A}$-ϕ Maxwell equations, Equations (2.15a) and (2.15b), we must choose a gauge. $\mathbf{A}$ and ϕ have an extra degree of freedom not present for $\mathbf{E}$ and $\mathbf{H}$. Choosing a gauge fixes $\mathbf{A}$ and ϕ, and a thoughtful choice can simplify difficult problems. The two most popular gauges are the Coulomb gauge and the Lorenz gauge.

2.2.2.1 The Coulomb Gauge

The Coulomb gauge is given as

$$\nabla \cdot \mathbf{A} = 0. \tag{2.16}$$

In free space, the Coulomb gauge reduces Equation (2.15b) to Poisson's equation

$$-\nabla^2 \phi = \frac{\rho}{\epsilon_0}. \tag{2.17}$$

However, to simplify Equations (2.15a) and (2.15b) for inhomogeneous media, we need a geralized Coulomb gauge

$$\nabla \cdot \epsilon \mathbf{A} = 0. \tag{2.18}$$

The Coulomb gauge is commonly used in quantum mechanics. In free space, the Coulomb gauge reduces Equation (2.15b) to

$$-\nabla \cdot \epsilon \nabla \phi = \rho, \tag{2.19}$$

which is Poisson's equation, a common equation solved by numerical solvers [].

The second equation, however, is not reduced to something as simple. The second equation ends up as

$$\nabla \times \frac{1}{\mu}(\nabla \times \mathbf{A}) = -\epsilon \frac{\partial^2}{\partial t^2}\mathbf{A} - \epsilon \frac{\partial}{\partial t}\nabla \phi + \mathbf{J}. \tag{2.20}$$

Since the ϕ term has a gradient operator, it is longitudinal or irrotational, which means it is zero when the curl is taken, like the identity in Equation (2.10). This implies that the current density can be written as two terms, the longitudinal/irrotational term and the transverse/solenoidal term

$$\mathbf{J} = \mathbf{J}_l + \mathbf{J}_t. \tag{2.21}$$

This implies the $\nabla \times \mathbf{J}_l = 0$ and $\nabla \cdot \mathbf{J}_t = 0$. The benefit of this, is that this separates Equation (2.20) into

$$\nabla \times \frac{1}{\mu}(\nabla \times \mathbf{A}) + \epsilon \frac{\partial^2}{\partial t^2}\mathbf{A} = \mathbf{J}_t, \tag{2.22a}$$

$$\epsilon \frac{\partial}{\partial t}\nabla\phi = \mathbf{J}_l. \tag{2.22b}$$

Equation (2.22a) is an inhomogeneous wave equation for $\mathbf{A}$. The second equation is a combination of Equation (2.19) and the continuity equation for electromagnetics, which is

$$\frac{\partial}{\partial t}\rho = -\nabla \cdot \mathbf{J}. \tag{2.23}$$

2.2.2.2 The Lorenz Gauge

The Lorenz gauge is given as

$$\nabla \cdot \mathbf{A} + \frac{1}{c}\partial_t \phi = 0. \tag{2.24}$$

The main benefit of the Lorenz gauge is that it aims to handle $\mathbf{A}$ and ϕ in similar ways. It also Lorentz invariant, which means it is independent of coordinate system. Using the Lorenz gauge separates Equations (2.15a) and (2.15b) in free space into two second-order inhomogeneous wave equations, one for $\mathbf{A}$, one for ϕ,

$$\nabla^2\mathbf{A} - \frac{1}{c^2}\frac{\partial^2}{\partial t^2}\mathbf{A} = -\mu_0\mathbf{J} \tag{2.25a}$$

$$\nabla^2\phi - \frac{1}{c^2}\frac{\partial^2}{\partial t^2}\phi = -\frac{\rho}{\epsilon_0} \tag{2.25b}$$

where they are coupled by the electromagnetic continuity equation relating $\mathbf{J}$ and ρ

$$\nabla \cdot \mathbf{J} + \frac{\partial \rho}{\partial t} = 0. \tag{2.26}$$

The generalized Lorenz gauge has also been used, such as in [53] and [14], and is written as

$$\epsilon^{-1}\nabla \cdot \epsilon\mathbf{A} = -\mu\epsilon\frac{\partial}{\partial t}\phi \tag{2.27}$$

The generalized Lorenz gauge separates Equations (2.15a) and (2.15b) into the inhomogeneous wave equations in inhomogeneous media

$$\nabla \cdot \epsilon\nabla\phi - \epsilon^2\mu\frac{\partial^2}{\partial t^2}\phi = -\rho \tag{2.28}$$

and

$$-\nabla \times \frac{1}{\mu}(\nabla \times \mathbf{A}) - \epsilon \frac{\partial^2}{\partial t^2}\mathbf{A} + \epsilon \nabla \epsilon^{-2}\mu^{-1}\nabla \cdot \epsilon \mathbf{A} = -\mathbf{J}. \tag{2.29}$$

Equations (2.28) and (2.29) are again coupled by the continuity equation, Equation (2.26). It is important to note that the standard Lorenz gauge does not separate the inhomogeneous wave equations for inhomogeneous media — this is why we need the generalized Lorenz gauge.

2.3 Gauge Transformation

Gauge transformations can be used to switch from one gauge to another. As given in [26], a magnetic vector potential $\mathbf{A}$ in one gauge can be transformed to $\mathbf{A}'$ in another gauge using

$$\mathbf{A}' = \mathbf{A} + \nabla \Lambda. \tag{2.30}$$

Here, Λ is an arbitrary scalar field. The same can be done to transform electric potential ϕ into the value ϕ' in another gauge

$$\phi' = \phi - \frac{1}{c}\partial_t \Lambda. \tag{2.31}$$

For potentials in the Lorenz gauge, there is an additional restriction on the value for Λ:

$$\nabla^2 \Lambda - \frac{1}{c^2}\partial_t^2 \Lambda = 0. \tag{2.32}$$

Most math for potentials is given in free space or homogenous materials rather than in inhomogeneous materials, which means the relations for gauge transformations may be different for the inhomogeneous wave equations in inhomogeneous materials.

2.4 Analytical Solution for a Square Current Loop

The vector potential can be calculated in the Coulomb gauge by integrating the current density using

$$\mathbf{A}(\mathbf{x}) = \frac{1}{c}\int d\mathbf{x}' \frac{\mathbf{J}(\mathbf{x}')}{|\mathbf{x} - \mathbf{x}'|} \tag{2.33}$$

from [26]. For an anylytical solution for a vector potential, we can solve this equation given a current density $\mathbf{J}$. One easy way to do this is to define a current density as a delta function. For

a realistic system that could be represented by a delta function current density, we can model a square wire loop in the $z = z_0$ plane with the current density

$$J_x(x, y, z) = J_0\delta(y - y_a)\delta(z - z_0), \quad x \in (x_a, x_b), \tag{2.34a}$$

$$J_y(x, y, z) = J_0\delta(x - x_b)\delta(z - z_0), \quad y \in (y_a, y_b), \tag{2.34b}$$

$$J_x(x, y, z) = -J_0\delta(y - y_b)\delta(z - z_0), \quad x \in (x_a, x_b), \tag{2.34c}$$

$$J_y(x, y, z) = -J_0\delta(x - x_a)\delta(z - z_0), \quad y \in (y_a, y_b), \tag{2.34d}$$

where J_0 is the magnitude of current in Amps. The postive current density J_x runs along a wire at $y = y_a$ for $x \in (x_a, x_b)$, a positive current density J_y runs along a wire at $x = x_b$ for $y \in (y_a, y_b)$, a negative current density J_x runs along a wire at $y = y_b$ for $x \in (x_a, x_b)$, and a negative current density J_y runs along a wire at $x = x_a$ for $y \in (y_a, y_b)$, forming a closed current loop. A square loop is more natural for a rectangular grid than the circular loop even though the circular loop has a simpler expression for current density. Evaluating the delta function parts of the integral for the definition of $\mathbf{A}$ gives us

$$\begin{aligned}\mathbf{A}(\mathbf{x}) = \frac{J_0}{c}\Big(&\int_{x_a}^{x_b} dx' \frac{\hat{x}}{\sqrt{(x - x')^2 + (y - y_a)^2 + (z - z_0)^2}} \\ &+ \int_{y_a}^{y_b} dy' \frac{\hat{y}}{\sqrt{(x - x_b)^2 + (y - y')^2 + (z - z_0)^2}} \\ &- \int_{x_a}^{x_b} dx' \frac{\hat{x}}{\sqrt{(x - x')^2 + (y - y_b)^2 + (z - z_0)^2}} \\ &- \int_{y_a}^{y_b} dy' \frac{\hat{y}}{\sqrt{(x - x_a)^2 + (y - y')^2 + (z - z_0)^2}}\Big),\end{aligned} \tag{2.35}$$

or

$$\begin{aligned}A_x(\mathbf{x}) = \frac{J_0}{c}\Big(&\int_{x_a}^{x_b} dx' \frac{1}{\sqrt{(x - x')^2 + (y - y_a)^2 + (z - z_0)^2}} \\ &- \int_{x_a}^{x_b} dx' \frac{1}{\sqrt{(x - x')^2 + (y - y_b)^2 + (z - z_0)^2}}\Big),\end{aligned} \tag{2.36}$$

$$\begin{aligned}A_y(\mathbf{x}) = \frac{J_0}{c}\Big(&\int_{y_a}^{y_b} dy' \frac{1}{\sqrt{(x - x_b)^2 + (y - y')^2 + (z - z_0)^2}} \\ &- \int_{y_a}^{y_b} dy' \frac{1}{\sqrt{(x - x_a)^2 + (y - y')^2 + (z - z_0)^2}}\Big),\end{aligned} \tag{2.37}$$

written in components of $\mathbf{A}$. Evaluating these integrals leads us to

$$\begin{aligned}\mathbf{A}(\mathbf{x}) = \frac{J_0}{c}(\hat{x}\tanh^{-1}&\left(\frac{-x+x'}{\sqrt{(x-x')^2+(y-y_a)^2+(z-z_0)^2}}\right)\Big|_{x_a}^{x_b}\\ &+\hat{y}\tanh^{-1}\left(\frac{-y+y'}{\sqrt{(x-xb)^2+(y-y')^2+(z-z_0)^2}}\right)\Big|_{y_a}^{y_b}\\ &-\hat{x}\tanh^{-1}\left(\frac{-x+x'}{\sqrt{(x-x')^2+(y-y_b)^2+(z-z_0)^2}}\right)\Big|_{x_a}^{x_b}\\ &-\hat{y}\tanh^{-1}\left(\frac{-y+y'}{\sqrt{(x-xa)^2+(y-y')^2+(z-z_0)^2}}\right)\Big|_{y_a}^{y_b}),\end{aligned} \quad (2.38)$$

which can be expanded to

$$\begin{aligned}\mathbf{A}(\mathbf{x}) = \frac{J_0}{c}(\hat{x}(\tanh^{-1}&\left(\frac{-x+x_b}{\sqrt{(x-x_b)^2+(y-y_a)^2+(z-z_0)^2}}\right)\\ &-\tanh^{-1}\left(\frac{-x+x_a}{\sqrt{(x-x_a)^2+(y-y_a)^2+(z-z_0)^2}}\right)\\ &-\tanh^{-1}\left(\frac{-x+x_b}{\sqrt{(x-x_b)^2+(y-y_b)^2+(z-z_0)^2}}\right)\\ &+\tanh^{-1}\left(\frac{-x+x_a}{\sqrt{(x-x_a)^2+(y-y_b)^2+(z-z_0)^2}}\right))\\ &+\hat{y}(\tanh^{-1}\left(\frac{-y+y_b}{\sqrt{(x-x_b)^2+(y-y_b)^2+(z-z_0)^2}}\right)\\ &-\tanh^{-1}\left(\frac{-y+y_a}{\sqrt{(x-x_b)^2+(y-y_a)^2+(z-z_0)^2}}\right)\\ &-\tanh^{-1}\left(\frac{-y+y_b}{\sqrt{(x-x_a)^2+(y-y_b)^2+(z-z_0)^2}}\right)\\ &+\tanh^{-1}\left(\frac{-y+y_a}{\sqrt{(x-x_a)^2+(y-y_a)^2+(z-z_0)^2}}\right))).\end{aligned} \quad (2.39)$$

Equation 2.39 is plotted in Figure 2.1 for a domain of $x \in (-1,3)$, $y \in (-1,3)$, and $z = 0$ where $x_a = 0$, $x_b = 2$, $y_a = 0$, and $y_b = 2$.

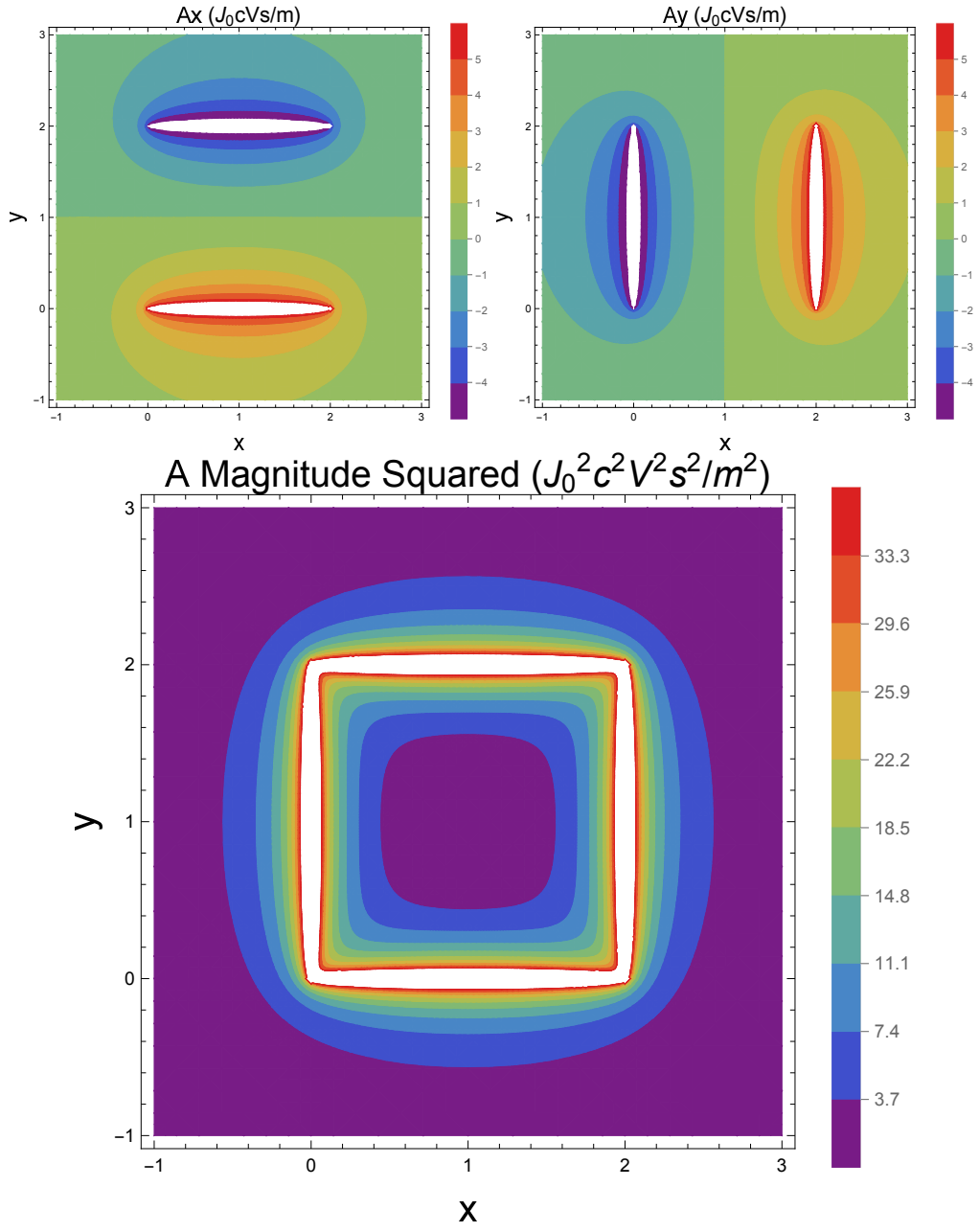

Figure 2.1: Colorized plots of the components of the vector potential (A_x in the top left panel and A_y in the top right panel) and its magnitude squared (bottom center) for a square current loop with the current density given in Eqs. (2.34).

Chapter 3

Equations on a Discrete Grid with the Finite-Difference Time-Domain Method

In order to solve Maxwell's equations presented in Section 2.1, we will use the finite-difference time-domain (FDTD) method. Conventional FDTD solves Maxwell's equations using updates for the electric and magnetic fields on a spatial Yee grid over time. In order to solve Maxwell's equations on a grid, first, we must discretize the equations such that field values are defined and updated on a discrete grid. FDTD is a well-develped and widely used technique [44], and is a basis of several open-source [47] and commercial computational electromagnetic tools [Lumerical etc]. Since we are developing a new FDTD method for potentials, in this chapter we first carefully examine the key concepts that underlie standard FDTD. We will also discuss how these concepts relate to potentials and a more rigorous formalism for finite differences for more complex FDTD equations.

3.1 Finite Differences

Finite differences are a way to approximate a derivative using values of a function at specific points. For FDTD, the specific points will be located on a grid. The finite difference for the partial derivative of x on a value f located at the spatial point (i, j, k) on a grid can be defined as

$$(\partial_x f)_{i,j,k} = \frac{f_{i+\frac{1}{2},j,k} - f_{i-\frac{1}{2},j,k}}{\Delta_x}. \tag{3.1}$$

In this equation, the partial derivative with respect to x for f at a point is calculated using values for f a half-step forward and behind the point as well as the spatial separation in x between the two points Δ_x. With knowledge of finite differences, we can discretize Maxwell's equations, the

equations for the conventional FDTD method. A more detailed formalism for finite differences and other vector calculus operations are presented in Section 3.4.

3.2 Conventional Finite-Difference Time-Domain Method

FDTD is a time-domain method, meaning that the algorithm is solved over time. For FDTD, this means the update equations need to march field values forward in time. The FDTD method is typically used in situations in which there is no spatial accumulation of free charge, meaning $\nabla \cdot \mathbf{E} = 0$. The $\mathbf{E}$ and $\mathbf{H}$ fields have no divergence, implying that both electric and magnetic fields are purely solenoidal. From Maxwell's equations, the curl equations solve for these solenoidal fields and also tell us about the change in the fields over time,

$$\mu \partial_t \mathbf{H} = -\nabla \times \mathbf{E}, \tag{3.2a}$$

$$\epsilon \partial_t \mathbf{E} = \nabla \times \mathbf{H} - \mathbf{J}. \tag{3.2b}$$

We can write these component-wise as

$$\epsilon \partial_t E_x = \partial_y H_z - \partial_z H_y - J_x, \tag{3.3a}$$

$$\epsilon \partial_t E_y = \partial_z H_x - \partial_x H_z - J_y, \tag{3.3b}$$

$$\epsilon \partial_t E_z = \partial_x H_y - \partial_y H_x - J_z, \tag{3.3c}$$

$$\mu \partial_t H_x = \partial_z E_y - \partial_y E_z, \tag{3.3d}$$

$$\mu \partial_t H_y = \partial_x E_z - \partial_z E_x, \tag{3.3e}$$

$$\mu \partial_t H_z = \partial_y E_x - \partial_x E_y. \tag{3.3f}$$

From this form, we can discretize Maxwell's equations using finite-differences; however, we need to know where these values are located on a grid and at what timestep they are updated. From our knowledge of finite differences, we know a derivative will spatially offset a value by a half-step. In order to solve Maxwell's equations in FDTD, we need to solve these equations for a future timestep. Say that the $\mathbf{E}$ field is defined at timestep n. This means, the partial derivative with respect to t can relate to the next timestep, $n + 1$ For a time derivative located at $n + \frac{1}{2}$, the

derivative can be written as

$$(\partial_t E_x)^{n+\frac{1}{2}} = \frac{E_x^{n+1} - E_x^n}{\Delta_t}. \tag{3.4}$$

The tricky part of these equations is knowing where these values are spatially defined. For instance, Equation (3.3a) tells us that E_x is located a half-step offset in z from H_y and y from H_z but at the same position for x, Equation (3.3b) tells us E_y is located a half-step offset in z from H_x and x from H_z but at the same position for y, and Equation (3.3c) tells us E_z is located a half-step offset in y from H_x and x in H_y but at the same position for z. Let us assume that, in the coordinate direction $\mathbf{E}$ components are not spatially offset from components of $\mathbf{H}$, components of $\mathbf{E}$ are located at a half-step. This assumption leads us to first making each term of Equation (3.3a) have consistent coordinate positions

$$\epsilon_{i+\frac{1}{2},j,k}(\partial_t E_x)^{n+\frac{1}{2}}_{i+\frac{1}{2},j,k} = (\partial_y H_z)^{n+\frac{1}{2}}_{i+\frac{1}{2},j,k} - (\partial_z H_y)^{n+\frac{1}{2}}_{i+\frac{1}{2},j,k} - J^{n+\frac{1}{2}}_{x\ i+\frac{1}{2},j,k}. \tag{3.5}$$

Making sure positions of fields are consistent with each other is important for the stability of FDTD. Not just any finite difference can be taken, the finite difference must be taken so that the points in the simulation are consistent in the equation. When expanded, Equation (3.5) gives us the full update including the positions of the fields

$$\begin{aligned}\epsilon_{i+\frac{1}{2},j,k}&\frac{E^{n+1}_{x\ i+\frac{1}{2},j,k} - E^n_{x\ i+\frac{1}{2},j,k}}{\Delta_t} \\ &= \frac{H^{n+1}_{z\ i+\frac{1}{2},j+\frac{1}{2},k} - H^n_{z\ i+\frac{1}{2},j-\frac{1}{2},k}}{\Delta_y} - \frac{H^{n+1}_{y\ i+\frac{1}{2},j,k+\frac{1}{2}} - H^n_{y\ i+\frac{1}{2},j,k-\frac{1}{2}}}{\Delta_z} - J^{n+\frac{1}{2}}_{x\ i+\frac{1}{2},j,k}.\end{aligned} \tag{3.6}$$

Using $\mathbf{J} = \sigma\mathbf{E}$ for a lossy medium, we can expand all fields to get the update equations for conventional FDTD

$$\begin{aligned}E^{n+1}_{x\ i+\frac{1}{2},j,k} = CA_{i+\frac{1}{2},j,k}&E^n_{x\ i+\frac{1}{2},j,k} + CB_{i+\frac{1}{2},j,k} \\ &[\frac{1}{\Delta_y}(H^{n+\frac{1}{2}}_{z\ i+\frac{1}{2},j+\frac{1}{2},k} - H^{n+\frac{1}{2}}_{z\ i+\frac{1}{2},j-\frac{1}{2},k}) + \frac{1}{\Delta_z}(H^{n+\frac{1}{2}}_{y\ i+\frac{1}{2},j,k-\frac{1}{2}} - H^{n+\frac{1}{2}}_{y\ i+\frac{1}{2},j,k+\frac{1}{2}})],\end{aligned} \tag{3.7a}$$

$$\begin{aligned}E^{n+1}_{y\ i,j+\frac{1}{2},k} = CA_{i,j+\frac{1}{2},k}&E^n_{y\ i,j+\frac{1}{2},k} + CB_{i,j+\frac{1}{2},k} \\ &[\frac{1}{\Delta_x}(H^{n+\frac{1}{2}}_{z\ i-\frac{1}{2},j+\frac{1}{2},k} - H^{n+\frac{1}{2}}_{z\ i+\frac{1}{2},j+\frac{1}{2},k}) + \frac{1}{\Delta_z}(H^{n+\frac{1}{2}}_{x\ i,j+\frac{1}{2},k+\frac{1}{2}} - H^{n+\frac{1}{2}}_{x\ i,j+\frac{1}{2},k-\frac{1}{2}})],\end{aligned} \tag{3.7b}$$

Variable	Value	$\sigma = 0$
$CA_{i,j,k}$	$\frac{1-\frac{\sigma_{i,j,k}\Delta_t}{2\epsilon_{i,j,k}}}{1+\frac{\sigma_{i,j,k}\Delta_t}{2\epsilon_{i,j,k}}}$	1
$CB_{i,j,k}$	$\frac{\frac{\Delta_t}{\epsilon_{i,j,k}}}{1+\frac{\sigma_{i,j,k}\Delta_t}{2\epsilon_{i,j,k}}}$	$\frac{\Delta_t}{\epsilon_{i,j,k}}$

Table 3.1: Update coefficients for $\mathbf{E}$ in Equations (3.7)

$$E^{n+1}_{z\ i,j,k+\frac{1}{2}} = CA_{i,j,k+\frac{1}{2}} E^{n}_{z\ i,j,k+\frac{1}{2}} + CB_{i,j,k+\frac{1}{2}} \\ [\frac{1}{\Delta_x}(H^{n+\frac{1}{2}}_{y\ i+\frac{1}{2},j,k+\frac{1}{2}} - H^{n+\frac{1}{2}}_{y\ i-\frac{1}{2},j,k+\frac{1}{2}}) + \frac{1}{\Delta_y}(H^{n+\frac{1}{2}}_{x\ i,j-\frac{1}{2},k+\frac{1}{2}} - H^{n+\frac{1}{2}}_{x\ i,j+\frac{1}{2},k+\frac{1}{2}})]. \quad (3.7c)$$

where the coeffiecients are given in Table 3.1.

$$H^{n+\frac{1}{2}}_{x\ i,j+\frac{1}{2},k+\frac{1}{2}} = H^{n-\frac{1}{2}}_{x\ i,j+\frac{1}{2},k+\frac{1}{2}} + \frac{\Delta_t}{\mu_0} \\ [\frac{1}{\Delta_y}(E^{n}_{z\ i,j,k+\frac{1}{2}} - E^{n}_{z\ i,j+1,k+\frac{1}{2}}) + \frac{1}{\Delta_z}(E^{n}_{y\ i,j+\frac{1}{2},k+1} - E^{n}_{y\ i,j+\frac{1}{2},k})], \quad (3.8a)$$

$$H^{n+\frac{1}{2}}_{y\ i+\frac{1}{2},j,k+\frac{1}{2}} = H^{n-\frac{1}{2}}_{y\ i+\frac{1}{2},j,k+\frac{1}{2}} + \frac{\Delta_t}{\mu_0} \\ [\frac{1}{\Delta_x}(E^{n}_{z\ i+1,j,k+\frac{1}{2}} - E^{n}_{z\ i,j,k+\frac{1}{2}}) + \frac{1}{\Delta_z}(E^{n}_{x\ i+\frac{1}{2},j,k} - E^{n}_{x\ i+\frac{1}{2},j,k+1})], \quad (3.8b)$$

$$H^{n+\frac{1}{2}}_{z\ i+\frac{1}{2},j+\frac{1}{2},k} = H^{n-\frac{1}{2}}_{z\ i+\frac{1}{2},j+\frac{1}{2},k} + \frac{\Delta_t}{\mu_0} \\ [\frac{1}{\Delta_x}(E^{n}_{z\ i,j,k+\frac{1}{2}} - E^{n}_{z\ i,j+1,k+\frac{1}{2}}) + \frac{1}{\Delta_y}(E^{n}_{y\ i,j+\frac{1}{2},k+1} - E^{n}_{y\ i,j+\frac{1}{2},k})]. \quad (3.8c)$$

The positions of these fields are located on the so-called Yee grid or Yee lattice discussed in Section 3.3 [54]. Figure 3.1 shows components of $\mathbf{E}$ and $\mathbf{H}$ for conventional FDTD.

3.3 Yee Grid for Fields and Potentials

In Section 3.2, we discretized Maxwell's equations by looking at the indices of finite differences and ensuring the field positions were consistent with each other. The grid these field positions

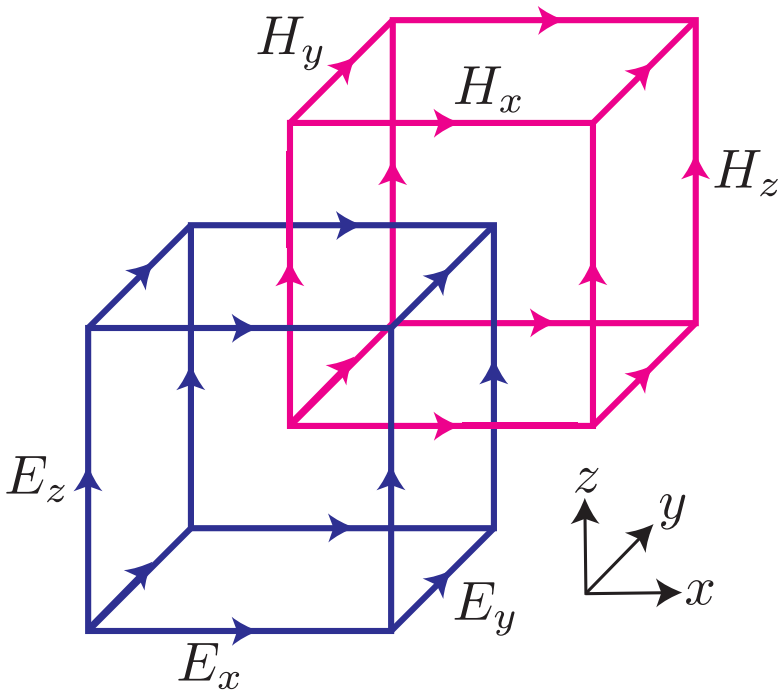

Figure 3.1: Representation of the Yee cell for fields **E** and **H**. Components of **E** and **H** are located on two boxes offset from each other in both time and space.

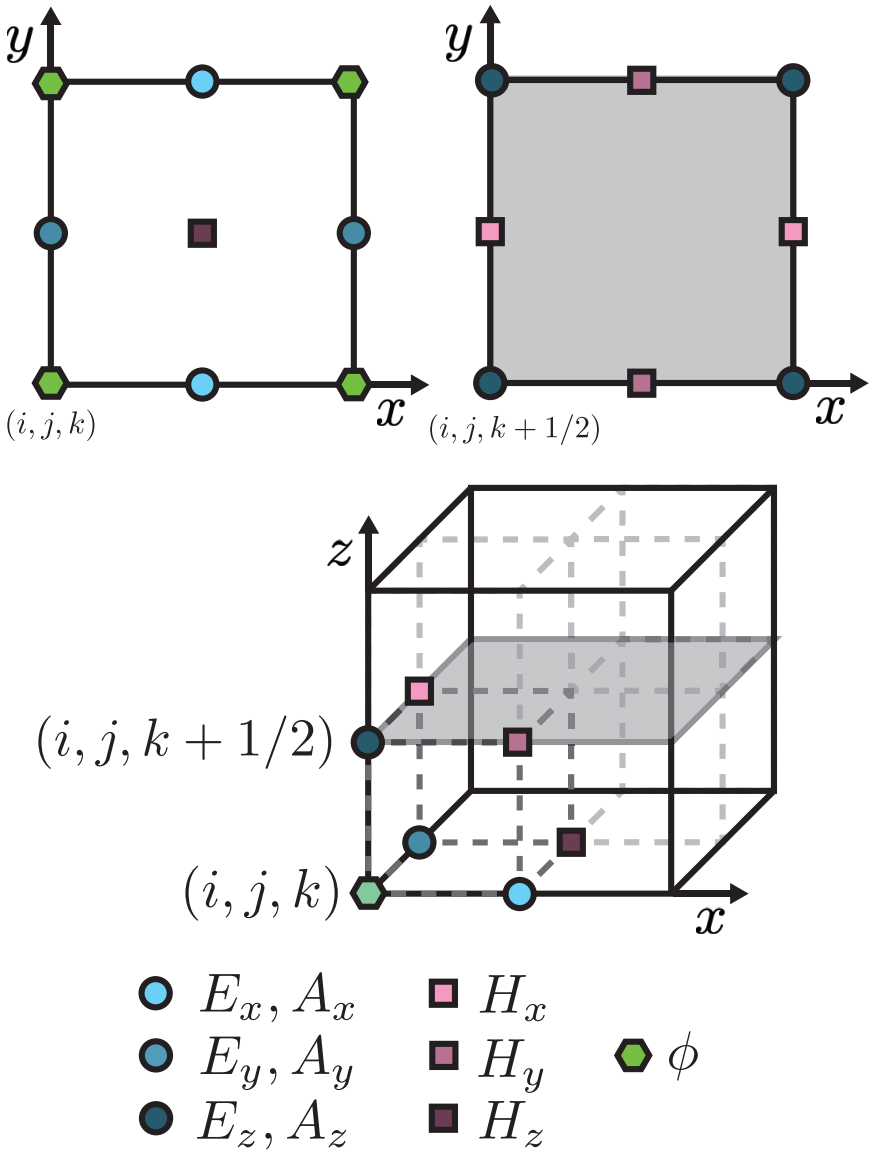

Figure 3.2: Locations of a set of fields and potentials on the Yee cell (bottom). All fields and potentials are shown for the Δ_z plane for integer-steps in z (top left) as well as for the $\Delta_z + \frac{1}{2}$ plane for half-steps in z (top right).

are located on is called the Yee grid or Yee lattice [54]. The Yee lattice can be further divided into smaller repeating components, or Yee cells. Yee cells make up the Yee lattice in a similar to the way to how unit cells make up a crystal lattice.

As discussed in Section 2.2, potentials can also be used to describe fields in electromagnetics. As we defined in Equations (2.6) and (2.12),

$$\mathbf{E} = -\partial_t \mathbf{A} - \nabla\phi, \tag{3.9a}$$

$$\mathbf{H} = \frac{1}{\mu}(\nabla \times \mathbf{A}). \tag{3.9b}$$

From these equations, we can see that $\mathbf{A}$ is located at the same spatial positions as $\mathbf{E}$ but is offset in time. We can also see ϕ is spatially offset from $\mathbf{E}$ in the direction corresponding to each component but is at the same timestep. Table 3.2 gives each field and potential location within the Yee cell.

Figure 3.2 shows the locations of fields and potentials in the Yee cell. ϕ and $\mathbf{E}$ are updated at one time step while $\mathbf{H}$ and $\mathbf{A}$ are updated at a half-timestep offset. The slices of the Δ_z and $\Delta_z + \frac{1}{2}$ planes show the positions of values in the full cell. The standard Yee cell is sometimes described as two intersecting cubes, where one cube contains $\mathbf{E}$ and one contains $\mathbf{H}$, that are offset by a half-step in all positions and time. This description does not work well with the addition of potentials because $\mathbf{A}$ would the colocated with $\mathbf{E}$ but is offset in time, and ϕ is a scalar field that is best described as being located on the corners of the $\mathbf{E}$ cube.

Values around points in the Yee cell can be used in the calculation of the central point, which results in the leapfrogging behavior of FDTD updates on the Yee grid. In the Δ_z plane, you can see that values of E_x and E_y or A_x and A_y surround H_z. Using both planes, we can see that E_x and E_z or A_x and A_z surround H_y and E_y and E_z or A_y and A_z surround H_x. This is consistent with conventional FDTD and gives us an understanding of how an FDTD for potentials would be updated. For example, ϕ is surrounded by values for $\mathbf{E}$ and $\mathbf{A}$, so those values could be good values to use to update ϕ, while $\mathbf{H}$ is not located in a beneficial place for the update. The value for A_x, for example, could be updated from E_x, ϕ, H_y or H_z.

Value	t-index	x-index	y-index	z-index
ϕ	n	i	j	k
E_x	n	$i+\frac{1}{2}$	j	k
E_y	n	i	$j+\frac{1}{2}$	k
E_z	n	i	j	$k+\frac{1}{2}$
A_x	$n+\frac{1}{2}$	$i+\frac{1}{2}$	j	k
A_y	$n+\frac{1}{2}$	i	$j+\frac{1}{2}$	k
A_z	$n+\frac{1}{2}$	i	j	$k+\frac{1}{2}$
H_x	$n+\frac{1}{2}$	i	$j+\frac{1}{2}$	$k+\frac{1}{2}$
H_y	$n+\frac{1}{2}$	$i+\frac{1}{2}$	j	$k+\frac{1}{2}$
H_z	$n+\frac{1}{2}$	$i+\frac{1}{2}$	$j+\frac{1}{2}$	k

Table 3.2: Timestep and positions for each field and potential value in the Yee cell.

3.4 Discrete Vector Calculus Formalism

In order to discretize calculus operations using finite differences, we need a written formalism. Generally, when evaulating finite differences for FDTD, a rigorous formalism isn't required to ensure the calculated value is at the central position. Due to the first-order nature of the equations in conventional FDTD, finite-differences can usually be evaluated by inspection. However, second-order equations are much more difficult due to evaulate due to multiple vector calculus operations acting on the same variable. In order to use second-order update equations, we must understand how they are discretized. In 1994, Chew originally discussed discretization of electromagnetic equations on a lattice; the details can be found in [55].

3.4.1 Finite Differences

A finite difference is a key building block for discrete vector calculus, and is a discrete approximation for taking the derivative. When taking the discrete derivative at a point, the derivative can be taken either in reference to a point ahead or behind the original; this matters for the location of the calculated derivative. Ensuring the location of the calculated value is consistent with the equations is important for stability. A finite difference operation on a spatial grid calculates the numerical derivative at a central point using the value at two points and the distance between those points. Say $f_m = f(m\Delta_x)$ where Δ_x corresponds to the grid length. We define a forward difference as

$$g_{m+\frac{1}{2}} = \tilde{\partial}_x f_m = \frac{f_{m+1} - f_m}{\Delta_x}, \tag{3.10}$$

and we define a backward difference as

$$g_{m-\frac{1}{2}} = \hat{\partial}_x f_m = \frac{f_m - f_{m-1}}{\Delta_x}. \tag{3.11}$$

Notice that both finite differences are located at half steps, where one is ahead of the initial point and one is behind. This spatial offset needs to be taken into account when taking multiple finite differences on the same variable, such as in second-order update equations.

3.4.2 Discrete Gradient

Since we defined the finite-difference operator, we can extend the definition to multiple dimensions with the gradient operator. Say a vector $\mathbf{g} = \nabla f$. The forward gradient can be written using forward differences as

$$\tilde{\mathbf{g}}_{\mathbf{mnp}} = \tilde{\nabla} f_{mnp} = \hat{x}\tilde{\partial}_x f_{mnp} + \hat{y}\tilde{\partial}_y f_{mnp} + \hat{z}\tilde{\partial}_z f_{mnp} \tag{3.12}$$

or

$$\tilde{\mathbf{g}}_{\mathbf{mnp}} = \hat{x}\frac{f_{m+1,n,p} - f_{m,n,p}}{\Delta_x} + \hat{y}\frac{f_{m,n+1,p} - f_{m,n,p}}{\Delta_y} + \hat{z}\frac{f_{m,n,p+1} - f_{m,n,p}}{\Delta_z}. \tag{3.13}$$

Notice that $\tilde{\mathbf{g}}_{\mathbf{mnp}}$ has an x-component located at $(m+\frac{1}{2}, n, p)$, y-component located at $(m, n+\frac{1}{2}, p)$, and z-component located at $(m, n, p+\frac{1}{2})$. Each component is located a half-step forward in the corresponding direction.

Similarly, the backward gradient can be written using backward differences as

$$\hat{\mathbf{g}}_{\mathbf{mnp}} = \hat{\nabla} f_{mnp} = \hat{x}\hat{\partial}_x f_{mnp} + \hat{y}\hat{\partial}_y f_{mnp} + \hat{z}\hat{\partial}_z f_{mnp} \tag{3.14}$$

or

$$\hat{\mathbf{g}}_{\mathbf{mnp}} = \hat{x}\frac{f_{m,n,p} - f_{m-1,n,p}}{\Delta_x} + \hat{y}\frac{f_{m,n,p} - f_{m,n-1,p}}{\Delta_y} + \hat{z}\frac{f_{m,n,p} - f_{m,n,p-1}}{\Delta_z}. \tag{3.15}$$

Each component is located a half-step backward in the corresponding direction.

3.4.3 Fore- and Back-Vectors

A fore-vector is defined as a vector with components a half-step in front of the corresponding direction. Fore-vector $\tilde{\mathbf{g}}_{\mathbf{mnp}}$ can be rewritten as

$$\tilde{\mathbf{g}}_{\mathbf{mnp}} = \hat{x}g_{m+\frac{1}{2},n,p} + \hat{y}g_{m,n+\frac{1}{2},p} + \hat{z}g_{m,n,p+\frac{1}{2}} \tag{3.16}$$

where $g_{m+\frac{1}{2},n,p}$ is defined at point $(m+\frac{1}{2}, n, p)$. This means that the $\hat{x}$, $\hat{y}$, and $\hat{z}$ components of $\hat{\mathbf{g}}_{\mathbf{mnp}}$ are defined at different points on the grid.

A back-vector is defined as a vector with components a half-step behind the corresponding direction. Back-vector $\hat{\mathbf{g}}_{\mathbf{mnp}}$ can be written as

$$\hat{\mathbf{g}}_{\mathbf{mnp}} = \hat{x}g_{m-\frac{1}{2},n,p} + \hat{y}g_{m,n-\frac{1}{2},p} + \hat{z}g_{m,n,p-\frac{1}{2}}. \tag{3.17}$$

3.4.4 Discrete Divergence

In order to calculate divergence, we need to define a fore- and a back-vector to operate on. We define fore-vector $\tilde{\mathbf{F}}_{\mathbf{mnp}}$ as

$$\tilde{\mathbf{F}}_{\mathbf{mnp}} = \hat{x} f^x_{m+\frac{1}{2},n,p} + \hat{y} f^y_{m,n+\frac{1}{2},p} + \hat{z} f^z_{m,n,p+\frac{1}{2}}. \tag{3.18}$$

and back-vector $\hat{\mathbf{F}}_{\mathbf{mnp}}$ as

$$\hat{\mathbf{F}}_{\mathbf{mnp}} = \hat{x} f^x_{m-\frac{1}{2},n,p} + \hat{y} f^y_{m,n-\frac{1}{2},p} + \hat{z} f^z_{m,n,p-\frac{1}{2}}. \tag{3.19}$$

In order for the divergence to be located around the central position of (m, n, p), the divergence of a fore-vector must be taken using backward differences. Similarly, the divergence of a back-vector must be taken using forward differences. The divergence of a fore-vector can be taken as

$$\hat{\nabla} \cdot \tilde{\mathbf{F}}_{\mathbf{mnp}} = \hat{\partial}_x f^x_{m+\frac{1}{2},n,p} + \hat{\partial}_y f^y_{m,n+\frac{1}{2},p} + \hat{\partial}_z \hat{z} f^z_{m,n,p+\frac{1}{2}} \tag{3.20}$$

or

$$\hat{\nabla} \cdot \tilde{\mathbf{F}}_{\mathbf{mnp}} = \frac{f^x_{m+\frac{1}{2},n,p} - f^x_{m-\frac{1}{2},n,p}}{\Delta_x} + \frac{f^y_{m,n+\frac{1}{2},p} - f^y_{m,n-\frac{1}{2},p}}{\Delta_y} + \frac{f^z_{m,n,p+\frac{1}{2},n,p} - f^z_{m,n,p-\frac{1}{2}}}{\Delta_z}. \tag{3.21}$$

The divergence of a back-vector can be taken as

$$\tilde{\nabla} \cdot \hat{\mathbf{F}}_{\mathbf{mnp}} = \tilde{\partial}_x f^x_{m-\frac{1}{2},n,p} + \tilde{\partial}_y f^y_{m,n-\frac{1}{2},p} + \tilde{\partial}_z \hat{z} f^z_{m,n,p-\frac{1}{2}} \tag{3.22}$$

or

$$\tilde{\nabla} \cdot \hat{\mathbf{F}}_{\mathbf{mnp}} = \frac{f^x_{m+\frac{1}{2},n,p} - f^x_{m-\frac{1}{2},n,p}}{\Delta_x} + \frac{f^y_{m,n+\frac{1}{2},p} - f^y_{m,n-\frac{1}{2},p}}{\Delta_y} + \frac{f^z_{m,n,p+\frac{1}{2},n,p} - f^z_{m,n,p-\frac{1}{2}}}{\Delta_z}. \tag{3.23}$$

Equations (3.21) and (3.23) show that the discrete divergence turns out to be the same in both cases.

3.4.5 Discrete Curl

Unlike the gradient and divergence, the process of taking the discrete curl causes forward and backward differences to operate on values located at whole rather than half steps. The result of

taking the curl is either a fore- or back-vector located at half-spatial step offset in all directions. The curl of a fore-vector is expanded as

$$\begin{aligned}\hat{\mathbf{B}}_{\mathbf{m}+\frac{\mathbf{1}}{\mathbf{2}},\mathbf{n}+\frac{\mathbf{1}}{\mathbf{2}},\mathbf{p}+\frac{\mathbf{1}}{\mathbf{2}}} &= \tilde{\nabla} \times \tilde{\mathbf{F}}_{m,n,p} \\ &= \hat{x}\left(\frac{f^z_{m,n+1,p+\frac{1}{2}} - f^z_{m,n,p+\frac{1}{2}}}{\Delta_y} - \frac{f^y_{m,n+\frac{1}{2},p+1} - f^y_{m,n+\frac{1}{2},p}}{\Delta_z}\right) \\ &+ \hat{y}\left(\frac{f^x_{m+\frac{1}{2},n,p+1} - f^x_{m+\frac{1}{2},n,p}}{\Delta_z} - \frac{f^z_{m+1,n,p+\frac{1}{2}} - f^z_{m,n,p+\frac{1}{2}}}{\Delta_z}\right) \\ &+ \hat{z}\left(\frac{f^y_{m+1,n+\frac{1}{2},p} - f^y_{m,n+\frac{1}{2},p}}{\Delta_x} - \frac{f^x_{m+\frac{1}{2},n+1,p} - f^x_{m+\frac{1}{2},n,p}}{\Delta_y}\right).\end{aligned} \tag{3.24}$$

We can see that $(m, n+\frac{1}{2}, p+\frac{1}{2})$ is the location of the x-component, $(m+\frac{1}{2}, n, p+\frac{1}{2})$ is the location of the y-component, and $(m+\frac{1}{2}, n+\frac{1}{2}, p)$ is the location of the z-component. These components show us that our new vector is located at $(m+\frac{1}{2}, n+\frac{1}{2}, p+\frac{1}{2})$ and the index related to the component is located a half-step backward, indicating the result is a back-vector.

The curl of a back-vector is expanded as

$$\begin{aligned}\tilde{\mathbf{B}}_{\mathbf{m}-\frac{\mathbf{1}}{\mathbf{2}},\mathbf{n}-\frac{\mathbf{1}}{\mathbf{2}},\mathbf{p}-\frac{\mathbf{1}}{\mathbf{2}}} &= \hat{\nabla} \times \hat{\mathbf{F}}_{m,n,p} \\ &= \hat{x}\left(\frac{f^z_{m,n,p-\frac{1}{2}} - f^z_{m,n-1,p-\frac{1}{2}}}{\Delta_y} - \frac{f^y_{m,n-\frac{1}{2},p} - f^y_{m,n-\frac{1}{2},p-1}}{\Delta_z}\right) \\ &+ \hat{y}\left(\frac{f^x_{m-\frac{1}{2},n,p} - f^x_{m-\frac{1}{2},n,p-1}}{\Delta_z} - \frac{f^z_{m,n,p-\frac{1}{2}} - f^z_{m-1,n,p-\frac{1}{2}}}{\Delta_z}\right) \\ &+ \hat{z}\left(\frac{f^y_{m,n-\frac{1}{2},p} - f^y_{m-1,n-\frac{1}{2},p}}{\Delta_x} - \frac{f^x_{m-\frac{1}{2},n,p} - f^x_{m-\frac{1}{2},n-1,p}}{\Delta_y}\right).\end{aligned} \tag{3.25}$$

We can see that $(m, n-\frac{1}{2}, p-\frac{1}{2})$ is the location of the x-component, $(m-\frac{1}{2}, n, p-\frac{1}{2})$ is the location of the y-component, and $(m-\frac{1}{2}, n-\frac{1}{2}, p)$ is the location of the z-component. These components show us that our new vector is located at $(m-\frac{1}{2}, n-\frac{1}{2}, p-\frac{1}{2})$ and the index related to the component is located a half-step forward, indicating the result is a fore-vector.

Taking the backward curl of a fore-vector or the forward curl of a back-vector would result in the values within the components of the vector not being located at a single point. For example, for the backward curl of a fore-vector, the x-component would have values located at both $(m, n-$

$\frac{1}{2}, p + \frac{1}{2})$ and $(m, n + \frac{1}{2}, p - \frac{1}{2})$. Values being located at consistent positions are important for stability of finite-difference schemes.

Chapter 4

Second-Order Field-Potential Finite-Difference Time-Domain

An existing FDTD formulation has been developed that solves the second-order inhomogeneous wave equations for potentials [14]. This method uses $\mathbf{J}$ and ρ as sources in order to update $\mathbf{A}$ and ϕ. The difficulty of this method lies in the second-order nature of the equations.

Second-order equations make implementation of an absorbing boundary layer difficult. Absorbing boundary layers are necessary to reduce computational domain size, and therefore computational resources, while also minimizing reflections.

4.1 Second Order Wave Equations

Maxwell's equations can be rewritten using the definitions of $\mathbf{A}$ and ϕ found in Section 2.2 in addition to a choice of gauge that can be found in Section 2.2.2. If we choose the generalized Lorenz Gauge generalized for inhomogeneous media, we can convert Maxwell's four first-order equations into two second-order equations, the inhomogeneous wave equations. The generalized Lorenz gauge is written as

$$\epsilon^{-1}\nabla \cdot \epsilon\mathbf{A} = -\mu\epsilon\frac{\partial}{\partial t}\phi \tag{4.1}$$

and can be further generalized to

$$\nabla \cdot \epsilon\mathbf{A} = -\chi\frac{\partial}{\partial t}\phi \tag{4.2}$$

where $\chi = \alpha\epsilon^2\mu$ and $\alpha = 1$.

We can insert Equation (4.1) into Equations (2.15a) and (2.15b) to obtain the $\mathbf{A}$-ϕ formulation of Maxwell's equations, the inhomogenous wave equations for $\mathbf{A}$ and ϕ. The inhomogenous wave

equations are

$$\nabla \cdot \epsilon \nabla \phi - \epsilon^2 \mu \frac{\partial^2}{\partial t^2} \phi = -\rho \tag{4.3}$$

and

$$-\nabla \times \frac{1}{\mu}(\nabla \times \mathbf{A}) - \epsilon \frac{\partial^2}{\partial t^2} \mathbf{A} + \epsilon \nabla \epsilon^{-2} \mu^{-1} \nabla \cdot \epsilon \mathbf{A} = -\mathbf{J}. \tag{4.4}$$

The first equation only depends on ϕ and ρ while the other is only in terms of $\mathbf{A}$ and $\mathbf{J}$, making the equations appear separated; however, ρ and $\mathbf{J}$ are coupled via the electromagnetic continuity equation

$$\nabla \cdot \mathbf{J} + \frac{\partial \rho}{\partial t} = 0. \tag{4.5}$$

4.2 Time-Stepping Equations for of $\mathbf{A}$-ϕ Formalism

The inhomogeneous wave equations in the generalized Lorenz gauge and the electromagnetic continuity equation will serve as update equations for the second-order $\mathbf{A}$-ϕ FDTD. In order to time-update these equations, we need to separate the term with time-derivative for each equation. The form of the update equations are given as

$$\frac{\partial \rho}{\partial t} = -\nabla \cdot \mathbf{J}, \tag{4.6a}$$

$$\epsilon^2 \mu \frac{\partial^2}{\partial t^2} \phi = \nabla \cdot \epsilon \nabla \phi + \rho, \tag{4.6b}$$

and

$$\epsilon \frac{\partial^2}{\partial t^2} \mathbf{A} = \epsilon \nabla \frac{1}{\epsilon^2 \mu} \nabla \cdot \epsilon \mathbf{A} - \nabla \times \frac{1}{\mu}(\nabla \times \mathbf{A}) + \mathbf{J}. \tag{4.6c}$$

When we discretize these equations, the time-derivatives will allow us to update the next time step in the algorithm. First-order derivatives will require one previous timestep of the update field, while second-order derivatives will require two. This means, for simulation-domain update equations, both $\mathbf{A}$ and ϕ update equations will require two previous timesteps stored in the memory, while $\mathbf{J}$ and ρ require just one.

4.3 Discretization of Vector Potential Formulation of Maxwell's Equations

Since the set of Equations (4.6a)-(4.6c) are continuous, we now need to discretize them. Assuming that all vectors are fore-vectors and all calculus operators are discrete, we can write Equations (4.6a)-(4.6c) using the rules from Section 3.4 as

$$\partial_t \rho = -\left(\hat{\nabla} \cdot \tilde{\mathbf{J}}_{i,j,k}^{n+\frac{1}{2}}\right), \tag{4.7}$$

$$\partial_t^2 \phi_{i,j,k}^n = \epsilon_{i,j,k}^{-2} \mu_{i,j,k}^{-1} \left(\hat{\nabla} \cdot \epsilon_{i,j,k} \tilde{\nabla} \phi_{i,j,k}^n + \rho_{i,j,k}^n\right), \tag{4.8}$$

and

$$\partial_t^2 \tilde{\mathbf{A}}_{i,j,k}^{n+\frac{1}{2}} = \epsilon_{i,j,k}^{-1} \left(-\hat{\nabla} \times \mu_{i+\frac{1}{2},j+\frac{1}{2},k+\frac{1}{2}}^{-1} \left(\tilde{\nabla} \times \tilde{\mathbf{A}}_{i,j,k}^n\right) + \epsilon_{i,j,k} \tilde{\nabla} \epsilon_{i,j,k}^{-2} \mu_{i,j,k}^{-1} \hat{\nabla} \cdot \epsilon_{i,j,k} \tilde{\mathbf{A}}_{i,j,k}^n + \tilde{\mathbf{J}}_{i,j,k}^n\right). \tag{4.9}$$

All fore-vectors and scalar values are located at point (i, j, k). The time-step are a half-step offset for $\mathbf{A}$ and $\mathbf{J}$ at n compared to ϕ and ρ at $n + \frac{1}{2}$. The details of spatial-steps and timesteps can be found in Section 3.3.

Next, we add the discretization of the time derivative, the first-order derivative is a forward-difference while the second-order time derivative is central difference. Expanding the time derivative in Equations (4.7)-(4.9) gives

$$\rho_{i,j,k}^n = \rho_{i,j,k}^{n-1} - \Delta_t \left(\hat{\nabla} \cdot \tilde{\mathbf{J}}_{i,j,k}^n\right), \tag{4.10}$$

$$\phi_{i,j,k}^{n+1} = 2\phi_{i,j,k}^n - \phi_{i,j,k}^{n-1} + \Delta_t^2 \epsilon_{i,j,k}^{-2} \mu_{i,j,k}^{-1} \left(\hat{\nabla} \cdot \epsilon_{i,j,k} \tilde{\nabla} \phi_{i,j,k}^n + \rho_{i,j,k}^n\right), \tag{4.11}$$

and

$$\begin{aligned} \tilde{\mathbf{A}}_{i,j,k}^{n+1} &= 2\tilde{\mathbf{A}}_{i,j,k}^n - \tilde{\mathbf{A}}_{i,j,k}^{n-1} \\ &+ \Delta_t^2 \epsilon_{i,j,k}^{-1} \left(-\hat{\nabla} \times \mu_{i+\frac{1}{2},j+\frac{1}{2},k+\frac{1}{2}}^{-1} \left(\tilde{\nabla} \times \tilde{\mathbf{A}}_{i,j,k}^n\right) + \epsilon_{i,j,k} \tilde{\nabla} \epsilon_{i,j,k}^{-2} \mu_{i,j,k}^{-1} \hat{\nabla} \cdot \epsilon_{i,j,k} \tilde{\mathbf{A}}_{i,j,k}^n + \tilde{\mathbf{J}}_{i,j,k}^n\right). \end{aligned} \tag{4.12}$$

The next sections are devoted to expanding the vector calculus operations in these equations. The second-nature of these equations makes the expansion of these equations nontrivial.

4.3.1 Expansion of ρ Update Equation

Using vector calculus definitions, we can expand Equation (4.10) into finite-differences of the values of current density. Writing out the discrete divergence in terms of backward differences and components of the current density gives us

$$\rho_{i,j,k}^{n+1} = \rho_{i,j,k}^{n} - \Delta_t^2 \left(\hat{\partial}_x J_{x\ i+\frac{1}{2},j,k}^{n+\frac{1}{2}} + \hat{\partial}_y J_{y\ i,j+\frac{1}{2},k}^{n+\frac{1}{2}} + \hat{\partial}_z J_{z\ i,j,k+\frac{1}{2}}^{n+\frac{1}{2}} \right). \tag{4.13}$$

By evaluating the backward differences on the fore-vector, we obtain

$$\rho_{i,j,k}^{n+1} = \rho_{i,j,k}^{n} - \Delta_t^2 \left(\frac{J_{x\ i+\frac{1}{2},j,k}^{n+\frac{1}{2}} - J_{x\ i-\frac{1}{2},j,k}^{n+\frac{1}{2}}}{\Delta_x} + \frac{J_{y\ i,j+\frac{1}{2},k}^{n+\frac{1}{2}} - J_{y\ i,j-\frac{1}{2},k}^{n+\frac{1}{2}}}{\Delta_y} + \frac{J_{z\ i,j,k+\frac{1}{2}}^{n+\frac{1}{2}} - J_{z\ i,j,k-\frac{1}{2}}^{n+\frac{1}{2}}}{\Delta_z} \right). \tag{4.14}$$

Since this equation is first-order, this is the most simple update equation for the $\mathbf{A}$-ϕ formalism.

4.3.2 Expansion of ϕ Update Equation

We can expand Equation (4.11) into finite-differences where ϕ updates in time from its own past values as well as a ρ source. First, we expand the gradient from Equation (4.11) into forward differences

$$\phi_{i,j,k}^{n+1} = 2\phi_{i,j,k}^{n} - \phi_{i,j,k}^{n-1} + \Delta_t^2 \epsilon_{i,j,k}^{-2} \mu_{i,j,k}^{-1} \left(\hat{\nabla} \cdot \epsilon_{i,j,k} \left(\hat{x}\tilde{\partial}_x \phi_{i,j,k}^{n} + \hat{y}\tilde{\partial}_y \phi_{i,j,k}^{n} + \hat{z}\tilde{\partial}_z \phi_{i,j,k}^{n} \right) + \rho_{i,j,k}^{n} \right). \tag{4.15}$$

Next, we can expand the forward differences into different values of ϕ

$$\phi_{i,j,k}^{n+1} = 2\phi_{i,j,k}^{n} - \phi_{i,j,k}^{n-1} + \Delta_t^2 \epsilon_{i,j,k}^{-2} \mu_{i,j,k}^{-1} \left(\hat{\nabla} \cdot \epsilon_{i,j,k} \left(\hat{x} \frac{\phi_{i+1,j,k}^{n} - \phi_{i,j,k}^{n}}{\Delta x} + \hat{y} \frac{\phi_{i,j+1,k}^{n} - \phi_{i,j,k}^{n}}{\Delta y} + \hat{z} \frac{\phi_{i,j,k+1}^{n} - \phi_{i,j,k}^{n}}{\Delta z} \right) + \rho_{i,j,k}^{n} \right). \tag{4.16}$$

The divergence can be separated into backward difference operators

$$\phi_{i,j,k}^{n+1} = 2\phi_{i,j,k}^{n} - \phi_{i,j,k}^{n-1} + \Delta_t^2 \epsilon_{i,j,k}^{-2} \mu_{i,j,k}^{-1} \left(\left(\hat{\partial}_x \left(\epsilon_{i,j,k} \frac{\phi_{i+1,j,k}^{n} - \phi_{i,j,k}^{n}}{\Delta_x} \right) + \hat{\partial}_y \left(\epsilon_{i,j,k} \frac{\phi_{i,j+1,k}^{n} - \phi_{i,j,k}^{n}}{\Delta_y} \right) + \hat{\partial}_z \left(\epsilon_{i,j,k} \frac{\phi_{i,j,k+1}^{n} - \phi_{i,j,k}^{n}}{\Delta_z} \right) \right) + \rho_{i,j,k}^{n} \right). \quad (4.17)$$

The backward difference can be taken on the entire expression

$$\phi_{i,j,k}^{n+1} = 2\phi_{i,j,k}^{n} - \phi_{i,j,k}^{n-1} + \Delta_t^2 \epsilon_{i,j,k}^{-2} \mu_{i,j,k}^{-1} \left(\left(\frac{1}{\Delta_x} \left(\left(\epsilon_{i,j,k} \frac{\phi_{i+1,j,k}^{n} - \phi_{i,j,k}^{n}}{\Delta_x} \right) - \left(\epsilon_{i-1,j,k} \frac{\phi_{i,j,k}^{n} - \phi_{i-1,j,k}^{n}}{\Delta_x} \right) \right) + \frac{1}{\Delta_y} \left(\left(\epsilon_{i,j,k} \frac{\phi_{i,j+1,k}^{n} - \phi_{i,j,k}^{n}}{\Delta_y} \right) - \left(\epsilon_{i,j-1,k} \frac{\phi_{i,j,k}^{n} - \phi_{i,j-1,k}^{n}}{\Delta_y} \right) \right) + \frac{1}{\Delta_z} \left(\left(\epsilon_{i,j,k} \frac{\phi_{i,j,k+1}^{n} - \phi_{i,j,k}^{n}}{\Delta_z} \right) - \left(\epsilon_{i,j,k-1} \frac{\phi_{i,j,k}^{n} - \phi_{i,j,k-1}^{n}}{\Delta_z} \right) \right) \right) + \rho_{i,j,k}^{n} \right). \quad (4.18)$$

After taking the backward difference, ϵ varies by position within the update equation. The assumption of inhomogeniety in the original equation is important because these values appear in discretization. Terms can be sorted by a coefficient times a value of ϕ

$$\phi_{i,j,k}^{n+1} = 2\phi_{i,j,k}^{n} - \phi_{i,j,k}^{n-1} + \Delta_t^2 \epsilon_{i,j,k}^{-2} \mu_{i,j,k}^{-1} \left(\left(\frac{\epsilon_{i,j,k}}{\Delta_x^2} \phi_{i+1,j,k}^{n} - \frac{\epsilon_{i,j,k} - \epsilon_{i-1,j,k}}{\Delta_x^2} \phi_{i,j,k}^{n} + \frac{\epsilon_{i-1,j,k}}{\Delta_x^2} \phi_{i-1,j,k}^{n} \right) + \left(\frac{\epsilon_{i,j,k}}{\Delta_y^2} \phi_{i,j+1,k}^{n} - \frac{\epsilon_{i,j,k} - \epsilon_{i,j-1,k}}{\Delta_y^2} \phi_{i,j,k}^{n} + \frac{\epsilon_{i,j-1,k}}{\Delta_y^2} \phi_{i,j-1,k}^{n} \right) + \left(\frac{\epsilon_{i,j,k}}{\Delta_z^2} \phi_{i,j,k+1}^{n} - \frac{\epsilon_{i,j,k} - \epsilon_{i,j,k-1}}{\Delta_z^2} \phi_{i,j,k}^{n} + \frac{\epsilon_{i,j,k-1}}{\Delta_z^2} \phi_{i,j,k-1}^{n} \right) + \rho_{i,j,k}^{n} \right). \quad (4.19)$$

4.3.3 Expansion of A Update Equation

We can expand Equation (4.12) by first separating the equation into mutliple terms. Say Equation (4.12) is now

$$\tilde{\mathbf{A}}_{i,j,k}^{n+\frac{3}{2}} = 2\tilde{\mathbf{A}}_{i,j,k}^{n+\frac{1}{2}} - \tilde{\mathbf{A}}_{i,j,k}^{n-\frac{1}{2}} + \Delta_t^2 \epsilon_{i,j,k}^{-1} \left(\mathbf{A}_{term1}^{n+\frac{1}{2}} + \mathbf{A}_{term2}^{n+\frac{1}{2}} + \tilde{\mathbf{J}}_{i,j,k}^{n+\frac{1}{2}} \right) \quad (4.20)$$

where

$$\mathbf{A}_{term1}^{n+\frac{1}{2}} = -\hat{\nabla} \times \mu^{-1}_{i+\frac{1}{2},j+\frac{1}{2},k+\frac{1}{2}} \left(\tilde{\nabla} \times \tilde{\mathbf{A}}_{i,j,k}^{n+\frac{1}{2}} \right) \tag{4.21}$$

and

$$\mathbf{A}_{term2}^{n+\frac{1}{2}} = \epsilon_{i,j,k} \tilde{\nabla} \epsilon^{-2}_{i,j,k} \mu^{-1}_{i,j,k} \hat{\nabla} \cdot \epsilon_{i,j,k} \tilde{\mathbf{A}}_{i,j,k}^{n+\frac{1}{2}}. \tag{4.22}$$

4.3.3.1 Expansion of $\mathbf{A}_{term1}$

Starting with Equation (4.21),

$$\mathbf{A}_{term1}^{n+\frac{1}{2}} = -\hat{\nabla} \times \mu^{-1}_{i+\frac{1}{2},j+\frac{1}{2},k+\frac{1}{2}} \left(\tilde{\nabla} \times \tilde{\mathbf{A}}_{i,j,k}^{n+\frac{1}{2}} \right), \tag{4.23}$$

we can evaulate the first curl as

$$\begin{aligned} \tilde{\nabla} \times \tilde{\mathbf{A}}_{i,j,k}^{n+\frac{1}{2}} = \hat{x} \left(\tilde{\partial}_y A_{z\ i,j,k+\frac{1}{2}}^{n+\frac{1}{2}} - \tilde{\partial}_z A_{y\ i,j+\frac{1}{2},k}^{n+\frac{1}{2}} \right) + \\ \hat{y} \left(\tilde{\partial}_z A_{x\ i+\frac{1}{2},j,k}^{n+\frac{1}{2}} - \tilde{\partial}_x A_{z\ i,j,k+\frac{1}{2}}^{n+\frac{1}{2}} \right) + \\ \hat{z} \left(\tilde{\partial}_x A_{y\ i,j+\frac{1}{2},k}^{n+\frac{1}{2}} - \tilde{\partial}_y A_{x\ i+\frac{1}{2},j,k}^{n+\frac{1}{2}} \right) \end{aligned} \tag{4.24}$$

which gives us the first term as

$$\begin{aligned} \mathbf{A}_{term1}^{n+\frac{1}{2}} = -\hat{\nabla} \times \mu^{-1}_{i+\frac{1}{2},j+\frac{1}{2},k+\frac{1}{2}} \\ \left(\hat{x} \left(\frac{A_{z\ i,j+1,k+\frac{1}{2}}^{n+\frac{1}{2}} - A_{z\ i,j,k+\frac{1}{2}}^{n+\frac{1}{2}}}{\Delta_y} - \frac{A_{y\ i,j+\frac{1}{2},k+1}^{n+\frac{1}{2}} - A_{y\ i,j+\frac{1}{2},k}^{n+\frac{1}{2}}}{\Delta_z} \right) + \right. \\ \hat{y} \left(\frac{A_{x\ i+\frac{1}{2},j,k+1}^{n+\frac{1}{2}} - A_{x\ i+\frac{1}{2}j,k}^{n+\frac{1}{2}}}{\Delta_z} - \frac{A_{z\ i+1,j,k+\frac{1}{2}}^{n+\frac{1}{2}} - A_{z\ i,j,k+\frac{1}{2}}^{n+\frac{1}{2}}}{\Delta_x} \right) + \\ \left. \hat{z} \left(\frac{A_{y\ i+1,j+\frac{1}{2},k}^{n+\frac{1}{2}} - A_{y\ i,j+\frac{1}{2},k}^{n+\frac{1}{2}}}{\Delta_x} - \frac{A_{x\ i+\frac{1}{2},j+1,k}^{n+\frac{1}{2}} - A_{x\ i+\frac{1}{2},j,k}^{n+\frac{1}{2}}}{\Delta_y} \right) \right). \end{aligned} \tag{4.25}$$

Taking the curl of this equation requires evaulating finite-differences for all components. We will simplify this again by separating the full expression into simpler terms.

In general, the curl can be written as

$$-\hat{\nabla} \times \mathbf{A} = -\hat{x}\left(\hat{\partial}_y a_z - \hat{\partial}_z a_y\right) - \hat{y}\left(\hat{\partial}_z a_x - \hat{\partial}_x a_z\right) - \hat{z}\left(\hat{\partial}_x a_y - \hat{\partial}_y a_x\right) \tag{4.26}$$

This means the components of $\mathbf{A}_{term1}$ can be written as

$$A_{x\ term1}^{n+\frac{1}{2}} = -\left(\hat{\partial}_y a_z - \hat{\partial}_z a_y\right), \tag{4.27a}$$

$$A_{y\ term1}^{n+\frac{1}{2}} = -\left(\hat{\partial}_z a_x - \hat{\partial}_x a_z\right), \tag{4.27b}$$

and

$$A_{z\ term1}^{n+\frac{1}{2}} = -\left(\hat{\partial}_x a_y - \hat{\partial}_y a_x\right) \tag{4.27c}$$

where

$$a_x = \left(\mu^{-1}_{i+\frac{1}{2},j+\frac{1}{2},k+\frac{1}{2}}\left(\frac{A_{z\ i,j+1,k+\frac{1}{2}}^{n+\frac{1}{2}} - A_{z\ i,j,k+\frac{1}{2}}^{n+\frac{1}{2}}}{\Delta_y} - \frac{A_{y\ i,j+\frac{1}{2},k+1}^{n+\frac{1}{2}} - A_{y\ i,j+\frac{1}{2},k}^{n+\frac{1}{2}}}{\Delta_z}\right)\right), \tag{4.28a}$$

$$a_y = \left(\mu^{-1}_{i+\frac{1}{2},j+\frac{1}{2},k+\frac{1}{2}}\left(\frac{A_{x\ i+\frac{1}{2},j,k+1}^{n+\frac{1}{2}} - A_{x\ i+\frac{1}{2}j,k}^{n+\frac{1}{2}}}{\Delta_z} - \frac{A_{z\ i+1,j,k+\frac{1}{2}}^{n+\frac{1}{2}} - A_{z\ i,j,k+\frac{1}{2}}^{n+\frac{1}{2}}}{\Delta_x}\right)\right), \tag{4.28b}$$

and

$$a_z = \left(\mu^{-1}_{i+\frac{1}{2},j+\frac{1}{2},k+\frac{1}{2}}\left(\frac{A_{y\ i+1,j+\frac{1}{2},k}^{n+\frac{1}{2}} - A_{y\ i,j+\frac{1}{2},k}^{n+\frac{1}{2}}}{\Delta_x} - \frac{A_{x\ i+\frac{1}{2},j+1,k}^{n+\frac{1}{2}} - A_{x\ i+\frac{1}{2},j,k}^{n+\frac{1}{2}}}{\Delta_y}\right)\right). \tag{4.28c}$$

Writing each term separately shows which component of finite differences need to be evaulated on each term

$$\begin{aligned} A_{x\ term1}^{n+\frac{1}{2}} = \\ -\hat{\partial}_y\left(\mu^{-1}_{i+\frac{1}{2},j+\frac{1}{2},k+\frac{1}{2}}\left(\frac{A_{y\ i+1,j+\frac{1}{2},k}^{n+\frac{1}{2}} - A_{y\ i,j+\frac{1}{2},k}^{n}}{\Delta_x} - \frac{A_{x\ i+\frac{1}{2},j+1,k}^{n+\frac{1}{2}} - A_{x\ i+\frac{1}{2},j,k}^{n}}{\Delta_y}\right)\right) + \\ \hat{\partial}_z\left(\mu^{-1}_{i+\frac{1}{2},j+\frac{1}{2},k+\frac{1}{2}}\left(\frac{A_{x\ i+\frac{1}{2},j,k+1}^{n+\frac{1}{2}} - A_{x\ i+\frac{1}{2}j,k}^{n}}{\Delta_z} - \frac{A_{z\ i+1,j,k+\frac{1}{2}}^{n+\frac{1}{2}} - A_{z\ i,j,k+\frac{1}{2}}^{n}}{\Delta_x}\right)\right), \end{aligned} \tag{4.29a}$$

$$A_{y\ term1}^{n+\frac{1}{2}} =$$
$$-\hat{\partial}_z\left(\mu^{-1}_{i+\frac{1}{2},j+\frac{1}{2},k+\frac{1}{2}}\left(\frac{A_{z\ i,j+1,k+\frac{1}{2}}^{n+\frac{1}{2}}-A_{z\ i,j,k+\frac{1}{2}}^{n+\frac{1}{2}}}{\Delta_y}-\frac{A_{y\ i,j+\frac{1}{2},k+1}^{n+\frac{1}{2}}-A_{y\ i,j+\frac{1}{2},k}^{n+\frac{1}{2}}}{\Delta_z}\right)\right)+$$
$$\hat{\partial}_x\left(\mu^{-1}_{i+\frac{1}{2},j+\frac{1}{2},k+\frac{1}{2}}\left(\frac{A_{y\ i+1,j+\frac{1}{2},k}^{n+\frac{1}{2}}-A_{y\ i,j+\frac{1}{2},k}^{n+\frac{1}{2}}}{\Delta_x}-\frac{A_{x\ i+\frac{1}{2},j+1,k}^{n+\frac{1}{2}}-A_{x\ i+\frac{1}{2},j,k}^{n+\frac{1}{2}}}{\Delta_y}\right)\right), \quad (4.29b)$$

and

$$A_{z\ term1}^{n+\frac{1}{2}} =$$
$$-\hat{\partial}_x\left(\mu^{-1}_{i+\frac{1}{2},j+\frac{1}{2},k+\frac{1}{2}}\left(\frac{A_{x\ i+\frac{1}{2},j,k+1}^{n+\frac{1}{2}}-A_{x\ i+\frac{1}{2}j,k}^{n+\frac{1}{2}}}{\Delta_z}-\frac{A_{z\ i+1,j,k+\frac{1}{2}}^{n+\frac{1}{2}}-A_{z\ i,j,k+\frac{1}{2}}^{n+\frac{1}{2}}}{\Delta_x}\right)\right)+$$
$$\hat{\partial}_y\left(\mu^{-1}_{i+\frac{1}{2},j+\frac{1}{2},k+\frac{1}{2}}\left(\frac{A_{z\ i,j+1,k+\frac{1}{2}}^{n+\frac{1}{2}}-A_{z\ i,j,k+\frac{1}{2}}^{n+\frac{1}{2}}}{\Delta_y}-\frac{A_{y\ i,j+\frac{1}{2},k+1}^{n+\frac{1}{2}}-A_{y\ i,j+\frac{1}{2},k}^{n+\frac{1}{2}}}{\Delta_z}\right)\right). \quad (4.29c)$$

Evaluating finite differences leads to doubling the number of field values within a term, giving the final expressions for the components of $\mathbf{A}_{term1}^{n+\frac{1}{2}}$ as

$$A_{x\ term1}^{n+\frac{1}{2}} =$$
$$-\frac{1}{\Delta_y}\left(\left(\mu^{-1}_{i+\frac{1}{2},j+\frac{1}{2},k+\frac{1}{2}}\left(\frac{A_{y\ i+1,j+\frac{1}{2},k}^{n+\frac{1}{2}}-A_{y\ i,j+\frac{1}{2},k}^{n+\frac{1}{2}}}{\Delta_x}-\frac{A_{x\ i+\frac{1}{2},j+1,k}^{n+\frac{1}{2}}-A_{x\ i+\frac{1}{2},j,k}^{n+\frac{1}{2}}}{\Delta_y}\right)\right)-\right.$$
$$\left.\left(\mu^{-1}_{i+\frac{1}{2},j-\frac{1}{2},k+\frac{1}{2}}\left(\frac{A_{y\ i+1,j-\frac{1}{2},k}^{n+\frac{1}{2}}-A_{y\ i,j-\frac{1}{2},k}^{n+\frac{1}{2}}}{\Delta_x}-\frac{A_{x\ i+\frac{1}{2},j,k}^{n+\frac{1}{2}}-A_{x\ i+\frac{1}{2},j-1,k}^{n+\frac{1}{2}}}{\Delta_y}\right)\right)\right)$$
$$+\frac{1}{\Delta_z}\left(\mu^{-1}_{i+\frac{1}{2},j+\frac{1}{2},k+\frac{1}{2}}\left(\frac{A_{x\ i+\frac{1}{2},j,k+1}^{n+\frac{1}{2}}-A_{x\ i+\frac{1}{2}j,k}^{n+\frac{1}{2}}}{\Delta_z}-\frac{A_{z\ i+1,j,k+\frac{1}{2}}^{n+\frac{1}{2}}-A_{z\ i,j,k+\frac{1}{2}}^{n+\frac{1}{2}}}{\Delta_x}\right)-\right.$$
$$\left.\mu^{-1}_{i+\frac{1}{2},j+\frac{1}{2},k-\frac{1}{2}}\left(\frac{A_{x\ i+\frac{1}{2},j,k}^{n+\frac{1}{2}}-A_{x\ i+\frac{1}{2}j,k-1}^{n+\frac{1}{2}}}{\Delta_z}-\frac{A_{z\ i+1,j,k-\frac{1}{2}}^{n+\frac{1}{2}}-A_{z\ i,j,k-\frac{1}{2}}^{n+\frac{1}{2}}}{\Delta_x}\right)\right), \quad (4.30a)$$

$$
\begin{aligned}
A_{y\ term1}^{n+\frac{1}{2}} = & \\
& -\frac{1}{\Delta_z}\left(\mu^{-1}_{i+\frac{1}{2},j+\frac{1}{2},k+\frac{1}{2}}\left(\frac{A^{n+\frac{1}{2}}_{z\ i,j+1,k+\frac{1}{2}} - A^{n+\frac{1}{2}}_{z\ i,j,k+\frac{1}{2}}}{\Delta_y} - \frac{A^{n+\frac{1}{2}}_{y\ i,j+\frac{1}{2},k+1} - A^{n+\frac{1}{2}}_{y\ i,j+\frac{1}{2},k}}{\Delta_z}\right) - \right. \\
& \left.\mu^{-1}_{i+\frac{1}{2},j+\frac{1}{2},k-\frac{1}{2}}\left(\frac{A^{n+\frac{1}{2}}_{z\ i,j+1,k-\frac{1}{2}} - A^{n+\frac{1}{2}}_{z\ i,j,k-\frac{1}{2}}}{\Delta_y} - \frac{A^{n+\frac{1}{2}}_{y\ i,j+\frac{1}{2},k} - A^{n+\frac{1}{2}}_{y\ i,j+\frac{1}{2},k-1}}{\Delta_z}\right)\right) \\
& +\frac{1}{\Delta_x}\left(\mu^{-1}_{i+\frac{1}{2},j+\frac{1}{2},k+\frac{1}{2}}\left(\frac{A^{n+\frac{1}{2}}_{y\ i+1,j+\frac{1}{2},k} - A^{n+\frac{1}{2}}_{y\ i,j+\frac{1}{2},k}}{\Delta_x} - \frac{A^{n+\frac{1}{2}}_{x\ i+\frac{1}{2},j+1,k} - A^{n+\frac{1}{2}}_{x\ i+\frac{1}{2},j,k}}{\Delta_y}\right) - \right. \\
& \left.\mu^{-1}_{i-\frac{1}{2},j+\frac{1}{2},k+\frac{1}{2}}\left(\frac{A^{n+\frac{1}{2}}_{y\ i,j+\frac{1}{2},k} - A^{n+\frac{1}{2}}_{y\ i-1,j+\frac{1}{2},k}}{\Delta_x} - \frac{A^{n+\frac{1}{2}}_{x\ i-\frac{1}{2},j+1,k} - A^{n+\frac{1}{2}}_{x\ i-\frac{1}{2},j,k}}{\Delta_y}\right)\right), \qquad (4.30b)
\end{aligned}
$$

and

$$
\begin{aligned}
A_{z\ term1}^{n+\frac{1}{2}} = & \\
& -\frac{1}{\Delta_x}\left(\mu^{-1}_{i+\frac{1}{2},j+\frac{1}{2},k+\frac{1}{2}}\left(\frac{A^{n+\frac{1}{2}}_{x\ i+\frac{1}{2},j,k+1} - A^{n+\frac{1}{2}}_{x\ i+\frac{1}{2}j,k}}{\Delta_z} - \frac{A^{n+\frac{1}{2}}_{z\ i+1,j,k+\frac{1}{2}} - A^{n+\frac{1}{2}}_{z\ i,j,k+\frac{1}{2}}}{\Delta_x}\right) - \right. \\
& \left.\mu^{-1}_{i-\frac{1}{2},j+\frac{1}{2},k+\frac{1}{2}}\left(\frac{A^{n+\frac{1}{2}}_{x\ i-\frac{1}{2},j,k+1} - A^{n+\frac{1}{2}}_{x\ i-\frac{1}{2}j,k}}{\Delta_z} - \frac{A^{n+\frac{1}{2}}_{z\ i,j,k+\frac{1}{2}} - A^{n+\frac{1}{2}}_{z\ i-1,j,k+\frac{1}{2}}}{\Delta_x}\right)\right) \\
& +\frac{1}{\Delta_y}\left(\mu^{-1}_{i+\frac{1}{2},j+\frac{1}{2},k+\frac{1}{2}}\left(\frac{A^{n+\frac{1}{2}}_{z\ i,j+1,k+\frac{1}{2}} - A^{n+\frac{1}{2}}_{z\ i,j,k+\frac{1}{2}}}{\Delta_y} - \frac{A^{n+\frac{1}{2}}_{y\ i,j+\frac{1}{2},k+1} - A^{n+\frac{1}{2}}_{y\ i,j+\frac{1}{2},k}}{\Delta_z}\right) - \right. \\
& \left.\mu^{-1}_{i+\frac{1}{2},j-\frac{1}{2},k+\frac{1}{2}}\left(\frac{A^{n+\frac{1}{2}}_{z\ i,j,k+\frac{1}{2}} - A^{n+\frac{1}{2}}_{z\ i,j,k+\frac{1}{2}}}{\Delta_y} - \frac{A^{n+\frac{1}{2}}_{y\ i,j+\frac{1}{2},k+1} - A^{n+\frac{1}{2}}_{y\ i,j+\frac{1}{2},k}}{\Delta_z}\right)\right). \qquad (4.30c)
\end{aligned}
$$

4.3.3.2 Expansion of $\mathbf{A}_{term2}$

Starting with Equation (4.22),

$$
\mathbf{A}^{n+\frac{1}{2}}_{term2} = \epsilon_{i,j,k}\tilde{\nabla}\epsilon^{-2}_{i,j,k}\mu^{-1}_{i,j,k}\hat{\nabla}\cdot\epsilon_{i,j,k}\tilde{\mathbf{A}}^{n+\frac{1}{2}}_{i,j,k}, \qquad (4.31)
$$

we can expand the first divergence into backward differences

$$\hat{\nabla} \cdot \epsilon_{i,j,k} \tilde{\mathbf{A}}_{i,j,k}^{n+\frac{1}{2}} = \hat{\partial}_x \epsilon_{i,j,k} A_{x\ i+\frac{1}{2},j,k}^{n+\frac{1}{2}} + \hat{\partial}_y \epsilon_{i,j,k} A_{y\ i,j+\frac{1}{2},k}^{n+\frac{1}{2}} + \hat{\partial}_z \epsilon_{i,j,k} A_{z\ i,j,k+\frac{1}{2}}^{n+\frac{1}{2}}. \tag{4.32}$$

The backward differences can be evaluated to obtain

$$\begin{aligned}\hat{\nabla} \cdot \epsilon_{i,j,k} \tilde{\mathbf{A}}_{i,j,k}^{n+\frac{1}{2}} = \frac{1}{\Delta x} \left(\epsilon_{i,j,k} A_{x\ i+\frac{1}{2},j,k}^{n+\frac{1}{2}} - \epsilon_{i-1,j,k} A_{x\ i-\frac{1}{2},j,k}^{n+\frac{1}{2}} \right) + \\ \frac{1}{\Delta y} \left(\epsilon_{i,j,k} A_{y\ i,j+\frac{1}{2},k}^{n+\frac{1}{2}} - \epsilon_{i,j-1,k} A_{y\ i,j-\frac{1}{2},k}^{n+\frac{1}{2}} \right) + \\ \frac{1}{\Delta z} \left(\epsilon_{i,j,k} A_{z\ i,j,k+\frac{1}{2}}^{n+\frac{1}{2}} - \epsilon_{i,j,k-1} A_{z\ i,j,k-\frac{1}{2}}^{n+\frac{1}{2}} \right).\end{aligned} \tag{4.33}$$

Next, we can take the backward gradient of Equation (4.33) to obtain the next part of $\mathbf{A}_{term2}^{n+\frac{1}{2}}$

$$\begin{aligned}\tilde{\nabla} \epsilon_{i,j,k}^{-2} \mu_{i,j,k}^{-1} \hat{\nabla} \cdot \epsilon_{i,j,k} \tilde{\mathbf{A}}_{i,j,k}^{n} = \tilde{\nabla} \\ \left(\frac{1}{\Delta x} \epsilon_{i,j,k}^{-2} \mu_{i,j,k}^{-1} \left(\epsilon_{i,j,k} A_{x\ i+\frac{1}{2},j,k}^{n+\frac{1}{2}} - \epsilon_{i-1,j,k} A_{x\ i-\frac{1}{2},j,k}^{n+\frac{1}{2}} \right) + \right. \\ \frac{1}{\Delta y} \epsilon_{i,j,k}^{-2} \mu_{i,j,k}^{-1} \left(\epsilon_{i,j,k} A_{y\ i,j+\frac{1}{2},k}^{n+\frac{1}{2}} - \epsilon_{i,j-1,k} A_{y\ i,j-\frac{1}{2},k}^{n+\frac{1}{2}} \right) + \\ \left. \frac{1}{\Delta z} \epsilon_{i,j,k}^{-2} \mu_{i,j,k}^{-1} \left(\epsilon_{i,j,k} A_{z\ i,j,k+\frac{1}{2}}^{n+\frac{1}{2}} - \epsilon_{i,j,k-1} A_{z\ i,j,k-\frac{1}{2}}^{n+\frac{1}{2}} \right) \right).\end{aligned} \tag{4.34}$$

Since we know the gradient is the last operation, we can divide $\mathbf{A}_{term2}^{n+\frac{1}{2}}$ into components to evaluate each separately

$$\mathbf{A}_{term2}^{n+\frac{1}{2}} = A_{x\ term2} \hat{x} + A_{y\ term2} \hat{y} + A_{z\ term2} \hat{z}\ . \tag{4.35}$$

The components are

$$\begin{aligned}A_{x\ term2}^{n+\frac{1}{2}} = \epsilon_{i,j,k} \tilde{\partial}_x \left(\frac{1}{\Delta_x} \epsilon_{i,j,k}^{-2} \mu_{i,j,k}^{-1} \left(\epsilon_{i,j,k} A_{x\ i+\frac{1}{2},j,k}^{n+\frac{1}{2}} - \epsilon_{i-1,j,k} A_{x\ i-\frac{1}{2},j,k}^{n+\frac{1}{2}} \right) + \right. \\ \frac{1}{\Delta_y} \epsilon_{i,j,k}^{-2} \mu_{i,j,k}^{-1} \left(\epsilon_{i,j,k} A_{y\ i,j+\frac{1}{2},k}^{n+\frac{1}{2}} - \epsilon_{i,j-1,k} A_{y\ i,j-\frac{1}{2},k}^{n+\frac{1}{2}} \right) + \\ \left. \frac{1}{\Delta_z} \epsilon_{i,j,k}^{-2} \mu_{i,j,k}^{-1} \left(\epsilon_{i,j,k} A_{z\ i,j,k+\frac{1}{2}}^{n+\frac{1}{2}} - \epsilon_{i,j,k-1} A_{z\ i,j,k-\frac{1}{2}}^{n+\frac{1}{2}} \right) \right),\end{aligned} \tag{4.36a}$$

$$A_{y\ term2}^{n+\frac{1}{2}} = \epsilon_{i,j,k}\tilde{\partial}_y \left(\frac{1}{\Delta_x}\epsilon_{i,j,k}^{-2}\mu_{i,j,k}^{-1}\left(\epsilon_{i,j,k}A_{x\ i+\frac{1}{2},j,k}^{n+\frac{1}{2}} - \epsilon_{i-1,j,k}A_{x\ i-\frac{1}{2},j,k}^{n+\frac{1}{2}}\right) + \right.$$
$$\frac{1}{\Delta_y}\epsilon_{i,j,k}^{-2}\mu_{i,j,k}^{-1}\left(\epsilon_{i,j,k}A_{y\ i,j+\frac{1}{2},k}^{n+\frac{1}{2}} - \epsilon_{i,j-1,k}A_{y\ i,j-\frac{1}{2},k}^{n+\frac{1}{2}}\right) +$$
$$\left.\frac{1}{\Delta_z}\epsilon_{i,j,k}^{-2}\mu_{i,j,k}^{-1}\left(\epsilon_{i,j,k}A_{z\ i,j,k+\frac{1}{2}}^{n+\frac{1}{2}} - \epsilon_{i,j,k-1}A_{z\ i,j,k-\frac{1}{2}}^{n+\frac{1}{2}}\right)\right), \quad (4.36b)$$

and

$$A_{z\ term2}^{n+\frac{1}{2}} = \epsilon_{i,j,k}\tilde{\partial}_z \left(\frac{1}{\Delta_x}\epsilon_{i,j,k}^{-2}\mu_{i,j,k}^{-1}\left(\epsilon_{i,j,k}A_{x\ i+\frac{1}{2},j,k}^{n+\frac{1}{2}} - \epsilon_{i-1,j,k}A_{x\ i-\frac{1}{2},j,k}^{n+\frac{1}{2}}\right) + \right.$$
$$\frac{1}{\Delta_y}\epsilon_{i,j,k}^{-2}\mu_{i,j,k}^{-1}\left(\epsilon_{i,j,k}A_{y\ i,j+\frac{1}{2},k}^{n+\frac{1}{2}} - \epsilon_{i,j-1,k}A_{y\ i,j-\frac{1}{2},k}^{n+\frac{1}{2}}\right) +$$
$$\left.\frac{1}{\Delta_z}\epsilon_{i,j,k}^{-2}\mu_{i,j,k}^{-1}\left(\epsilon_{i,j,k}A_{z\ i,j,k+\frac{1}{2}}^{n+\frac{1}{2}} - \epsilon_{i,j,k-1}A_{z\ i,j,k-\frac{1}{2}}^{n+\frac{1}{2}}\right)\right). \quad (4.36c)$$

After evaluating the forward differences, the components become

$$A_{x\ term2}^{n+\frac{1}{2}} = \epsilon_{i,j,k}\left(\left(\frac{1}{\Delta_x}\epsilon_{i+1,j,k}^{-2}\mu_{i+1,j,k}^{-1}\left(\epsilon_{i+1,j,k}A_{x\ i+\frac{3}{2},j,k}^{n+\frac{1}{2}} - \epsilon_{i,j,k}A_{x\ i+\frac{1}{2},j,k}^{n+\frac{1}{2}}\right) + \right.\right.$$
$$\frac{1}{\Delta_y}\epsilon_{i+1,j,k}^{-2}\mu_{i+1,j,k}^{-1}\left(\epsilon_{i+1,j,k}A_{y\ i+1,j+\frac{1}{2},k}^{n+\frac{1}{2}} - \epsilon_{i+1,j-1,k}A_{y\ i+1,j-\frac{1}{2},k}^{n+\frac{1}{2}}\right) +$$
$$\left.\frac{1}{\Delta_z}\epsilon_{i+1,j,k}^{-2}\mu_{i+1,j,k}^{-1}\left(\epsilon_{i+1,j,k}A_{z\ i+1,j,k+\frac{1}{2}}^{n+\frac{1}{2}} - \epsilon_{i+1,j,k-1}A_{z\ i+1,j,k-\frac{1}{2}}^{n+\frac{1}{2}}\right)\right) -$$
$$\left(\frac{1}{\Delta_x}\epsilon_{i,j,k}^{-2}\mu_{i,j,k}^{-1}\left(\epsilon_{i,j,k}A_{x\ i+\frac{1}{2},j,k}^{n+\frac{1}{2}} - \epsilon_{i-1,j,k}A_{x\ i-\frac{1}{2},j,k}^{n+\frac{1}{2}}\right) + \right.$$
$$\frac{1}{\Delta_y}\epsilon_{i,j,k}^{-2}\mu_{i,j,k}^{-1}\left(\epsilon_{i,j,k}A_{y\ i,j+\frac{1}{2},k}^{n+\frac{1}{2}} - \epsilon_{i,j-1,k}A_{y\ i,j-\frac{1}{2},k}^{n+\frac{1}{2}}\right) +$$
$$\left.\left.\left.\frac{1}{\Delta_z}\epsilon_{i,j,k}^{-2}\mu_{i,j,k}^{-1}\left(\epsilon_{i,j,k}A_{z\ i,j,k+\frac{1}{2}}^{n+\frac{1}{2}} - \epsilon_{i,j,k-1}A_{z\ i,j,k-\frac{1}{2}}^{n+\frac{1}{2}}\right)\right)\right)/\Delta_x, \quad (4.37a)$$

$$A_{y\ term2}^{n+\frac{1}{2}} = \epsilon_{i,j,k}\Bigg(\Bigg(\frac{1}{\Delta_x}\epsilon_{i,j+1,k}^{-2}\mu_{i,j+1,k}^{-1}\left(\epsilon_{i,j+1,k}A_{x\ i+\frac{1}{2},j+1,k}^{n+\frac{1}{2}} - \epsilon_{i-1,j+1,k}A_{x\ i-\frac{1}{2},j+1,k}^{n+\frac{1}{2}}\right) + \frac{1}{\Delta_y}\epsilon_{i,j+1,k}^{-2}\mu_{i,j+1,k}^{-1}\left(\epsilon_{i,j+1,k}A_{y\ i,j+\frac{3}{2},k}^{n+\frac{1}{2}} - \epsilon_{i,j,k}A_{y\ i,j+\frac{1}{2},k}^{n+\frac{1}{2}}\right) + \frac{1}{\Delta_z}\epsilon_{i,j+1,k}^{-2}\mu_{i,j+1,k}^{-1}\left(\epsilon_{i,j+1,k}A_{z\ i,j+1,k+\frac{1}{2}}^{n+\frac{1}{2}} - \epsilon_{i,j+1,k-1}A_{z\ i,j+1,k-\frac{1}{2}}^{n+\frac{1}{2}}\right)\Bigg) - \Bigg(\frac{1}{\Delta_x}\epsilon_{i,j,k}^{-2}\mu_{i,j,k}^{-1}\left(\epsilon_{i,j,k}A_{x\ i+\frac{1}{2},j,k}^{n+\frac{1}{2}} - \epsilon_{i-1,j,k}A_{x\ i-\frac{1}{2},j,k}^{n+\frac{1}{2}}\right) + \frac{1}{\Delta_y}\epsilon_{i,j,k}^{-2}\mu_{i,j,k}^{-1}\left(\epsilon_{i,j,k}A_{y\ i,j+\frac{1}{2},k}^{n+\frac{1}{2}} - \epsilon_{i,j-1,k}A_{y\ i,j-\frac{1}{2},k}^{n+\frac{1}{2}}\right) + \frac{1}{\Delta_z}\epsilon_{i,j,k}^{-2}\mu_{i,j,k}^{-1}\left(\epsilon_{i,j,k}A_{z\ i,j,k+\frac{1}{2}}^{n+\frac{1}{2}} - \epsilon_{i,j,k-1}A_{z\ i,j,k-\frac{1}{2}}^{n+\frac{1}{2}}\right)\Bigg)\Bigg)/\Delta_y, \quad (4.37b)$$

and

$$A_{z\ term2}^{n+\frac{1}{2}} = \epsilon_{i,j,k}\Bigg(\Bigg(\frac{1}{\Delta_x}\epsilon_{i,j,k+1}^{-2}\mu_{i,j,k+1}^{-1}\left(\epsilon_{i,j,k+1}A_{x\ i+\frac{1}{2},j,k+1}^{n+\frac{1}{2}} - \epsilon_{i-1,j,k+1}A_{x\ i-\frac{1}{2},j,k+1}^{n+\frac{1}{2}}\right) + \frac{1}{\Delta_y}\epsilon_{i,j,k+1}^{-2}\mu_{i,j,k+1}^{-1}\left(\epsilon_{i,j,k+1}A_{y\ i,j+\frac{1}{2},k+1}^{n+\frac{1}{2}} - \epsilon_{i,j-1,k+1}A_{y\ i,j-\frac{1}{2},k+1}^{n+\frac{1}{2}}\right) + \frac{1}{\Delta_z}\epsilon_{i,j,k+1}^{-2}\mu_{i,j,k+1}^{-1}\left(\epsilon_{i,j,k+1}A_{z\ i,j,k+\frac{3}{2}}^{n+\frac{1}{2}} - \epsilon_{i,j,k}A_{z\ i,j,k+\frac{1}{2}}^{n+\frac{1}{2}}\right)\Bigg) - \Bigg(\frac{1}{\Delta_x}\epsilon_{i,j,k}^{-2}\mu_{i,j,k}^{-1}\left(\epsilon_{i,j,k}A_{x\ i+\frac{1}{2},j,k}^{n+\frac{1}{2}} - \epsilon_{i-1,j,k}A_{x\ i-\frac{1}{2},j,k}^{n+\frac{1}{2}}\right) + \frac{1}{\Delta_y}\epsilon_{i,j,k}^{-2}\mu_{i,j,k}^{-1}\left(\epsilon_{i,j,k}A_{y\ i,j+\frac{1}{2},k}^{n+\frac{1}{2}} - \epsilon_{i,j-1,k}A_{y\ i,j-\frac{1}{2},k}^{n+\frac{1}{2}}\right) + \frac{1}{\Delta_z}\epsilon_{i,j,k}^{-2}\mu_{i,j,k}^{-1}\left(\epsilon_{i,j,k}A_{z\ i,j,k+\frac{1}{2}}^{n+\frac{1}{2}} - \epsilon_{i,j,k-1}A_{z\ i,j,k-\frac{1}{2}}^{n+\frac{1}{2}}\right)\Bigg)\Bigg)/\Delta_z. \quad (4.37c)$$

4.3.3.3 A Update Equation - All Terms

The final **A** update equations by component are as follows:

$$A_{x\ i,j,k}^{n+\frac{3}{2}} = 2A_{x\ i,j,k}^{n+\frac{1}{2}} - A_{x\ i,j,k}^{n-\frac{1}{2}} + \epsilon_{i,j,k}^{-1}\left(A_{x\ term1}^{n+\frac{1}{2}} + A_{x\ term2}^{n+\frac{1}{2}} + J_{x\ i,j,k}^{n+\frac{1}{2}}\right), \quad (4.38a)$$

$$A_{y\ i,j,k}^{n+\frac{3}{2}} = 2A_{y\ i,j,k}^{n+\frac{1}{2}} - A_{y\ i,j,k}^{n-\frac{1}{2}} + \epsilon_{i,j,k}^{-1}\left(A_{y\ term1}^{n+\frac{1}{2}} + A_{y\ term2}^{n+\frac{1}{2}} + J_{y\ i,j,k}^{n+\frac{1}{2}}\right), \quad (4.38b)$$

and

$$A_{z\ i,j,k}^{n+\frac{3}{2}} = 2A_{z\ i,j,k}^{n+\frac{1}{2}} - A_{z\ i,j,k}^{n-\frac{1}{2}} + \epsilon_{i,j,k}^{-1}\left(A_{z\ term1}^{n+\frac{1}{2}} + A_{z\ term2}^{n+\frac{1}{2}} + J_{z\ i,j,k}^{n+\frac{1}{2}}\right) \quad (4.38c)$$

where the components of $\mathbf{A}_{term1}^{n+\frac{1}{2}}$ are

$$
\begin{aligned}
A_{x\ term1}^{n+\frac{1}{2}} = & \\
& \frac{1}{\Delta_y}\left(\left(\mu^{-1}_{i+\frac{1}{2},j-\frac{1}{2},k+\frac{1}{2}}\left(\frac{A^{n+\frac{1}{2}}_{y\ i+1,j-\frac{1}{2},k}-A^{n+\frac{1}{2}}_{y\ i,j-\frac{1}{2},k}}{\Delta_x}-\frac{A^{n+\frac{1}{2}}_{x\ i+\frac{1}{2},j,k}-A^{n+\frac{1}{2}}_{x\ i+\frac{1}{2},j-1,k}}{\Delta_y}\right)\right)- \right. \\
& \left.\left(\mu^{-1}_{i+\frac{1}{2},j+\frac{1}{2},k+\frac{1}{2}}\left(\frac{A^{n+\frac{1}{2}}_{y\ i+1,j+\frac{1}{2},k}-A^{n+\frac{1}{2}}_{y\ i,j+\frac{1}{2},k}}{\Delta_x}-\frac{A^{n+\frac{1}{2}}_{x\ i+\frac{1}{2},j+1,k}-A^{n+\frac{1}{2}}_{x\ i+\frac{1}{2},j,k}}{\Delta_y}\right)\right)\right) \\
& +\frac{1}{\Delta_z}\left(\mu^{-1}_{i+\frac{1}{2},j+\frac{1}{2},k+\frac{1}{2}}\left(\frac{A^{n+\frac{1}{2}}_{x\ i+\frac{1}{2},j,k+1}-A^{n+\frac{1}{2}}_{x\ i+\frac{1}{2}j,k}}{\Delta_z}-\frac{A^{n+\frac{1}{2}}_{z\ i+1,j,k+\frac{1}{2}}-A^{n+\frac{1}{2}}_{z\ i,j,k+\frac{1}{2}}}{\Delta_x}\right)- \right. \\
& \left.\mu^{-1}_{i+\frac{1}{2},j+\frac{1}{2},k-\frac{1}{2}}\left(\frac{A^{n+\frac{1}{2}}_{x\ i+\frac{1}{2},j,k}-A^{n+\frac{1}{2}}_{x\ i+\frac{1}{2}j,k-1}}{\Delta_z}-\frac{A^{n+\frac{1}{2}}_{z\ i+1,j,k-\frac{1}{2}}-A^{n+\frac{1}{2}}_{z\ i,j,k-\frac{1}{2}}}{\Delta_x}\right)\right), \quad \text{(4.39a)}
\end{aligned}
$$

$$
\begin{aligned}
A_{y\ term1}^{n+\frac{1}{2}} = & \\
& \frac{1}{\Delta_z}\left(\mu^{-1}_{i+\frac{1}{2},j+\frac{1}{2},k-\frac{1}{2}}\left(\frac{A^{n+\frac{1}{2}}_{z\ i,j+1,k-\frac{1}{2}}-A^{n+\frac{1}{2}}_{z\ i,j,k-\frac{1}{2}}}{\Delta_y}-\frac{A^{n+\frac{1}{2}}_{y\ i,j+\frac{1}{2},k}-A^{n+\frac{1}{2}}_{y\ i,j+\frac{1}{2},k-1}}{\Delta_z}\right)- \right. \\
& \left.\mu^{-1}_{i+\frac{1}{2},j+\frac{1}{2},k+\frac{1}{2}}\left(\frac{A^{n+\frac{1}{2}}_{z\ i,j+1,k+\frac{1}{2}}-A^{n+\frac{1}{2}}_{z\ i,j,k+\frac{1}{2}}}{\Delta_y}-\frac{A^{n+\frac{1}{2}}_{y\ i,j+\frac{1}{2},k+1}-A^{n+\frac{1}{2}}_{y\ i,j+\frac{1}{2},k}}{\Delta_z}\right)\right) \\
& +\frac{1}{\Delta_x}\left(\mu^{-1}_{i+\frac{1}{2},j+\frac{1}{2},k+\frac{1}{2}}\left(\frac{A^{n+\frac{1}{2}}_{y\ i+1,j+\frac{1}{2},k}-A^{n+\frac{1}{2}}_{y\ i,j+\frac{1}{2},k}}{\Delta_x}-\frac{A^{n+\frac{1}{2}}_{x\ i+\frac{1}{2},j+1,k}-A^{n+\frac{1}{2}}_{x\ i+\frac{1}{2},j,k}}{\Delta_y}\right)- \right. \\
& \left.\mu^{-1}_{i-\frac{1}{2},j+\frac{1}{2},k+\frac{1}{2}}\left(\frac{A^{n+\frac{1}{2}}_{y\ i,j+\frac{1}{2},k}-A^{n+\frac{1}{2}}_{y\ i-1,j+\frac{1}{2},k}}{\Delta_x}-\frac{A^{n+\frac{1}{2}}_{x\ i-\frac{1}{2},j+1,k}-A^{n+\frac{1}{2}}_{x\ i-\frac{1}{2},j,k}}{\Delta_y}\right)\right), \quad \text{(4.39b)}
\end{aligned}
$$

and

$$A^{n+\frac{1}{2}}_{z\ term1} = \frac{1}{\Delta_x}\left(\mu^{-1}_{i-\frac{1}{2},j+\frac{1}{2},k+\frac{1}{2}}\left(\frac{A^{n+\frac{1}{2}}_{x\ i-\frac{1}{2},j,k+1} - A^{n+\frac{1}{2}}_{x\ i-\frac{1}{2}j,k}}{\Delta_z} - \frac{A^{n+\frac{1}{2}}_{z\ i,j,k+\frac{1}{2}} - A^{n+\frac{1}{2}}_{z\ i-1,j,k+\frac{1}{2}}}{\Delta_x}\right) - \mu^{-1}_{i+\frac{1}{2},j+\frac{1}{2},k+\frac{1}{2}}\left(\frac{A^{n+\frac{1}{2}}_{x\ i+\frac{1}{2},j,k+1} - A^{n+\frac{1}{2}}_{x\ i+\frac{1}{2}j,k}}{\Delta_z} - \frac{A^{n+\frac{1}{2}}_{z\ i+1,j,k+\frac{1}{2}} - A^{n+\frac{1}{2}}_{z\ i,j,k+\frac{1}{2}}}{\Delta_x}\right)\right) + \frac{1}{\Delta_y}\left(\mu^{-1}_{i+\frac{1}{2},j+\frac{1}{2},k+\frac{1}{2}}\left(\frac{A^{n+\frac{1}{2}}_{z\ i,j+1,k+\frac{1}{2}} - A^{n+\frac{1}{2}}_{z\ i,j,k+\frac{1}{2}}}{\Delta_y} - \frac{A^{n+\frac{1}{2}}_{y\ i,j+\frac{1}{2},k+1} - A^{n+\frac{1}{2}}_{y\ i,j+\frac{1}{2},k}}{\Delta_z}\right) - \mu^{-1}_{i+\frac{1}{2},j-\frac{1}{2},k+\frac{1}{2}}\left(\frac{A^{n+\frac{1}{2}}_{z\ i,j,k+\frac{1}{2}} - A^{n+\frac{1}{2}}_{z\ i,j,k+\frac{1}{2}}}{\Delta_y} - \frac{A^{n+\frac{1}{2}}_{y\ i,j+\frac{1}{2},k+1} - A^{n+\frac{1}{2}}_{y\ i,j+\frac{1}{2},k}}{\Delta_z}\right)\right), \quad (4.39c)$$

and the components of $\mathbf{A}^{n+\frac{1}{2}}_{term2}$ are

$$A^{n+\frac{1}{2}}_{x\ term2} = \epsilon_{i,j,k}\left(\left(\frac{1}{\Delta_x}\epsilon^{-2}_{i+1,j,k}\mu^{-1}_{i+1,j,k}\left(\epsilon_{i+1,j,k}A^{n+\frac{1}{2}}_{x\ i+\frac{3}{2},j,k} - \epsilon_{i,j,k}A^{n+\frac{1}{2}}_{x\ i+\frac{1}{2},j,k}\right) + \frac{1}{\Delta_y}\epsilon^{-2}_{i+1,j,k}\mu^{-1}_{i+1,j,k}\left(\epsilon_{i+1,j,k}A^{n+\frac{1}{2}}_{y\ i+1,j+\frac{1}{2},k} - \epsilon_{i+1,j-1,k}A^{n+\frac{1}{2}}_{y\ i+1,j-\frac{1}{2},k}\right) + \frac{1}{\Delta_z}\epsilon^{-2}_{i+1,j,k}\mu^{-1}_{i+1,j,k}\left(\epsilon_{i+1,j,k}A^{n+\frac{1}{2}}_{z\ i+1,j,k+\frac{1}{2}} - \epsilon_{i+1,j,k-1}A^{n+\frac{1}{2}}_{z\ i+1,j,k-\frac{1}{2}}\right)\right) - \left(\frac{1}{\Delta_x}\epsilon^{-2}_{i,j,k}\mu^{-1}_{i,j,k}\left(\epsilon_{i,j,k}A^{n+\frac{1}{2}}_{x\ i+\frac{1}{2},j,k} - \epsilon_{i-1,j,k}A^{n+\frac{1}{2}}_{x\ i-\frac{1}{2},j,k}\right) + \frac{1}{\Delta_y}\epsilon^{-2}_{i,j,k}\mu^{-1}_{i,j,k}\left(\epsilon_{i,j,k}A^{n+\frac{1}{2}}_{y\ i,j+\frac{1}{2},k} - \epsilon_{i,j-1,k}A^{n+\frac{1}{2}}_{y\ i,j-\frac{1}{2},k}\right) + \frac{1}{\Delta_z}\epsilon^{-2}_{i,j,k}\mu^{-1}_{i,j,k}\left(\epsilon_{i,j,k}A^{n+\frac{1}{2}}_{z\ i,j,k+\frac{1}{2}} - \epsilon_{i,j,k-1}A^{n+\frac{1}{2}}_{z\ i,j,k-\frac{1}{2}}\right)\right)\right)/\Delta_x, \quad (4.40a)$$

$$A_{y\ term2}^{n+\frac{1}{2}} = \epsilon_{i,j,k}\left(\left(\frac{1}{\Delta_x}\epsilon_{i,j+1,k}^{-2}\mu_{i,j+1,k}^{-1}\left(\epsilon_{i,j+1,k}A_{x\ i+\frac{1}{2},j+1,k}^{n+\frac{1}{2}} - \epsilon_{i-1,j+1,k}A_{x\ i-\frac{1}{2},j+1,k}^{n+\frac{1}{2}}\right) + \frac{1}{\Delta_y}\epsilon_{i,j+1,k}^{-2}\mu_{i,j+1,k}^{-1}\left(\epsilon_{i,j+1,k}A_{y\ i,j+\frac{3}{2},k}^{n+\frac{1}{2}} - \epsilon_{i,j,k}A_{y\ i,j+\frac{1}{2},k}^{n+\frac{1}{2}}\right) + \frac{1}{\Delta_z}\epsilon_{i,j+1,k}^{-2}\mu_{i,j+1,k}^{-1}\left(\epsilon_{i,j+1,k}A_{z\ i,j+1,k+\frac{1}{2}}^{n+\frac{1}{2}} - \epsilon_{i,j+1,k-1}A_{z\ i,j+1,k-\frac{1}{2}}^{n+\frac{1}{2}}\right)\right) - \left(\frac{1}{\Delta_x}\epsilon_{i,j,k}^{-2}\mu_{i,j,k}^{-1}\left(\epsilon_{i,j,k}A_{x\ i+\frac{1}{2},j,k}^{n+\frac{1}{2}} - \epsilon_{i-1,j,k}A_{x\ i-\frac{1}{2},j,k}^{n+\frac{1}{2}}\right) + \frac{1}{\Delta_y}\epsilon_{i,j,k}^{-2}\mu_{i,j,k}^{-1}\left(\epsilon_{i,j,k}A_{y\ i,j+\frac{1}{2},k}^{n+\frac{1}{2}} - \epsilon_{i,j-1,k}A_{y\ i,j-\frac{1}{2},k}^{n+\frac{1}{2}}\right) + \frac{1}{\Delta_z}\epsilon_{i,j,k}^{-2}\mu_{i,j,k}^{-1}\left(\epsilon_{i,j,k}A_{z\ i,j,k+\frac{1}{2}}^{n+\frac{1}{2}} - \epsilon_{i,j,k-1}A_{z\ i,j,k-\frac{1}{2}}^{n+\frac{1}{2}}\right)\right)\right)/\Delta_y, \quad (4.40b)$$

and

$$A_{z\ term2}^{n+\frac{1}{2}} = \epsilon_{i,j,k}\left(\left(\frac{1}{\Delta_x}\epsilon_{i,j,k+1}^{-2}\mu_{i,j,k+1}^{-1}\left(\epsilon_{i,j,k+1}A_{x\ i+\frac{1}{2},j,k+1}^{n+\frac{1}{2}} - \epsilon_{i-1,j,k+1}A_{x\ i-\frac{1}{2},j,k+1}^{n+\frac{1}{2}}\right) + \frac{1}{\Delta_y}\epsilon_{i,j,k+1}^{-2}\mu_{i,j,k+1}^{-1}\left(\epsilon_{i,j,k+1}A_{y\ i,j+\frac{1}{2},k+1}^{n+\frac{1}{2}} - \epsilon_{i,j-1,k+1}A_{y\ i,j-\frac{1}{2},k+1}^{n+\frac{1}{2}}\right) + \frac{1}{\Delta z}\epsilon_{i,j,k+1}^{-2}\mu_{i,j,k+1}^{-1}\left(\epsilon_{i,j,k+1}A_{z\ i,j,k+\frac{3}{2}}^{n+\frac{1}{2}} - \epsilon_{i,j,k}A_{z\ i,j,k+\frac{1}{2}}^{n+\frac{1}{2}}\right)\right) - \left(\frac{1}{\Delta_x}\epsilon_{i,j,k}^{-2}\mu_{i,j,k}^{-1}\left(\epsilon_{i,j,k}A_{x\ i+\frac{1}{2},j,k}^{n+\frac{1}{2}} - \epsilon_{i-1,j,k}A_{x\ i-\frac{1}{2},j,k}^{n+\frac{1}{2}}\right) + \frac{1}{\Delta_y}\epsilon_{i,j,k}^{-2}\mu_{i,j,k}^{-1}\left(\epsilon_{i,j,k}A_{y\ i,j+\frac{1}{2},k}^{n+\frac{1}{2}} - \epsilon_{i,j-1,k}A_{y\ i,j-\frac{1}{2},k}^{n+\frac{1}{2}}\right) + \frac{1}{\Delta_z}\epsilon_{i,j,k}^{-2}\mu_{i,j,k}^{-1}\left(\epsilon_{i,j,k}A_{z\ i,j,k+\frac{1}{2}}^{n+\frac{1}{2}} - \epsilon_{i,j,k-1}A_{z\ i,j,k-\frac{1}{2}}^{n+\frac{1}{2}}\right)\right)\right)/\Delta_z. \quad (4.40c)$$

4.4 Discretization of Vector Potential Formulation of Maxwell for Graded Mesh

To implement a graded mesh for this system, the distance between points needs to be indexed. Here, I show how to write the second-order equations for a graded mesh. This is nontrivial due to the index now corresponding to location of difference.

By defining the index for the graded mesh at position i to be the difference of the positions a half-step in either direction,

$$\Delta x_i = x_{i+\frac{1}{2}} - x_{i-\frac{1}{2}} \quad (4.41)$$

we can discretize Equations (4.10)-(4.12) for a graded mesh.

There are multiple ways of looking at the problem of an inhomogeneous mesh. One important consideration is computational resources; increasing the number operations required can increase computational cost for each time-step. Conversely, an incorrectly graded mesh can lead to inaccuracy and instability in the FDTD algorithm. Cost and accuracy factors must be considered when implementing a graded mesh.

4.4.1 Expansion of ρ Update Equation for Graded Mesh

First, we again take the discrete divergence of Equation (4.10) to obtain

$$\rho^n_{i,j,k} = \rho^{n-1}_{i,j,k} - \Delta_t \left(\hat{\partial}_x J^n_{x\ i+\frac{1}{2},j,k} + \hat{\partial}_y J^n_{y\ i,j+\frac{1}{2},k} + \hat{\partial}_z J^n_{z\ i,j,k+\frac{1}{2}} \right). \tag{4.42}$$

Now, by altering the vector calculus definitions to have the spatial offset vary by position, we can take the backward difference for the result for a graded mesh

$$\rho^n_{i,j,k} = \rho^{n-1}_{i,j,k} - \Delta_t \left(\frac{J^n_{x\ i+\frac{1}{2},j,k} - J^n_{x\ i-\frac{1}{2},j,k}}{\Delta x_i} + \frac{J^n_{y\ i,j+\frac{1}{2},k} - J^n_{y\ i,j-\frac{1}{2},k}}{\Delta y_j} + \frac{J^n_{z\ i,j,k+\frac{1}{2}} - J^n_{z\ i,j,k-\frac{1}{2}}}{\Delta z_k} \right). \tag{4.43}$$

4.4.2 Expansion of ϕ Update Equation for Graded Mesh

Starting with Equation (4.11), we evaluate the forward gradient to get

$$\phi^{n+1}_{i,j,k} = 2\phi^n_{i,j,k} - \phi^{n-1}_{i,j,k} + \Delta_t^2 \epsilon^{-2}_{i,j,k} \mu^{-1}_{i,j,k} \left(\hat{\nabla} \cdot \epsilon_{i,j,k} \left(\hat{x}\tilde{\partial}_x \phi^n_{i,j,k} + \hat{y}\tilde{\partial}_y \phi^n_{i,j,k} + \hat{z}\tilde{\partial}_z \phi^n_{i,j,k} \right) + \rho^n_{i,j,k} \right). \tag{4.44}$$

The forward differences can be evaluated on the graded mesh as

$$\phi^{n+1}_{i,j,k} = 2\phi^n_{i,j,k} - \phi^{n-1}_{i,j,k} + \Delta_t^2 \epsilon^{-2}_{i,j,k} \mu^{-1}_{i,j,k} \left(\hat{\nabla} \cdot \epsilon_{i,j,k} \left(\hat{x} \frac{\phi^n_{i+1,j,k} - \phi^n_{i,j,k}}{\Delta x_{i+\frac{1}{2}}} + \hat{y} \frac{\phi^n_{i,j+1,k} - \phi^n_{i,j,k}}{\Delta y_{j+\frac{1}{2}}} + \hat{z} \frac{\phi^n_{i,j,k+1} - \phi^n_{i,j,k}}{\Delta z_{k+\frac{1}{2}}} \right) + \rho^n_{i,j,k} \right). \tag{4.45}$$

Expanding the backward divergence into backward differences gives

$$\phi^{n+1}_{i,j,k} = 2\phi^{n}_{i,j,k} - \phi^{n-1}_{i,j,k} + \Delta_t^2 \epsilon^{-2}_{i,j,k}\mu^{-1}_{i,j,k} \left(\hat{\partial}_x \left(\epsilon_{i,j,k} \frac{\phi^n_{i+1,j,k} - \phi^n_{i,j,k}}{\Delta x_{i+\frac{1}{2}}} \right) + \hat{\partial}_y \left(\epsilon_{i,j,k} \frac{\phi^n_{i,j+1,k} - \phi^n_{i,j,k}}{\Delta y_{j+\frac{1}{2}}} \right) + \hat{\partial}_z \left(\epsilon_{i,j,k} \frac{\phi^n_{i,j,k+1} - \phi^n_{i,j,k}}{\Delta z_{k+\frac{1}{2}}} \right) + \rho^n_{i,j,k} \right). \quad (4.46)$$

From here, there are two different ways to evaulate the backward difference. Either the finite differences can be evaluated with the original fields in the equation or, in order to simplify, assume each term already evaluated with a finite difference is located at its average point. By taking the finite difference of each value, the expression we obtain for ϕ update with a graded index is

$$\begin{aligned}\phi^{n+1}_{i,j,k} = 2\phi^{n}_{i,j,k} - \phi^{n-1}_{i,j,k} + \Delta_t^2 \epsilon^{-2}_{i,j,k}\mu^{-1}_{i,j,k} \\ \left(\frac{1}{\Delta x_{i+\frac{1}{2}}} \left(\left(\epsilon_{i,j,k} \frac{\phi^n_{i+1,j,k} - \phi^n_{i,j,k}}{\Delta x_{i+\frac{1}{2}}} \right) - \left(\epsilon_{i-1,j,k} \frac{\phi^n_{i,j,k} - \phi^n_{i-1,j,k}}{\Delta x_{i-\frac{1}{2}}} \right) \right) + \right. \\ \frac{1}{\Delta y_{j+\frac{1}{2}}} \left(\left(\epsilon_{i,j,k} \frac{\phi^n_{i,j+1,k} - \phi^n_{i,j,k}}{\Delta y_{j+\frac{1}{2}}} \right) - \left(\epsilon_{i,j-1,k} \frac{\phi^n_{i,j,k} - \phi^n_{i,j-1,k}}{\Delta y_{j-\frac{1}{2}}} \right) \right) + \\ \left. \frac{1}{\Delta z_{k+\frac{1}{2}}} \left(\left(\epsilon_{i,j,k} \frac{\phi^n_{i,j,k+1} - \phi^n_{i,j,k}}{\Delta z_{k+\frac{1}{2}}} \right) - \left(\epsilon_{i,j,k-1} \frac{\phi^n_{i,j,k} - \phi^n_{i,j,k-1}}{\Delta z_{k-\frac{1}{2}}} \right) \right) + \rho^n_{i,j,k} \right). \quad (4.47)\end{aligned}$$

The more computationally inexpensive version for a ϕ update with simpliying assumptions about the graded mesh would be

$$\begin{aligned}\phi^{n+1}_{i,j,k} = 2\phi^{n}_{i,j,k} - \phi^{n-1}_{i,j,k} + \Delta_t^2 \epsilon^{-2}_{i,j,k}\mu^{-1}_{i,j,k} \\ \left(\frac{1}{\Delta x^2_{i+\frac{1}{2}}} \left(\left(\epsilon_{i,j,k} \left(\phi^n_{i+1,j,k} - \phi^n_{i,j,k} \right) \right) - \left(\epsilon_{i-1,j,k} \left(\phi^n_{i,j,k} - \phi^n_{i-1,j,k} \right) \right) \right) + \right. \\ \frac{1}{\Delta y^2_{j+\frac{1}{2}}} \left(\left(\epsilon_{i,j,k} \left(\phi^n_{i,j+1,k} - \phi^n_{i,j,k} \right) \right) - \left(\epsilon_{i,j-1,k} \left(\phi^n_{i,j,k} - \phi^n_{i,j-1,k} \right) \right) \right) + \\ \left. \frac{1}{\Delta z^2_{k+\frac{1}{2}}} \left(\left(\epsilon_{i,j,k} \left(\phi^n_{i,j,k+1} - \phi^n_{i,j,k} \right) \right) - \left(\epsilon_{i,j,k-1} \left(\phi^n_{i,j,k} - \phi^n_{i,j,k-1} \right) \right) \right) + \rho^n_{i,j,k} \right). \quad (4.48)\end{aligned}$$

Equation (4.48) requires fewer operations than Equation (4.47) to compute values on a graded mesh; however, Equation (4.47) does not make simplifying assumptions about the distance between values, thus is more accurate. Since ϕ only has a single update equation, we implemented Equation (4.47) for increased accuracy and stability.

4.4.3 Expansion of A Update Equation for Graded Mesh

Assume again

$$\tilde{\mathbf{A}}_{i,j,k}^{n+\frac{3}{2}} = 2\tilde{\mathbf{A}}_{i,j,k}^{n+\frac{1}{2}} - \tilde{\mathbf{A}}_{i,j,k}^{n-\frac{1}{2}} + \Delta_t^2 \epsilon_{i,j,k}^{-1} \left(\mathbf{A}_{term1}^{n+\frac{1}{2}} + \mathbf{A}_{term2}^{n+\frac{1}{2}} + \tilde{\mathbf{J}}_{i,j,k}^{n+\frac{1}{2}} \right) \tag{4.49}$$

where

$$\mathbf{A}_{term1}^{n+\frac{1}{2}} = -\hat{\nabla} \times \mu_{i+\frac{1}{2},j+\frac{1}{2},k+\frac{1}{2}}^{-1} \left(\tilde{\nabla} \times \tilde{\mathbf{A}}_{i,j,k}^{n+\frac{1}{2}} \right) \tag{4.50}$$

and

$$\mathbf{A}_{term2}^{n+\frac{1}{2}} = \epsilon_{i,j,k} \tilde{\nabla} \epsilon_{i,j,k}^{-2} \mu_{i,j,k}^{-1} \hat{\nabla} \cdot \epsilon_{i,j,k} \tilde{\mathbf{A}}_{i,j,k}^{n+\frac{1}{2}}. \tag{4.51}$$

4.4.3.1 Expansion of $\mathbf{A}_{term1}$ for Graded Mesh

Starting with Equation (4.50), evaluate the discrete curl

$$\begin{aligned} \tilde{\nabla} \times \tilde{\mathbf{A}}_{i,j,k}^{n} = \hat{x} \left(\tilde{\partial}_y A_{z\ i,j,k+\frac{1}{2}}^{n} - \tilde{\partial}_z A_{y\ i,j+\frac{1}{2},k}^{n} \right) + \\ \hat{y} \left(\tilde{\partial}_z A_{x\ i+\frac{1}{2},j,k}^{n} - \tilde{\partial}_x A_{z\ i,j,k+\frac{1}{2}}^{n} \right) + \\ \hat{z} \left(\tilde{\partial}_x A_{y\ i,j+\frac{1}{2},k}^{n} - \tilde{\partial}_y A_{x\ i+\frac{1}{2},j,k}^{n} \right) \end{aligned} \tag{4.52}$$

and the forward differences

$$\begin{aligned} \tilde{\nabla} \times \tilde{\mathbf{A}}_{i,j,k}^{n} = \hat{x} \left(\frac{A_{z\ i,j+1,k+\frac{1}{2}}^{n} - A_{z\ i,j,k+\frac{1}{2}}^{n}}{\Delta y_{j+\frac{1}{2}}} - \frac{A_{y\ i,j+\frac{1}{2},k+1}^{n} - A_{y\ i,j+\frac{1}{2},k}^{n}}{\Delta z_{k+\frac{1}{2}}} \right) + \\ \hat{y} \left(\frac{A_{x\ i+\frac{1}{2},j,k+1}^{n} - A_{x\ i+\frac{1}{2}j,k}^{n}}{\Delta z_{k+\frac{1}{2}}} - \frac{A_{z\ i+1,j,k+\frac{1}{2}}^{n} - A_{z\ i,j,k+\frac{1}{2}}^{n}}{\Delta x_{i+\frac{1}{2}}} \right) + \\ \hat{z} \left(\frac{A_{y\ i+1,j+\frac{1}{2},k}^{n} - A_{y\ i,j+\frac{1}{2},k}^{n}}{\Delta x_{i+\frac{1}{2}}} - \frac{A_{x\ i+\frac{1}{2},j+1,k}^{n} - A_{x\ i+\frac{1}{2},j,k}^{n}}{\Delta y_{j+\frac{1}{2}}} \right). \end{aligned} \tag{4.53}$$

Putting this term back into the entire term

$$\mathbf{A}_{term1}^{n+\frac{1}{2}} = -\hat{\nabla} \times \mu^{-1}_{i+\frac{1}{2},j+\frac{1}{2},k+\frac{1}{2}} \left(\hat{x} \left(\frac{A^n_{z\ i,j+1,k+\frac{1}{2}} - A^n_{z\ i,j,k+\frac{1}{2}}}{\Delta y_{j+\frac{1}{2}}} - \frac{A^n_{y\ i,j+\frac{1}{2},k+1} - A^n_{y\ i,j+\frac{1}{2},k}}{\Delta z_{k+\frac{1}{2}}} \right) + \hat{y} \left(\frac{A^n_{x\ i+\frac{1}{2},j,k+1} - A^n_{x\ i+\frac{1}{2}j,k}}{\Delta z_{k+\frac{1}{2}}} - \frac{A^n_{z\ i+1,j,k+\frac{1}{2}} - A^n_{z\ i,j,k+\frac{1}{2}}}{\Delta x_{i+\frac{1}{2}}} \right) + \hat{z} \left(\frac{A^n_{y\ i+1,j+\frac{1}{2},k} - A^n_{y\ i,j+\frac{1}{2},k}}{\Delta x_{i+\frac{1}{2}}} - \frac{A^n_{x\ i+\frac{1}{2},j+1,k} - A^n_{x\ i+\frac{1}{2},j,k}}{\Delta y_{j+\frac{1}{2}}} \right) \right) \tag{4.54}$$

Simplify the term by separating into components,

$$-\hat{\nabla} \times \mathbf{A} = -\hat{x} \left(\hat{\partial}_y a_z - \hat{\partial}_z a_y \right) - \hat{y} \left(\hat{\partial}_z a_x - \hat{\partial}_x a_z \right) - \hat{z} \left(\hat{\partial}_x a_y - \hat{\partial}_y a_x \right), \tag{4.55}$$

where

$$A_{x\ term1} = -\left(\hat{\partial}_y a_z - \hat{\partial}_z a_y \right), \tag{4.56a}$$

$$A_{y\ term1} = -\left(\hat{\partial}_z a_x - \hat{\partial}_x a_z \right), \tag{4.56b}$$

$$A_{z\ term1} = -\left(\hat{\partial}_x a_y - \hat{\partial}_y a_x \right), \tag{4.56c}$$

and

$$a_x = \left(\mu^{-1}_{i+\frac{1}{2},j+\frac{1}{2},k+\frac{1}{2}} \left(\frac{A^n_{z\ i,j+1,k+\frac{1}{2}} - A^n_{z\ i,j,k+\frac{1}{2}}}{\Delta y_{j+\frac{1}{2}}} - \frac{A^n_{y\ i,j+\frac{1}{2},k+1} - A^n_{y\ i,j+\frac{1}{2},k}}{\Delta z_{k+\frac{1}{2}}} \right) \right), \tag{4.57a}$$

$$a_y = \left(\mu^{-1}_{i+\frac{1}{2},j+\frac{1}{2},k+\frac{1}{2}} \left(\frac{A^n_{x\ i+\frac{1}{2},j,k+1} - A^n_{x\ i+\frac{1}{2}j,k}}{\Delta z_{k+\frac{1}{2}}} - \frac{A^n_{z\ i+1,j,k+\frac{1}{2}} - A^n_{z\ i,j,k+\frac{1}{2}}}{\Delta x_{i+\frac{1}{2}}} \right) \right), \tag{4.57b}$$

$$a_z = \left(\mu^{-1}_{i+\frac{1}{2},j+\frac{1}{2},k+\frac{1}{2}} \left(\frac{A^n_{y\ i+1,j+\frac{1}{2},k} - A^n_{y\ i,j+\frac{1}{2},k}}{\Delta x_{i+\frac{1}{2}}} - \frac{A^n_{x\ i+\frac{1}{2},j+1,k} - A^n_{x\ i+\frac{1}{2},j,k}}{\Delta y_{j+\frac{1}{2}}} \right) \right). \tag{4.57c}$$

Here are A_{term1} components

$$A_{x\ term1} = -\hat{\partial}_y \left(\mu^{-1}_{i+\frac{1}{2},j+\frac{1}{2},k+\frac{1}{2}} \left(\frac{A^n_{y\ i+1,j+\frac{1}{2},k} - A^n_{y\ i,j+\frac{1}{2},k}}{\Delta x_{i+\frac{1}{2}}} - \frac{A^n_{x\ i+\frac{1}{2},j+1,k} - A^n_{x\ i+\frac{1}{2},j,k}}{\Delta y_{j+\frac{1}{2}}} \right) \right) + \hat{\partial}_z \left(\mu^{-1}_{i+\frac{1}{2},j+\frac{1}{2},k+\frac{1}{2}} \left(\frac{A^n_{x\ i+\frac{1}{2},j,k+1} - A^n_{x\ i+\frac{1}{2}j,k}}{\Delta z_{k+\frac{1}{2}}} - \frac{A^n_{z\ i+1,j,k+\frac{1}{2}} - A^n_{z\ i,j,k+\frac{1}{2}}}{\Delta x_{i+\frac{1}{2}}} \right) \right), \tag{4.58a}$$

$$
\begin{aligned}
A_{y\ term1} = & \\
& -\hat{\partial}_z \left(\mu^{-1}_{i+\frac{1}{2},j+\frac{1}{2},k+\frac{1}{2}} \left(\frac{A^n_{z\ i,j+1,k+\frac{1}{2}} - A^n_{z\ i,j,k+\frac{1}{2}}}{\Delta y_{j+\frac{1}{2}}} - \frac{A^n_{y\ i,j+\frac{1}{2},k+1} - A^n_{y\ i,j+\frac{1}{2},k}}{\Delta z_{k+\frac{1}{2}}} \right) \right) + \\
& \hat{\partial}_x \left(\mu^{-1}_{i+\frac{1}{2},j+\frac{1}{2},k+\frac{1}{2}} \left(\frac{A^n_{y\ i+1,j+\frac{1}{2},k} - A^n_{y\ i,j+\frac{1}{2},k}}{\Delta x_{i+\frac{1}{2}}} - \frac{A^n_{x\ i+\frac{1}{2},j+1,k} - A^n_{x\ i+\frac{1}{2},j,k}}{\Delta y_{j+\frac{1}{2}}} \right) \right), \quad (4.58b)
\end{aligned}
$$

and

$$
\begin{aligned}
A_{z\ term1} = & \\
& -\hat{\partial}_x \left(\mu^{-1}_{i+\frac{1}{2},j+\frac{1}{2},k+\frac{1}{2}} \left(\frac{A^n_{x\ i+\frac{1}{2},j,k+1} - A^n_{x\ i+\frac{1}{2}j,k}}{\Delta z_{k+\frac{1}{2}}} - \frac{A^n_{z\ i+1,j,k+\frac{1}{2}} - A^n_{z\ i,j,k+\frac{1}{2}}}{\Delta x_{i+\frac{1}{2}}} \right) \right) + \\
& \hat{\partial}_y \left(\mu^{-1}_{i+\frac{1}{2},j+\frac{1}{2},k+\frac{1}{2}} \left(\frac{A^n_{z\ i,j+1,k+\frac{1}{2}} - A^n_{z\ i,j,k+\frac{1}{2}}}{\Delta y_{j+\frac{1}{2}}} - \frac{A^n_{y\ i,j+\frac{1}{2},k+1} - A^n_{y\ i,j+\frac{1}{2},k}}{\Delta z_{k+\frac{1}{2}}} \right) \right). \quad (4.58c)
\end{aligned}
$$

Since each equation contains 8 terms, taking the backward difference of each term will result in a total of 16 terms per component. The most detailed grated grid evaluation of finite difference would require 3 different grid differences while the most simple would require 1. Due to the number of operations already present of each component, we evaluate the grated grid as the most simple version. Here are A_{term1} components in the most simple evaluation of the backward difference

$$
\begin{aligned}
A_{x\ term1} = & \\
& -\frac{1}{\Delta y_j} \left(\left(\mu^{-1}_{i+\frac{1}{2},j+\frac{1}{2},k+\frac{1}{2}} \left(\frac{A^n_{y\ i+1,j+\frac{1}{2},k} - A^n_{y\ i,j+\frac{1}{2},k}}{\Delta x_{i+\frac{1}{2}}} - \frac{A^n_{x\ i+\frac{1}{2},j+1,k} - A^n_{x\ i+\frac{1}{2},j,k}}{\Delta y_{j+\frac{1}{2}}} \right) \right) - \right. \\
& \left. \left(\mu^{-1}_{i+\frac{1}{2},j-\frac{1}{2},k+\frac{1}{2}} \left(\frac{A^n_{y\ i+1,j-\frac{1}{2},k} - A^n_{y\ i,j-\frac{1}{2},k}}{\Delta x_{i+\frac{1}{2}}} - \frac{A^n_{x\ i+\frac{1}{2},j,k} - A^n_{x\ i+\frac{1}{2},j-1,k}}{\Delta y_{j+\frac{1}{2}}} \right) \right) \right) \\
& + \frac{1}{\Delta z_k} \left(\mu^{-1}_{i+\frac{1}{2},j+\frac{1}{2},k+\frac{1}{2}} \left(\frac{A^n_{x\ i+\frac{1}{2},j,k+1} - A^n_{x\ i+\frac{1}{2}j,k}}{\Delta z_{k+\frac{1}{2}}} - \frac{A^n_{z\ i+1,j,k+\frac{1}{2}} - A^n_{z\ i,j,k+\frac{1}{2}}}{\Delta x_{i+\frac{1}{2}}} \right) - \right. \\
& \left. \mu^{-1}_{i+\frac{1}{2},j+\frac{1}{2},k-\frac{1}{2}} \left(\frac{A^n_{x\ i+\frac{1}{2},j,k} - A^n_{x\ i+\frac{1}{2}j,k-1}}{\Delta z_{k+\frac{1}{2}}} - \frac{A^n_{z\ i+1,j,k-\frac{1}{2}} - A^n_{z\ i,j,k-\frac{1}{2}}}{\Delta x_{i+\frac{1}{2}}} \right) \right), \quad (4.59a)
\end{aligned}
$$

$$
\begin{aligned}
A_{y\ term1} = & \\
& -\frac{1}{\Delta z_k}\left(\mu^{-1}_{i+\frac{1}{2},j+\frac{1}{2},k+\frac{1}{2}}\left(\frac{A^n_{z\ i,j+1,k+\frac{1}{2}}-A^n_{z\ i,j,k+\frac{1}{2}}}{\Delta y}-\frac{A^n_{y\ i,j+\frac{1}{2},k+1}-A^n_{y\ i,j+\frac{1}{2},k}}{\Delta z}\right)-\right. \\
& \left.\mu^{-1}_{i+\frac{1}{2},j+\frac{1}{2},k-\frac{1}{2}}\left(\frac{A^n_{z\ i,j+1,k-\frac{1}{2}}-A^n_{z\ i,j,k-\frac{1}{2}}}{\Delta y}-\frac{A^n_{y\ i,j+\frac{1}{2},k}-A^n_{y\ i,j+\frac{1}{2},k-1}}{\Delta z}\right)\right) \\
& +\frac{1}{\Delta x_i}\left(\mu^{-1}_{i+\frac{1}{2},j+\frac{1}{2},k+\frac{1}{2}}\left(\frac{A^n_{y\ i+1,j+\frac{1}{2},k}-A^n_{y\ i,j+\frac{1}{2},k}}{\Delta x}-\frac{A^n_{x\ i+\frac{1}{2},j+1,k}-A^n_{x\ i+\frac{1}{2},j,k}}{\Delta y}\right)-\right. \\
& \left.\mu^{-1}_{i-\frac{1}{2},j+\frac{1}{2},k+\frac{1}{2}}\left(\frac{A^n_{y\ i,j+\frac{1}{2},k}-A^n_{y\ i-1,j+\frac{1}{2},k}}{\Delta x}-\frac{A^n_{x\ i-\frac{1}{2},j+1,k}-A^n_{x\ i-\frac{1}{2},j,k}}{\Delta y}\right)\right), \qquad (4.59b)
\end{aligned}
$$

$$
\begin{aligned}
A_{z\ term1} = & \\
& -\frac{1}{\Delta x_i}\left(\mu^{-1}_{i+\frac{1}{2},j+\frac{1}{2},k+\frac{1}{2}}\left(\frac{A^n_{x\ i+\frac{1}{2},j,k+1}-A^n_{x\ i+\frac{1}{2}j,k}}{\Delta z_{k+\frac{1}{2}}}-\frac{A^n_{z\ i+1,j,k+\frac{1}{2}}-A^n_{z\ i,j,k+\frac{1}{2}}}{\Delta x_{i+\frac{1}{2}}}\right)-\right. \\
& \left.\mu^{-1}_{i-\frac{1}{2},j+\frac{1}{2},k+\frac{1}{2}}\left(\frac{A^n_{x\ i-\frac{1}{2},j,k+1}-A^n_{x\ i-\frac{1}{2}j,k}}{\Delta z_{k+\frac{1}{2}}}-\frac{A^n_{z\ i,j,k+\frac{1}{2}}-A^n_{z\ i-1,j,k+\frac{1}{2}}}{\Delta x_{i+\frac{1}{2}}}\right)\right) \\
& +\frac{1}{\Delta y_j}\left(\mu^{-1}_{i+\frac{1}{2},j+\frac{1}{2},k+\frac{1}{2}}\left(\frac{A^n_{z\ i,j+1,k+\frac{1}{2}}-A^n_{z\ i,j,k+\frac{1}{2}}}{\Delta y_{j+\frac{1}{2}}}-\frac{A^n_{y\ i,j+\frac{1}{2},k+1}-A^n_{y\ i,j+\frac{1}{2},k}}{\Delta z_{k+\frac{1}{2}}}\right)-\right. \\
& \left.\mu^{-1}_{i+\frac{1}{2},j-\frac{1}{2},k+\frac{1}{2}}\left(\frac{A^n_{z\ i,j,k+\frac{1}{2}}-A^n_{z\ i,j,k+\frac{1}{2}}}{\Delta y_{j+\frac{1}{2}}}-\frac{A^n_{y\ i,j+\frac{1}{2},k+1}-A^n_{y\ i,j+\frac{1}{2},k}}{\Delta z_{k+\frac{1}{2}}}\right)\right). \qquad (4.59c)
\end{aligned}
$$

Notice these update equations still contain a large number of operations. These equations need to be updated every timestep, so keeping the number of operations is small is important.

4.4.3.2 Expansion of $\mathbf{A}_{term2}$ for Graded Mesh

Starting from Equation (4.51), evaluate divergence term

$$
\hat{\nabla}\cdot\epsilon_{i,j,k}\tilde{\mathbf{A}}^n_{i,j,k}=\hat{\partial}_x\epsilon_{i,j,k}A^x_{i+\frac{1}{2},j,k}+\hat{\partial}_y\epsilon_{i,j,k}A^y_{i,j+\frac{1}{2},k}+\hat{\partial}_z\epsilon_{i,j,k}A^z_{i,j,k+\frac{1}{2}} \qquad (4.60)
$$

and evaluate backward difference

$$\hat{\nabla}\cdot\epsilon_{i,j,k}\tilde{\mathbf{A}}^n_{i,j,k} = \frac{1}{\Delta x_i}\left(\epsilon_{i,j,k}A^n_{x\ i+\frac{1}{2},j,k} - \epsilon_{i-1,j,k}A^n_{x\ i-\frac{1}{2},j,k}\right) + \frac{1}{\Delta y_j}\left(\epsilon_{i,j,k}A^n_{y\ i,j+\frac{1}{2},k} - \epsilon_{i,j-1,k}A^n_{y\ i,j-\frac{1}{2},k}\right) + \frac{1}{\Delta z_k}\left(\epsilon_{i,j,k}A^n_{z\ i,j,k+\frac{1}{2}} - \epsilon_{i,j,k-1}A^n_{z\ i,j,k-\frac{1}{2}}\right). \quad (4.61)$$

The entire term can be written as

$$\tilde{\nabla}\epsilon^{-2}_{i,j,k}\mu^{-1}_{i,j,k}\hat{\nabla}\cdot\epsilon_{i,j,k}\tilde{\mathbf{A}}^n_{i,j,k} = \tilde{\nabla}\left(\frac{1}{\Delta x_i}\epsilon^{-2}_{i,j,k}\mu^{-1}_{i,j,k}\left(\epsilon_{i,j,k}A^n_{x\ i+\frac{1}{2},j,k} - \epsilon_{i-1,j,k}A^n_{x\ i-\frac{1}{2},j,k}\right) + \frac{1}{\Delta y_j}\epsilon^{-2}_{i,j,k}\mu^{-1}_{i,j,k}\left(\epsilon_{i,j,k}A^n_{y\ i,j+\frac{1}{2},k} - \epsilon_{i,j-1,k}A^n_{y\ i,j-\frac{1}{2},k}\right) + \frac{1}{\Delta z_k}\epsilon^{-2}_{i,j,k}\mu^{-1}_{i,j,k}\left(\epsilon_{i,j,k}A^n_{z\ i,j,k+\frac{1}{2}} - \epsilon_{i,j,k-1}A^n_{z\ i,j,k-\frac{1}{2}}\right)\right). \quad (4.62)$$

Divide into components

$$A_{x\ term2} = \epsilon_{i,j,k}\tilde{\partial}_x\left(\frac{1}{\Delta x_i}\epsilon^{-2}_{i,j,k}\mu^{-1}_{i,j,k}\left(\epsilon_{i,j,k}A^n_{x\ i+\frac{1}{2},j,k} - \epsilon_{i-1,j,k}A^n_{x\ i-\frac{1}{2},j,k}\right) + \frac{1}{\Delta y_j}\epsilon^{-2}_{i,j,k}\mu^{-1}_{i,j,k}\left(\epsilon_{i,j,k}A^n_{y\ i,j+\frac{1}{2},k} - \epsilon_{i,j-1,k}A^n_{y\ i,j-\frac{1}{2},k}\right) + \frac{1}{\Delta z_k}\epsilon^{-2}_{i,j,k}\mu^{-1}_{i,j,k}\left(\epsilon_{i,j,k}A^n_{z\ i,j,k+\frac{1}{2}} - \epsilon_{i,j,k-1}A^n_{z\ i,j,k-\frac{1}{2}}\right)\right), \quad (4.63a)$$

$$A_{y\ term2} = \epsilon_{i,j,k}\tilde{\partial}_y\left(\frac{1}{\Delta x_i}\epsilon^{-2}_{i,j,k}\mu^{-1}_{i,j,k}\left(\epsilon_{i,j,k}A^n_{x\ i+\frac{1}{2},j,k} - \epsilon_{i-1,j,k}A^n_{x\ i-\frac{1}{2},j,k}\right) + \frac{1}{\Delta y_j}\epsilon^{-2}_{i,j,k}\mu^{-1}_{i,j,k}\left(\epsilon_{i,j,k}A^n_{y\ i,j+\frac{1}{2},k} - \epsilon_{i,j-1,k}A^n_{y\ i,j-\frac{1}{2},k}\right) + \frac{1}{\Delta z_k}\epsilon^{-2}_{i,j,k}\mu^{-1}_{i,j,k}\left(\epsilon_{i,j,k}A^n_{z\ i,j,k+\frac{1}{2}} - \epsilon_{i,j,k-1}A^n_{z\ i,j,k-\frac{1}{2}}\right)\right), \quad (4.63b)$$

$$A_{z\ term2} = \epsilon_{i,j,k}\tilde{\partial}_z\left(\frac{1}{\Delta x_i}\epsilon^{-2}_{i,j,k}\mu^{-1}_{i,j,k}\left(\epsilon_{i,j,k}A^n_{x\ i+\frac{1}{2},j,k} - \epsilon_{i-1,j,k}A^n_{x\ i-\frac{1}{2},j,k}\right) + \frac{1}{\Delta y_j}\epsilon^{-2}_{i,j,k}\mu^{-1}_{i,j,k}\left(\epsilon_{i,j,k}A^n_{y\ i,j+\frac{1}{2},k} - \epsilon_{i,j-1,k}A^n_{y\ i,j-\frac{1}{2},k}\right) + \frac{1}{\Delta z_k}\epsilon^{-2}_{i,j,k}\mu^{-1}_{i,j,k}\left(\epsilon_{i,j,k}A^n_{z\ i,j,k+\frac{1}{2}} - \epsilon_{i,j,k-1}A^n_{z\ i,j,k-\frac{1}{2}}\right)\right). \quad (4.63c)$$

Make the same assumption to simplify the graded mesh that was made for $\mathbf{A}_{term1}$ and evaluate the forward difference

$$
\begin{aligned}
A_{x\ term2} = \epsilon_{i,j,k} \Bigg(\Bigg(& \frac{1}{\Delta x_i} \epsilon^{-2}_{i+1,j,k} \mu^{-1}_{i+1,j,k} \left(\epsilon_{i+1,j,k} A^n_{x\ i+\frac{3}{2},j,k} - \epsilon_{i,j,k} A^n_{x\ i+\frac{1}{2},j,k} \right) + \\
& \frac{1}{\Delta y_j} \epsilon^{-2}_{i+1,j,k} \mu^{-1}_{i+1,j,k} \left(\epsilon_{i+1,j,k} A^n_{y\ i+1,j+\frac{1}{2},k} - \epsilon_{i+1,j-1,k} A^n_{y\ i+1,j-\frac{1}{2},k} \right) + \\
& \frac{1}{\Delta z_k} \epsilon^{-2}_{i+1,j,k} \mu^{-1}_{i+1,j,k} \left(\epsilon_{i+1,j,k} A^n_{z\ i+1,j,k+\frac{1}{2}} - \epsilon_{i+1,j,k-1} A^n_{z\ i+1,j,k-\frac{1}{2}} \right) \Bigg) - \\
& \Bigg(\frac{1}{\Delta x_i} \epsilon^{-2}_{i,j,k} \mu^{-1}_{i,j,k} \left(\epsilon_{i,j,k} A^n_{x\ i+\frac{1}{2},j,k} - \epsilon_{i-1,j,k} A^n_{x\ i-\frac{1}{2},j,k} \right) + \\
& \frac{1}{\Delta y_j} \epsilon^{-2}_{i,j,k} \mu^{-1}_{i,j,k} \left(\epsilon_{i,j,k} A^n_{y\ i,j+\frac{1}{2},k} - \epsilon_{i,j-1,k} A^n_{y\ i,j-\frac{1}{2},k} \right) + \\
& \frac{1}{\Delta z_k} \epsilon^{-2}_{i,j,k} \mu^{-1}_{i,j,k} \left(\epsilon_{i,j,k} A^n_{z\ i,j,k+\frac{1}{2}} - \epsilon_{i,j,k-1} A^n_{z\ i,j,k-\frac{1}{2}} \right) \Bigg) \Bigg) / \Delta x_{i+\frac{1}{2}}, \quad \text{(4.64a)}
\end{aligned}
$$

$$
\begin{aligned}
A_{y\ term2} = \epsilon_{i,j,k} \Bigg(\Bigg(& \frac{1}{\Delta x_i} \epsilon^{-2}_{i,j+1,k} \mu^{-1}_{i,j+1,k} \left(\epsilon_{i,j+1,k} A^n_{x\ i+\frac{1}{2},j+1,k} - \epsilon_{i-1,j+1,k} A^n_{x\ i-\frac{1}{2},j+1,k} \right) + \\
& \frac{1}{\Delta y_j} \epsilon^{-2}_{i,j+1,k} \mu^{-1}_{i,j+1,k} \left(\epsilon_{i,j+1,k} A^n_{y\ i,j+\frac{3}{2},k} - \epsilon_{i,j,k} A^n_{y\ i,j+\frac{1}{2},k} \right) + \\
& \frac{1}{\Delta z_k} \epsilon^{-2}_{i,j+1,k} \mu^{-1}_{i,j+1,k} \left(\epsilon_{i,j+1,k} A^n_{z\ i,j+1,k+\frac{1}{2}} - \epsilon_{i,j+1,k-1} A^n_{z\ i,j+1,k-\frac{1}{2}} \right) \Bigg) - \\
& \Bigg(\frac{1}{\Delta x_i} \epsilon^{-2}_{i,j,k} \mu^{-1}_{i,j,k} \left(\epsilon_{i,j,k} A^n_{x\ i+\frac{1}{2},j,k} - \epsilon_{i-1,j,k} A^n_{x\ i-\frac{1}{2},j,k} \right) + \\
& \frac{1}{\Delta y_j} \epsilon^{-2}_{i,j,k} \mu^{-1}_{i,j,k} \left(\epsilon_{i,j,k} A^n_{y\ i,j+\frac{1}{2},k} - \epsilon_{i,j-1,k} A^n_{y\ i,j-\frac{1}{2},k} \right) + \\
& \frac{1}{\Delta z_k} \epsilon^{-2}_{i,j,k} \mu^{-1}_{i,j,k} \left(\epsilon_{i,j,k} A^n_{z\ i,j,k+\frac{1}{2}} - \epsilon_{i,j,k-1} A^n_{z\ i,j,k-\frac{1}{2}} \right) \Bigg) \Bigg) / \Delta y_{j+\frac{1}{2}}, \quad \text{(4.64b)}
\end{aligned}
$$

$$A_{z\ term2} = \epsilon_{i,j,k}\Bigg(\Bigg(\frac{1}{\Delta x_i}\epsilon^{-2}_{i,j,k+1}\mu^{-1}_{i,j,k+1}\left(\epsilon_{i,j,k+1}A^n_{x\ i+\frac{1}{2},j,k+1} - \epsilon_{i-1,j,k+1}A^n_{x\ i-\frac{1}{2},j,k+1}\right) + \frac{1}{\Delta y_j}\epsilon^{-2}_{i,j,k+1}\mu^{-1}_{i,j,k+1}\left(\epsilon_{i,j,k+1}A^n_{y\ i,j+\frac{1}{2},k+1} - \epsilon_{i,j-1,k+1}A^n_{y\ i,j-\frac{1}{2},k+1}\right) + \frac{1}{\Delta z_k}\epsilon^{-2}_{i,j,k+1}\mu^{-1}_{i,j,k+1}\left(\epsilon_{i,j,k+1}A^n_{z\ i,j,k+\frac{3}{2}} - \epsilon_{i,j,k}A^n_{z\ i,j,k+\frac{1}{2}}\right)\Bigg) - \Bigg(\frac{1}{\Delta x_i}\epsilon^{-2}_{i,j,k}\mu^{-1}_{i,j,k}\left(\epsilon_{i,j,k}A^n_{x\ i+\frac{1}{2},j,k} - \epsilon_{i-1,j,k}A^n_{x\ i-\frac{1}{2},j,k}\right) + \frac{1}{\Delta y_j}\epsilon^{-2}_{i,j,k}\mu^{-1}_{i,j,k}\left(\epsilon_{i,j,k}A^n_{y\ i,j+\frac{1}{2},k} - \epsilon_{i,j-1,k}A^n_{y\ i,j-\frac{1}{2},k}\right) + \frac{1}{\Delta z_k}\epsilon^{-2}_{i,j,k}\mu^{-1}_{i,j,k}\left(\epsilon_{i,j,k}A^n_{z\ i,j,k+\frac{1}{2}} - \epsilon_{i,j,k-1}A^n_{z\ i,j,k-\frac{1}{2}}\right)\Bigg)\Bigg)/\Delta z_{k+\frac{1}{2}}. \quad (4.64c)$$

4.4.3.3 A Update Equations for Graded Mesh - All Terms

The **A** update equations for a graded mesh are given below.

$$\tilde{\mathbf{A}}^{n+\frac{3}{2}}_{i,j,k} = 2\tilde{\mathbf{A}}^{n+\frac{1}{2}}_{i,j,k} - \tilde{\mathbf{A}}^{n-\frac{1}{2}}_{i,j,k} + \Delta_t^2\epsilon^{-1}_{i,j,k}\left(\mathbf{A}^{n+\frac{1}{2}}_{term1} + \mathbf{A}^{n+\frac{1}{2}}_{term2} + \tilde{\mathbf{J}}^{n+\frac{1}{2}}_{i,j,k}\right) \quad (4.65)$$

where

$$\mathbf{A}^{n+\frac{1}{2}}_{term1} = -\hat{\nabla}\times\mu^{-1}_{i+\frac{1}{2},j+\frac{1}{2},k+\frac{1}{2}}\left(\tilde{\nabla}\times\tilde{\mathbf{A}}^{n+\frac{1}{2}}_{i,j,k}\right) \quad (4.66)$$

and

$$\mathbf{A}^{n+\frac{1}{2}}_{term2} = \epsilon_{i,j,k}\tilde{\nabla}\epsilon^{-2}_{i,j,k}\mu^{-1}_{i,j,k}\hat{\nabla}\cdot\epsilon_{i,j,k}\tilde{\mathbf{A}}^{n+\frac{1}{2}}_{i,j,k}. \quad (4.67)$$

Each update term contains many operations even with the simplifying assumptions about the graded mesh. The equations for the first term are

$$
\begin{aligned}
A_{x\ term1} = & \\
& \frac{1}{\Delta y_j}\left(\left(\mu^{-1}_{i+\frac{1}{2},j-\frac{1}{2},k+\frac{1}{2}}\left(\frac{A^n_{y\ i+1,j-\frac{1}{2},k}-A^n_{y\ i,j-\frac{1}{2},k}}{\Delta x_{i+\frac{1}{2}}}-\frac{A^n_{x\ i+\frac{1}{2},j,k}-A^n_{x\ i+\frac{1}{2},j-1,k}}{\Delta y_{j+\frac{1}{2}}}\right)\right)-\right. \\
& \left.\left(\mu^{-1}_{i+\frac{1}{2},j+\frac{1}{2},k+\frac{1}{2}}\left(\frac{A^n_{y\ i+1,j+\frac{1}{2},k}-A^n_{y\ i,j+\frac{1}{2},k}}{\Delta x_{i+\frac{1}{2}}}-\frac{A^n_{x\ i+\frac{1}{2},j+1,k}-A^n_{x\ i+\frac{1}{2},j,k}}{\Delta y_{j+\frac{1}{2}}}\right)\right)\right) \\
& +\frac{1}{\Delta z_k}\left(\mu^{-1}_{i+\frac{1}{2},j+\frac{1}{2},k+\frac{1}{2}}\left(\frac{A^n_{x\ i+\frac{1}{2},j,k+1}-A^n_{x\ i+\frac{1}{2}j,k}}{\Delta z_{k+\frac{1}{2}}}-\frac{A^n_{z\ i+1,j,k+\frac{1}{2}}-A^n_{z\ i,j,k+\frac{1}{2}}}{\Delta x_{i+\frac{1}{2}}}\right)-\right. \\
& \left.\mu^{-1}_{i+\frac{1}{2},j+\frac{1}{2},k-\frac{1}{2}}\left(\frac{A^n_{x\ i+\frac{1}{2},j,k}-A^n_{x\ i+\frac{1}{2}j,k-1}}{\Delta z_{k+\frac{1}{2}}}-\frac{A^n_{z\ i+1,j,k-\frac{1}{2}}-A^n_{z\ i,j,k-\frac{1}{2}}}{\Delta x_{i+\frac{1}{2}}}\right)\right), \qquad (4.68a)
\end{aligned}
$$

$$
\begin{aligned}
A_{y\ term1} = & \\
& \frac{1}{\Delta z_k}\left(\mu^{-1}_{i+\frac{1}{2},j+\frac{1}{2},k-\frac{1}{2}}\left(\frac{A^n_{z\ i,j+1,k-\frac{1}{2}}-A^n_{z\ i,j,k-\frac{1}{2}}}{\Delta y_{j+\frac{1}{2}}}-\frac{A^n_{y\ i,j+\frac{1}{2},k}-A^n_{y\ i,j+\frac{1}{2},k-1}}{\Delta z_{k+\frac{1}{2}}}\right)-\right. \\
& \left.\mu^{-1}_{i+\frac{1}{2},j+\frac{1}{2},k+\frac{1}{2}}\left(\frac{A^n_{z\ i,j+1,k+\frac{1}{2}}-A^n_{z\ i,j,k+\frac{1}{2}}}{\Delta y_{j+\frac{1}{2}}}-\frac{A^n_{y\ i,j+\frac{1}{2},k+1}-A^n_{y\ i,j+\frac{1}{2},k}}{\Delta z_{k+\frac{1}{2}}}\right)\right) \\
& +\frac{1}{\Delta x_i}\left(\mu^{-1}_{i+\frac{1}{2},j+\frac{1}{2},k+\frac{1}{2}}\left(\frac{A^n_{y\ i+1,j+\frac{1}{2},k}-A^n_{y\ i,j+\frac{1}{2},k}}{\Delta x_{i+\frac{1}{2}}}-\frac{A^n_{x\ i+\frac{1}{2},j+1,k}-A^n_{x\ i+\frac{1}{2},j,k}}{\Delta y_{j+\frac{1}{2}}}\right)-\right. \\
& \left.\mu^{-1}_{i-\frac{1}{2},j+\frac{1}{2},k+\frac{1}{2}}\left(\frac{A^n_{y\ i,j+\frac{1}{2},k}-A^n_{y\ i-1,j+\frac{1}{2},k}}{\Delta x_{i+\frac{1}{2}}}-\frac{A^n_{x\ i-\frac{1}{2},j+1,k}-A^n_{x\ i-\frac{1}{2},j,k}}{\Delta y_{j+\frac{1}{2}}}\right)\right), \qquad (4.68b)
\end{aligned}
$$

and

$$
\begin{aligned}
A_{z\ term1} = & \\
& \frac{1}{\Delta x_i}\left(\mu^{-1}_{i-\frac{1}{2},j+\frac{1}{2},k+\frac{1}{2}}\left(\frac{A^n_{x\ i-\frac{1}{2},j,k+1}-A^n_{x\ i-\frac{1}{2}j,k}}{\Delta z_{k+\frac{1}{2}}}-\frac{A^n_{z\ i,j,k+\frac{1}{2}}-A^n_{z\ i-1,j,k+\frac{1}{2}}}{\Delta x_{i+\frac{1}{2}}}\right)-\right. \\
& \left.\mu^{-1}_{i+\frac{1}{2},j+\frac{1}{2},k+\frac{1}{2}}\left(\frac{A^n_{x\ i+\frac{1}{2},j,k+1}-A^n_{x\ i+\frac{1}{2}j,k}}{\Delta z_{k+\frac{1}{2}}}-\frac{A^n_{z\ i+1,j,k+\frac{1}{2}}-A^n_{z\ i,j,k+\frac{1}{2}}}{\Delta x_{i+\frac{1}{2}}}\right)\right) \\
& +\frac{1}{\Delta y_j}\left(\mu^{-1}_{i+\frac{1}{2},j+\frac{1}{2},k+\frac{1}{2}}\left(\frac{A^n_{z\ i,j+1,k+\frac{1}{2}}-A^n_{z\ i,j,k+\frac{1}{2}}}{\Delta y_{j+\frac{1}{2}}}-\frac{A^n_{y\ i,j+\frac{1}{2},k+1}-A^n_{y\ i,j+\frac{1}{2},k}}{\Delta z_{k+\frac{1}{2}}}\right)-\right. \\
& \left.\left.\mu^{-1}_{i+\frac{1}{2},j-\frac{1}{2},k+\frac{1}{2}}\left(\frac{A^n_{z\ i,j,k+\frac{1}{2}}-A^n_{z\ i,j,k+\frac{1}{2}}}{\Delta y_{j+\frac{1}{2}}}-\frac{A^n_{y\ i,j+\frac{1}{2},k+1}-A^n_{y\ i,j+\frac{1}{2},k}}{\Delta z_{k+\frac{1}{2}}}\right)\right)\right. . \qquad (4.68c)
\end{aligned}
$$

The equations for the second term are

$$
\begin{aligned}
A_{x\ term2} = \epsilon_{i,j,k}\Bigg(\Bigg(\Bigg(\frac{1}{\Delta x_i}\epsilon^{-2}_{i+1,j,k}\mu^{-1}_{i+1,j,k}\left(\epsilon_{i+1,j,k}A^n_{x\ i+\frac{3}{2},j,k}-\epsilon_{i,j,k}A^n_{x\ i+\frac{1}{2},j,k}\right)+ \\
\frac{1}{\Delta y_j}\epsilon^{-2}_{i+1,j,k}\mu^{-1}_{i+1,j,k}\left(\epsilon_{i+1,j,k}A^n_{y\ i+1,j+\frac{1}{2},k}-\epsilon_{i+1,j-1,k}A^n_{y\ i+1,j-\frac{1}{2},k}\right)+ \\
\frac{1}{\Delta z_k}\epsilon^{-2}_{i+1,j,k}\mu^{-1}_{i+1,j,k}\left(\epsilon_{i+1,j,k}A^n_{z\ i+1,j,k+\frac{1}{2}}-\epsilon_{i+1,j,k-1}A^n_{z\ i+1,j,k-\frac{1}{2}}\right)\Bigg)- \\
\Bigg(\frac{1}{\Delta x_i}\epsilon^{-2}_{i,j,k}\mu^{-1}_{i,j,k}\left(\epsilon_{i,j,k}A^n_{x\ i+\frac{1}{2},j,k}-\epsilon_{i-1,j,k}A^n_{x\ i-\frac{1}{2},j,k}\right)+ \\
\frac{1}{\Delta y_j}\epsilon^{-2}_{i,j,k}\mu^{-1}_{i,j,k}\left(\epsilon_{i,j,k}A^n_{y\ i,j+\frac{1}{2},k}-\epsilon_{i,j-1,k}A^n_{y\ i,j-\frac{1}{2},k}\right)+ \\
\frac{1}{\Delta z_k}\epsilon^{-2}_{i,j,k}\mu^{-1}_{i,j,k}\left(\epsilon_{i,j,k}A^n_{z\ i,j,k+\frac{1}{2}}-\epsilon_{i,j,k-1}A^n_{z\ i,j,k-\frac{1}{2}}\right)\Bigg)\Bigg)/\Delta x_{i+\frac{1}{2}}, \qquad (4.69a)
\end{aligned}
$$

$$A_{y\ term2} = \epsilon_{i,j,k}\left(\left(\frac{1}{\Delta x_i}\epsilon^{-2}_{i,j+1,k}\mu^{-1}_{i,j+1,k}\left(\epsilon_{i,j+1,k}A^n_{x\ i+\frac{1}{2},j+1,k} - \epsilon_{i-1,j+1,k}A^n_{x\ i-\frac{1}{2},j+1,k}\right) + \right.\right.$$
$$\frac{1}{\Delta y_j}\epsilon^{-2}_{i,j+1,k}\mu^{-1}_{i,j+1,k}\left(\epsilon_{i,j+1,k}A^n_{y\ i,j+\frac{3}{2},k} - \epsilon_{i,j,k}A^n_{y\ i,j+\frac{1}{2},k}\right) +$$
$$\left.\left.\frac{1}{\Delta z_k}\epsilon^{-2}_{i,j+1,k}\mu^{-1}_{i,j+1,k}\left(\epsilon_{i,j+1,k}A^n_{z\ i,j+1,k+\frac{1}{2}} - \epsilon_{i,j+1,k-1}A^n_{z\ i,j+1,k-\frac{1}{2}}\right)\right) -\right.$$
$$\left(\frac{1}{\Delta x_i}\epsilon^{-2}_{i,j,k}\mu^{-1}_{i,j,k}\left(\epsilon_{i,j,k}A^n_{x\ i+\frac{1}{2},j,k} - \epsilon_{i-1,j,k}A^n_{x\ i-\frac{1}{2},j,k}\right) +\right.$$
$$\frac{1}{\Delta y_j}\epsilon^{-2}_{i,j,k}\mu^{-1}_{i,j,k}\left(\epsilon_{i,j,k}A^n_{y\ i,j+\frac{1}{2},k} - \epsilon_{i,j-1,k}A^n_{y\ i,j-\frac{1}{2},k}\right) +$$
$$\left.\left.\left.\frac{1}{\Delta z_k}\epsilon^{-2}_{i,j,k}\mu^{-1}_{i,j,k}\left(\epsilon_{i,j,k}A^n_{z\ i,j,k+\frac{1}{2}} - \epsilon_{i,j,k-1}A^n_{z\ i,j,k-\frac{1}{2}}\right)\right)\right)\right)/\Delta y_{j+\frac{1}{2}}, \quad (4.69b)$$

and

$$A_{z\ term2} = \epsilon_{i,j,k}\left(\left(\frac{1}{\Delta x_i}\epsilon^{-2}_{i,j,k+1}\mu^{-1}_{i,j,k+1}\left(\epsilon_{i,j,k+1}A^n_{x\ i+\frac{1}{2},j,k+1} - \epsilon_{i-1,j,k+1}A^n_{x\ i-\frac{1}{2},j,k+1}\right) + \right.\right.$$
$$\frac{1}{\Delta y_j}\epsilon^{-2}_{i,j,k+1}\mu^{-1}_{i,j,k+1}\left(\epsilon_{i,j,k+1}A^n_{y\ i,j+\frac{1}{2},k+1} - \epsilon_{i,j-1,k+1}A^n_{y\ i,j-\frac{1}{2},k+1}\right) +$$
$$\left.\left.\frac{1}{\Delta z_k}\epsilon^{-2}_{i,j,k+1}\mu^{-1}_{i,j,k+1}\left(\epsilon_{i,j,k+1}A^n_{z\ i,j,k+\frac{3}{2}} - \epsilon_{i,j,k}A^n_{z\ i,j,k+\frac{1}{2}}\right)\right) -\right.$$
$$\left(\frac{1}{\Delta x_i}\epsilon^{-2}_{i,j,k}\mu^{-1}_{i,j,k}\left(\epsilon_{i,j,k}A^n_{x\ i+\frac{1}{2},j,k} - \epsilon_{i-1,j,k}A^n_{x\ i-\frac{1}{2},j,k}\right) +\right.$$
$$\frac{1}{\Delta y_j}\epsilon^{-2}_{i,j,k}\mu^{-1}_{i,j,k}\left(\epsilon_{i,j,k}A^n_{y\ i,j+\frac{1}{2},k} - \epsilon_{i,j-1,k}A^n_{y\ i,j-\frac{1}{2},k}\right) +$$
$$\left.\left.\left.\frac{1}{\Delta z_k}\epsilon^{-2}_{i,j,k}\mu^{-1}_{i,j,k}\left(\epsilon_{i,j,k}A^n_{z\ i,j,k+\frac{1}{2}} - \epsilon_{i,j,k-1}A^n_{z\ i,j,k-\frac{1}{2}}\right)\right)\right)\right)/\Delta z_{k+\frac{1}{2}}. \quad (4.69c)$$

4.5 Simulation Results

We have implemented the discretized equations for a uniform mesh (Sections 4.3.2 and 4.3.3.3) and for a graded mesh (Sections 4.4.2 and 4.4.3.3). The simulation was on a $90 \times 100 \times 110$ grid in free space. We give our simulation a current source, a dipole source with a wavelength of 940 nm. The source is located at the center of the simulation.

$$J_z\left(\frac{i_{\max}}{2}, \frac{j_{\max}}{2}, \frac{k_{\max}}{2}\right) = 1 - \cos(\omega t). \quad (4.70)$$

The graded mesh has varying values of grid spacing but still must not violate the Courant stability condition

$$\Delta_t < \frac{1}{c\sqrt{\Delta_{x\,\min}^{-2} + \Delta_{y\,\min}^{-2} + \Delta_{z\,\min}^{-2}}}, \tag{4.71}$$

where $\Delta_{i\,\min}$ is the minimum mesh separation in the i-direction. We use

$$\Delta_t = \frac{0.99}{c\sqrt{\Delta_{x\,\min}^{-2} + \Delta_{y\,\min}^{-2} + \Delta_{z\,\min}^{-2}}}. \tag{4.72}$$

The timestep is calculated to be $\Delta_t = 0.090$ fs, and $\Delta_{i\,\min} = \frac{\lambda}{20}$ for standard grid sampling.

The $\mathbf{E}$ and $\mathbf{H}$ fields can be obtained by discretization of the definitions from $\mathbf{A}$ and ϕ. This is useful if someone wanted to compare values to conventional FDTD or visually confirm the behavior of the electromagnetic fields is not unexpected. The values for $\mathbf{A}$ and ϕ are less intuitive than the standard $\mathbf{E}$ and $\mathbf{H}$ fields.

4.5.1 Uniform Mesh

Figure 4.1 shows field values for $\mathbf{A}$ and ϕ as well as $\mathbf{E}$ and $\mathbf{H}$ for $t = 50\Delta_t$ or $t = 4.4805$ fs. Figure 4.1a gives values of $\mathbf{A}$ and ϕ calculated directly from the simulation. Figure 4.1b gives values of $\mathbf{E}$ and $\mathbf{H}$ calculated from the discretized definitions of $\mathbf{E}$ and $\mathbf{H}$ in terms of $\mathbf{A}$ and ϕ. We observe a circular wave propagating outwards from the center for the z-components, as well as ϕ, as expected. Other components appear symmetric about the origin and seem to have stable propagation characteristics. One thing to note is that the values appear smooth along the wavefront; this indicates a stable simulation.

Figure 4.2 shows field values for $\mathbf{A}$ and ϕ as well as $\mathbf{E}$ and $\mathbf{H}$ for $t = 500\Delta_t$ or $t = 44.805$ fs. Figure 4.2a and Figure 4.2b are calculated in the same way as in Figure 4.1. These results appear a little rough. I think this is due to lack of consideration of edges of the simulation. The benefit is that, in coding, all updates were evaluated in one loop, speeding up computation time. This differs from conventional FDTD because the second-order update equations are uncoupled, so the previous values only depend on prior timesteps, not the position-dependent values of another field at the same timestep. However, if I were to work on this simulation again, I would put ρ, ϕ, and $\mathbf{A}$

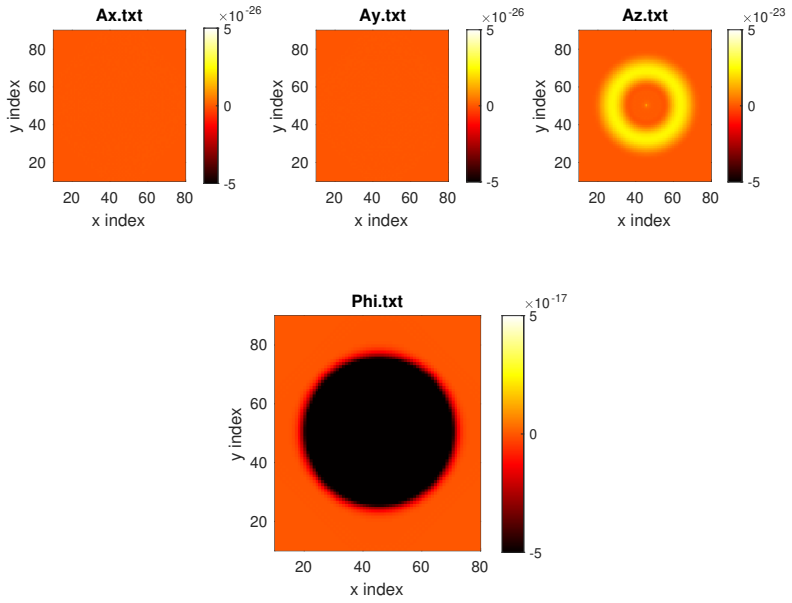

(a) Values for $\mathbf{A}$ and ϕ calculated from the second-order $\mathbf{A}$-ϕ FDTD at $t = 4.4805$ fs

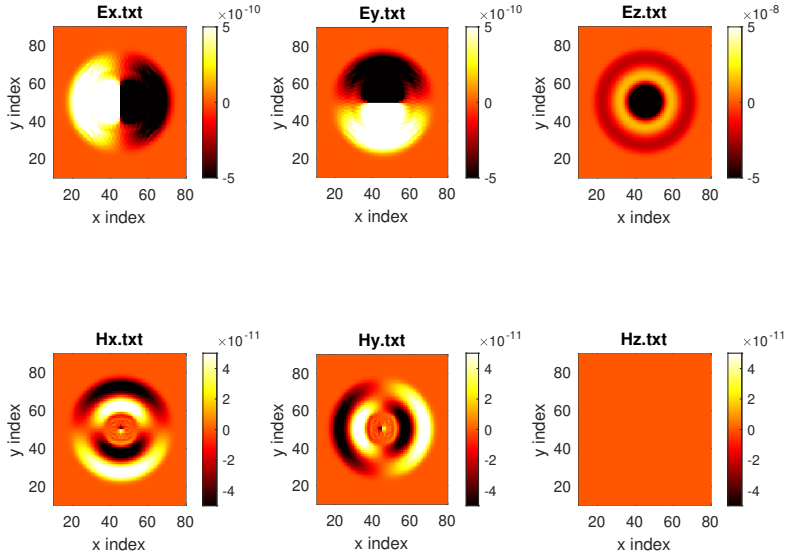

(b) Field values $\mathbf{E}$ and $\mathbf{H}$ calculated from $\mathbf{A}$ and ϕ in the second-order $\mathbf{A}$-ϕ FDTD at $t = 4.4805$ fs

Figure 4.1: Shows $\mathbf{A}$, ϕ, $\mathbf{H}$, and $\mathbf{E}$ values calculated from the second-order $\mathbf{A}$-ϕ FDTD at $t = 50\Delta_t = 4.4805$ fs for a dipole current source J_z in Equation (4.70).

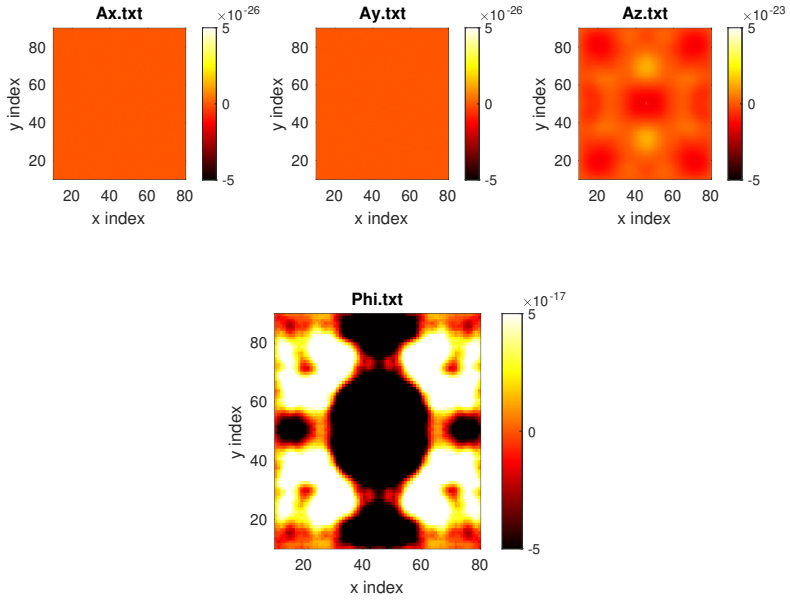

(a) Values for $\mathbf{A}$ and ϕ calculated from the second-order $\mathbf{A}$-ϕ FDTD at $t = 44.805$fs

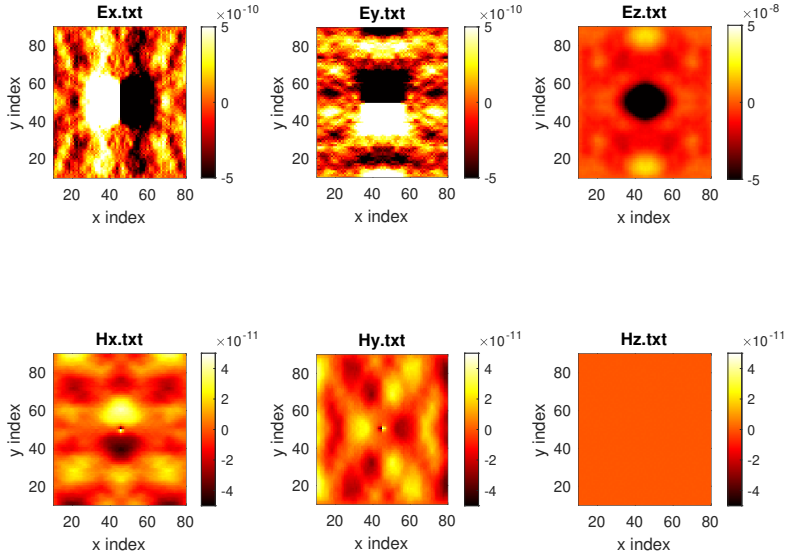

(b) Field values $\mathbf{E}$ and $\mathbf{H}$ calculated from $\mathbf{A}$ and ϕ in the second-order $\mathbf{A}$-ϕ FDTD at $t = 44.805$ fs

Figure 4.2: Shows $\mathbf{A}$, ϕ, $\mathbf{H}$, and $\mathbf{E}$ values calculated from the second-order $\mathbf{A}$-ϕ FDTD at $t = 500\Delta_t$, $t = 44.805$ fs for a dipole current source J_z in Equation (4.70).

in separate update loops with appropriate indices for grid termination. Iteration through multiple loops would be more computationally expensive, but it would allow for the creation of a symmetric domain. Another method to create a symmetric domain and minimize loops could be by creating a second loop with just the boundary value updates. How to determine boundaries for FDTD loops is covered in a later section for the development of FiPo.

4.5.2 Nonuniform Mesh

The nonuniform mesh is defined at both half and whole steps for each coordinate. We consider a graded mesh where the size of the cell varies linearly with position. The slope of the grading is found by

$$\text{slope} = \frac{\text{gradeScale} * \Delta_{x\ min}}{i_{\max} - \text{mid}} \tag{4.73}$$

and spatial steps calculations for the first half of the grid (1 to mid) are defined as

$$\Delta_x = -\text{slope} * (ii - \text{mid}) + \Delta_{x\ \min} \tag{4.74a}$$

$$\Delta_x = -\text{slope} * (ii - \text{mid} + 0.5) + \Delta_{x\ \min} \tag{4.74b}$$

The equations for the second half of the grid (mid to $i_{\max}$) are calculated in the same way except with a slope of the opposite sign. We defined a mesh grading scale gradeScale of 0.10 that changes how quickly the spatial variation of the grid changes. We chose a value of 0.10 in order to not vary too much and make the simulation unstable but also have a nonnegligible spatial variation. The value mid is the center point of the simulation.

Figure 4.3 shows field values for $\mathbf{A}$ and ϕ as well as $\mathbf{E}$ and $\mathbf{H}$ for $t = 50\Delta_t$ or $t = 4.4805$ fs for a nonuniform mesh. Figure 4.3a gives values of $\mathbf{A}$ and ϕ calculated directly from the simulation. Figure 4.3b gives values of $\mathbf{E}$ and $\mathbf{H}$ calculated from the discretized definitions of $\mathbf{E}$ and $\mathbf{H}$ in terms of $\mathbf{A}$ and ϕ. Similar to the uniform simulation, we observe a circular wave propagating outwards from the center for the z-components as well as ϕ, as expected. However, ϕ now has both positive and negative values and there are now differences for the now non-negligible components for A_x and A_y. There appears to be some roughness at the edge of E_x and E_y that could be due to

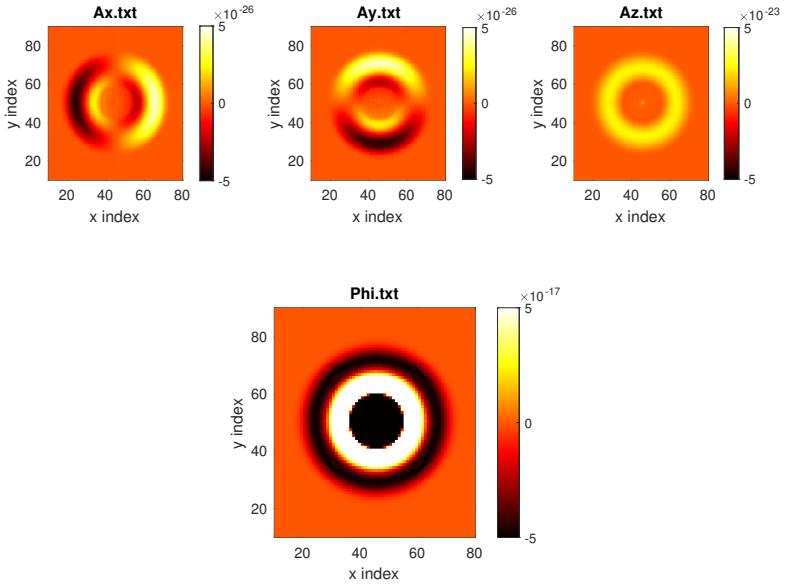

(a) Values for $\mathbf{A}$ and ϕ calculated from the second-order $\mathbf{A}$-ϕ FDTD with nonuniform mesh at $t = 4.4805$ fs

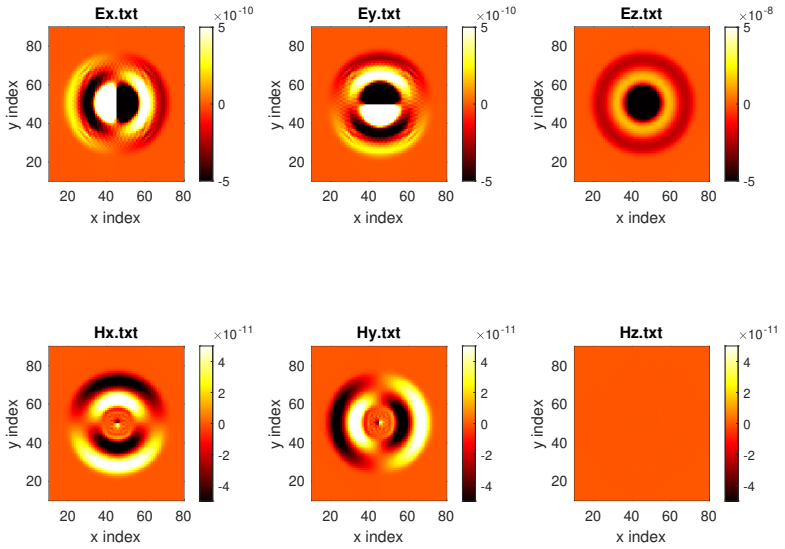

(b) Field values $\mathbf{E}$ and $\mathbf{H}$ calculated from $\mathbf{A}$ and ϕ in the second-order $\mathbf{A}$-ϕ FDTD with nonuniform mesh at $t = 4.4805$ fs

Figure 4.3: $\mathbf{A}$, ϕ, $\mathbf{H}$, and $\mathbf{E}$ values calculated from the second-order $\mathbf{A}$-ϕ FDTD with nonuniform mesh at $\Delta_t = 50$, $t = 4.4805$ fs for a dipole current source J_z.

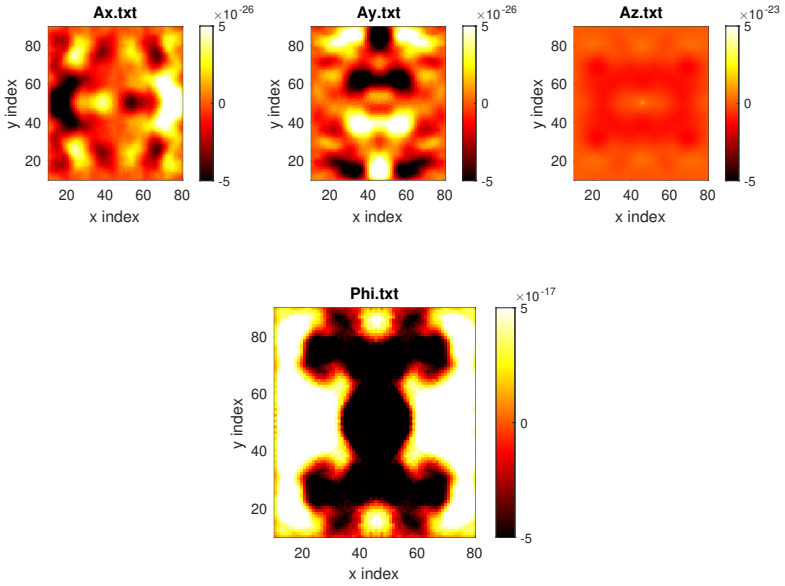

(a) Values for $\mathbf{A}$ and ϕ calculated from the second-order $\mathbf{A}$-ϕ FDTD with nonuniform mesh at $t = 44.805$ fs

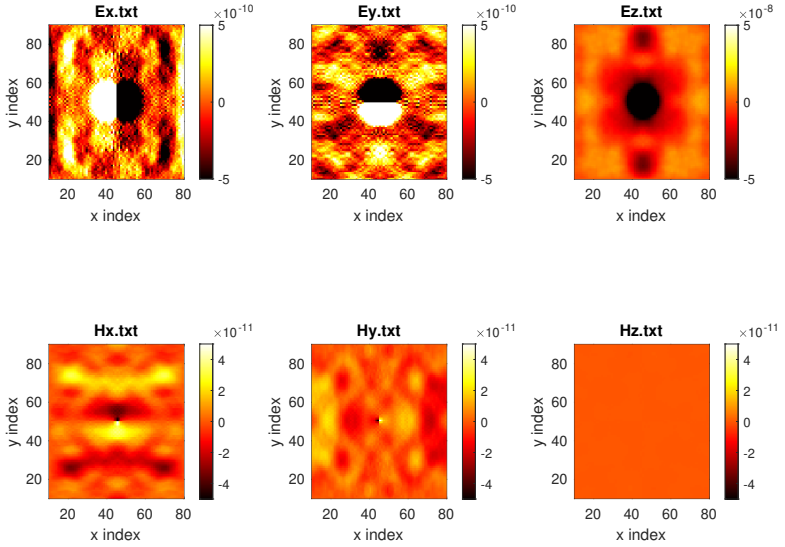

(b) Field values $\mathbf{E}$ and $\mathbf{H}$ calculated from $\mathbf{A}$ and ϕ in the second-order $\mathbf{A}$-ϕ FDTD with nonuniform mesh at $t = 44.805$ fs

Figure 4.4: $\mathbf{A}$, ϕ, $\mathbf{H}$, and $\mathbf{E}$ values calculated from the second-order $\mathbf{A}$-ϕ FDTD with nonuniform mesh at $\Delta_t = 500$, $t = 44.805$ fs for a dipole current source J_z.

instabilities arising from the nonuniform mesh. The results have some differences from Figure 4.3 that could be a result of error from the nonuniform mesh.

Conventional first-order FDTD can be troublesome to implement if not careful of the indices; the second-order equations are much worse in this regard. I ended up implementing the operations in code rather than opting for writing out individual values because when I tried, they were extremely prone to error. This method of programming operations, however, results in unsimplified equations and increases overall compuatational cost. It would be better to simplify in terms of coefficients and field values of the same position and timestep. The problem is that there are so many different field values for a single update equation that the solution is a mess. As you could see in the derivation, I divided the A update equation into multiple terms where each term was complicated with many different values. Details of implementation were not included in Ryu *et al.* [14], but due to the complexity of this method, the amount of work necessary to recreate the FDTD is impractical for use of those who are not well-versed in FDTD.

4.6 Discussion of PML for Second-Order Equations

The $\mathbf{A}$-ϕ FDTD works well enough for a sample simulation; however, to use this method for device simulation, absorbing boundary conditions need to be implemented. This section will go over the PML implemented in Ryu *et al.* [14]. We have already discussed the impractical nature of the second-order update equations, but the complexity of the second-order update equations really shines in PML implementation. We can demonstrate the difficulty of PML implementation

by looking at the update equation for $A_x^{n+\frac{1}{2}}$, given as

$$\frac{\partial_y H_z^{n-\frac{1}{2}} - 2\partial_y H_z^{n-\frac{3}{2}} + \partial_y H_z^{n-\frac{5}{2}}}{\Delta_t^2} + \frac{\sigma_z}{\epsilon}\frac{\partial_y H_z^{n-\frac{1}{2}} - \partial_y H_z^{n-\frac{5}{2}}}{2\Delta_t} - \frac{\partial_z H_y^{n-\frac{1}{2}} - 2\partial_z H_y^{n-\frac{3}{2}} + \partial_z H_y^{n-\frac{5}{2}}}{\Delta_t^2}$$
$$- \frac{\sigma_y}{\epsilon}\frac{\partial_z H_y^{n-\frac{1}{2}} - \partial_z H_y^{n-\frac{5}{2}}}{2\Delta_t} + \epsilon\frac{A_x^{n+\frac{1}{2}} - 4A_x^{n-\frac{1}{2}} + 6A_x^{n-\frac{3}{2}} - 4A_x^{n-\frac{5}{2}} + A_x^{n-\frac{7}{2}}}{\Delta_t^4}$$
$$+ (\sigma_y + \sigma_z)\frac{\frac{1}{2}A_x^{n+\frac{1}{2}} - A_x^{n-\frac{1}{2}} + A_x^{n-\frac{5}{2}} - \frac{1}{2}A_x^{n-\frac{7}{2}}}{\Delta_t^3} + \frac{\sigma_y\sigma_z}{\epsilon}\frac{A_x^{n-\frac{1}{2}} - 2A_x^{n-\frac{3}{2}} + A_x^{n-\frac{5}{2}}}{\Delta_t^2}$$
$$- \epsilon\frac{[\nabla_s f]_x^{n-\frac{1}{2}} - 2[\nabla_s f]_x^{n-\frac{3}{2}} + [\nabla_s f]_x^{n-\frac{5}{2}}}{\Delta_t^2} - (\sigma_y + \sigma_z)\frac{[\nabla_s f]_x^{n-\frac{1}{2}} - [\nabla_s f]_x^{n-\frac{5}{2}}}{2\Delta_t} - \frac{\sigma_y\sigma_z}{\epsilon}[\nabla_s f]_x^{n-\frac{3}{2}}$$
$$= \frac{J_x^{n-\frac{1}{2}} - 2J_x^{n-\frac{3}{2}} + J_x^{n-\frac{5}{2}}}{\Delta_t^2} \quad (4.75)$$

Note, the original paper appears to contain a typo where there is a multiplication of the $[\nabla_s f]_x^{n-\frac{5}{2}}$ term rather than addition — this term is altered here. Notice that in the form given, the update equation still needs to be solved for $A_x^{n+\frac{1}{2}}$ in order to update the next timestep. By inspection, we can tell this equation is the update equation for $A_x^{n+\frac{1}{2}}$ because there is only one value at the $n + \frac{1}{2}$ timestep, whereas the rest are at $n - \frac{1}{2}$ or lower. We can see from the indices listed on the values in the update equation, that we will need to store four previous timesteps of values in addition to the value being updated. Storing five fields for one variable at once is a notable concern for computational demand. The benefit of first-order FDTD is that only one previous timestep is stored for simulation updates, resulting in two total. For the second-order FDTD simulation region, two previous timesteps are required to be stored, three total. With the addition of the PML, the second-order method requires storage of five total timesteps for a single variable. Table 4.1 shows how many timesteps are required for each variable.

In the simulation domain for the $\mathbf{A}$-ϕ FDTD, only ρ, ϕ, and $\mathbf{A}$ are updated. $\mathbf{J}$ should be provided and stored in the simulation as a source. In this update equation, on top of the extra timesteps, we now have the additional values of $\mathbf{H}$ and $[\nabla_s f]$. $\mathbf{H}$ and $[\nabla_s f]$ appear as simple values, but their calculation is also somewhat involved.

In the paper, Ryu *et al.* [14] claims

$$\mathbf{H} = \mu^{-1}\nabla_s \times \mathbf{A}, \quad (4.76)$$

Variable Requires	Timesteps	Number of Stored Timesteps
A_x	$n+\frac{1}{2}, n-\frac{1}{2}, n-\frac{3}{2}, n-\frac{5}{2}, n-\frac{7}{2}$	5
H_y	$n-\frac{1}{2}, n-\frac{3}{2}, n-\frac{5}{2}$	3
H_z	$n-\frac{1}{2}, n-\frac{3}{2}, n-\frac{5}{2}$	3
$[\nabla f]_x$	$n-\frac{1}{2}, n-\frac{3}{2}, n-\frac{5}{2}$	3
J_x	$n-\frac{1}{2}, n-\frac{3}{2}, n-\frac{5}{2}$	3

Table 4.1: Shows variables required for update of Equation (4.75), the timesteps that require storage, and the number of stored timesteps per variable.

which takes the definition of $\mathbf{H}$ in terms of the vector potential $\mathbf{A}$ and changes the curl operator to be a stretched-coordinate operator. The occurence of the stretched-coordinate operator in this definition seems logical but, due to the lack of a time-derivative in the equation, may not necessarily hold in terms of physics. I will discuss the presence of the stretched-coordinate operator in this equation in a later derivation in this thesis.

The calculation of $\mathbf{H}$ is not just a simple calculation from $\mathbf{A}$, however. The authors of [14] claim the calculation of one component of $\mathbf{H}$ takes 3 variables, such that $H_x = H_{s_x,x} + H_{s_y,x} + H_{s_z,x}$. where $H_{s_y,x}$ and $H_{s_z,x}$ can be calculated by solving

$$\frac{A_y^{n-\frac{1}{2}}(i+1,j+\frac{1}{2},k) - A_y^{n-\frac{1}{2}}(i,j+\frac{1}{2},k)}{\Delta_x} = \mu H_{s_x,z}^{n-\frac{1}{2}} + \frac{\sigma_x \mu}{\epsilon}\left(\sum_{m=1}^{n-1} H_{s_x,z}^{m-\frac{1}{2}} + \frac{1}{2}H_{s_x,z}^{n-\frac{1}{2}}\right)\Delta_t \quad (4.77)$$

and

$$-\frac{A_z^{n-\frac{1}{2}}(i+1,j,k+\frac{1}{2}) - A_z^{n-\frac{1}{2}}(i,j,k+\frac{1}{2})}{\Delta_x} = \mu H_{s_x,y}^{n-\frac{1}{2}} + \frac{\sigma_x \mu}{\epsilon}\left(\sum_{m=1}^{n-1} H_{s_x,y}^{m-\frac{1}{2}} + \frac{1}{2}H_{s_x,y}^{n-\frac{1}{2}}\right)\Delta_t. \quad (4.78)$$

No equation is given for $H_{s_x,x}$; I assume it is included in the equation for completeness, but does not actually exist due to the nature of the derivation and how the components come from the curl.. From these equations, $H_{s_x,z}^{n-\frac{1}{2}}$ can be calculated from $A_y^{n-\frac{1}{2}}$ and $H_{s_x,y}^{n-\frac{1}{2}}$ can be calculated from $A_z^{n-\frac{1}{2}}$ for the A_x PML. One important thing to note here is that the integration of the component of $\mathbf{H}$ is over all timesteps. This means that, for every timestep, an integration variable must be stored in addition to the stretched-component field value.

Similar to the calculation of $\mathbf{H}$, f can be calculated as $f = f_{s_x} + f_{s_y} + f_{s_z}$. $f_{s_x}^{n-\frac{1}{2}}$ can be found from $A_x^{n-\frac{1}{2}}$ by solving

$$f_{s_x}^{n-\frac{1}{2}} + \frac{\sigma_x}{\epsilon}\left(\sum_{m=1}^{n-1} f_{s_x}^{m-\frac{1}{2}} + \frac{1}{2}f_{s_x}^{n-\frac{1}{2}}\right)\Delta_t = \frac{1}{\mu\epsilon^2}\frac{\epsilon(i+\frac{1}{2},j,k)A_x^{n-\frac{1}{2}} - \epsilon(i-\frac{1}{2},j,k)A_x^{n-\frac{1}{2}}}{\Delta_x}. \quad (4.79)$$

This equation looks similar to the $\mathbf{H}$ update and requires the storage of integration variables as well as values for $f_{s_x,y,z}$. f only has a single component instead of three like $\mathbf{H}$, but we also need to update the gradient for this value for the PML update equation. In order to update the value for

the gradient, we need to solve

$$\frac{f^{n-\frac{1}{2}}(i+1,j,k)-f^{n-\frac{1}{2}}(i,j,k)}{\Delta_x}=[\nabla_s f]_x^{n-\frac{1}{2}}+\frac{\sigma_x}{\epsilon}\left(\sum_{m=1}^{n-1}[\nabla_s f]_x^{m-\frac{1}{2}}+\frac{1}{2}[\nabla_s f]_x^{n-\frac{1}{2}}\right)\Delta_t. \quad (4.80)$$

There is another typo in this equation that was changed here; [14] uses n instead of m for the index of the $[\nabla_s f]_x$ in the sum. Again, this equation will require the storage of components and integration variables.

A summary of update equations, update variables required, and integration variables required can be found in Table 4.2. For the update of the A_x PML alone, 17 variables are required to be stored for direct calculation. Integration variables and intermediate update variables require additional memory for storage. The equations to update intermediate variables as well as the update equation contain many operations. Second-order PML is computationally expensive, memory intensive, and nonintuitive, and this is why we chose to develop a new method rather than to use the method that has already been developed. We do not know how well this PML performs because, unlike most papers on PML implementation, no data was given in Ryu *et al.* [14] to show PML performance [56].

Update Equation	Required Update Variables	Required Integration Variables
$H_{s_x,y}$	A_z	$H_{s_x,y}$
$H_{s_x,z}$	A_y	$H_{s_x,z}$
$H_{s_y,z}$	A_x	$H_{s_y,z}$
$H_{s_y,x}$	A_z	$H_{s_y,x}$
$H_{s_z,x}$	A_y	$H_{s_z,x}$
$H_{s_z,y}$	A_x	$H_{s_z,y}$
H_x	$H_{s_x,x}, H_{s_y,x}, H_{s_z,x}$	None
H_y	$H_{s_x,y}, H_{s_y,y}, H_{s_z,y}$	None
H_z	$H_{s_x,z}, H_{s_y,z}, H_{s_z,z}$	None
f_{s_x}	A_x	f_{s_x}
f_{s_y}	A_y	f_{s_y}
f_{s_z}	A_z	f_{s_z}
f	$f_{s_x}, f_{s_y}, f_{s_z}$	None
$[\nabla f]_x$	f	$[\nabla f]_x$
$[\nabla f]_y$	f	$[\nabla f]_y$
$[\nabla f]_z$	f	$[\nabla f]_z$

Table 4.2: Required update equations for the PML for second-order $\mathbf{A}$-ϕ FDTD, the variables required for the update equation, and variables that require integration.

Chapter 5

Field–Potential FDTD Method

We have established that second-order FDTD for potentials is not a very practical method. The update equations have many variables to store and operations to perform, and the PML is even worse in that regard. The second-order nature of the equations makes the method complicated. When you look at conventional FDTD, update equations are first order and easier to handle, and the formalism has already been extensively developed. We wanted a method to solve for potentials that would be able to use the advancements already made for conventional FDTD, like a PML, and that requires a first-order method.

5.1 First-Order Equations

5.1.1 A New Set of Update Equations

In order to develop first-order equations, we need to look at possible FDTD update equations for the potentials. FDTD update equations utilize discretization of the time derivative in order to march a variable update forward in time. From the definitions, we see

$$\mathbf{E} = -\partial_t \mathbf{A} - \nabla\phi \tag{5.1}$$

is a good candidate for an $\mathbf{A}$ update equation. We can rewrite the update equation as

$$\partial_t \mathbf{A} = -\mathbf{E} - \nabla\phi \tag{5.2}$$

and see that the time update for $\mathbf{A}$ requires values for $\mathbf{E}$ and ϕ.

The tricky term in Equation (5.2) is ϕ because the definition for $\mathbf{E}$ in Equation (5.1) is the only place ϕ appears in the field definitions. The only other equation that could contain ϕ is potentially

the choice of gauge. This means that the restriction for the gauge must mean it would ideally have a time-derivative of ϕ in order to be an update equation.

Luckily, a common gauge, the Lorenz gauge, contains a time derivative of ϕ. Since our domain for FDTD is likely to be an inhomogeneous material, we can choose our update equation as the generalized Lorenz gauge for inhomogeneous media [32, 53]

$$\epsilon\mu\partial_t\phi = -\epsilon^{-1}\nabla\cdot(\epsilon\mathbf{A}). \tag{5.3}$$

Other than requiring ϕ, Equation (5.2) also requires $\mathbf{E}$. This is convenient because we know that conventional FDTD already is able to solve for $\mathbf{E}$. From conventional FDTD, we have an update equation for $\mathbf{E}$

$$\epsilon\partial_t\mathbf{E} = \nabla\times\mathbf{H} - \mathbf{J}, \tag{5.4}$$

which requires $\mathbf{H}$ as well as a current source $\mathbf{J}$. Since $\mathbf{J}$ is often given as a source in simulations, this just leaves the update for $\mathbf{H}$.

$\mathbf{H}$ is also updated in conventional FDTD, so a previous update equation exists, but $\mathbf{H}$ is also defined in terms of potential $\mathbf{A}$. This gives a couple options for updating $\mathbf{H}$. The update equation from conventional FDTD is

$$\mu\partial_t\mathbf{H} = -\nabla\times\mathbf{E}. \tag{5.5}$$

This equation uses $\mathbf{E}$ to update $\mathbf{H}$. To obtain $\mathbf{H}$ from potentials we can use the definition

$$\mu\mathbf{H} = \nabla\times\mathbf{A}. \tag{5.6}$$

This equation uses $\mathbf{A}$ to update $\mathbf{H}$. An important note here is that *there is no time-derivative for the calculation of* $\mathbf{H}$ in this equation.

5.1.2 Update Order for New Equations

We have gathered four equations to calculate values we need to update the potentials. The equation to update $\mathbf{H}$ is a choice we will discuss. The five possibilities of update equations are

$$\partial_t \mathbf{A} = -\mathbf{E} - \nabla\phi, \tag{5.7a}$$

$$\epsilon^2\mu\partial_t\phi = -\nabla\cdot(\epsilon\mathbf{A}), \tag{5.7b}$$

$$\epsilon\partial_t\mathbf{E} = \nabla\times\mathbf{H} - \mathbf{J}, \tag{5.7c}$$

$$\mu\mathbf{H} = \nabla\times\mathbf{A}, \tag{5.7d}$$

$$\mu\partial_t\mathbf{H} = -\nabla\times\mathbf{E}. \tag{5.7e}$$

From Equation (5.7a) and our knowledge of the Yee grid (see Section 3.3), we can tell $\mathbf{A}$ is located a half timestep from $\mathbf{E}$ and ϕ and that $\mathbf{E}$ and ϕ are updated at the same timestep. $\mathbf{E}$ and $\mathbf{H}$ fields should be consistent with the conventional Yee grid. From Equation (5.7d), it is obvious from the lack of time derivative that $\mathbf{H}$ and $\mathbf{A}$ are located at the same timestep. This means $\mathbf{E}$ and ϕ should be updated in one timestep, and $\mathbf{H}$ and $\mathbf{A}$ should be updated in another. The update order of which set first should not matter but requires a choice. Since the update equation for $\mathbf{E}$ contains a source, it makes sense to update it first, so that the result of adding a source can be present in the entire timestep. This means we place $\mathbf{E}$ and ϕ are at timestep n, and $\mathbf{H}$ and $\mathbf{A}$ are at timestep $n+\frac{1}{2}$. In terms of update order, whether $\mathbf{E}$ and ϕ are first should not matter since they do not depend on each other. The update for $\mathbf{A}$, however, must come before $\mathbf{H}$ for the Equation (5.7d), so we will update $\mathbf{H}$ after $\mathbf{A}$ in the FDTD algorithm. The ordered set of equations is:

$$\epsilon^2\mu\partial_t\phi = -\nabla\cdot(\epsilon\mathbf{A}), \tag{5.8a}$$

$$\epsilon\partial_t\mathbf{E} = \nabla\times\mathbf{H} - \mathbf{J}, \tag{5.8b}$$

$$\partial_t \mathbf{A} = -\mathbf{E} - \nabla\phi, \tag{5.8c}$$

$$\mu\mathbf{H} = \nabla\times\mathbf{A}, \tag{5.8d}$$

$$\mu\partial_t\mathbf{H} = -\nabla\times\mathbf{E}. \tag{5.8e}$$

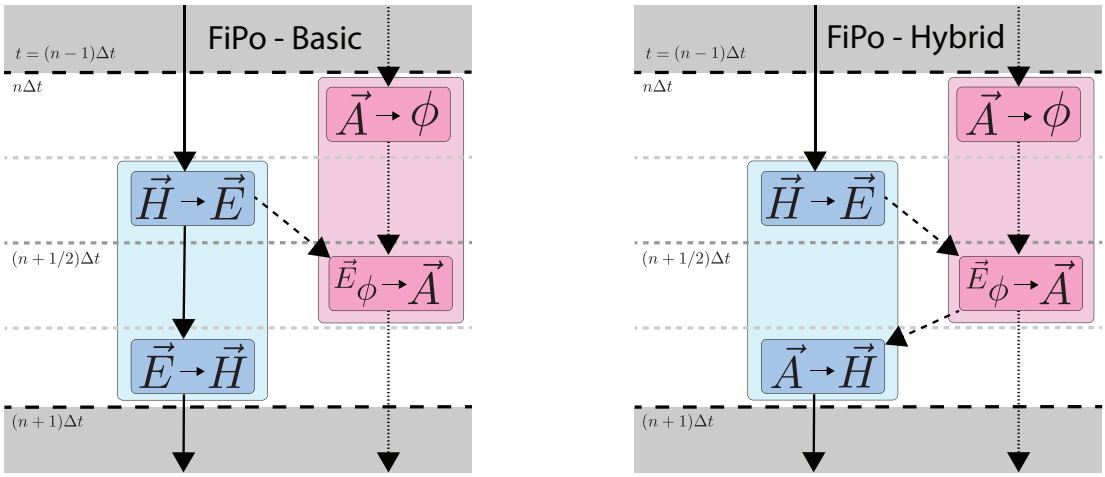

(a) FiPo Basic

(b) FiPo Hybrid

Figure 5.1: Diagram of ϕ, $\mathbf{E}$, $\mathbf{A}$, and $\mathbf{H}$ update positions at respective timesteps for the FiPo algorithm. Field updates are given in blue on the left, and potential updates are pink on the right. Arrows show the progression of field values through the update equations.

Since Equations (5.8a)-(5.8e) update both fields and potentials, we can start to develop what we call Field-Potential (FiPo) FDTD. Equations (5.8d) and (5.8e) present two different methods for updating $\mathbf{H}$. The algorithm using Equation (5.8e) as the $\mathbf{H}$ update is called FiPo Basic since this method is conventional FDTD with the addition of update equations for potentials. The downside of this method is that information from $\mathbf{A}$ or ϕ is not fed back into the update equations for $\mathbf{E}$ and $\mathbf{H}$. The algorithm using Equation (5.8d) as the $\mathbf{H}$ update is called FiPo Hybrid since this equation self-consistently updates all field and potential values, creating a hybrid method of conventional FDTD with new update equations for potentials. Figure 5.1 shows the FiPo Basic and FiPo Hybrid algorithms and follows the updated values for a single timestep.

Figure 5.1 shows the update algorithm for both FiPo Hybrid and FiPo Basic. The center represents a single timestep for integer step n and half-integer step $n + \frac{1}{2}$; the top and bottom are grey and represent the previous and next timesteps, respectively. Each labelled box with gives the variable being updated as well as those needed to do the update. Arrows show the progression of updates in the order of the algorithm. ϕ is first updated from the previous $\mathbf{A}$. Next, $\mathbf{E}$ is updated

from the previous $\mathbf{H}$, as well as a source $\mathbf{J}$. Moving to the half timestep, $\mathbf{A}$ is updated from $\mathbf{E}$ and ϕ. Finally, $\mathbf{H}$ is updated differently in each algorithm — from $\mathbf{E}$ in FiPo Basic and $\mathbf{A}$ in FiPo Hybrid. Values from $\mathbf{H}$ and $\mathbf{A}$ are then used in the next timestep to move forward in time. The fields (blue) and potentials (pink) are differentiated by color in order to show the exchange of information between the two sets of variables. Notice information only moves to the right, from fields to potentials, in FiPo Basic, but information moves from potentials back to fields in FiPo Hybrid. You can see conventional FDTD represented in Figure 5.1a by looking at blue-box quantities and arrows with solid lines.

To explicitly write out the update equations, the FiPo Basic update equations are

$$\epsilon^2 \mu \partial_t \phi = -\nabla \cdot (\epsilon \mathbf{A}), \tag{5.9a}$$

$$\epsilon \partial_t \mathbf{E} = \nabla \times \mathbf{H} - \mathbf{J}, \tag{5.9b}$$

$$\partial_t \mathbf{A} = -\mathbf{E} - \nabla \phi, \tag{5.9c}$$

$$\mu \partial_t \mathbf{H} = -\nabla \times \mathbf{E}, \tag{5.9d}$$

and the FiPo Hybrid update equations are

$$\epsilon^2 \mu \partial_t \phi = -\nabla \cdot (\epsilon \mathbf{A}), \tag{5.10a}$$

$$\epsilon \partial_t \mathbf{E} = \nabla \times \mathbf{H} - \mathbf{J}, \tag{5.10b}$$

$$\partial_t \mathbf{A} = -\mathbf{E} - \nabla \phi, \tag{5.10c}$$

$$\mu \mathbf{H} = \nabla \times \mathbf{A}. \tag{5.10d}$$

Notice that FiPo Basic and FiPo Hybrid are the same except for the update equation for $\mathbf{H}$. Each of these sets of equations has four equations now instead of the total five we have been working with because there are two options for $\mathbf{H}$ updates, and we split the $\mathbf{H}$ update options into two different methods, FiPo Basic and FiPo Hybrid.

These equations written component-wise are

$$\epsilon^2\mu\partial_t\phi = -(\partial_x(\epsilon A_x) + \partial_y(\epsilon A_y) + \partial_z(\epsilon A_z)), \tag{5.11a}$$

$$\epsilon\partial_t E_x = \partial_y H_z - \partial_z H_y - J_x, \tag{5.11b}$$

$$\epsilon\partial_t E_y = \partial_z H_x - \partial_x H_z - J_y, \tag{5.11c}$$

$$\epsilon\partial_t E_z = \partial_x H_y - \partial_y H_x - J_z, \tag{5.11d}$$

$$\partial_t A_x = -E_x - \partial_x\phi, \tag{5.11e}$$

$$\partial_t A_y = -E_y - \partial_y\phi, \tag{5.11f}$$

$$\partial_t A_z = -E_z - \partial_z\phi, \tag{5.11g}$$

$$\mu H_x = \partial_y A_z - \partial_z A_y, \tag{5.11h}$$

$$\mu H_y = \partial_z A_x - \partial_x A_z, \tag{5.11i}$$

$$\mu H_z = \partial_x A_y - \partial_y A_x, \tag{5.11j}$$

$$\mu\partial_t H_x = \partial_z E_y - \partial_y E_z, \tag{5.11k}$$

$$\mu\partial_t H_y = \partial_x E_z - \partial_z E_x, \tag{5.11l}$$

$$\mu\partial_t H_z = \partial_y E_x - \partial_x E_y. \tag{5.11m}$$

The first two variables updated in FiPo, ϕ and $\mathbf{E}$, are interchangable in update order. One reason we chose the order ϕ-$\mathbf{E}$-$\mathbf{A}$-$\mathbf{H}$ was due to the symmetry of updating a potential first and then the field in a single half-timestep, so the algorithm updates potential-field-potential-field. However, arbitrary update orders are not allowed for all variables in FiPo. The main restriction is which fields are at n and which are at $n + \frac{1}{2}$. After the timestep update consideration, we must then consider if a variable depends on a value updated at the same timestep. For this reason, $\mathbf{H}$ must be updated before $\mathbf{A}$ in FiPo Hybrid, and it makes sense to keep the update order the same for the same variables in both FiPo algorithms. However, in FiPo Basic, the update order for $\mathbf{H}$ and $\mathbf{A}$ is interchangable just as ϕ and $\mathbf{E}$ are in both FiPo algorithms. The update for the simulation source appears in the update equation for $\mathbf{E}$, but the same timestep for ϕ only receives information from the simulation source at the next timestep. ϕ^{n+1} updates from $\mathbf{A}^{n+\frac{1}{2}}$, $\mathbf{A}^{n+\frac{1}{2}}$ comes from $\mathbf{E}^n$ and ϕ^n, $\mathbf{E}^n$ receives information from the source $\mathbf{J}^{n-\frac{1}{2}}$, so ϕ^{n+1} receives information from $\mathbf{J}^{n-\frac{1}{2}}$ when

it updates. Note, the second-order update equation for ϕ, Equation (4.19), updates ϕ^{n+1} from ρ^n. The discretized continuity equation would act as an update equation for ρ^n from $\mathbf{J}^{n-\frac{1}{2}}$. The FiPo update for ϕ comes from an equivalent source as the update for ϕ in Ryu *et al.* [14].

5.2 Discretization

FiPo's first-order update equations are much simpler to discretize than the second-order equations in Section 4.3. The update equation for discretized ϕ is

$$\phi^{n+1}_{i,j,k} = \phi^{n}_{i,j,k} - \frac{\Delta_t}{\epsilon^2_{i,j,k}\mu_{i,j,k}} \left(\left(\epsilon_{i+\frac{1}{2},j,k} A^{n+\frac{1}{2}}_{x\ i+\frac{1}{2},j,k} - \epsilon_{i-\frac{1}{2},j,k} A^{n+\frac{1}{2}}_{x\ i-\frac{1}{2},j,k} \right) + \left(\epsilon_{i,j+\frac{1}{2},k} A^{n+\frac{1}{2}}_{y\ i,j+\frac{1}{2},k} - \epsilon_{i,j-\frac{1}{2},k} A^{n+\frac{1}{2}}_{y\ i,j-\frac{1}{2},k} \right) + \left(\epsilon_{i,j,k+\frac{1}{2}} A^{n+\frac{1}{2}}_{z\ i,j,k+\frac{1}{2}} - \epsilon_{i,j,k-\frac{1}{2}} A^{n+\frac{1}{2}}_{z\ i,j,k-\frac{1}{2}} \right) \right). \quad (5.12)$$

The update equations for discretized $\mathbf{E}$ components are

$$E^{n+1}_{x\ i+\frac{1}{2},j,k} = CA_{i+\frac{1}{2},j,k} E^{n}_{x\ i+\frac{1}{2},j,k} + CB_{i+\frac{1}{2},j,k} \left[\frac{1}{\Delta_y} \left(H^{n+\frac{1}{2}}_{z\ i+\frac{1}{2},j+\frac{1}{2},k} - H^{n+\frac{1}{2}}_{z\ i+\frac{1}{2},j-\frac{1}{2},k} \right) + \frac{1}{\Delta_z} \left(H^{n+\frac{1}{2}}_{y\ i+\frac{1}{2},j,k-\frac{1}{2}} - H^{n+\frac{1}{2}}_{y\ i+\frac{1}{2},j,k+\frac{1}{2}} \right) \right], \quad (5.13a)$$

$$E^{n+1}_{y\ i,j+\frac{1}{2},k} = CA_{i,j+\frac{1}{2},k} E^{n}_{y\ i,j+\frac{1}{2},k} + CB_{i,j+\frac{1}{2},k} \left[\frac{1}{\Delta_x} \left(H^{n+\frac{1}{2}}_{z\ i-\frac{1}{2},j+\frac{1}{2},k} - H^{n+\frac{1}{2}}_{z\ i+\frac{1}{2},j+\frac{1}{2},k} \right) + \frac{1}{\Delta_z} \left(H^{n+\frac{1}{2}}_{x\ i,j+\frac{1}{2},k+\frac{1}{2}} - H^{n+\frac{1}{2}}_{x\ i,j+\frac{1}{2},k-\frac{1}{2}} \right) \right], \quad (5.13b)$$

$$E^{n+1}_{z\ i,j,k+\frac{1}{2}} = CA_{i,j,k+\frac{1}{2}} E^{n}_{z\ i,j,k+\frac{1}{2}} + CB_{i,j,k+\frac{1}{2}} \left[\frac{1}{\Delta_x} \left(H^{n+\frac{1}{2}}_{y\ i+\frac{1}{2},j,k+\frac{1}{2}} - H^{n+\frac{1}{2}}_{y\ i-\frac{1}{2},j,k+\frac{1}{2}} \right) + \frac{1}{\Delta_y} \left(H^{n+\frac{1}{2}}_{x\ i,j-\frac{1}{2},k+\frac{1}{2}} - H^{n+\frac{1}{2}}_{x\ i,j+\frac{1}{2},k+\frac{1}{2}} \right) \right]. \quad (5.13c)$$

where the coeffiecients are given in Table 5.1.

The update equations for discretized $\mathbf{A}$ components are

$$A^{n+\frac{1}{2}}_{x\ i+\frac{1}{2},j,k} = A^{n-\frac{1}{2}}_{x\ i+\frac{1}{2},j,k} - \Delta_t \left(E^{n}_{x\ i+\frac{1}{2},j,k} + \frac{1}{\Delta_x} \left(\phi^{n}_{i+1,j,k} - \phi^{n}_{i,j,k} \right) \right), \quad (5.14a)$$

Variable	Value	Value with $\sigma = 0$
$CA_{i,j,k}$	$\frac{1-\frac{\sigma_{i,j,k}\Delta_t}{2\epsilon_{i,j,k}}}{1+\frac{\sigma_{i,j,k}\Delta_t}{2\epsilon_{i,j,k}}}$	1
$CB_{i,j,k}$	$\frac{\frac{\Delta_t}{\epsilon_{i,j,k}}}{1+\frac{\sigma_{i,j,k}\Delta_t}{2\epsilon_{i,j,k}}}$	$\frac{\Delta_t}{\epsilon_{i,j,k}}$

Table 5.1: Update coefficients for $\mathbf{E}$ in Equations (5.13)

$$A_{y\ i,j+\frac{1}{2},k}^{n+\frac{1}{2}} = A_{y\ i,j+\frac{1}{2},k}^{n-\frac{1}{2}} - \Delta_t \left(E_{y\ i,j+\frac{1}{2},k}^{n} + \frac{1}{\Delta_y} \left(\phi_{i,j+1,k}^{n} - \phi_{i,j,k}^{n} \right) \right), \tag{5.14b}$$

$$A_{z\ i,j,k+\frac{1}{2}}^{n+\frac{1}{2}} = A_{z\ i,j,k+\frac{1}{2}}^{n-\frac{1}{2}} - \Delta_t \left(E_{z\ i,j,k+\frac{1}{2}}^{n} + \frac{1}{\Delta_z} \left(\phi_{i,j,k+1}^{n} - \phi_{i,j,k}^{n} \right) \right). \tag{5.14c}$$

The update equations for discretized $\mathbf{H}$ components for FiPo Basic are

$$H_{x\ i,j+\frac{1}{2},k+\frac{1}{2}}^{n+\frac{1}{2}} = H_{x\ i,j+\frac{1}{2},k+\frac{1}{2}}^{n-\frac{1}{2}} + \frac{\Delta_t}{\mu_0} \left[\frac{1}{\Delta_y} \left(E_{z\ i,j,k+\frac{1}{2}}^{n} - E_{z\ i,j+1,k+\frac{1}{2}}^{n} \right) + \frac{1}{\Delta_z} \left(E_{y\ i,j+\frac{1}{2},k+1}^{n} - E_{y\ i,j+\frac{1}{2},k}^{n} \right) \right], \tag{5.15a}$$

$$H_{y\ i+\frac{1}{2},j,k+\frac{1}{2}}^{n+\frac{1}{2}} = H_{y\ i+\frac{1}{2},j,k+\frac{1}{2}}^{n-\frac{1}{2}} + \frac{\Delta_t}{\mu_0} \left[\frac{1}{\Delta_x} \left(E_{z\ i+1,j,k+\frac{1}{2}}^{n} - E_{z\ i,j,k+\frac{1}{2}}^{n} \right) + \frac{1}{\Delta_z} \left(E_{x\ i+\frac{1}{2},j,k}^{n} - E_{x\ i+\frac{1}{2},j,k+1}^{n} \right) \right], \tag{5.15b}$$

$$H_{z\ i+\frac{1}{2},j+\frac{1}{2},k}^{n+\frac{1}{2}} = H_{z\ i+\frac{1}{2},j+\frac{1}{2},k}^{n-\frac{1}{2}} + \frac{\Delta_t}{\mu_0} \left[\frac{1}{\Delta_x} \left(E_{z\ i,j,k+\frac{1}{2}}^{n} - E_{z\ i,j+1,k+\frac{1}{2}}^{n} \right) + \frac{1}{\Delta_y} \left(E_{y\ i,j+\frac{1}{2},k+1}^{n} - E_{y\ i,j+\frac{1}{2},k}^{n} \right) \right]. \tag{5.15c}$$

The update equations for discretized $\mathbf{H}$ components for FiPo Hybrid are

$$H_{x\ i,j+\frac{1}{2},k+\frac{1}{2}}^{n+\frac{1}{2}} = \frac{1}{\mu_0} \left[\frac{1}{\Delta_y} \left(A_{z\ i,j+1,k+\frac{1}{2}}^{n+\frac{1}{2}} - A_{z\ i,j,k+\frac{1}{2}}^{n+\frac{1}{2}} \right) + \frac{1}{\Delta_z} \left(A_{y\ i,j+\frac{1}{2},k}^{n+\frac{1}{2}} - A_{y\ i,j+\frac{1}{2},k+1}^{n+\frac{1}{2}} \right) \right], \tag{5.16a}$$

$$H_{y\ i+\frac{1}{2},j,k+\frac{1}{2}}^{n+\frac{1}{2}} = \frac{1}{\mu_0} \left[\frac{1}{\Delta_x} \left(A_{z\ i,j,k+\frac{1}{2}}^{n+\frac{1}{2}} - A_{z\ i+1,j,k+\frac{1}{2}}^{n+\frac{1}{2}} \right) + \frac{1}{\Delta_z} \left(A_{x\ i+\frac{1}{2},j,k+1}^{n+\frac{1}{2}} - A_{x\ i+\frac{1}{2},j,k}^{n+\frac{1}{2}} \right) \right], \tag{5.16b}$$

$$H_{z\ i+\frac{1}{2},j+\frac{1}{2},k}^{n+\frac{1}{2}} = \frac{1}{\mu_0}\left[\frac{1}{\Delta_x}\left(A_{y\ i+1,j+\frac{1}{2},k}^{n+\frac{1}{2}} - A_{y\ i,j+\frac{1}{2},k}^{n+\frac{1}{2}}\right) + \frac{1}{\Delta_y}\left(A_{x\ i+\frac{1}{2},j,k}^{n+\frac{1}{2}} - A_{x\ i+\frac{1}{2},j+1,k}^{n+\frac{1}{2}}\right)\right]. \tag{5.16c}$$

5.3 Results

In order to test the FiPo a algorithm, we simulated a differentiated Gaussian pulse in free space ($\epsilon_r = 1$, $\sigma = 0$). The z-component of the current density is located at the center of the simulation and can be expressed as

$$J_z(t) = -J_0 \frac{t - t_0}{t_w} e^{-\frac{t-t_0}{t_w}^2} \tag{5.17}$$

where t_0 adjusts pulse start time, t_w adjusts the duration the pulse, and the coefficient J_0 is an adjustment to the magnitude of the current-density source.

For this simulation, we chose a pulse width that corresponds to a 6 GHz bandwidth $t_w = (\pi\text{bandwidth})^{-1} = 0.053052$ ns and $t_0 = 4t_w \approx 0.21$ ns. The simulation was run on a $300 \times 300 \times 300$ grid with $\Delta_x = \Delta_y = \Delta_z = 1$ mm for a total of 2000 timesteps with dt calculated to be smaller than the stability condition as $\Delta_t = 0.9/(c\sqrt{(\Delta_x^{-2} + \Delta_y^{-2} + \Delta_z^{-2})}) \approx 1.73$ ps. J_0 is defined as 2.0×10^{-3}, where the factor of two comes from the differentiation of the Gaussian. Since J_z is a source for E_z, our main magnetic field components should be in H_x and H_y. Additionally, we should see the largest $\mathbf{A}$ values for A_z, the same directional component as $\mathbf{E}$ field, and ϕ. Figure 5.2 shows pulse for these fields and potentials at $t = 300\Delta_t \approx 0.52$ ns for FiPo Basic. Results for FiPo Basic and FiPo Hybrid appear the same for the simulation with reflective boundaries.

In Figure 5.2, we can see the propagation characteristics are the same for both FiPo Basic and FiPo Hybrid simulations. For both simulations, the wave propagates symmetrically outwards from the source in the center of the simulation. Since the results for the simualtions are identical for both methods, Figure 5.3 shows a later timestep of only the FiPo Basic simulation after the wavefront has reached and reflected from the outer boundary of the simulation. The simulation appears to remain stable after reflection, indicating field indices at the boundary are implemented correctly. These results show our set of first order equations propagate waves as expected.

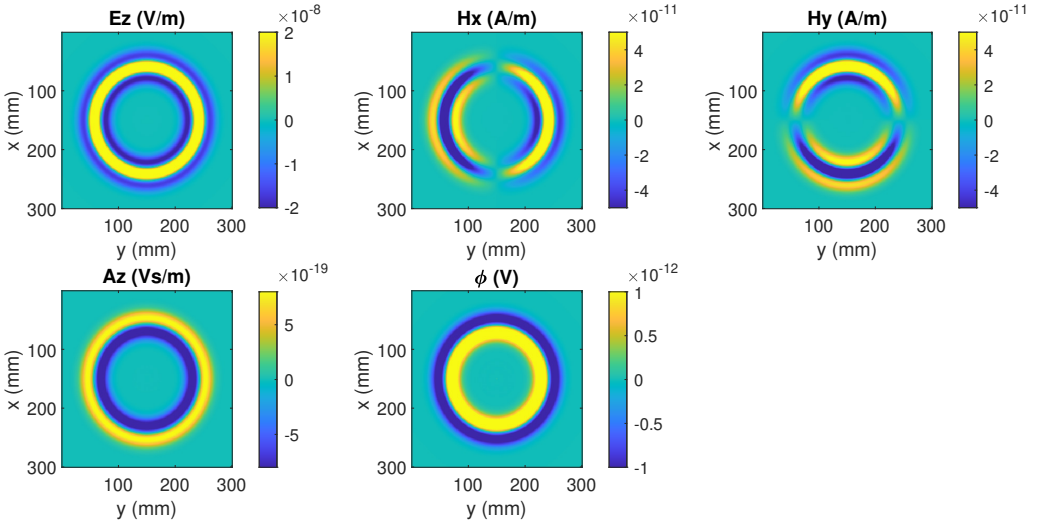

(a) FiPo Basic

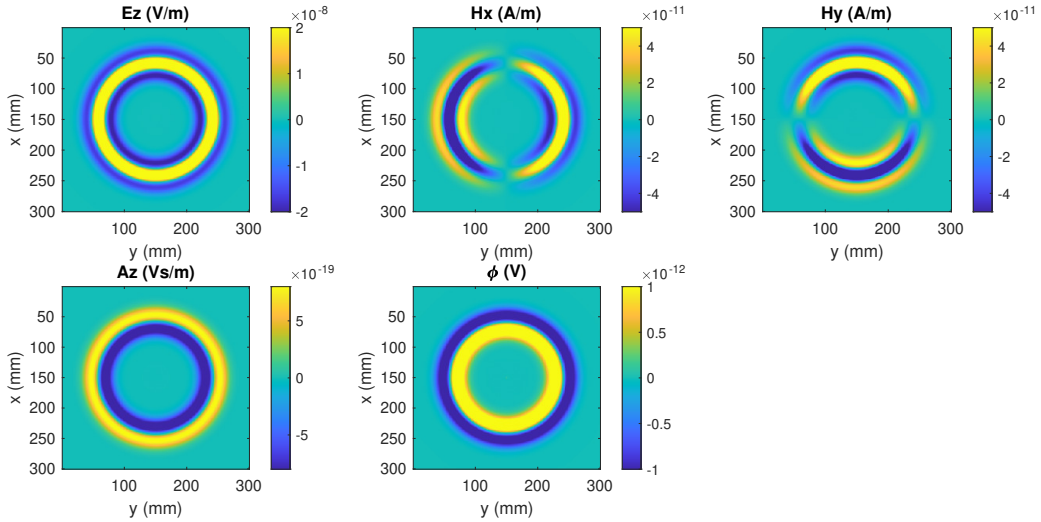

(b) FiPo Hybrid

Figure 5.2: Spatial profile of (top row) E_x, H_x, and H_y, as well as (bottom row) A_z and ϕ for a differentiated Gaussian current source from Eq. (5.17) at time $t = 0.52$ ns ($300\Delta_t$ or $9.801t_w$) after start of the simulation.

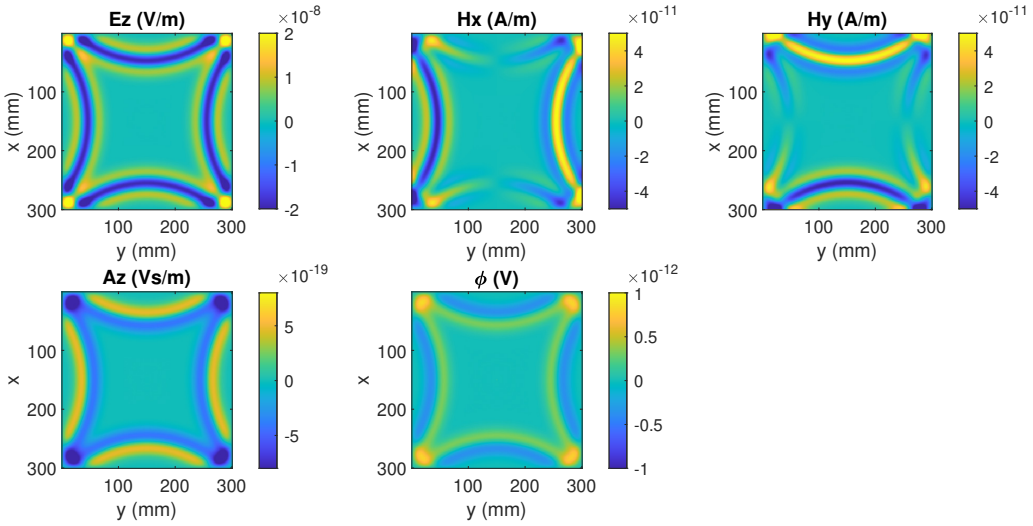

Figure 5.3: Spatial profile of (top row) E_x, H_x, and H_y, as well as (bottom row) A_z and ϕ for a differentiated Gaussian current source from Eq. (5.17) at time $t = 0.87$ ns ($500\Delta_t$ or $16.335t_w$) after start of the FiPo Basic simulation.

5.4 Implementation

One difficulty with implementation is knowing where to define fields and potentials. We know spatially where they are located on the Yee grid, but we also need to know how to properly terminate our simulation boundary with our defined fields. A table with fields and potentials with respective positions on the Yee grid, update timestep, array size, and range of updates for the variable are given in Table 5.2.

Correctly defining the boundary is important. We choose the values on the boundary such that integer indices are located on the boundary. This has implications for defining array sizes. Anything with an integer index will have n_i grid points. Anything with a half-integer index will have $n_i - 1$ grid points since they lie in between integer grid points, and integer grid points are on the boundary.

A variable with a integer-index in a direction will be on the boundary for that direction, and is set to zero for reflecting boundary conditions. In a direction of an integer-index, the updates are restricted to $2 : n_i - 1$ to avoid rewriting the boundary. For the variable ϕ, all indices are integers, so it is defined from $1 : n_i$ in all directions and updates inside the boundary from $2 : n_i$. For E_i, the dimension for i is a half-integer, so we will can use the range $1 : n_i$ in the i-direction without overwriting our boundary condition. However, if we take into account array size since it's a half-integer, it is only defined for $1 : n_i - 1$, so those are our update bounds. For the rest, we need to avoid updating beyond the boundary, so they are $2 : n_i - 1$. Since $\mathbf{A}$ is defined at the same grid points as $\mathbf{E}$, the update ranges are the same. For $\mathbf{H}$, we follow the same pattern, but two indices are half-integers and one is integer and on the boundary.

Field	Array Size	Update Range
$\phi^n_{i,j,k}$	n_x, n_y, n_z	$2:n_x-1, 2:n_y-1, 2:n_z-1$
$E^n_{x\ i+\frac{1}{2},j,k}$	n_x-1, n_y, n_z	$1:n_x-1, 2:n_y-1, 2:n_z-1$
$E^n_{y\ i,j+\frac{1}{2},k}$	n_x, n_y-1, n_z	$2:n_x-1, 1:n_y-1, 2:n_z-1$
$E^n_{z\ i,j,k+\frac{1}{2}}$	n_x, n_y, n_z-1	$2:n_x-1, 2:n_y-1, 1:n_z-1$
$A^{n+\frac{1}{2}}_{x\ i+\frac{1}{2},j,k}$	n_x-1, n_y, n_z	$1:n_x-1, 2:n_y-1, 2:n_z-1$
$A^{n+\frac{1}{2}}_{y\ i,j+\frac{1}{2},k}$	n_x, n_y-1, n_z	$2:n_x-1, 1:n_y-1, 2:n_z-1$
$A^{n+\frac{1}{2}}_{z\ i,j,k+\frac{1}{2}}$	n_x, n_y, n_z-1	$2:n_x-1, 2:n_y-1, 1:n_z-1$
$H^{n+\frac{1}{2}}_{x\ i,j+\frac{1}{2},k+\frac{1}{2}}$	n_x, n_y-1, n_z-1	$2:n_x-1, 1:n_y-1, 1:n_z-1$
$H^{n+\frac{1}{2}}_{y\ i+\frac{1}{2},j,k+\frac{1}{2}}$	n_x-1, n_y, n_z-1	$1:n_x-1, 2:n_y-1, 1:n_z-1$
$H^{n+\frac{1}{2}}_{z\ i+\frac{1}{2},j+\frac{1}{2},k}$	n_x-1, n_y-1, n_z	$1:n_x-1, 1:n_y-1, 2:n_z-1$

Table 5.2: Update ranges for FDTD loops and array sizes for fields and potentials updated at the specified time and position on the Yee grid.

Chapter 6

Perfectly Matched Layer Absorbing Boundary Conditions

In order to simulate structures in a finite domain, absorbing boundary conditions are necessary to minimize reflection error. Reflection error happens when waves travel to the boundary of the simulation and reflect back into the simulation domain. A perfectly matched layer (PML) absorbing boundary layer is a layer of cells generally placed next to the boundary of the simulation that acts as a material that ”matches” the one in the simulation domain but is designed to absorb waves. This ”matching” paired with gradual varying of the material properties in the PML allows the wave to enter and be absorbed without the reflections associated with an abrupt change of material properties.

Many PML methods have been formulated for FDTD since the original formulation of PML in Berenger's split-field PML method [57, 58, 59, 60, 44]. Chew and Weedon formulated a stretched-coordinate formalism for PML, which is a compact formalism to write Berenger's split-field [61]. Uniaxial PML (UPML) [62, 63], another common method, has been shown to have equivalent reflection error to Berenger's split-field PML [44, 64]. The convolutional PML (CPML) method has lower reflection error and is more efficient than the above methods [44]. CPML uses the recursive convolution (RC) technique to handle convolution, and is widely used and efficient, so we will implement a CPML for our first order equations [56, 65, 44]. Both the auxiliary differential equation (ADE) [66, 67] and piecewise linear recursive convolution (PLRC) [68, 69] are similar methods capable of handling the convolution and are used to model dispersive media [44]. Higher-order CPML, a CPML with additional auxiliary variables, is able to reduce the error with respect to the original CPML formulation and could be used to lower reflection error as an extension to CPML [70].

6.1 Stretched Coordinate Derivation

Stretched coordinates are a common formalism to describe how PMLs absorb [61, 71]. Introducing a stretched coordinate allows us to have Maxwell's equations within a PML medium but have them look like standard Maxwell's equations just in a complex coordinate system. In order to introduce this formalism for potentials, we start with the frequency-domain update equations for both FiPo Hybrid and FiPo Basic

$$j\omega\epsilon^2\mu\phi = -\nabla\cdot(\epsilon\mathbf{A}), \tag{6.1a}$$

$$j\omega\epsilon\mathbf{E} = \nabla\times\mathbf{H}, \tag{6.1b}$$

$$j\omega\mathbf{A} = -\mathbf{E} - \nabla\phi, \tag{6.1c}$$

$$j\omega\mu\mathbf{H} = -\nabla\times\mathbf{E}, \tag{6.1d}$$

$$\mu\mathbf{H} = \nabla\times\mathbf{A}. \tag{6.1e}$$

Notice that in Equations (6.1a)-(6.1a), no current density has been introduced yet. In order for fields and potentials to decay in the PML, our system must contain a physical mechanism for fields and potentials to be absorbed. Electric current density $\mathbf{J}^E$ contains information about how electric charges move over time. These charges regulate how the electric field is absorbed and decays. In order for the PML to cause fields to decay, we must introduce analagous ficticious charges for both fields and potentials, meaing we must introduce terms for current densities for these charges. We include the real electric current density $\mathbf{J}^E$ and the commonly used, but ficticious, magnetic current density $\mathbf{M} = \mathbf{J}^H$. Here, we introduce the idea of two additional ficticious quantities: the magnetic vector potential current density $\mathbf{J}^A$ and electric potential current density $\mathbf{J}^\phi$. We do not add a ficticious current density to the $\mathbf{H}$ update equation for FiPo Hybrid, Equation (6.1e), since $\mathbf{J}^H$ contains information about how the ficticious magnetic charges move over time, and there is no time derivative acting on $\mathbf{H}$.

$$j\omega\epsilon^2\mu\phi = -\nabla\cdot(\epsilon\mathbf{A}) - J^{\phi}, \tag{6.2a}$$

$$j\omega\epsilon\mathbf{E} = \nabla\times\mathbf{H} - \mathbf{J}^{E}, \tag{6.2b}$$

$$j\omega\mathbf{A} = -\mathbf{E} - \nabla\phi - \mathbf{J}^{A}, \tag{6.2c}$$

$$j\omega\mu\mathbf{H} = -\nabla\times\mathbf{E} - \mathbf{J}^{H}, \tag{6.2d}$$

$$\mu\mathbf{H} = \nabla\times\mathbf{A}. \tag{6.2e}$$

Next, we need to split fields into components for stretched coordinates s_x, s_y, s_z like in [61]. This is done in order for absorption in each direction to be handled separately. The components added together should return the original field

$$\phi = \phi_{s_x} + \phi_{s_y} + \phi_{s_z}, \tag{6.3a}$$

$$\mathbf{E} = \mathbf{E}_{s_x} + \mathbf{E}_{s_y} + \mathbf{E}_{s_z}, \tag{6.3b}$$

$$\mathbf{A} = \mathbf{A}_E + A_{s_x}\hat{x} + A_{s_y}\hat{y} + A_{s_z}\hat{z}, \tag{6.3c}$$

$$\mathbf{H} = \mathbf{H}_{s_x} + \mathbf{H}_{s_y} + \mathbf{H}_{s_z}, \tag{6.3d}$$

$$\mathbf{H} = \mathbf{H}_{s_x} + \mathbf{H}_{s_y} + \mathbf{H}_{s_z}. \tag{6.3e}$$

Notice that Equation (6.3c) contains the extra term $\mathbf{A}_E$. This difference is due to Equation (6.2c) containing a term with $\mathbf{E}$ with no derivative. Stretched coordinates act with the derivative operator, and with no operator present, the coordinate cannot be stretched. Equation (6.3c) is unique in ing this term because $\mathbf{A}$ and $\mathbf{E}$ are offset in time but not position, so the value for $\mathbf{E}$ doesn't need to be stretched since it is colocated with $\mathbf{A}$ on the lattice. This concept could also be considered in terms of thinking of current densities as movement of charges over time. Since the value for $\mathbf{E}$ and $\mathbf{A}$ are located at the same position, the charges are not moving, meaning the part of $\mathbf{A}$ related to $\mathbf{E}$ doesn't contain information on moving charges.

Using the components from Equations (6.3a)-(6.3e), the component-separated Equations (6.2a)-(6.2e) can be written as

$$j\omega\epsilon^2\mu\phi_{s_x} = -\partial_x(\epsilon A_x) - J^{\phi}_{s_x}, \tag{6.4a}$$

$$j\omega\epsilon^2\mu\phi_{s_y} = -\partial_y(\epsilon A_y) - J^{\phi}_{s_y}, \tag{6.4b}$$

$$j\omega\epsilon^2\mu\phi_{s_z} = -\partial_z(\epsilon A_z) - J^{\phi}_{s_z}, \tag{6.4c}$$

$$j\omega\epsilon\mathbf{E}_{s_x} = \partial_x\hat{\mathbf{x}} \times \mathbf{H} - \mathbf{J}^{E}_{s_x}, \tag{6.4d}$$

$$j\omega\epsilon\mathbf{E}_{s_y} = \partial_y\hat{\mathbf{y}} \times \mathbf{H} - \mathbf{J}^{E}_{s_y}, \tag{6.4e}$$

$$j\omega\epsilon\mathbf{E}_{s_z} = \partial_z\hat{\mathbf{z}} \times \mathbf{H} - \mathbf{J}^{E}_{s_z}, \tag{6.4f}$$

$$j\omega\mathbf{A}_E = -\mathbf{E}, \tag{6.4g}$$

$$j\omega A_{s_x} = -\partial_x\phi - J^{A}_{s_x}, \tag{6.4h}$$

$$j\omega A_{s_y} = -\partial_y\phi - J^{A}_{s_y}, \tag{6.4i}$$

$$j\omega A_{s_z} = -\partial_z\phi - J^{A}_{s_z}, \tag{6.4j}$$

$$j\omega\epsilon\mathbf{H}_{s_x} = -\partial_x\hat{\mathbf{x}} \times \mathbf{E} - \mathbf{J}^{H}_{s_x}, \tag{6.4k}$$

$$j\omega\epsilon\mathbf{H}_{s_y} = -\partial_y\hat{\mathbf{y}} \times \mathbf{E} - \mathbf{J}^{H}_{s_y}, \tag{6.4l}$$

$$j\omega\epsilon\mathbf{H}_{s_z} = -\partial_z\hat{\mathbf{z}} \times \mathbf{E} - \mathbf{J}^{H}_{s_z}, \tag{6.4m}$$

$$\mu\mathbf{H}_{s_x} = \partial_x\hat{\mathbf{x}} \times \mathbf{A}, \tag{6.4n}$$

$$\mu\mathbf{H}_{s_y} = \partial_y\hat{\mathbf{y}} \times \mathbf{A}, \tag{6.4o}$$

$$\mu\mathbf{H}_{s_z} = \partial_z\hat{\mathbf{z}} \times \mathbf{A}. \tag{6.4p}$$

Since we now have information in the equations on how the charges move in each direction of the PML, we can introduce how they decay. Electric conductivity represents material absorption of electric field, we can use this property to introduce a lossy medium and absorb the field. We need analogous material properties for the all fields and potentials in order to absorb them as well. Here we introduce a lossy medium with conductivity σ^E, magnetic loss σ^H, magnetic vector potential loss σ^A, and electric potential loss σ^ϕ such that $\vec{J}^E = \sigma^E\vec{E}$, $\vec{M} = \vec{J}^H = \sigma^H\vec{H}$, $\vec{J}^A = \sigma^A\vec{A}$, and

$J^{\phi} = \sigma^{\phi}\phi$. We can put these relations into Equations (6.4a)-(6.4p) to obtain

$$j\omega\epsilon^2\mu\phi_{s_x} = -\partial_x(\epsilon A_x) - \sigma_x^{\phi}\phi_{s_x}, \tag{6.5a}$$

$$j\omega\epsilon^2\mu\phi_{s_y} = -\partial_y(\epsilon A_y) - \sigma_y^{\phi}\phi_{s_y}, \tag{6.5b}$$

$$j\omega\epsilon^2\mu\phi_{s_z} = -\partial_z(\epsilon A_z) - \sigma_z^{\phi}\phi_{s_z}, \tag{6.5c}$$

$$j\omega\epsilon\mathbf{E}_{s_x} = \partial_x\hat{\mathbf{x}} \times \mathbf{H} - \sigma_x^{E}\mathbf{E}_{s_x}, \tag{6.5d}$$

$$j\omega\epsilon\mathbf{E}_{s_y} = \partial_y\hat{\mathbf{y}} \times \mathbf{H} - \sigma_y^{E}\mathbf{E}_{s_y}, \tag{6.5e}$$

$$j\omega\epsilon\mathbf{E}_{s_z} = \partial_z\hat{\mathbf{z}} \times \mathbf{H} - \sigma_z^{E}\mathbf{E}_{s_z}, \tag{6.5f}$$

$$j\omega\mathbf{A}_E = -\mathbf{E}, \tag{6.5g}$$

$$j\omega\mathbf{A}_{s_x} = -\partial_x\phi - \sigma_x^{A}\mathbf{A}_{s_x}, \tag{6.5h}$$

$$j\omega\mathbf{A}_{s_y} = -\partial_y\phi - \sigma_y^{A}\mathbf{A}_{s_y}, \tag{6.5i}$$

$$j\omega\mathbf{A}_{s_z} = -\partial_z\phi - \sigma_z^{A}\mathbf{A}_{s_z}, \tag{6.5j}$$

$$j\omega\epsilon\mathbf{H}_{s_x} = -\partial_x\hat{\mathbf{x}} \times \mathbf{E} - \sigma_x^{H}\mathbf{H}_{s_x}, \tag{6.5k}$$

$$j\omega\epsilon\mathbf{H}_{s_y} = -\partial_y\hat{\mathbf{y}} \times \mathbf{E} - \sigma_y^{H}\mathbf{H}_{s_y}, \tag{6.5l}$$

$$j\omega\epsilon\mathbf{H}_{s_z} = -\partial_z\hat{\mathbf{z}} \times \mathbf{E} - \sigma_z^{H}\mathbf{H}_{s_z}, \tag{6.5m}$$

$$\mu\mathbf{H}_{s_x} = \partial_x\hat{\mathbf{x}} \times \mathbf{A}, \tag{6.5n}$$

$$\mu\mathbf{H}_{s_y} = \partial_y\hat{\mathbf{y}} \times \mathbf{A}, \tag{6.5o}$$

$$\mu\mathbf{H}_{s_z} = \partial_z\hat{\mathbf{z}} \times \mathbf{A}. \tag{6.5p}$$

In order to give the stretched coordinate a similar form in all equations, we introduce values of κ^K where $K = E, H, A,$ or ϕ. For $\mathbf{E}$ and $\mathbf{H}$ these values have physical meanings - κ^E is the relative electric permittivity and κ^H is the relative magnetic permeability. The analogous values we introduce for $\mathbf{A}$ and ϕ don't have the same direct physical meaning but are denoted κ^A and κ^{ϕ}. Values of κ^K written in terms of materials properties are $\epsilon = \epsilon_0\kappa^E$, $\mu = \mu_0\kappa^H$, $1 = \kappa^A$, and $\epsilon^2\mu = \epsilon_0^2\mu_0\kappa^{\phi}$. We know that the physically, higher values of relative permittivity κ^E slow the propagation of the electric field in a material. Higher values for the relative permeability κ^H also slow the propagation of the magnetic field in a material. This tells us that increases in κ^K, as a

material property, slows the propagation of the wave for the value it corresponds to. In the PML, defining a κ^K is beneficial because by slowing the wave, the wave spends more time in the lossy region in which the wave decays. However, if κ^K changes abruptly, there is risk of reflections at the boundary. We can simplify Equations (6.5a)-(6.5p) by moving the conductivity term to the left

side and introducing κ

$$\epsilon_0^2\mu_0 j\omega\left(\kappa_x^\phi + \frac{\sigma_x^\phi}{j\omega\epsilon_0^2\mu_0}\right)\phi_{s_x} = -\partial_x(\epsilon A_x), \tag{6.6a}$$

$$\epsilon_0^2\mu_0 j\omega\left(\kappa_y^\phi + \frac{\sigma_y^\phi}{j\omega\epsilon_0^2\mu_0}\right)\phi_{s_y} = -\partial_y(\epsilon A_y), \tag{6.6b}$$

$$\epsilon_0^2\mu_0 j\omega\left(\kappa_z^\phi + \frac{\sigma_z^\phi}{j\omega\epsilon_0^2\mu_0}\right)\phi_{s_z} = -\partial_z(\epsilon A_z), \tag{6.6c}$$

$$\epsilon_0 j\omega\left(\kappa_x^E + \frac{\sigma_x^E}{j\omega\epsilon_0}\right)\mathbf{E}_{s_x} = \partial_x\hat{\mathbf{x}}\times\mathbf{H}, \tag{6.6d}$$

$$\epsilon_0 j\omega\left(\kappa_y^E + \frac{\sigma_y^E}{j\omega\epsilon_0}\right)\mathbf{E}_{s_y} = \partial_y\hat{\mathbf{y}}\times\mathbf{H}, \tag{6.6e}$$

$$\epsilon_0 j\omega\left(\kappa_z^E + \frac{\sigma_z^E}{j\omega\epsilon_0}\right)\mathbf{E}_{s_z} = \partial_z\hat{\mathbf{z}}\times\mathbf{H}, \tag{6.6f}$$

$$j\omega\mathbf{A}_E = -\mathbf{E}, \tag{6.6g}$$

$$j\omega\left(\kappa_x^A + \frac{\sigma_x^A}{j\omega}\right)\mathbf{A}_{s_x} = -\partial_x\phi, \tag{6.6h}$$

$$j\omega\left(\kappa_y^A + \frac{\sigma_y^A}{j\omega}\right)\mathbf{A}_{s_y} = -\partial_y\phi, \tag{6.6i}$$

$$j\omega\left(\kappa_z^A + \frac{\sigma_z^A}{j\omega}\right)\mathbf{A}_{s_z} = -\partial_z\phi, \tag{6.6j}$$

$$\mu_0 j\omega\left(\kappa_x^H + \frac{\sigma_x^H}{j\omega\mu_0}\right)\mathbf{H}_{s_x} = -\partial_x\hat{\mathbf{x}}\times\mathbf{E}, \tag{6.6k}$$

$$\mu_0 j\omega\left(\kappa_y^H + \frac{\sigma_y^H}{j\omega\mu_0}\right)\mathbf{H}_{s_y} = -\partial_y\hat{\mathbf{y}}\times\mathbf{E}, \tag{6.6l}$$

$$\mu_0 j\omega\left(\kappa_z^H + \frac{\sigma_z^H}{j\omega\mu_0}\right)\mathbf{H}_{s_z} = -\partial_z\hat{\mathbf{z}}\times\mathbf{E}, \tag{6.6m}$$

$$\mu\mathbf{H}_{s_x} = \partial_x\hat{\mathbf{x}}\times\mathbf{A}, \tag{6.6n}$$

$$\mu\mathbf{H}_{s_y} = \partial_y\hat{\mathbf{y}}\times\mathbf{A}, \tag{6.6o}$$

$$\mu\mathbf{H}_{s_z} = \partial_z\hat{\mathbf{z}}\times\mathbf{A}. \tag{6.6p}$$

Here, we introduce the definition for stretched coordinate. The variable terms for s_ν^E include the electric permittivity and the conductivity.

$$s_\nu^\phi = \kappa_\nu^\phi + \frac{\sigma_\nu^\phi}{j\omega\epsilon_0^2\mu_0}, \quad \nu = x, y, z, \tag{6.7a}$$

$$s_\nu^E = \kappa_\nu^E + \frac{\sigma_\nu^E}{j\omega\epsilon_0}, \quad \nu = x, y, z, \tag{6.7b}$$

$$s_\nu^A = \kappa_\nu^A + \frac{\sigma_\nu^A}{j\omega}, \quad \nu = x, y, z, \tag{6.7c}$$

$$s_\nu^H = \kappa_\nu^H + \frac{\sigma_\nu^H}{j\omega\mu_0}, \quad \nu = x, y, z. \tag{6.7d}$$

Now, we introduce the stretched coordinate into our equations and move the stretched coordinate term to the side with the spatial derivative.

$$\epsilon^2 \mu j\omega \phi_{s_x} = -\frac{1}{s_x^\phi} \partial_x \left(\epsilon A_x\right), \tag{6.8a}$$

$$\epsilon^2 \mu j\omega \phi_{s_y} = -\frac{1}{s_y^\phi} \partial_y \left(\epsilon A_y\right), \tag{6.8b}$$

$$\epsilon^2 \mu j\omega \phi_{s_z} = -\frac{1}{s_z^\phi} \partial_z \left(\epsilon A_z\right), \tag{6.8c}$$

$$\epsilon j\omega \mathbf{E}_{s_x} = \frac{1}{s_x^E} \partial_x \hat{\mathbf{x}} \times \mathbf{H}, \tag{6.8d}$$

$$\epsilon j\omega \mathbf{E}_{s_y} = \frac{1}{s_y^E} \partial_y \hat{\mathbf{y}} \times \mathbf{H}, \tag{6.8e}$$

$$\epsilon j\omega \mathbf{E}_{s_z} = \frac{1}{s_z^E} \partial_z \hat{\mathbf{z}} \times \mathbf{H}, \tag{6.8f}$$

$$j\omega \mathbf{A}_E = -\mathbf{E}, \tag{6.8g}$$

$$j\omega \mathbf{A}_{s_x} = -\frac{1}{s_x^A} \partial_x \phi, \tag{6.8h}$$

$$j\omega \mathbf{A}_{s_y} = -\frac{1}{s_y^A} \partial_y \phi, \tag{6.8i}$$

$$j\omega \mathbf{A}_{s_z} = -\frac{1}{s_z^A} \partial_z \phi, \tag{6.8j}$$

$$\epsilon j\omega \mathbf{H}_{s_x} = -\frac{1}{s_x^H} \partial_x \hat{\mathbf{x}} \times \mathbf{E}, \tag{6.8k}$$

$$\epsilon j\omega \mathbf{H}_{s_y} = -\frac{1}{s_y^H} \partial_y \hat{\mathbf{y}} \times \mathbf{E}, \tag{6.8l}$$

$$\epsilon j\omega \mathbf{H}_{s_z} = -\frac{1}{s_z^H} \partial_z \hat{\mathbf{z}} \times \mathbf{E}, \tag{6.8m}$$

$$\mu \mathbf{H}_{s_x} = \partial_x \hat{\mathbf{x}} \times \mathbf{A}, \tag{6.8n}$$

$$\mu \mathbf{H}_{s_y} = \partial_y \hat{\mathbf{y}} \times \mathbf{A}, \tag{6.8o}$$

$$\mu \mathbf{H}_{s_z} = \partial_z \hat{\mathbf{z}} \times \mathbf{A}. \tag{6.8p}$$

From here, we can recombine the field components into the full fields in terms of the stretched coordinate. We want to see this form of the stretched coordinate because all operators $\frac{1}{s_i^K}$ are paired with a spatial derivate ∂_i. In this form, applying the stretched coordinate is like making an adjustment to the spatial derivate operator.

$$\epsilon^2 \mu j\omega\phi = -\frac{1}{s_x^\phi}\partial_x(\epsilon A_x) - \frac{1}{s_y^\phi}\partial_y(\epsilon A_y) - \frac{1}{s_z^\phi}\partial_z(\epsilon A_z), \tag{6.9a}$$

$$\epsilon j\omega \mathbf{E}_{s_x} = \frac{1}{s_x^E}\partial_x \hat{\mathbf{x}} \times \mathbf{H} + \frac{1}{s_y^E}\partial_y \hat{\mathbf{y}} \times \mathbf{H} + \frac{1}{s_z^E}\partial_z \hat{\mathbf{z}} \times \mathbf{H}, \tag{6.9b}$$

$$j\omega \mathbf{A}_E = -\mathbf{E} - \frac{1}{s_x^A}\partial_x\phi - \frac{1}{s_y^A}\partial_y\phi - \frac{1}{s_z^A}\partial_z\phi, \tag{6.9c}$$

$$\epsilon j\omega \mathbf{H}_{s_x} = -\frac{1}{s_x^H}\partial_x \hat{\mathbf{x}} \times \mathbf{E} - \frac{1}{s_y^H}\partial_y \hat{\mathbf{y}} \times \mathbf{E} - \frac{1}{s_z^H}\partial_z \hat{\mathbf{z}} \times \mathbf{E}, \tag{6.9d}$$

$$\mu \mathbf{H}_{s_x} = \partial_x \hat{\mathbf{x}} \times \mathbf{A} + \partial_y \hat{\mathbf{y}} \times \mathbf{A} + \partial_z \hat{\mathbf{z}} \times \mathbf{A}. \tag{6.9e}$$

We can define a streched coordinate form of the operater ∇ as

$$\nabla_s^K = \frac{1}{s_x^K}\partial_x \hat{\mathbf{x}} + \frac{1}{s_y^K}\partial_y \hat{\mathbf{y}} + \frac{1}{s_z^K}\partial_z \hat{\mathbf{z}}. \tag{6.10}$$

This leaves us with FiPo equations with stretched coordinate operators in the frequency domain

$$j\omega\epsilon^2\mu\phi = -\nabla_s^\phi \cdot (\epsilon \mathbf{A}), \tag{6.11a}$$

$$j\omega\epsilon \mathbf{E} = \nabla_s^E \times \mathbf{H}, \tag{6.11b}$$

$$j\omega \mathbf{A} = -\mathbf{E} - \nabla_s^A \phi, \tag{6.11c}$$

$$j\omega\mu \mathbf{H} = -\nabla_s^H \times \mathbf{E}, \tag{6.11d}$$

$$\mu \mathbf{H} = \nabla \times \mathbf{A}. \tag{6.11e}$$

From here, we can introduce the stretched coordinate used in [56]. A shift in the frequency-dependent pole was introduced by [72] and aids in the absorption of evanescent waves. Evanescent waves are a source of numerical error in the PML [73]. We introduce an α in our stretched coordinates for each quantity

$$s_\nu^\phi = \kappa_\nu^\phi + \frac{\sigma_\nu^\phi}{\alpha^\phi + j\omega\epsilon_0^2\mu_0}, \nu = x, y, z, \tag{6.12a}$$

$$s_\nu^E = \kappa_\nu^E + \frac{\sigma_\nu^E}{\alpha^E + j\omega\epsilon_0}, \nu = x, y, z, \tag{6.12b}$$

$$s_\nu^A = \kappa_\nu^A + \frac{\sigma_\nu^A}{\alpha^A + j\omega}, \nu = x, y, z, \tag{6.12c}$$

$$s_\nu^H = \kappa_\nu^H + \frac{\sigma_\nu^H}{\alpha^H + j\omega\mu_0}, \nu = x, y, z. \tag{6.12d}$$

We can simplify the above to the complex frequency-shifted (CFS) tensor coefficient [60, 56, 44],

$$s_\nu^K = \kappa_\nu^K + \frac{\bar{\sigma_\nu}^K}{\bar{\alpha}^K + j\omega}, \quad \nu = x, y, z, \tag{6.13}$$

where we define bar values as

$$\bar{\sigma_\nu}^\phi = \frac{\sigma_\nu^\phi}{\epsilon_0^2\mu_0}, \tag{6.14a}$$

$$\bar{\sigma_\nu}^E = \frac{\sigma_\nu^E}{\epsilon_0}, \tag{6.14b}$$

$$\bar{\sigma_\nu}^H = \frac{\sigma_\nu^H}{\mu_0}, \tag{6.14c}$$

$$\bar{\sigma_\nu}^A = \sigma_\nu^A, \tag{6.14d}$$

$$\bar{\alpha_\nu}^\phi = \frac{\alpha_\nu^\phi}{\epsilon_0^2\mu_0}, \tag{6.14e}$$

$$\bar{\alpha_\nu}^E = \frac{\alpha_\nu^E}{\epsilon_0}, \tag{6.14f}$$

$$\bar{\alpha_\nu}^H = \frac{\alpha_\nu^H}{\mu_0}, \tag{6.14g}$$

$$\bar{\alpha_\nu}^A = \alpha_\nu^A. \tag{6.14h}$$

A PML using the CFS tensor coefficient in the stretched coordinate is typically called a CFS-PML.

One thing to also note is that FiPo Hybrid equations imply the following vector identity:

$$\nabla_s^K \cdot \nabla \times \mathbf{A} = 0. \tag{6.15}$$

The identity in Equation (6.15) should hold because we can expand this relation to be

$$\frac{1}{s^K}(\nabla \cdot \nabla \times \mathbf{A}) = 0 \tag{6.16}$$

where $\nabla \cdot \nabla \times \mathbf{A} = 0$ is a known vector identity.

6.2 Convolutional Perfectly Matched Layer (CPML) Derivation

Since we understand how coordinate stretching relates to our new FDTD update equaions, we are able to derive a PML absorbing boundary layer to attenuate the fields and potentials. We will derive the update equations for a convolutional PML (CPML) [56]. The CPML in [56] was originally formulated for fields, but we show that this method can also be applied to potentials.

The stretched coordinate for a CFS-PML in frequency-domain is given in Equation (6.13) as

$$s_\nu^K = \kappa_\nu^K + \frac{\bar{\sigma_\nu}^K}{\bar{\alpha}^K + j\omega}, \quad \nu = x, y, z, \tag{6.17}$$

where K denotes which field or potential $\mathbf{E}, \mathbf{H}, \mathbf{A}$, or ϕ the values $\kappa, \bar{\sigma}$, and $\bar{\alpha}$ relate to. Taking the inverse Fourier transform, as in [56], we can utilize Laplace transform theory to obtain

$$\bar{s}_\nu^K(t) = \frac{\delta(t)}{\kappa_\nu^K} - \frac{\bar{\sigma}_\nu^K}{(\kappa_\nu^K)^2} \exp\left[-\left(\frac{\bar{\sigma}_\nu^K}{\kappa_\nu^K} + \bar{\alpha}_\nu^K\right) t\right] u(t), \tag{6.18}$$

which we can write as

$$\bar{s}_\nu^K(t) = \frac{\delta(t)}{\kappa_\nu^K} + \xi_\nu^K(t), \tag{6.19}$$

where $u(t)$ is a Heaviside step function and $\delta(t)$ is the Dirac delta function, also referred to as the impulse function.

We can start from Equations (6.11a)-(6.11e), the FiPo update equations in the frequency-domain,

$$j\omega\epsilon^2\mu\phi = -\nabla_s^\phi \cdot (\epsilon\mathbf{A}), \tag{6.20a}$$

$$j\omega\epsilon\mathbf{E} = \nabla_s^E \times \mathbf{H}, \tag{6.20b}$$

$$j\omega\mathbf{A} = -\mathbf{E} - \nabla_s^A\phi, \tag{6.20c}$$

$$j\omega\mu\mathbf{H} = -\nabla_s^H \times \mathbf{E}, \tag{6.20d}$$

$$\mu\mathbf{H} = \nabla \times \mathbf{A}. \tag{6.20e}$$

For the CPML derivation, we will look only at the x-component for vector-valued fields and potentials. We can transform Equations (6.20a)-(6.20e) back into the time domain where $\circledast$ denotes a convolution

$$\epsilon^2\mu\partial_t\phi = -\left(\bar{s}_x^{\phi} \circledast \partial_x\left(\epsilon A_x\right) + \bar{s}_y^{\phi} \circledast \partial_y\left(\epsilon A_y\right) + \bar{s}_z^{\phi} \circledast \partial_z\left(\epsilon A_z\right)\right), \tag{6.21a}$$

$$\epsilon\partial_t E_x + \sigma E_x = \bar{s}_y^{E} \circledast \partial_y H_z - \bar{s}_z^{E} \circledast \partial_z H_y, \tag{6.21b}$$

$$\partial_t A_x = -E_x - \bar{s}_x^{A} \circledast \partial_x\phi, \tag{6.21c}$$

$$\mu\partial_t H_x = \bar{s}_z^{H} \circledast \partial_z E_y - \bar{s}_y^{H} \circledast \partial_y E_z, \tag{6.21d}$$

$$\mu H_x = \partial_y A_z - \partial_z A_y. \tag{6.21e}$$

By applying the definition for s from Equation (6.19) to Equations (6.21a)-(6.21e) gives

$$\begin{aligned}\epsilon^2\mu\partial_t\phi = -\Bigg(&\frac{1}{\kappa_x^{\phi}}\partial_x\left(\epsilon A_x\right) + \frac{1}{\kappa_y^{\phi}}\partial_y\left(\epsilon A_y\right) + \frac{1}{\kappa_z^{\phi}}\partial_z\left(\epsilon A_z\right) \\ &+ \xi_x^{\phi} \circledast \partial_x\left(\epsilon A_x\right) + \xi_y^{\phi} \circledast \partial_y\left(\epsilon A_y\right) + \xi_z^{\phi} \circledast \partial_z\left(\epsilon A_z\right)\Bigg),\end{aligned} \tag{6.22a}$$

$$\begin{aligned}\epsilon\partial_t E_x + \sigma E_x = &\frac{1}{\kappa_y^{E}}\partial_y H_z - \frac{1}{\kappa_z^{E}}\partial_z H_y \\ &+ \xi_y^{E} \circledast \partial_y H_z - \xi_z^{E} \circledast \partial_z H_y,\end{aligned} \tag{6.22b}$$

$$\partial_t A_x = -E_x - \frac{1}{\kappa_x^{A}}\partial_x\phi - \xi_x^{A} \circledast \partial_x\phi, \tag{6.22c}$$

$$\begin{aligned}\mu\partial_t H_x = &\frac{1}{\kappa_z^{H}}\partial_z E_y - \frac{1}{\kappa_y^{H}}\partial_y E_z \\ &+ \xi_z^{H} \circledast \partial_z E_y - \xi_y^{H} \circledast \partial_y E_z,\end{aligned} \tag{6.22d}$$

$$\mu H_x = \partial_y A_z - \partial_z A_y. \tag{6.22e}$$

In order to discretize our equations containing the convolution, we need to define the discrete impulse response of ξ_ν as

$$Z_\nu^K(m) = \int_{m\Delta_t}^{(m+1)\Delta_t} \xi_\nu(\tau)d\tau, \tag{6.23a}$$

$$= -\frac{\bar{\sigma_\nu}^K}{(\kappa_\nu^K)^2}\int_{m\Delta_t}^{(m+1)\Delta_t} \exp\left[-\left(\frac{\bar{\sigma_\nu}^K}{\kappa_\nu^K} + \bar{\alpha}_\nu^K\right)\tau\right]d\tau, \tag{6.23b}$$

$$= a_\nu \exp\left[\left(\frac{\bar{\sigma}_\nu}{\kappa_\nu} + \bar{\alpha}_\nu\right)m\Delta_t\right], \tag{6.23c}$$

where

$$a_\nu^K = \frac{\bar{\sigma}_\nu^K}{\bar{\sigma}_\nu^K \kappa_\nu^K + (\kappa_\nu^K)^2 \bar{\alpha}_\nu^K} \left(\exp\left[-\left(\frac{\bar{\sigma}_\nu^K}{\kappa_\nu^K} + \bar{\alpha}_\nu^K \right) \Delta_t \right] - 1.0 \right). \tag{6.24}$$

Note that Equation (6.22e) contains no convolution, so we will drop it out of the derivation. Using Equations (6.23c) and (6.24), we can discretize Equations (6.22a)-(6.22d) as

$$\begin{aligned}
&\frac{\epsilon^2 \mu}{\Delta_t}(\phi_{i,j,k}^{n+1} - \phi_{i,j,k}^{n}) = \qquad (6.25a)\\
&- \left(\frac{1}{\kappa_x^\phi \Delta_x} \partial_x \left(\epsilon_{i+\frac{1}{2},j,k} A_{x\ i+\frac{1}{2},j,k}^{n+\frac{1}{2}} - \epsilon_{i-\frac{1}{2},j,k} A_{x\ i-\frac{1}{2},j,k}^{n+\frac{1}{2}} \right) \right.\\
&+ \frac{1}{\kappa_y^\phi \Delta_y} \partial_y \left(\epsilon_{i,j+\frac{1}{2},k} A_{y\ i,j+\frac{1}{2},k}^{n+\frac{1}{2}} - \epsilon_{i,j-\frac{1}{2},k} A_{y\ i,j-\frac{1}{2},k}^{n+\frac{1}{2}} \right)\\
&+ \frac{1}{\kappa_z^\phi \Delta_z} \partial_z \left(\epsilon_{i,j,k+\frac{1}{2}} A_{z\ i,j,k+\frac{1}{2}}^{n+\frac{1}{2}} - \epsilon_{i,j,k-\frac{1}{2}} A_{z\ i,j,k-\frac{1}{2}}^{n+\frac{1}{2}} \right)\\
&+ \sum_{m=0}^{N-1} Z_x^\phi(m) \frac{1}{\Delta_x} \left(\epsilon_{i+\frac{1}{2},j,k} A_{x\ i+\frac{1}{2},j,k}^{n-m+\frac{1}{2}} - \epsilon_{i-\frac{1}{2},j,k} A_{x\ i-\frac{1}{2},j,k}^{n-m+\frac{1}{2}} \right)\\
&+ \sum_{m=0}^{N-1} Z_y^\phi(m) \frac{1}{\Delta_y} \left(\epsilon_{i,j+\frac{1}{2},k} A_{y\ i,j+\frac{1}{2},k}^{n-m+\frac{1}{2}} - \epsilon_{i,j-\frac{1}{2},k} A_{y\ i,j-\frac{1}{2},k}^{n-m+\frac{1}{2}} \right)\\
&\left. + \sum_{m=0}^{N-1} Z_z^\phi(m) \frac{1}{\Delta_z} \left(\epsilon_{i,j,k+\frac{1}{2}} A_{z\ i,j,k+\frac{1}{2}}^{n-m+\frac{1}{2}} - \epsilon_{i,j,k-\frac{1}{2}} A_{z\ i,j,k-\frac{1}{2}}^{n-m+\frac{1}{2}} \right) \right),
\end{aligned}$$

$$\begin{aligned}
&\frac{\epsilon_r \epsilon_0}{\Delta_t} \left(E_{x\ i+\frac{1}{2},j,k}^{n+1} - E_{x\ i+\frac{1}{2},j,k}^{n} \right) + \frac{\sigma}{2} \left(E_{x\ i+\frac{1}{2},j,k}^{n+1} + E_{x\ i+\frac{1}{2},j,k}^{n} \right) = \qquad (6.25b)\\
&\quad \frac{1}{\kappa_y^E \Delta_y} \left(H_{z\ i+\frac{1}{2},j+\frac{1}{2},k}^{n+\frac{1}{2}} - H_{z\ i+\frac{1}{2},j-\frac{1}{2},k}^{n+\frac{1}{2}} \right)\\
&- \frac{1}{\kappa_z^E \Delta_z} \left(H_{y\ i+\frac{1}{2},j,k+\frac{1}{2}}^{n+\frac{1}{2}} - H_{y\ i+\frac{1}{2},j,k-\frac{1}{2}}^{n+\frac{1}{2}} \right)\\
&+ \sum_{m=0}^{N-1} Z_y^E(m) \frac{1}{\Delta_y} \left(H_{z\ i+\frac{1}{2},j+\frac{1}{2},k}^{n-m+\frac{1}{2}} - H_{z\ i+\frac{1}{2},j-\frac{1}{2},k}^{n-m+\frac{1}{2}} \right)\\
&- \sum_{m=0}^{N-1} Z_z^E(m) \frac{1}{\Delta_z} \left(H_{y\ i+\frac{1}{2},j,k+\frac{1}{2}}^{n-m+\frac{1}{2}} - H_{y\ i+\frac{1}{2},j,k-\frac{1}{2}}^{n-m+\frac{1}{2}} \right),
\end{aligned}$$

$$\frac{1}{\Delta t}\left(A^{n+\frac{1}{2}}_{x\ i+\frac{1}{2},j,k} - A^{n-\frac{1}{2}}_{x\ i+\frac{1}{2},j,k}\right) = \tag{6.25c}$$
$$- E^{n}_{x\ i+\frac{1}{2},j,k} - \frac{1}{\kappa^{A}_{x}\Delta_x}\left(\phi^{n}_{i+1,j,k} - \phi^{n}_{i,j,k}\right)$$
$$- \sum_{m=0}^{N-1} Z^{A}_{x}(m)\frac{1}{\Delta_x}\left(\phi^{n-m}_{i+1,j,k} - \phi^{n-m}_{i,j,k}\right),$$

$$\frac{\mu_r\mu_0}{\Delta_t}\left(H^{n+\frac{1}{2}}_{x\ i,j+\frac{1}{2},k+\frac{1}{2}} - H^{n-\frac{1}{2}}_{x\ i,j+\frac{1}{2},k+\frac{1}{2}}\right) = \tag{6.25d}$$
$$\frac{1}{\kappa^{H}_{z}\Delta_z}\left(E^{n}_{y\ i,j+\frac{1}{2},k+1} - E^{n}_{y\ i,j+\frac{1}{2},k}\right)$$
$$- \frac{1}{\kappa^{H}_{y}\Delta_y}\left(E^{n}_{z\ i,j+1,k+\frac{1}{2}} - E^{n}_{z\ i,j,k+\frac{1}{2}}\right)$$
$$+ \sum_{m=0}^{N-1} Z^{H}_{z}(m)\frac{1}{\Delta_z}\left(E^{n-m}_{y\ i,j+\frac{1}{2},k+1} - E^{n-m}_{y\ i,j+\frac{1}{2},k}\right)$$
$$- \sum_{m=0}^{N-1} Z^{H}_{y}(m)\frac{1}{\Delta_y}\left(E^{n-m}_{z\ i,j+1,k+\frac{1}{2}} - E^{n-m}_{z\ i,j,k+\frac{1}{2}}\right).$$

The details of discretizing the equations can be found in [74]. However, in their current form, the discrete sums that evaluate the convolution would be expensive to perform. In order to reduce the computational cost of these sums, we can utilize the recursive convolution (RC) method [75, 76]. The RC convolution method works by introducing an auxiliary variable ψ that is updated in order to recursively evaluate the convolution summation. The update equations with the auxiliary variables are written as

$$\frac{\epsilon^2\mu}{\Delta_t}\left(\phi^{n+1}_{i,j,k} - \phi^{n}_{i,j,k}\right) = \tag{6.26a}$$
$$- \Bigg(\frac{1}{\kappa^{\phi}_{x}\Delta_x}\left(\epsilon_{i+\frac{1}{2},j,k}A^{n+\frac{1}{2}}_{x\ i+\frac{1}{2},j,k} - \epsilon_{i-\frac{1}{2},j,k}A^{n+\frac{1}{2}}_{x\ i-\frac{1}{2},j,k}\right)$$
$$+ \frac{1}{\kappa^{\phi}_{y}\Delta_y}\left(\epsilon_{i,j+\frac{1}{2},k}A^{n+\frac{1}{2}}_{y\ i,j+\frac{1}{2},k} - \epsilon_{i,j-\frac{1}{2},k}A^{n+\frac{1}{2}}_{y\ i,j-\frac{1}{2},k}\right)$$
$$+ \frac{1}{\kappa^{\phi}_{z}\Delta_z}\left(\epsilon_{i,j,k+\frac{1}{2}}A^{n+\frac{1}{2}}_{z\ i,j,k+\frac{1}{2}} - \epsilon_{i,j,k-\frac{1}{2}}A^{n+\frac{1}{2}}_{z\ i,j,k-\frac{1}{2}}\right)$$
$$+ \psi^{n+\frac{1}{2}}_{\phi\ x\ i,j,k} + \psi^{n+\frac{1}{2}}_{\phi\ y\ i,j,k} + \psi^{n+\frac{1}{2}}_{\phi\ z\ i,j,k}\Bigg),$$

$$\frac{\epsilon_r\epsilon_0}{\Delta_t}\left(E^{n+1}_{x\ i+\frac{1}{2},j,k} - E^{n}_{x\ i+\frac{1}{2},j,k}\right) = \tag{6.26b}$$
$$+\frac{\sigma}{2}\left(E^{n+1}_{x\ i+\frac{1}{2},j,k} + E^{n}_{x\ i+\frac{1}{2},j,k}\right) =$$
$$\frac{1}{\kappa^E_y\Delta_y}\left(H^{n+\frac{1}{2}}_{z\ i+\frac{1}{2},j+\frac{1}{2},k} - H^{n+\frac{1}{2}}_{z\ i+\frac{1}{2},j-\frac{1}{2},k}\right)$$
$$-\frac{1}{\kappa^E_z\Delta_z}\left(H^{n+\frac{1}{2}}_{y\ i+\frac{1}{2},j,k+\frac{1}{2}} - H^{n+\frac{1}{2}}_{y\ i+\frac{1}{2},j,k-\frac{1}{2}}\right)$$
$$+\psi^{n+\frac{1}{2}}_{E\ xy\ i+\frac{1}{2},j,k} - \psi^{n+\frac{1}{2}}_{E\ xz\ i+\frac{1}{2},j,k},$$

$$\frac{1}{\Delta t}\left(A^{n+\frac{1}{2}}_{x\ i+\frac{1}{2},j,k} - A^{n-\frac{1}{2}}_{x\ i+\frac{1}{2},j,k}\right) = \tag{6.26c}$$
$$-E^{n}_{x\ i+\frac{1}{2},j,k} - \frac{1}{\kappa^A_x\Delta_x}\left(\phi^n_{i+1,j,k} - \phi^n_{i,j,k}\right)$$
$$-\psi^n_{A\ x\ i+\frac{1}{2},j,k},$$

$$\frac{\mu_r\mu_0}{\Delta_t}\left(H^{n+\frac{1}{2}}_{x\ i,j+\frac{1}{2},k+\frac{1}{2}} - H^{n-\frac{1}{2}}_{x\ i,j+\frac{1}{2},k+\frac{1}{2}}\right) = \tag{6.26d}$$
$$\frac{1}{\kappa^H_z\Delta_z}\left(E^{n}_{y\ i,j+\frac{1}{2},k+1} - E^{n}_{y\ i,j+\frac{1}{2},k}\right)$$
$$-\frac{1}{\kappa^H_y\Delta_y}\left(E^{n}_{z\ i,j+1,k+\frac{1}{2}} - E^{n}_{z\ i,j,k+\frac{1}{2}}\right)$$
$$+\psi^n_{H\ xz\ i,j+\frac{1}{2},k+\frac{1}{2}} - \psi^n_{H\ xy\ i,j+\frac{1}{2},k+\frac{1}{2}}.$$

Notice that the auxiliary variable for ϕ in Equation (6.26a) only contains one subscript component in the notation. We do this as a convenience to due to the partial derivative always being taken for the respective component of the potential. This means we write the auxiliary variables for ϕ as $\psi_{\phi\ xx} = \psi_{\phi\ x}$. For other auxiliary variables, the first subscript is component of field updated and the second subscript is the component of the partial derivative. The update equations for $\mathbf{E}$ and $\mathbf{H}$ require a total of six auxiliary variables total (two per component), $\mathbf{A}$ requires three, and ϕ requires three. The auxiliary update equations needed for Equations (6.26a)-(6.26d) are written as

$$\psi^{n+\frac{1}{2}}_{\phi\ x\ i,j,k} = b^\phi_x\psi^{n-\frac{1}{2}}_{\phi\ x\ i,j,k} \tag{6.27a}$$
$$+a^\phi_x\frac{1}{\Delta_x}\left(\epsilon_{i+\frac{1}{2},j,k}A^{n+\frac{1}{2}}_{x\ i+\frac{1}{2},j,k} - \epsilon_{i-\frac{1}{2},j,k}A^{n+\frac{1}{2}}_{x\ i-\frac{1}{2},j,k}\right),$$

$$\psi^{n+\frac{1}{2}}_{\phi\ y\ i,j,k} = b^{\phi}_{y}\psi^{n-\frac{1}{2}}_{\phi\ y\ i,j,k} + a^{\phi}_{y}\frac{1}{\Delta_y}\left(\epsilon_{i,j+\frac{1}{2},k}A^{n+\frac{1}{2}}_{y\ i,j+\frac{1}{2},k} - \epsilon_{i,j-\frac{1}{2},k}A^{n+\frac{1}{2}}_{y\ i,j-\frac{1}{2},k}\right), \tag{6.27b}$$

$$\psi^{n+\frac{1}{2}}_{\phi\ z\ i,j,k} = b^{\phi}_{z}\psi^{n-\frac{1}{2}}_{\phi\ z\ i,j,k} + a^{\phi}_{z}\frac{1}{\Delta_z}\left(\epsilon_{i,j,k+\frac{1}{2}}A^{n+\frac{1}{2}}_{z\ i,j,k+\frac{1}{2}} - \epsilon_{i,j,k-\frac{1}{2}}A^{n+\frac{1}{2}}_{z\ i,j,k-\frac{1}{2}}\right), \tag{6.27c}$$

$$\psi^{n+\frac{1}{2}}_{E\ xy\ i+\frac{1}{2},j,k} = b^{E}_{y}\psi^{n-\frac{1}{2}}_{E\ xy\ i+\frac{1}{2},j,k} + a^{E}_{y}\frac{1}{\Delta_y}\left(H^{n+\frac{1}{2}}_{z\ i+\frac{1}{2},j+\frac{1}{2},k} - H^{n+\frac{1}{2}}_{z\ i+\frac{1}{2},j-\frac{1}{2},k}\right), \tag{6.27d}$$

$$\psi^{n+\frac{1}{2}}_{E\ xz\ i+\frac{1}{2},j,k} = b^{E}_{z}\psi^{n-\frac{1}{2}}_{E\ xz\ i+\frac{1}{2},j,k} + a^{E}_{z}\frac{1}{\Delta_z}\left(H^{n+\frac{1}{2}}_{y\ i+\frac{1}{2},j,k+\frac{1}{2}} - H^{n+\frac{1}{2}}_{y\ i+\frac{1}{2},j,k-\frac{1}{2}}\right), \tag{6.27e}$$

$$\psi^{n}_{A\ x\ i+\frac{1}{2},j,k} = b^{A}_{x}\psi^{n-1}_{A\ x\ i+\frac{1}{2},j,k} \tag{6.27f}$$

$$+ a^{A}_{x}\frac{1}{\Delta_x}\left(\phi^{n}_{i+1,j,k} - \phi^{n}_{i,j,k}\right), \tag{6.27g}$$

$$\psi^{n}_{H\ xy\ i,j+\frac{1}{2},k+\frac{1}{2}} = b^{H}_{y}\psi^{n-1}_{H\ xy\ i,j+\frac{1}{2},k+\frac{1}{2}} + a^{H}_{y}\frac{1}{\Delta_y}\left(E^{n}_{z\ i,j+1,k+\frac{1}{2}} - E^{n}_{z\ i,j,k+\frac{1}{2}}\right), \tag{6.27h}$$

$$\psi^{n}_{H\ xz\ i,j+\frac{1}{2},k+\frac{1}{2}} = b^{H}_{z}\psi^{n-1}_{H\ xz\ i,j+\frac{1}{2},k+\frac{1}{2}} + a^{H}_{z}\frac{1}{\Delta_z}\left(E^{n}_{y\ i,j+\frac{1}{2},k+1} - E^{n}_{y\ i,j+\frac{1}{2},k}\right), \tag{6.27i}$$

where

$$a^{K}_{\nu} = \frac{\bar{\sigma}^{K}_{\nu}}{\bar{\sigma}^{K}_{\nu}\kappa^{K}_{\nu} + \left(\kappa^{K}_{\nu}\right)^{2}\bar{\alpha}^{K}_{\nu}}\left(b^{K}_{\nu} - 1.0\right), \tag{6.28a}$$

$$b^{K}_{\nu} = \exp\left[-\left(\frac{\bar{\sigma}^{K}_{\nu}}{\kappa^{K}_{\nu}} + \bar{\alpha}^{K}_{\nu}\right)\Delta_t\right]. \tag{6.28b}$$

Method	$\mathbf{E}$	ψ_E	$\mathbf{H}$	ψ_H	$\mathbf{A}$	ψ_A	ϕ	ψ_ϕ	Total
Conventional FDTD	3	6	3	6	**0**	**0**	**0**	**0**	18
FiPo Basic	3	6	3	6	3	3	1	3	28
FiPo Hybrid	3	6	3	**0**	3	3	1	3	22

Table 6.1: Required number of arrays for storing fields, potentials, and auxiliary variables for conventional FDTD, FiPo Basic, and FiPo Hybrid.

The update equations for the components of $\mathbf{E}$, $\mathbf{H}$, and $\mathbf{A}$ not written here can be derived similarly.

The amount of memory required by the algorithm depends on the number of fields that have to be stored. The number of fields includes the components of each field as well as each auxiliary variable needed for field decay in the PML. Table 6.1 lists the number of variables required to be stored in each method. Conventional FDTD requires a total of 18 varaibles. FiPo Basic requires 10 additional fields from conventional FDTD, including fields for $\mathbf{A}$ and ϕ and the associated auxiliary variables, for a total of 28. FiPo Hybrid requires 6 less variables than FiPo Basic due to the removal of auxiliary variables for $\mathbf{H}$.

6.2.1 All CPML Update Equations

For reference and completeness, all CPML update equations for fields, potentials, and their auxiliary variables are given here.

6.2.1.1 Fields and Potentials

The PML update equation for ϕ is

$$\begin{aligned}
&\frac{\epsilon^2\mu}{\Delta_t}\left(\phi^{n+1}_{i,j,k} - \phi^{n}_{i,j,k}\right) = \\
&-\left(\frac{1}{\kappa^{\phi}_{x}\Delta_x}\left(\epsilon_{i+\frac{1}{2},j,k}A^{n+\frac{1}{2}}_{x\ i+\frac{1}{2},j,k} - \epsilon_{i-\frac{1}{2},j,k}A^{n+\frac{1}{2}}_{x\ i-\frac{1}{2},j,k}\right)\right. \\
&+\frac{1}{\kappa^{\phi}_{y}\Delta_y}\left(\epsilon_{i,j+\frac{1}{2},k}A^{n+\frac{1}{2}}_{y\ i,j+\frac{1}{2},k} - \epsilon_{i,j-\frac{1}{2},k}A^{n+\frac{1}{2}}_{y\ i,j-\frac{1}{2},k}\right) \\
&+\frac{1}{\kappa^{\phi}_{z}\Delta_z}\left(\epsilon_{i,j,k+\frac{1}{2}}A^{n+\frac{1}{2}}_{z\ i,j,k+\frac{1}{2}} - \epsilon_{i,j,k-\frac{1}{2}}A^{n+\frac{1}{2}}_{z\ i,j,k-\frac{1}{2}}\right) \\
&\left.+\psi^{n+\frac{1}{2}}_{\phi\ x\ i,j,k} + \psi^{n+\frac{1}{2}}_{\phi\ y\ i,j,k} + \psi^{n+\frac{1}{2}}_{\phi\ z\ i,j,k}\right).
\end{aligned} \tag{6.29}$$

The PML update equations for **E** are

$$\begin{aligned}
&\frac{\epsilon_r\epsilon_0}{\Delta_t}\left(E^{n+1}_{x\ i+\frac{1}{2},j,k} - E^{n}_{x\ i+\frac{1}{2},j,k}\right) = \\
&+\frac{\sigma}{2}\left(E^{n+1}_{x\ i+\frac{1}{2},j,k} + E^{n}_{x\ i+\frac{1}{2},j,k}\right) = \\
&\quad\frac{1}{\kappa^{E}_{y}\Delta_y}\left(H^{n+\frac{1}{2}}_{z\ i+\frac{1}{2},j+\frac{1}{2},k} - H^{n+\frac{1}{2}}_{z\ i+\frac{1}{2},j-\frac{1}{2},k}\right) \\
&-\frac{1}{\kappa^{E}_{z}\Delta_z}\left(H^{n+\frac{1}{2}}_{y\ i+\frac{1}{2},j,k+\frac{1}{2}} - H^{n+\frac{1}{2}}_{y\ i+\frac{1}{2},j,k-\frac{1}{2}}\right) \\
&+\psi^{n+\frac{1}{2}}_{E\ xy\ i+\frac{1}{2},j,k} - \psi^{n+\frac{1}{2}}_{E\ xz\ i+\frac{1}{2},j,k},
\end{aligned} \tag{6.30a}$$

$$\begin{aligned}
&\frac{\epsilon_r\epsilon_0}{\Delta_t}\left(E^{n+1}_{y\ i,j+\frac{1}{2},k} - E^{n}_{y\ i,j+\frac{1}{2},k}\right) = \\
&+\frac{\sigma}{2}\left(E^{n+1}_{y\ i,j+\frac{1}{2},k} + E^{n}_{y\ i,j+\frac{1}{2},k}\right) = \\
&\quad\frac{1}{\kappa^{E}_{z}\Delta_z}\left(H^{n+\frac{1}{2}}_{x\ i,j+\frac{1}{2},k+\frac{1}{2}} - H^{n+\frac{1}{2}}_{x\ i,j+\frac{1}{2},k-\frac{1}{2}}\right) \\
&-\frac{1}{\kappa^{E}_{x}\Delta_x}\left(H^{n+\frac{1}{2}}_{z\ i+\frac{1}{2},j+\frac{1}{2},k} - H^{n+\frac{1}{2}}_{z\ i-\frac{1}{2},j+\frac{1}{2},k}\right) \\
&+\psi^{n+\frac{1}{2}}_{E\ yz\ i,j+\frac{1}{2},k} - \psi^{n+\frac{1}{2}}_{E\ yx\ i,j+\frac{1}{2},k},
\end{aligned} \tag{6.30b}$$

$$\frac{\epsilon_r\epsilon_0}{\Delta_t}\left(E^{n+1}_{z\ i,j,k+\frac{1}{2}} - E^{n}_{z\ i,j,k+\frac{1}{2}}\right) = \tag{6.30c}$$
$$+\frac{\sigma}{2}\left(E^{n+1}_{z\ i,j,k+\frac{1}{2}} + E^{n}_{z\ i,j,k+\frac{1}{2}}\right) =$$
$$\frac{1}{\kappa^E_x\Delta_x}\left(H^{n+\frac{1}{2}}_{y\ i+\frac{1}{2},j,k+\frac{1}{2}} - H^{n+\frac{1}{2}}_{y\ i-\frac{1}{2},j,k+\frac{1}{2}}\right)$$
$$-\frac{1}{\kappa^E_y\Delta_y}\left(H^{n+\frac{1}{2}}_{x\ i,j+\frac{1}{2},k+\frac{1}{2}} - H^{n+\frac{1}{2}}_{x\ i,j-\frac{1}{2},k+\frac{1}{2}}\right)$$
$$+\psi^{n+\frac{1}{2}}_{E\ zx\ i,j,k+\frac{1}{2}} - \psi^{n+\frac{1}{2}}_{E\ zy\ i,j,k+\frac{1}{2}}.$$

The PML update equations for **A** are

$$\frac{1}{\Delta t}\left(A^{n+\frac{1}{2}}_{x\ i+\frac{1}{2},j,k} - A^{n-\frac{1}{2}}_{x\ i+\frac{1}{2},j,k}\right) = \tag{6.31a}$$
$$-E^{n}_{x\ i+\frac{1}{2},j,k} - \frac{1}{\kappa^A_x\Delta_x}\left(\phi^n_{i+1,j,k} - \phi^n_{i,j,k}\right)$$
$$-\psi^n_{A\ x\ i+\frac{1}{2},j,k},$$

$$\frac{1}{\Delta t}\left(A^{n+\frac{1}{2}}_{y\ i,j+\frac{1}{2},k} - A^{n-\frac{1}{2}}_{y\ i,j+\frac{1}{2},k}\right) = \tag{6.31b}$$
$$-E^{n}_{y\ i,j+\frac{1}{2},k} - \frac{1}{\kappa^A_y\Delta_y}\left(\phi^n_{i,j+1,k} - \phi^n_{i,j,k}\right)$$
$$-\psi^n_{A\ y\ i,j+\frac{1}{2},k},$$

$$\frac{1}{\Delta t}\left(A^{n+\frac{1}{2}}_{z\ i,j,k+\frac{1}{2}} - A^{n-\frac{1}{2}}_{z\ i,j,k+\frac{1}{2}}\right) = \tag{6.31c}$$
$$-E^{n}_{z\ i,j,k+\frac{1}{2}} - \frac{1}{\kappa^A_z\Delta_z}\left(\phi^n_{i,j,k+1} - \phi^n_{i,j,k}\right)$$
$$-\psi^n_{A\ z\ i,j,k+\frac{1}{2}}.$$

The PML update equations for **H** for FiPo Basic are

$$\frac{\mu_r\mu_0}{\Delta_t}\left(H^{n+\frac{1}{2}}_{x\ i,j+\frac{1}{2},k+\frac{1}{2}} - H^{n-\frac{1}{2}}_{x\ i,j+\frac{1}{2},k+\frac{1}{2}}\right) = \tag{6.32a}$$
$$\frac{1}{\kappa^H_z\Delta_z}\left(E^{n}_{y\ i,j+\frac{1}{2},k+1} - E^{n}_{y\ i,j+\frac{1}{2},k}\right)$$
$$-\frac{1}{\kappa^H_y\Delta_y}\left(E^{n}_{z\ i,j+1,k+\frac{1}{2}} - E^{n}_{z\ i,j,k+\frac{1}{2}}\right)$$
$$+\psi^n_{H\ xz\ i,j+\frac{1}{2},k+\frac{1}{2}} - \psi^n_{H\ xy\ i,j+\frac{1}{2},k+\frac{1}{2}},$$

$$\frac{\mu_r\mu_0}{\Delta_t}\left(H^{n+\frac{1}{2}}_{y\ i+\frac{1}{2},j,k+\frac{1}{2}} - H^{n-\frac{1}{2}}_{y\ i+\frac{1}{2},j,k+\frac{1}{2}}\right) = \tag{6.32b}$$
$$\frac{1}{\kappa^H_x\Delta_x}\left(E^n_{z\ i+1,j,k+\frac{1}{2}} - E^n_{z\ i,j,k+\frac{1}{2}}\right)$$
$$-\frac{1}{\kappa^H_z\Delta_z}\left(E^n_{x\ i+\frac{1}{2},j,k+1} - E^n_{z\ i,j,k+\frac{1}{2}}\right)$$
$$+\psi^n_{H\ yx\ i+\frac{1}{2},j,k+\frac{1}{2}} - \psi^n_{H\ yz\ i+\frac{1}{2},j,k+\frac{1}{2}},$$

$$\frac{\mu_r\mu_0}{\Delta_t}\left(H^{n+\frac{1}{2}}_{z\ i+\frac{1}{2},j+\frac{1}{2},k} - H^{n-\frac{1}{2}}_{z\ i+\frac{1}{2},j+\frac{1}{2},k}\right) = \tag{6.32c}$$
$$\frac{1}{\kappa^H_y\Delta_y}\left(E^n_{x\ i+\frac{1}{2},j+1,k} - E^n_{x\ i+\frac{1}{2},j,k}\right)$$
$$-\frac{1}{\kappa^H_x\Delta_x}\left(E^n_{y\ i+1,j+\frac{1}{2},k+\frac{1}{2}} - E^n_{y\ i,j+\frac{1}{2},k}\right)$$
$$+\psi^n_{H\ zy\ i+\frac{1}{2},j+\frac{1}{2},k} - \psi^n_{H\ zx\ i+\frac{1}{2},j+\frac{1}{2},k}.$$

The PML update equations for **H** for FiPo Hybrid do not exist because no PML is implemented for the FiPo Hybrid **H** update due to the lack of time derivative.

6.2.1.2 Auxiliary Variables

The auxiliary equations for ϕ are

$$\psi^{n+\frac{1}{2}}_{\phi\ x\ i,j,k} = b^\phi_{x\ i}\psi^{n-\frac{1}{2}}_{\phi\ x\ i,j,k} \tag{6.33a}$$
$$+a^\phi_{x\ i}\frac{1}{\Delta_x}\left(\epsilon_{i+\frac{1}{2},j,k}A^{n+\frac{1}{2}}_{x\ i+\frac{1}{2},j,k} - \epsilon_{i-\frac{1}{2},j,k}A^{n+\frac{1}{2}}_{x\ i-\frac{1}{2},j,k}\right),$$

$$\psi^{n+\frac{1}{2}}_{\phi\ y\ i,j,k} = b^\phi_{y\ j}\psi^{n-\frac{1}{2}}_{\phi\ x\ i,j,k} \tag{6.33b}$$
$$+a^\phi_{y\ j}\frac{1}{\Delta_y}\left(\epsilon_{i,j+\frac{1}{2},k}A^{n+\frac{1}{2}}_{y\ i,j+\frac{1}{2},k} - \epsilon_{i,j-\frac{1}{2},k}A^{n+\frac{1}{2}}_{y\ i,j-\frac{1}{2},k}\right),$$

$$\psi^{n+\frac{1}{2}}_{\phi\ z\ i,j,k} = b^\phi_{z\ k}\psi^{n-\frac{1}{2}}_{\phi\ x\ i,j,k} \tag{6.33c}$$
$$+a^\phi_{z\ k}\frac{1}{\Delta_z}\left(\epsilon_{i,j,k+\frac{1}{2}}A^{n+\frac{1}{2}}_{z\ i,j,k+\frac{1}{2}} - \epsilon_{i,j,k-\frac{1}{2}}A^{n+\frac{1}{2}}_{z\ i,j,k-\frac{1}{2}}\right).$$

The auxiliary equations for **E** are

$$\psi^{n+\frac{1}{2}}_{E\ xy\ i+\frac{1}{2},j,k} = b^{E}_{y\ j}\psi^{n-\frac{1}{2}}_{E\ xy\ i+\frac{1}{2},j,k} + a^{E}_{y\ j}\frac{1}{\Delta_y}\left(H^{n+\frac{1}{2}}_{z\ i+\frac{1}{2},j+\frac{1}{2},k} - H^{n+\frac{1}{2}}_{z\ i+\frac{1}{2},j-\frac{1}{2},k}\right), \tag{6.34a}$$

$$\psi^{n+\frac{1}{2}}_{E\ xz\ i+\frac{1}{2},j,k} = b^{E}_{z\ k}\psi^{n-\frac{1}{2}}_{E\ xz\ i+\frac{1}{2},j,k} + a^{E}_{z\ k}\frac{1}{\Delta_z}\left(H^{n+\frac{1}{2}}_{y\ i+\frac{1}{2},j,k+\frac{1}{2}} - H^{n+\frac{1}{2}}_{y\ i+\frac{1}{2},j,k-\frac{1}{2}}\right), \tag{6.34b}$$

$$\psi^{n+\frac{1}{2}}_{E\ yx\ i,j+\frac{1}{2},k} = b^{E}_{x\ i}\psi^{n-\frac{1}{2}}_{E\ xy\ i,j+\frac{1}{2},k} + a^{E}_{x\ i}\frac{1}{\Delta_x}\left(H^{n+\frac{1}{2}}_{z\ i+\frac{1}{2},j+\frac{1}{2},k} - H^{n+\frac{1}{2}}_{z\ i-\frac{1}{2},j+\frac{1}{2},k}\right), \tag{6.34c}$$

$$\psi^{n+\frac{1}{2}}_{E\ yz\ i,j+\frac{1}{2},k} = b^{E}_{z\ k}\psi^{n-\frac{1}{2}}_{E\ xz\ i,j+\frac{1}{2},k} + a^{E}_{z\ k}\frac{1}{\Delta_z}\left(H^{n+\frac{1}{2}}_{x\ i,j+\frac{1}{2},k+\frac{1}{2}} - H^{n+\frac{1}{2}}_{x\ i,j+\frac{1}{2},k-\frac{1}{2}}\right), \tag{6.34d}$$

$$\psi^{n+\frac{1}{2}}_{E\ zx\ i,j,k+\frac{1}{2}} = b^{E}_{x\ i}\psi^{n-\frac{1}{2}}_{E\ xy\ i,j,k+\frac{1}{2}} + a^{E}_{x\ i}\frac{1}{\Delta_x}\left(H^{n+\frac{1}{2}}_{y\ i+\frac{1}{2},j,k+\frac{1}{2}} - H^{n+\frac{1}{2}}_{y\ i-\frac{1}{2},j,k+\frac{1}{2}}\right), \tag{6.34e}$$

$$\psi^{n+\frac{1}{2}}_{E\ zy\ i,j,k+\frac{1}{2}} = b^{E}_{y\ j}\psi^{n-\frac{1}{2}}_{E\ xz\ i,j,k+\frac{1}{2}} + a^{E}_{y\ j}\frac{1}{\Delta_y}\left(H^{n+\frac{1}{2}}_{x\ i,j+\frac{1}{2},k+\frac{1}{2}} - H^{n+\frac{1}{2}}_{x\ i,j-\frac{1}{2},k+\frac{1}{2}}\right). \tag{6.34f}$$

The auxiliary equations for **A** are

$$\psi^{n}_{A\ x\ i+\frac{1}{2},j,k} = b^{A}_{x\ i+\frac{1}{2}}\psi^{n-1}_{A\ x\ i+\frac{1}{2},j,k} + a^{A}_{x\ i+\frac{1}{2}}\frac{1}{\Delta_x}\left(\phi^{n}_{i+1,j,k} - \phi^{n}_{i,j,k}\right), \tag{6.35a}$$

$$\psi^{n}_{A\ y\ i,j+\frac{1}{2},k} = b^{A}_{y\ j+\frac{1}{2}}\psi^{n-1}_{A\ y\ i,j+\frac{1}{2},k} + a^{A}_{y\ j+\frac{1}{2}}\frac{1}{\Delta_y}\left(\phi^{n}_{i,j+1,k} - \phi^{n}_{i,j,k}\right), \tag{6.35b}$$

$$\psi^n_{A\ z\ i,j,k+\frac{1}{2}} = b^A_{z\ k+\frac{1}{2}} \psi^{n-1}_{A\ z\ i,j,k+\frac{1}{2}} + a^A_{z\ k+\frac{1}{2}} \frac{1}{\Delta_z} \left(\phi^n_{i,j,k+1} - \phi^n_{i,j,k} \right). \tag{6.35c}$$

The auxiliary equations for **H** are

$$\psi^n_{H\ xy\ i,j+\frac{1}{2},k+\frac{1}{2}} = b^H_{y\ j+\frac{1}{2}} \psi^{n-1}_{H\ xy\ i,j+\frac{1}{2},k+\frac{1}{2}} + a^H_{y\ j+\frac{1}{2}} \frac{1}{\Delta_y} \left(E^n_{z\ i,j+1,k+\frac{1}{2}} - E^n_{z\ i,j,k+\frac{1}{2}} \right), \tag{6.36a}$$

$$\psi^n_{H\ xz\ i,j+\frac{1}{2},k+\frac{1}{2}} = b^H_{z\ k+\frac{1}{2}} \psi^{n-1}_{H\ xz\ i,j+\frac{1}{2},k+\frac{1}{2}} + a^H_{z\ k+\frac{1}{2}} \frac{1}{\Delta_z} \left(E^n_{y\ i,j+\frac{1}{2},k+1} - E^n_{y\ i,j+\frac{1}{2},k} \right), \tag{6.36b}$$

$$\psi^n_{H\ yx\ i+\frac{1}{2},j,k+\frac{1}{2}} = b^H_{x\ i+\frac{1}{2}} \psi^{n-1}_{H\ yx\ i+\frac{1}{2},j,k+\frac{1}{2}} + a^H_{x\ i+\frac{1}{2}} \frac{1}{\Delta_x} \left(E^n_{z\ i+1,j,k+\frac{1}{2}} - E^n_{z\ i,j,k+\frac{1}{2}} \right), \tag{6.36c}$$

$$\psi^n_{H\ yz\ i+\frac{1}{2},j,k+\frac{1}{2}} = b^H_{z\ k+\frac{1}{2}} \psi^{n-1}_{H\ yz\ i+\frac{1}{2},j,k+\frac{1}{2}} + a^H_{z\ k+\frac{1}{2}} \frac{1}{\Delta_z} \left(E^n_{x\ i+\frac{1}{2},j,k+1} - E^n_{x\ i+\frac{1}{2},j,k} \right), \tag{6.36d}$$

$$\psi^n_{H\ zx\ i+\frac{1}{2},j+\frac{1}{2},k} = b^H_{x\ i+\frac{1}{2}} \psi^{n-1}_{H\ zx\ i+\frac{1}{2},j+\frac{1}{2},k} + a^H_{x\ i+\frac{1}{2}} \frac{1}{\Delta_x} \left(E^n_{y\ i+1,j+\frac{1}{2},k+1} - E^n_{y\ i,j+\frac{1}{2},k} \right), \tag{6.36e}$$

$$\psi^n_{H\ zy\ i+\frac{1}{2},j+\frac{1}{2},k} = b^H_{y\ j+\frac{1}{2}} \psi^{n-1}_{H\ zy\ i+\frac{1}{2},j+\frac{1}{2},k} + a^H_{y\ j+\frac{1}{2}} \frac{1}{\Delta_y} \left(E^n_{x\ i+\frac{1}{2},j+1,k+\frac{1}{2}} - E^n_{x\ i+\frac{1}{2},j,k+\frac{1}{2}} \right). \tag{6.36f}$$

For these equations,

$$a^K_\nu = \frac{\bar{\sigma}^K_\nu}{\bar{\sigma}^K_\nu \kappa^K_\nu + \left(\kappa^K_\nu\right)^2 \bar{\alpha}^K_\nu} \left(b^K_\nu - 1.0 \right), \tag{6.37a}$$

$$b^K_\nu = \exp\left[- \left(\frac{\bar{\sigma}^K_\nu}{\kappa^K_\nu} + \bar{\alpha}^K_\nu \right) \Delta_t \right]. \tag{6.37b}$$

6.3 Relationship Between Parameters for Perfectly Matched Layer

Implementation of a CPML typically involves utilizing the same values for CPML parameters for both $\mathbf{E}$ and $\mathbf{H}$ fields offset by a half position step [44]. The ability to define the CPML parameters with only one set of variables is a consequence of impedance matching. Here, we show this relation holds for the potentials in the FiPo algorithm.

6.3.1 Fields in a Lossy Half Space

The first step in PML analysis is to find and minimize the reflection coefficient. In order to minimize the reflection coefficient, we need to define the fields and potentials in a system that models waves from the simulation region impinging on the PML. We model this by defining a wave incident on a lossy half space like in Taflove and Hagness [44]. Region I is lossless and is characterized by μ_1 and ϵ_1. Region II is lossy and characterized by $\mu_2 = \kappa^H \mu_0$ and $\epsilon_2 = \kappa^E \epsilon_0$ as well as conductivity σ^E and loss values for each other field and potential σ^H, σ^A, and σ^ϕ. The boundary between Region I and II is at $x = 0$, where Region I is defined for $x < 0$ and Region II is defined for $x > 0$. The incoming wave is TE$_z$-polarized at an arbitrary angle θ relative to the x-axis.

The magnetic field for a TE$_z$-polarized wave in Region I can be written as

$$H_z^I = H_0 \left(1 + \Gamma e^{2j\beta_{1x}x}\right) e^{-j\beta_{1x}x - j\beta_{1y}y}, \tag{6.38}$$

where Γ is the reflection coefficient and β is the propagation constant. Using Ampere's law, we can use Equation (6.38) to solve for the components of the electric field $\mathbf{E}$ in Region I, resulting in

$$E_x^I = -\frac{1}{\omega\epsilon_1}\beta_{1y} H_0 \left(1 + \Gamma e^{2j\beta_{1x}x}\right) e^{-j\beta_{1x}x - j\beta_{1y}y}, \tag{6.39a}$$

$$E_y^I = \frac{1}{\omega\epsilon_1}\beta_{1x} H_0 \left(1 - \Gamma e^{2j\beta_{1x}x}\right) e^{-j\beta_{1x}x - j\beta_{1y}y}, \tag{6.39b}$$

The magnetic field with loss for a TE$_z$-polarized wave in Region II can be written as

$$H_z^{II} = H_0 \tau e^{-j\beta_{2x}x - j\beta_{2y}y} \tag{6.40}$$

where τ is the transmission coefficient. Using Ampere's law again, we can use Equation (6.40) to solve for the components of electric field $\mathbf{E}$ in Region II, resulting in

$$E_x^{II} = -\frac{1}{\omega\epsilon_0}\frac{1}{s_x^E}\beta_{2y}H_0\tau e^{-j\beta_{2x}x-j\beta_{2y}y}, \tag{6.41a}$$

$$E_y^{II} = \frac{1}{\omega\epsilon_0}\frac{1}{s_y^E}\beta_{2x}H_0\tau e^{-j\beta_{2x}x-j\beta_{2y}y}. \tag{6.41b}$$

These fields are fairly common and given in [44]. In order to examine FiPo equations, however, we have to use these fields to derive the corresponding potentials. For Region I, we can use Equations (6.38), (6.39a), and (6.39b) to derive values for $\mathbf{A}$ from the definition of $\mathbf{H}$ in terms of $\mathbf{A}$, Equation (2.6), which gives us

$$A_x^I = -\frac{H_0}{2}\frac{j\mu_1}{\beta_{1y}}\left(1+\Gamma e^{2j\beta_{1x}x}\right)e^{-j\beta_{1x}x-j\beta_{1y}y}, \tag{6.42a}$$

$$A_y^I = \frac{H_0}{2}\frac{j\mu_1}{\beta_{1x}}\left(1-\Gamma e^{2j\beta_{1x}x}\right)e^{-j\beta_{1x}x-j\beta_{1y}y}. \tag{6.42b}$$

For Region II, we can use Equations (6.40), (6.41a), and (6.41b) with Equation (2.6), resulting in

$$A_x^{II} = -\frac{H_0}{2}\frac{j\mu_2}{\beta_{2y}}\tau e^{-j\beta_{2x}x-j\beta_{2y}y}, \tag{6.43a}$$

$$A_y^{II} = \frac{H_0}{2}\frac{j\mu_2}{\beta_{2x}}\tau e^{-j\beta_{2x}x-j\beta_{2y}y}. \tag{6.43b}$$

We can get ϕ using the gauge condition, the generalized Lorenz gauge from Equation (2.27). The definitions for ϕ also assume that materials properties vary such that $\partial_i\epsilon = \epsilon\partial_i$. This assumption should hold for ϵ that varies slowly on the grid. Since we are trying to analyze the reflection coefficient for these equations, we are looking at the boundary between Regions I and II in particular. At the boundary between these two materials, this assumption should hold. ϕ in Regions I and II can be written as

$$\phi^I = \frac{1}{j\omega\epsilon_1^2}\frac{H_0}{2}\left(\frac{\beta_{1x}}{\beta_{1y}}\left(1-\Gamma e^{2j\beta_{1x}x}\right)-\frac{\beta_{1y}}{\beta_{1x}}\left(1+\Gamma e^{2j\beta_{1x}x}\right)\right)e^{-j\beta_{1x}x-j\beta_{1y}y}, \tag{6.44}$$

$$\phi^{II} = \frac{\mu_2}{j\omega\epsilon_0^2\mu_0}\frac{H_0}{2}\frac{1}{s^\phi}\left(\frac{\beta_{2y}}{\beta_{2x}}-\frac{\beta_{2x}}{\beta_{2y}}\right)\tau e^{-j\beta_{2x}x-j\beta_{2y}y}. \tag{6.45}$$

Knowing the definitions of fields for all fields and potentials should allow us to analyze the reflection coefficients for all fields and potentials. This analysis will give us the relationship between the stretched coordinates.

6.3.2 Propagation Constant and Impedance

We need to clearly define the propagation constant and how it relates to materials properties. We can express the propagation constant β in Region I and II as

$$\beta_1^2 = \beta_{1x}^2 + \beta_{1y}^2 = k_1^2 = \omega^2 \epsilon_1 \mu_1, \tag{6.46a}$$

$$\beta_2^2 = \beta_{2x}^2 + \beta_{2y}^2 = k_0^2 s^E s^H = \omega^2 \epsilon_0 \mu_0 s^E s^H, \tag{6.46b}$$

where the components of β can be expressed as

$$\beta_{1x} = k_1 cos(\theta), \tag{6.47a}$$

$$\beta_{1y} = k_1 sin(\theta), \tag{6.47b}$$

$$\beta_{2x} = \sqrt{k_0^2 s^E s^H - \beta_{2y}^2}. \tag{6.47c}$$

Assuming $s_x^E = s_y^E$, the impedance in Region I can be written as

$$\eta_1 = \sqrt{\frac{\mu_1}{\epsilon_1}}, \tag{6.48}$$

and the impedance in Region II can be derived from the ratio of the electric and magnetic field amplitudes as

$$\eta_2 = \frac{|\mathbf{E}|}{|\mathbf{H}|} = \sqrt{\frac{1}{\omega^2 \epsilon_0^2} \left(\frac{1}{s^E}\right)^2 \beta_2^2}, \tag{6.49}$$

$$= \sqrt{\frac{1}{\omega^2 \epsilon_0^2} \left(\frac{1}{s^E}\right)^2 \omega^2 \mu_0 \epsilon_0 s^H s^E}, \tag{6.50}$$

$$= \sqrt{\frac{\mu_0}{\epsilon_0} \left(\frac{s^H}{s^E}\right)}, \tag{6.51}$$

$$= \sqrt{\frac{\mu_0 \left(\kappa^H + \frac{\sigma^H}{j\omega\mu_0}\right)}{\epsilon_0 \left(\kappa^E + \frac{\sigma^E}{j\omega\epsilon_0}\right)}}, \tag{6.52}$$

$$= \sqrt{\frac{\mu_2 \left(1 + \frac{\sigma^H}{j\omega\mu_2}\right)}{\epsilon_2 \left(1 + \frac{\sigma^E}{j\omega\epsilon_2}\right)}}. \tag{6.53}$$

Note that the analysis is being done on a definition of the stretched coordinate that doesn't include the CFS term α introduced by Kuzuoglu and Mittra [72] and included in the stretched coordinate defined in [56].

6.3.3 Impedance Matching for E and H

By enforcing continuity of tangential fields at $x = 0$, we set $E_y^I(x = 0) = E_y^{II}(x = 0)$. Enforcing continuity gives us $\beta_{1y} = \beta_{2y} = k_1 \sin(\theta)$, and the reflection coefficient is be found to be

$$\Gamma = \frac{\frac{\beta_{1x}}{\epsilon_1} - \frac{\beta_{2x}}{\epsilon_0 s^E}}{\frac{\beta_{1x}}{\epsilon_1} + \frac{\beta_{2x}}{\epsilon_0 s^E}}. \tag{6.54}$$

The general reflection coefficient is nonzero for arbitrary angle. We examine the case of normal incidence where $\theta = 0$. This means the y-components of β are 0 ($\beta_{1y} = \beta_{2y} = 0$), and the x-components of β are

$$\beta_{1x} = k_1 = \omega\sqrt{\mu_1\epsilon_1}, \tag{6.55}$$

$$\beta_{2x} = \sqrt{k_2^2 s^E s^H} = \omega\sqrt{\mu_0\epsilon_0 s^E s^H} = \omega\sqrt{\mu_2\epsilon_2(1 + \sigma^E/j\omega\epsilon_2)(1 + \sigma^H/j\omega\mu_2))}. \tag{6.56}$$

Inserting the definitions from Equations (6.55) and (6.56) into Equation (6.54), we can simplify Γ to be

$$\Gamma = \frac{\sqrt{\frac{\mu_1}{\epsilon_1}} - \sqrt{\frac{\mu_2}{\epsilon_2}}\sqrt{\frac{1+\sigma^H/j\omega\mu_2}{1+\sigma^E/j\omega\epsilon_2}}}{\sqrt{\frac{\mu_1}{\epsilon_1}} + \sqrt{\frac{\mu_2}{\epsilon_2}}\sqrt{\frac{1+\sigma^H/j\omega\mu_2}{1+\sigma^E/j\omega\epsilon_2}}}. \tag{6.57}$$

We can be write Equation (6.57) in terms of impedance as

$$\Gamma = \frac{\eta_1 - \eta_2}{\eta_1 + \eta_2} \tag{6.58}$$

The reflection coefficient is minimized ($\Gamma = 0$) when $\eta_1 = \eta_2$. When the PML material is impedance-matched with the simulation, we can write

$$\sqrt{\frac{\mu_1}{\epsilon_1}} = \sqrt{\frac{\mu_2\left(1 + \frac{\sigma^H}{j\omega\mu_2}\right)}{\epsilon_2\left(1 + \frac{\sigma^E}{j\omega\epsilon_2}\right)}}. \tag{6.59}$$

The easiest way to solve this equation is to set $\epsilon = \epsilon_1$=ϵ_2 and $\mu = \mu_1$=μ_2

$$\sqrt{\frac{\mu_1}{\epsilon_1}} = \sqrt{\frac{\mu_1\left(1+\frac{\sigma^H}{j\omega\mu_1}\right)}{\epsilon_1\left(1+\frac{\sigma^E}{j\omega\epsilon_1}\right)}}, \tag{6.60}$$

which can be simplified to

$$\frac{\sigma^E}{\epsilon_1} = \frac{\sigma^H}{\mu_1}. \tag{6.61}$$

By solving for σ_E, we see the relationship between the σ_E and σ_H is

$$\sigma^E = \frac{\epsilon}{\mu}\sigma^H. \tag{6.62}$$

When the material is impedance-matched, this relationship between σ^E and σ^H holds. This relationship also implies the stretched coordinates for $\mathbf{E}$ and $\mathbf{H}$ are equal $s^E = s^H$ if we defined the materials parameters in the PML such that $\kappa^E = \kappa^H$. Now, we need to find conditions for σ^A and σ^ϕ for an impedance-matched medium.

6.3.4 Impedance Matching for A and ϕ

The definition of $\mathbf{E}$ in terms of potentials shows $\mathbf{E}$ and $\mathbf{A}$ are related by a time-derivative and no other operations. This should mean that the boundary conditions for $\mathbf{A}$ are the same as those for $\mathbf{E}$. Doing the same analysis as the previous section, we should have continuity of tangential components of $\mathbf{A}$. By setting $A_y^I(x=0) = A_y^{II}(x=0)$, the reflection coefficient is

$$\Gamma = \frac{\frac{\mu_1}{\beta_{1x}} - \frac{\mu_2}{\beta_{2x}}}{\frac{\mu_1}{\beta_{1x}} + \frac{\mu_2}{\beta_{2x}}}. \tag{6.63}$$

If we assume the case of normal incidence ($\theta = 0$), it becomes

$$\Gamma = \frac{\sqrt{\frac{\epsilon_1}{\mu_1}} - \sqrt{\frac{\epsilon_2}{\mu_2}}\sqrt{\frac{1+\sigma^E/j\omega\epsilon_2}{1+\sigma^H/j\omega\mu_2}}}{\sqrt{\frac{\epsilon_1}{\mu_1}} + \sqrt{\frac{\epsilon_2}{\mu_2}}\sqrt{\frac{1+\sigma^E/j\omega\epsilon_2}{1+\sigma^H/j\omega\mu_2}}} \tag{6.64}$$

which can be written as

$$\Gamma = \frac{\frac{1}{\eta_1} - \frac{1}{\eta_2}}{\frac{1}{\eta_1} + \frac{1}{\eta_2}} \tag{6.65}$$

Minimization of this reflection coefficient results in the same relationship between σ^E and σ^H as the continuity analysis for $\mathbf{E}$. The result is consistent, but since our expression for $\mathbf{A}$ was derived from the definition of $\mathbf{H}$, there is no stretched coordinate in the equation to give us a relationship between σ^A and another known value. We will use a different method to obtain the relationship after doing the analysis for ϕ.

ϕ must be continuous across the interface, so we can do the same continuity analysis for ϕ such that $\phi^I(x=0) = \phi^{II}(x=0)$

$$\Gamma = \frac{\frac{1}{\epsilon_1^2}\left(\frac{\beta_{1y}}{\beta_{1x}} - \frac{\beta_{1x}}{\beta_{1y}}\right) + \frac{\mu_2}{\epsilon_0^2\mu_0 s^\phi}\left(\frac{\beta_{2x}}{\beta_{2y}} - \frac{\beta_{2y}}{\beta_{2x}}\right)}{-\frac{1}{\epsilon_1^2}\left(\frac{\beta_{1y}}{\beta_{1x}} + \frac{\beta_{1x}}{\beta_{1y}}\right) - \frac{\mu_2}{\epsilon_0^2\mu_0 s^\phi}\left(\frac{\beta_{2x}}{\beta_{2y}} - \frac{\beta_{2y}}{\beta_{2x}}\right)}. \tag{6.66}$$

If we assume the case of normal incidence ($\theta = 0$), it simplifies to

$$\Gamma = \frac{\frac{1}{\epsilon_1^2}\beta_{1x} - \frac{\mu_2}{\epsilon_0^2\mu_0 s^\phi}\beta_{2x}}{\frac{1}{\epsilon_1^2}\beta_{1x} + \frac{\mu_2}{\epsilon_0^2\mu_0 s^\phi}\beta_{2x}}, \tag{6.67}$$

which can be expanded to

$$\Gamma = \frac{\sqrt{\frac{\mu_1}{\epsilon_1}}\frac{1}{\epsilon_1} - \frac{\mu_2\sqrt{\mu_0\epsilon_0}}{\epsilon_0^2\mu_0 s^\phi}\sqrt{s^E s^H}}{\sqrt{\frac{\mu_1}{\epsilon_1}}\frac{1}{\epsilon_1} + \frac{\mu_2\sqrt{\mu_0\epsilon_0}}{\epsilon_0^2\mu_0 s^\phi}\sqrt{s^E s^H}}. \tag{6.68}$$

We know the stretched coordinates for E and H are equal ($s^E = s^H$), so we can insert the definition for the stretched coordinate to get a result in terms of κ^ϕ

$$\Gamma = \frac{\sqrt{\frac{\mu_1}{\epsilon_1}}\frac{1}{\epsilon_1} - \frac{\mu_2\sqrt{\mu_2\epsilon_2}}{\epsilon_0^2\mu_0\kappa^\phi}\frac{1+\sigma^E/j\omega\epsilon_2}{1+\sigma^\phi/j\omega\epsilon_2^2\mu_2}}{\sqrt{\frac{\mu_1}{\epsilon_1}}\frac{1}{\epsilon_1} + \frac{\mu_2\sqrt{\mu_2\epsilon_2}}{\epsilon_0^2\mu_0\kappa^\phi}\frac{1+\sigma^E/j\omega\epsilon_2}{1+\sigma^\phi/j\omega\epsilon_2^2\mu_2}}. \tag{6.69}$$

Inserting the definition of κ^ϕ results in

$$\Gamma = \frac{\sqrt{\frac{\mu_1}{\epsilon_1}}\frac{1}{\epsilon_1} - \frac{\mu_2\sqrt{\mu_2\epsilon_2}}{\epsilon_2^2\mu_2\kappa^\phi}\frac{1+\sigma^E/j\omega\epsilon_2}{1+\sigma^\phi/j\omega\epsilon_2^2\mu_2}}{\sqrt{\frac{\mu_1}{\epsilon_1}}\frac{1}{\epsilon_1} + \frac{\mu_2\sqrt{\mu_2\epsilon_2}}{\epsilon_2^2\mu_2}\frac{1+\sigma^E/j\omega\epsilon_2}{1+\sigma^\phi/j\omega\epsilon_2^2\mu_2}}, \tag{6.70}$$

which simplifies to

$$\Gamma = \frac{\sqrt{\frac{\mu_1}{\epsilon_1}}\frac{1}{\epsilon_1} - \sqrt{\frac{\mu_2}{\epsilon_2}}\frac{1}{\epsilon_2}\frac{1+\sigma^E/j\omega\epsilon_2}{1+\sigma^\phi/j\omega\epsilon_2^2\mu_2}}{\sqrt{\frac{\mu_1}{\epsilon_1}}\frac{1}{\epsilon_1} + \sqrt{\frac{\mu_2}{\epsilon_2}}\frac{1}{\epsilon_2}\frac{1+\sigma^E/j\omega\epsilon_2}{1+\sigma^\phi/j\omega\epsilon_2^2\mu_2}}. \tag{6.71}$$

We can now minimize the reflection coefficient by assuming $\epsilon = \epsilon_1$=ϵ_2 and $\mu = \mu_1$=μ_2. This results in an equation for σ^E in terms of σ^ϕ.

$$\sigma^E = \frac{1}{\epsilon\mu}\sigma^\phi \tag{6.72}$$

This implies $s^E = s^\phi$. So far we have proven $s^E = s^H = s^\phi$, but now we need to find the relation for s^A.

Recall the problem with minimizing the reflection coefficient was that our definition for $\mathbf{A}$ does not contain s^A. This is because our $\mathbf{A}$ field was calculated using the update equation for $\mathbf{H}$ in FiPo Hybrid, which does not contain a time derivative, which is necessary for an equation to have to have a stretched coordinate. Unfortunately, even though the update equation for $\mathbf{H}$ in FiPo Basic contains a stretched coordinate s^H, it does not contain $\mathbf{A}$ and will not allow us to calculate s^A. The equation that contains the term s^A is the update equation for $\mathbf{A}$, or the definition of $\mathbf{E}$ in terms of $\mathbf{A}$ and ϕ. We could not do this originally because we needed to find $\mathbf{A}$ from $\mathbf{H}$ before being able to calculate ϕ. Since we have all fields and potentials, we can insert out definitions for $\mathbf{E}$, $\mathbf{A}$, and ϕ into the definition of the y-component of $\mathbf{E}$ in terms of ϕ and $\mathbf{A}$ and arrive at

$$\omega^2\mu_0\epsilon_0 s^A = \left(\frac{2}{s^E} - \frac{1}{s^\phi}\right)\beta_{2x}^2 + \frac{1}{s^\phi}\beta_{2y}^2. \tag{6.73}$$

We can use the previously derived $s^E = s^\phi$ to simplify this to

$$\omega^2\mu_0\epsilon_0 s^A s^E = \beta^2. \tag{6.74}$$

Since we know β in terms of s^E and s^H, we now show that $s^H = s^A$. This means we have proven $s^E = s^H = s^A = s^\phi$.

Stretched coordinates being equal is an important result because it allows us to assume CPML coefficients a and b from Equations (6.28a) and (6.28b) are equal for all fields and potentials, such that $a_\nu^E = a_\nu^H = a_\nu^A = a_\nu^\phi$ and $b_\nu^E = b_\nu^H = b_\nu^A = b_\nu^\phi$. For different values, a and b are located at different positions, but no extra coefficients need to be calculated or stored in a conventional FDTD CPML versus a FiPo CPML since the coefficients are already calculated at both integer and half-integer position steps. In a conventional FDTD CPML, a_ν^E is calculated at integer steps due to

the positions of auxiliary variables ψ_E. a_ν^H is calculated at half-integer steps due to the positions of auxiliary variables ψ_H. By looking at the positions of ψ_A and ψ_ϕ, we know that a_ν^E is calculated at the same position as a_ν^ϕ, and a_ν^H is calculated at the same position as a_ν^A. Since all a_ν^K are equal, no extra CPML parameters need to be calculated or stored for the FiPo CPML - the same applies to b_ν^K. The auxiliary variables ψ_A and ψ_ϕ still require extra storage, but the coefficients to update these variables do not.

6.4 PML Parameters

The PML is a material designed to absorb waves with minimal reflection, and in order for the PML to absorb, we need to assign it values for its material properties. The PML is defined for the E field such that it has a conductivity σ^E, a dielectric constant κ^E, and a complex frequency shifting (CFS) parameter α^E. Introducing σ allows the wave to decay in the material, increasing κ slows the wave, and adding α can increase absorption of evanescent waves. Analogous quantities are defined for PMLs for $\mathbf{H}$, $\mathbf{A}$, and ϕ. A sudden change in materials parameters causes reflections, so grading these values over the PML domain is important for minimizing reflections. We do this for κ and σ by increasing their values deeper in the PML with a polynomial grading as found in [44]. The addition of α reduces reflection error at low frequencies but causes propagating waves to not attenuate well [44]. This can be remedied by grading α with its maximum value at the PML interface and scaling it to 0 deeper in the PML. Polynomial gradings for σ, κ, and α can be written as

$$\sigma_x(x) = \sigma_{x,\max}\left(\frac{x}{d}\right)^m \tag{6.75a}$$

$$\kappa_x(x) = 1 + (\kappa_{x,\max} - 1)\left(\frac{x}{d}\right)^m \tag{6.75b}$$

$$\alpha_x(x) = \alpha_{x,\max}\left(\frac{d-x}{x}\right)^{m_a} \tag{6.75c}$$

where each value varies with respect to position and depends on the size of the PML d, maximum paramter value, and a scaling order m. Large m means lower values for the parameter near the surface of the PML and a steep increase deeper in. Deeper in the PML, fields have decayed significantly and reflections due to discretization error have less of an impact [44]. Values in the

Variable K	K Unit	κ^K Unit	σ^K, α^K Unit
E	$\mathrm{V/m}$	none	$\mathrm{s^3\ A^2\ m^{-3}\ kg^{-1} = S/m}$
H	$\mathrm{A/m}$	none	$\mathrm{kg\ m\ s^{-2}\ A^{-2}}$
A	$\mathrm{Vs/m}$	none	$\mathrm{s^{-1}}$
ϕ	V	none	$\mathrm{s^5\ A^2\ m^{-5}\ kg^{-1}}$

Table 6.2: Variable K denotes a field or potential in column one. Units for fields and potentials are given in second column. Units for CPML parameters κ^K, σ^K, and α^K for fields and potentials are given in columns three and four.

range of $3 \leq m \leq 4$ are typically optimal for minimizing reflections [77, 57, 64, 78]. We have chosen linear scaling for α ($m_a = 1$) and $m = 3$. These scalings are different due to the different behavior these parameters have at the interface. While σ and κ must start small and gradually increase to minimize reflections in the PML, α must be nonzero at the interface and become smaller further in to not hinder the absorption of propagating waves where the values of σ and κ are largest. If $\sigma_{\max}$ is too large, discretization error will dominate in the simulation. Choosing $\sigma_{\max}$ aims to balance reflection error and discretization error [44]. The following are definitions for maximum values for σ, κ, α for a polynomial grading:

$$\sigma_{x,\max} = -\frac{(m+1)\ln[R(0)]}{2\eta d} \tag{6.76a}$$

$$\kappa_{x,\max} = 15 \tag{6.76b}$$

$$\alpha_{x,\max} = 0.24. \tag{6.76c}$$

Reflection error $R(\theta)$ at normal incidence is reffered to as optimal reflection error $R(0)$. $R(0)$ depends on size of PML and has been shown to be $R(0) = e^{-16}$ for a ten-cell PML and $R(0) = e^{-8}$ for a five-cell PML [64, 44]. For a ten-cell PML, this leads to an expression for σ_{opt} of

$$\sigma_{\mathrm{opt}} = \frac{0.8(m+1)}{\eta_0 \Delta \sqrt{\mu_r \epsilon_r}}. \tag{6.77}$$

Table 6.2 gives units for PML parameters for fields and potentials. The first column gives fields and potentials as a variable K, and the second column gives the unit of the fields and potentials. The third column is present for completeness but shows that the value of κ for each field and potential is unitless. The fourth column combines the units for σ and α because they are the same and gives the units for all fields and potentials. The unit for σ^E is the standard unit for conductivity. Since σ^H, σ^A, σ^ϕ are all ficticious values for loss, the units are not commonly defined, so they are given here.

The choice of parameters has a large impact on PML performance, although it is only one factor of many that impacts the absorption properties of the PML. If parameters are chosen without care, discretization or reflection error can dominate the simulation. Since CPML is a commonly-used method for conventional FDTD, the choice of parameters are well-documented. For FiPo FDTD, we have shown in Section 6.3.2 that the parameters for conventional FDTD can be utilized for the CPML for potentials, eliminating the need to rederive or reoptimize parameters for our new method.

6.5 Simulation Results

In order to test the CPML developed for FiPo, we consider four different test simulations. The first example is the simulation in Section 5.3 with an added CPML boundary layer. It is a basic differentiated Gaussian source launched from the center of the simulation in free space. The example is intuitive and allows us to visually examine the effectiveness of the PML. The second, third, and fourth simulations are similar in order to compare the effect of material and adding a scatterer to the simulation. The second simulation is similar to the first with the addition of a PEC and source moved 2 points up in the z-direction. The source for the third and fourth simulations is the same as the second. The third and fourth examples use the materials properties from Roden and Gedney's original CPML paper [56] for a PEC in soil. The third simulation is only the differentiated Gaussian pulse launched in soil. The fourth simulation is like the third with the addition of a PEC.

Relative error plots are a common way to evaluate the effectiveness of a PML. Generally, a large simulation will be run with a PML, as well as a smaller simulation, also with a PML. A receiver is placed at a location in each simulation such that, if the simulations were overlayed, the receiver would be at the same position in each. The field values for the large simulation can be checked at this point to ensure no reflections are present at the receiver for the reference simulation. The values of the field are recorded at the receiver for each simulation, and the relative error between the two simulations is calculated and plotted over time. The maximum error in dB is generally a good indicator of the performance of the PML.

6.5.1 Free-space Simulations

6.5.1.1 Resonant Cavity with CPML

In order to first test the PML, we again look at the simulation of the resonant cavity first dicussed in Section 5.3. We use the CPML parameters discussed in Section 6.4. To make the reference simulation for the resonant cavity with CPML, we added a ten-cell PML to the FiPo Basic simulation of a resonant cavity from Section 5.3.

Figure 6.1 shows snapshots of FiPo Basic (Figure 6.1a) and FiPo Hybrid (Figure6.1b) with CPML as the wave is impinging on the absorbing layer. Both simulations appear to have identical propagation characteristics prior to wave decay in PML. Figure 6.2 shows snapshots of FiPo Basic with no PML (Figure 6.2a) shortly after the wave reflects from the reflective boundary in the reference simulation as well as FiPo Basic (Figure 6.2b) and FiPo Hybrid (Figure 6.2c) with CPML after wave decay in the PML. We observe very little visible reflection for FiPo Basic with CPML, but we do see reflection for FiPo Hybrid with CPML, although the method still decreases the magnitude of the wave compared to the reference. In particular, the visible reflections for ϕ for FiPo Hybrid with CPML are negligible and appear to be identical for FiPo Basic and Hybrid with CPML. A difference in absorption between FiPo Basic and Hybrid is to be expected because of the nature of their update equations - the FiPo Hybrid update equations are Equations (5.16), and FiPo Basic update equations are Equations (6.32). The FiPo Basic CPML algorithm uses auxiliary variables to attenuate the wave in $\mathbf{H}$, while the FiPo Hybrid $\mathbf{H}$ is updated directly from $\mathbf{A}$ and does

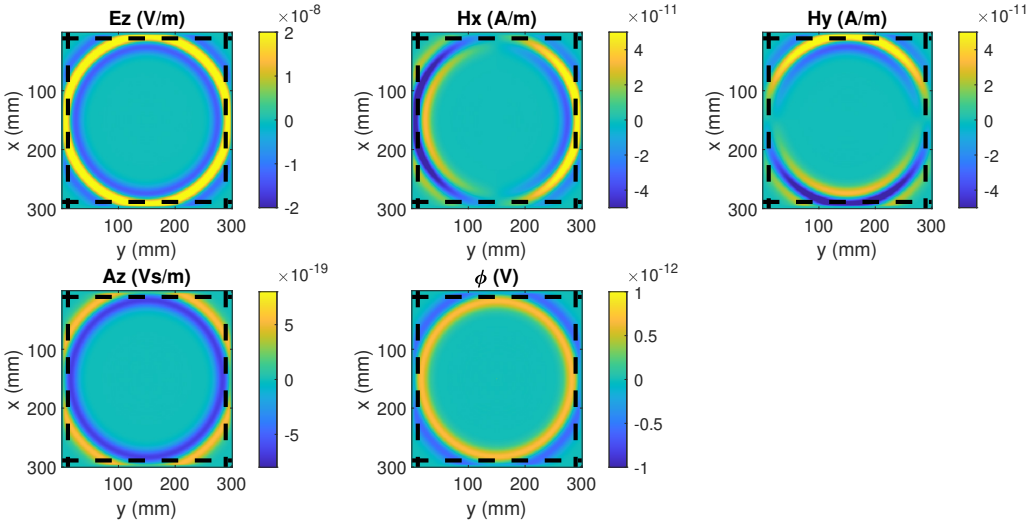

(a) FiPo Basic

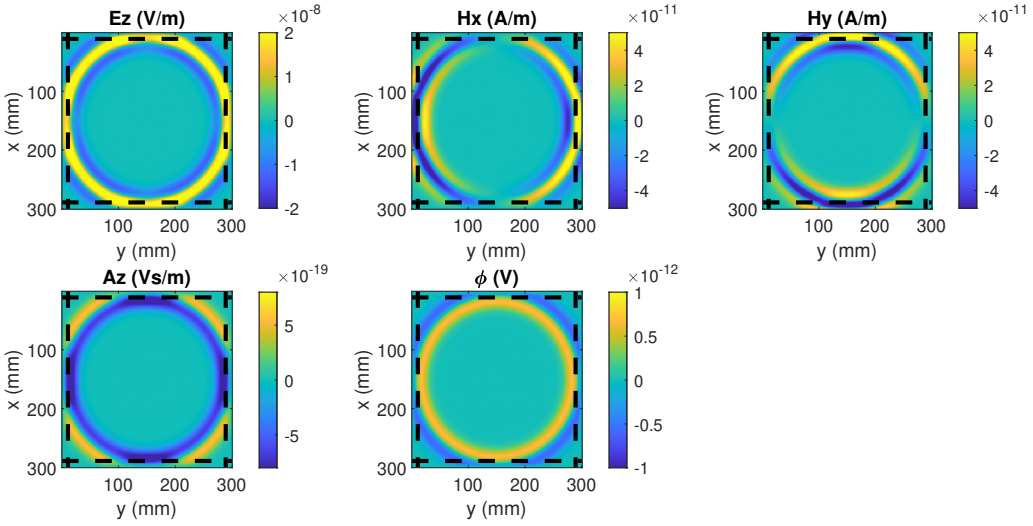

(b) FiPo Hybrid

Figure 6.1: Spatial profile of (top row) E_x, H_x, and H_y, as well as (bottom row) A_z and ϕ for a differentiated Gaussian current source from Eq. (5.17) in free space at time $t = 0.69$ ns ($400\Delta_t$ or $13.0684t_w$) after start of the simulation. Dashed black line represents CPML boundary.

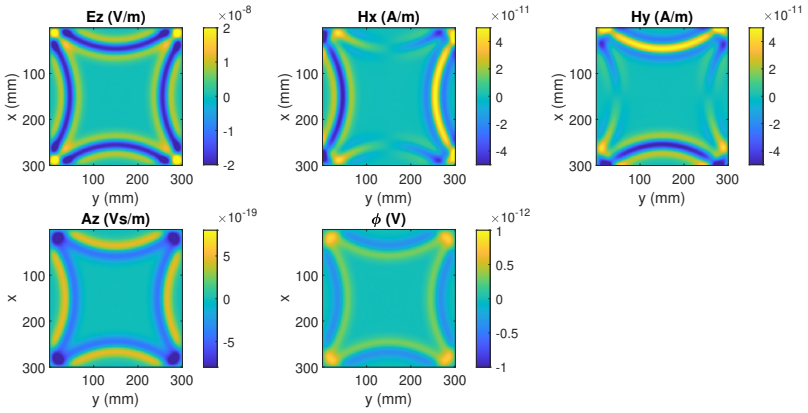

(a) FiPo Basic

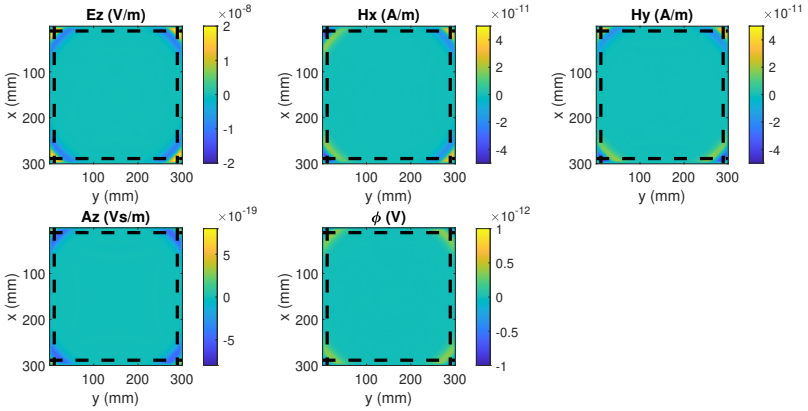

(b) FiPo Basic with CPML

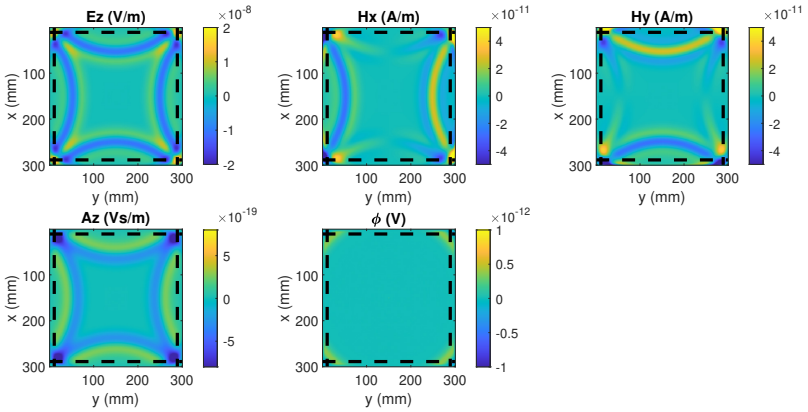

(c) FiPo Hybrid with CPML

Figure 6.2: Spatial profile of (top row) E_x, H_x, and H_y, as well as (bottom row) A_z and ϕ for a differentiated Gaussian current source from Eq. (5.17) in free space at time $t = 0.87$ ns ($500\Delta_t$ or $16.3355t_w$) after start of the simulation. Dashed black line represents CPML boundary.

not decay in the PML region. H_x and H_y update equations cumulatively have four more auxiliary variables in FiPo Basic than in FiPo Hybrid. This is due to each component of $\mathbf{H}$ containing two auxiliary variables, as can be seen in Equations (6.32a) and (6.32b). The update for $\mathbf{H}$ contains no auxiliary variables in FiPo Hybrid, and is the same as its update equation in the simulation region. Additionally, the ϕ update equation, Equation (6.29), contains more auxiliary variables than other CPML update equations. We attribute to the improved absorption to be a result of Equation (6.29) containing more auxiliary variables. The number of auxiliary variables in an update equation depends on how many spatial derivatives are present in that equation as well as the method used to derive the CPML.

In order to test the absorption of the PML, we ran simulations for FiPo Basic and FiPo Hybrid scaled to $71 \times 71 \times 71$ and compared them with a reference simulation of the previous FiPo Basic simulation for Figures 6.1a and 6.2b. A receiver placed 5 points away from the PML boundary in x and in the same plane as the source in y and z captures the fields and potentials, and the field magnitude was checked to make sure no reflections from boundary were observed from the reference. The calculation for relative error from [56] is written as

$$\text{error}_{\text{dB}}(t) = 20\ \log_{10} \frac{|\chi_i(t) - \chi_{i_{\text{ref}}}(t)|}{|\chi_{i_{\text{ref}_{\text{max}}}}|} \tag{6.78}$$

where $\chi_i(t)$ is the value of a time-dependent component of a field or potential, $\chi_{i_{\text{ref}}}(t)$ is the value of a time-dependent component of the field or potential in the reference simulation, and $\chi_{i_{\text{ref}_{\text{max}}}}$ is the maximum value of $\chi_{i_{\text{ref}}}(t)$ over the full simulation time. The relative error for the magnitude of fields and potentials for this simulation is plotted in Figure 6.3. The results confirm our initial obeservations from Figure 6.2. The error being below 0dB indiciates that the waves are being absorbed, indicating that the PML is working as expected. The reflection error for FiPo Basic peaks well below -50 dB, confirming the low reflections we see in Figure 6.1a. For FiPo Hybrid, however, the reflection error is above -50 dB for $\mathbf{E}$, $\mathbf{H}$, and $\mathbf{E}$, explaining the reflections we see for those fields and potentials. The reflection error for ϕ in FiPo Hybrid peaks for a value below -50 dB and appears to be similar to the error for ϕ in FiPo Basic, which is congruent with our previous observations from Figures 6.1a and 6.2b. The difference in error between these two methods is due to the lack of auxiliary variables in the update for the $\mathbf{H}$ in FiPo Hybrid compared to FiPo Basic.

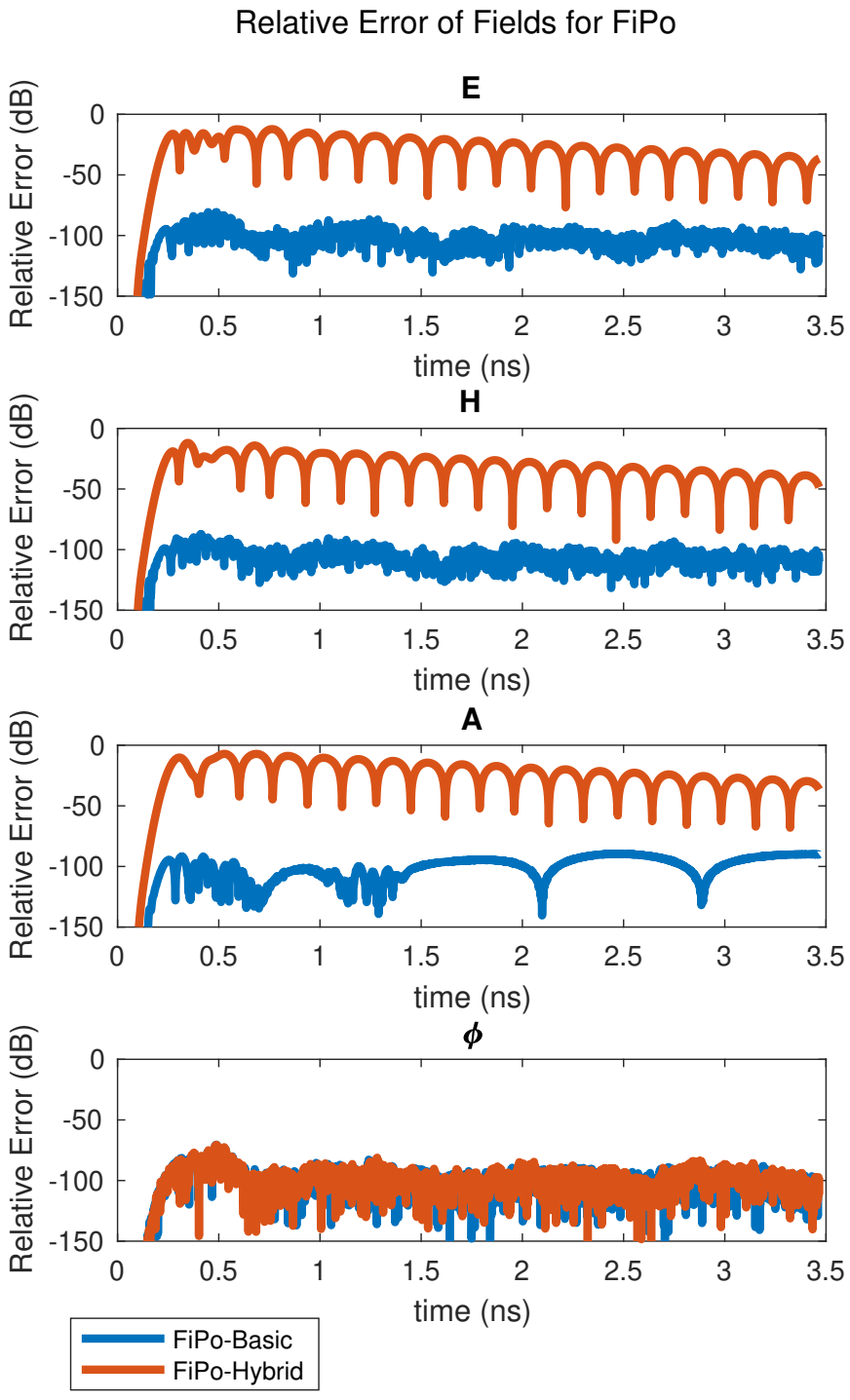

Figure 6.3: Relative error of fields and potentials for FiPo Basic and FiPo Hybrid simulations for a wave propagating in free space.

6.5.1.2 Resonant Cavity with PEC and CPML

The PEC is defined in free space ($\epsilon_r = 1$, $\sigma = 0$) from $x \in [30\text{ mm}, 40\text{ mm}]$ and $y \in [30\text{ mm}, 40\text{ mm}]$ where z is at the center of the simulation. The plate is illuminated by the current density J_z source from Section 5.3 paced two points above the plate in the z-direction (i.e., above the plane of observation). The simulation is run on $71 \times 71 \times 71$ cell lattice with a ten-cell PML. The reference simulation using FiPo Basic is run on a $300 \times 300 \times 300$ grid with a ten-cell PML. The reference fields were recorded five points away from the x PML boundary and in the center of the y–z plane. For parameters, we use $m = 3$ and $m_a = 1$. PML parameters are defined as

$$\sigma_{\max} = 1.1\frac{m+1}{150\pi\Delta\sqrt{\epsilon_r}}, \tag{6.79a}$$

$$\kappa_{\max} = 15, \tag{6.79b}$$

$$\alpha = 0.24. \tag{6.79c}$$

The waves from FiPo Basic and Hybrid appear identical propagating from the source at $t = 100\Delta_t$ in Figure 6.4. Once the wave impinges on the PML at $t = 200\Delta_t$ in Figure 6.5, the waves appear to be well absorbed by FiPo Basic because the wavefront still appears circular, unaltered by reflections. The wavefront from FiPo Hybrid is no longer spherical and has been altered by reflections at $t = 200\Delta_t$. The wave has been absorbed in FiPo Basic's PML at $t = 300\Delta_t$ in Figure 6.6, but waves in FiPo Hybrid still propagate in the simulation. Figure 6.7 shows the relative error of FiPo Basic and FiPo Hybrid. The difference in error between FiPo Basic and FiPo Hybrid is similar to difference in error in Figure 6.3, where FiPo Hybrid's error is above -50 dB and FiPo Basic's error is below -50 dB. The simulations for Figure 6.3 and 6.7 differ by the addition of a scatterer, the change made for $\sigma_{\max}$, and the source being moved by two points. The most notable increase in error is for ϕ in FiPo Hybrid. The increase in error from ϕ could come from the self-consistency of the FiPo Hybrid algorithm, where the unattenuated values of other fields and potentials can contribute to reflection error for ϕ. ϕ, in other simulations, seems to be able to compensate for this error with its three-auxilary variable PML. The PEC scatterer affects values of ϕ, however, and this effect can be seen as non-zero ϕ values in Figure 6.6 for FiPo Hybrid.

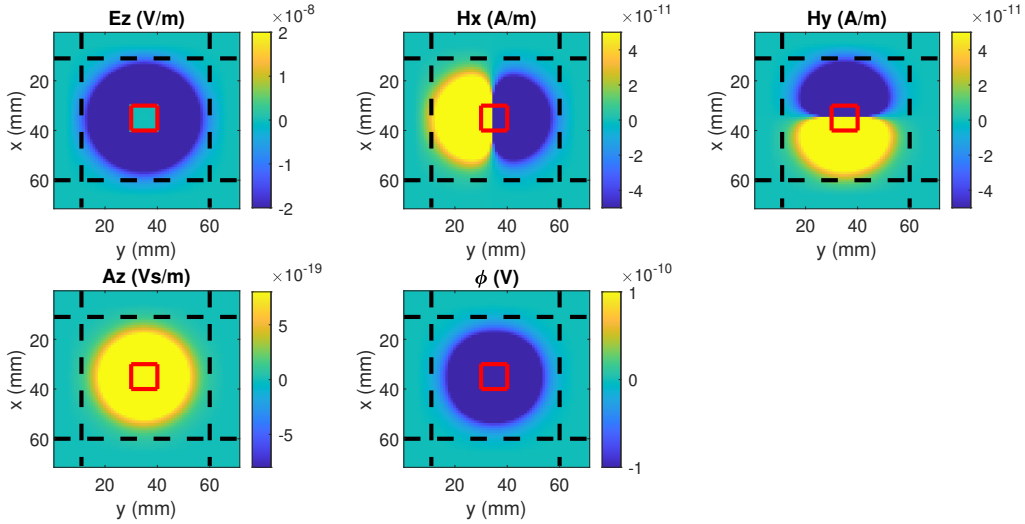

(a) FiPo Basic

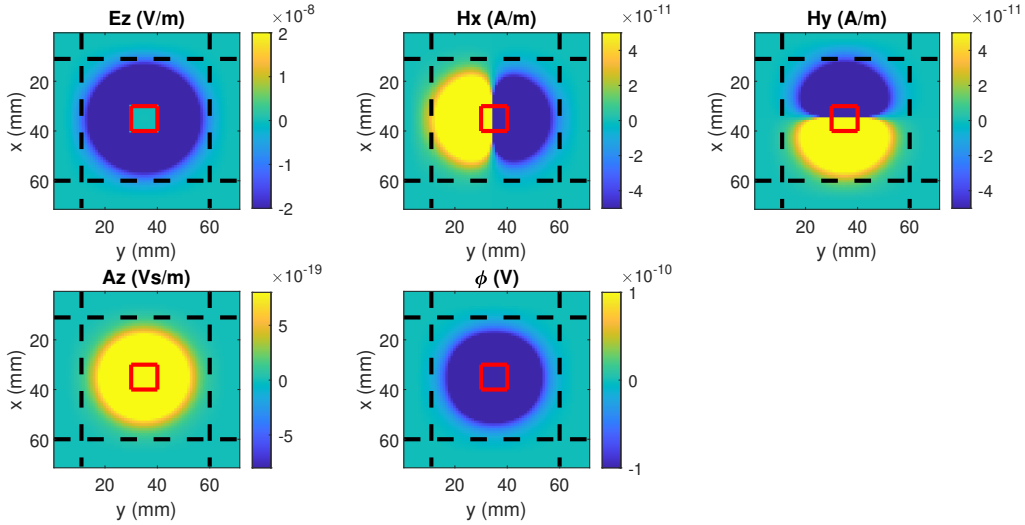

(b) FiPo Hybrid

Figure 6.4: Spatial profile of (top row) E_x, H_x, and H_y, as well as (bottom row) A_z and ϕ for a differentiated Gaussian current source from Eq. (5.17) in free space at time $t = 0.17$ ns ($100\Delta_t$ or $3.2671t_w$) after start of the simulation. Dashed black line represents CPML boundary. Solid red line outlines the region defined as a PEC.

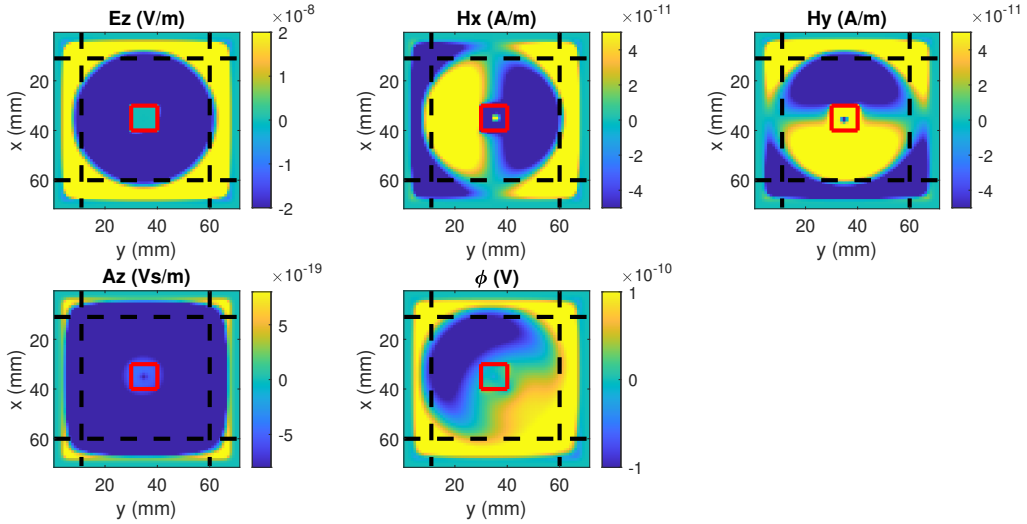

(a) FiPo Basic

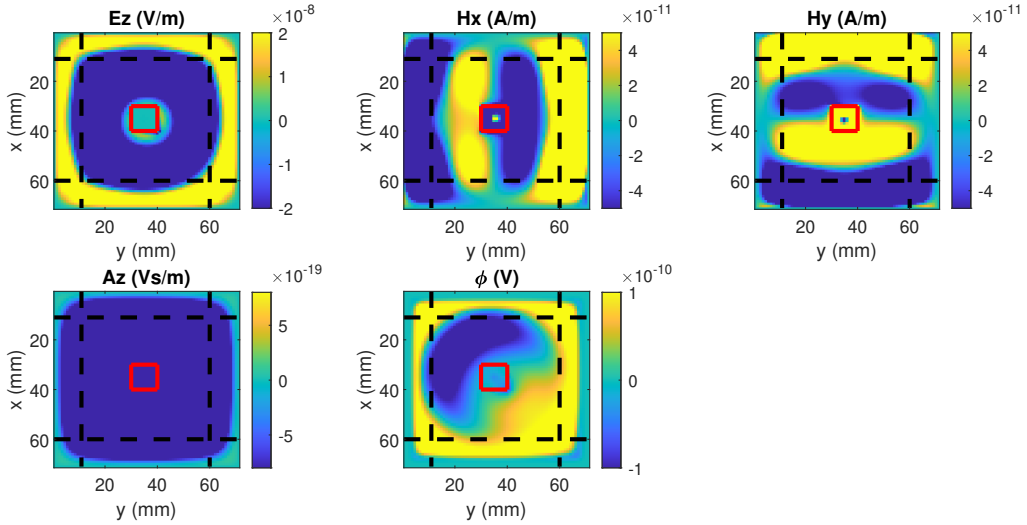

(b) FiPo Hybrid

Figure 6.5: Spatial profile of (top row) E_x, H_x, and H_y, as well as (bottom row) A_z and ϕ for a differentiated Gaussian current source from Eq. (5.17) in free space at time $t = 0.35$ ns ($200\Delta_t$ or $6.5342t_w$) after start of the simulation. Dashed black line represents CPML boundary. Solid red line outlines the region defined as a PEC.

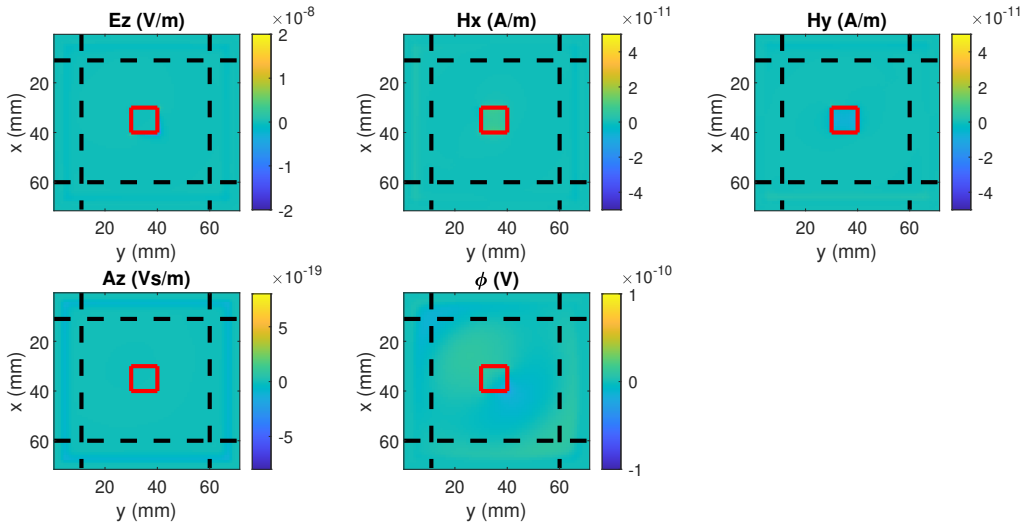

(a) FiPo Basic

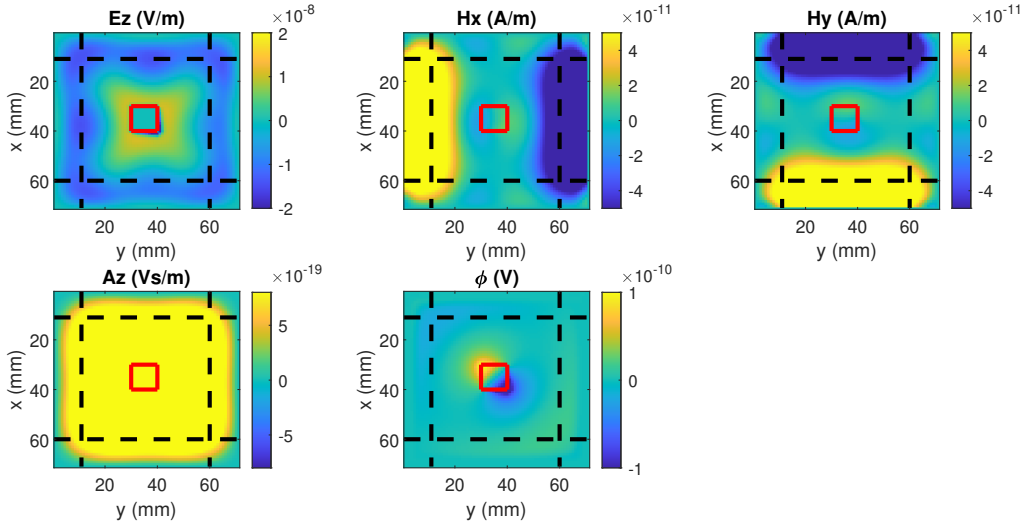

(b) FiPo Hybrid

Figure 6.6: Spatial profile of (top row) E_x, H_x, and H_y, as well as (bottom row) A_z and ϕ for a differentiated Gaussian current source from Eq. (5.17) in free space at time $t = 0.52$ ns ($300\Delta_t$ or $9.8013t_w$) after start of the simulation. Dashed black line represents CPML boundary. Solid red line outlines the region defined as a PEC.

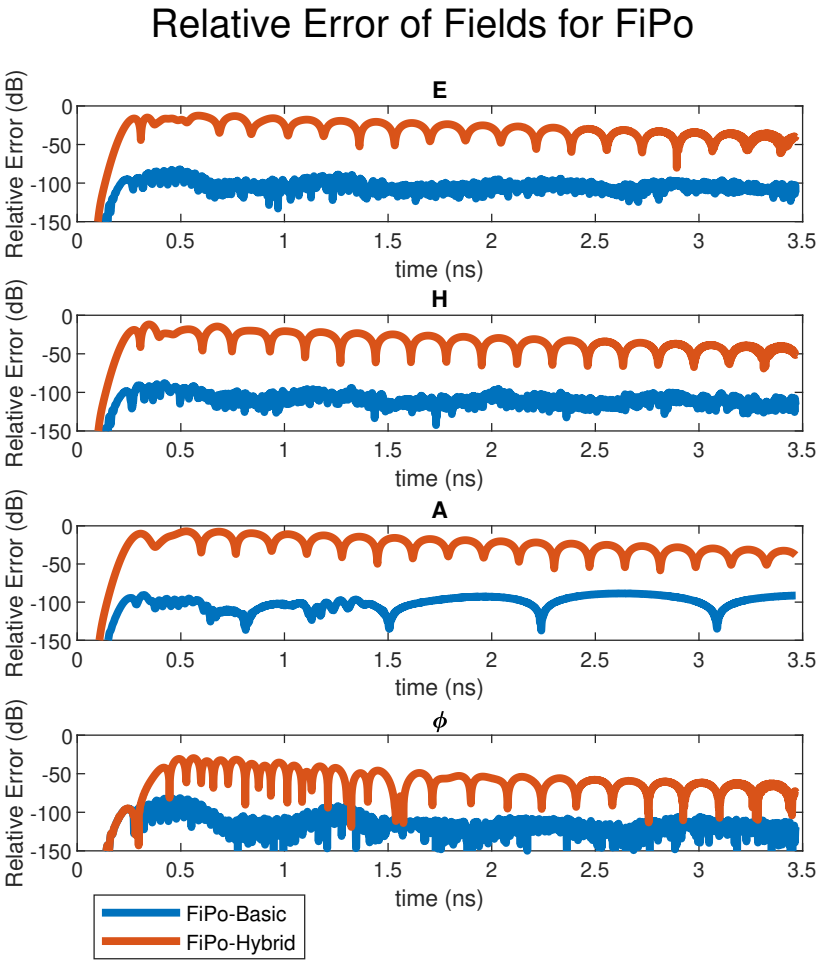

Figure 6.7: Relative error of fields and potentials for FiPo Basic and FiPo Hybrid simulations for a wave propagating around a PEC in free space.

6.5.2 Soil

The background material for the simulations in this section are defined for soil in [56] as $\epsilon_r = 7.73$ and $\sigma = 0.273$. The simulations are run on $71 \times 71 \times 71$ cell lattice with a ten-cell PML. The reference simulations using FiPo Basic are run on a $300 \times 300 \times 300$ grid with a ten-cell PML. The reference fields were recorded five points away from the x PML boundary and in the center of the y–z plane. For parameters, we use $m = 3$ and $m_a = 1$. PML parameters are defined as

$$\sigma_{\max} = 1.1 \frac{m+1}{150\pi\Delta\sqrt{\epsilon_r}}, \tag{6.80a}$$

$$\kappa_{\max} = 15, \tag{6.80b}$$

$$\alpha = 0.24. \tag{6.80c}$$

The simulation is sourced by the current-density J_z source from Section 5.3 two points above the midpoint in the z-direction.

6.5.2.1 No Scatterer in Soil

Figure 6.8 shows identical wave propagation characteristics for FiPo Basic and FiPo Hybrid at $t = 200\Delta_t$, before the wave impinges on the PML. As the wave propagates into the PML at $t = 350\Delta_t$ in Figure 6.9, we can see the wave in slowed in both cases, and FiPo Hybrid has visible reflections. ϕ looks identical in both FiPo Basic and FiPo Hybrid simulations. At $t = 500\Delta_t$ in Figure 6.10, FiPo Hybrid values have more reflection than FiPo Basic with the exception of ϕ, which appears identical in both simulations. When comparing the relative error in Figure 6.11, we see that reflection error is higher for FiPo Hybrid compared to FiPo Basic, but the error is much closer for the two algorithms compared to free-space simulations in Figures 6.3 and 6.7. FiPo Hybrid peaks above -50 dB and decreases to around -100 dB. FiPo Basic peaks at about -50 dB and decreases to around the same level as FiPo Hybrid. Reflection error in FiPo Basic is most likely reduced because of the added loss from the nonzero conductivity of soil. In this simulation, reflection error for ϕ appears identical for FiPo Basic and FiPo Hybrid.

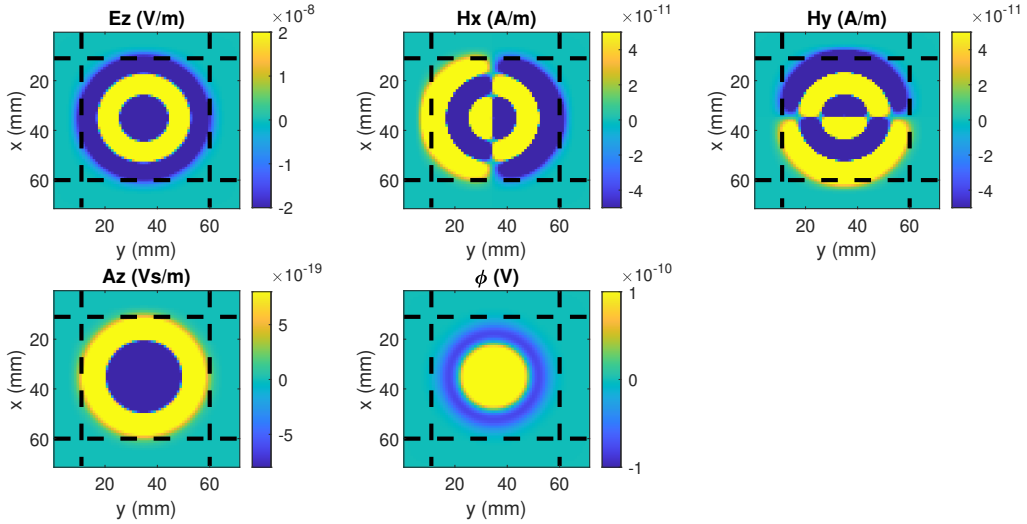

(a) FiPo Basic

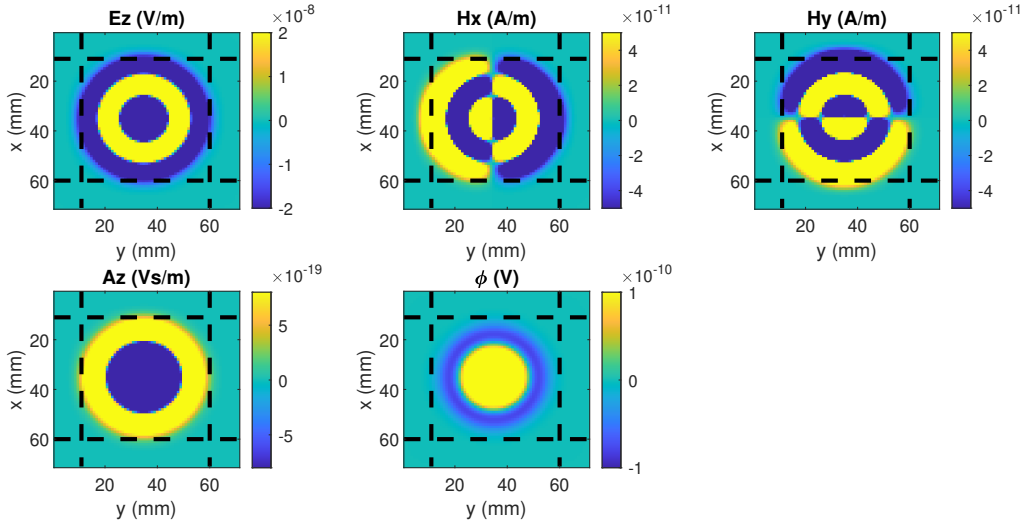

(b) FiPo Hybrid

Figure 6.8: Spatial profile of (top row) E_x, H_x, and H_y, as well as (bottom row) A_z and ϕ for a differentiated Gaussian current source from Eq. (5.17) in soil at time $t = 0.35$ ns ($200\Delta_t$ or $6.5t_w$) after start of the simulation. Dashed black line represents CPML boundary.

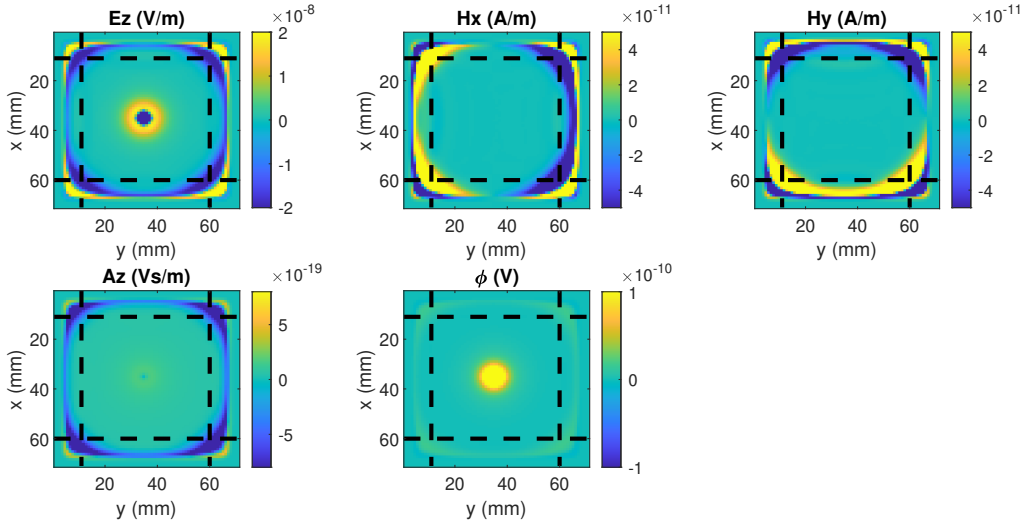

(a) FiPo Basic

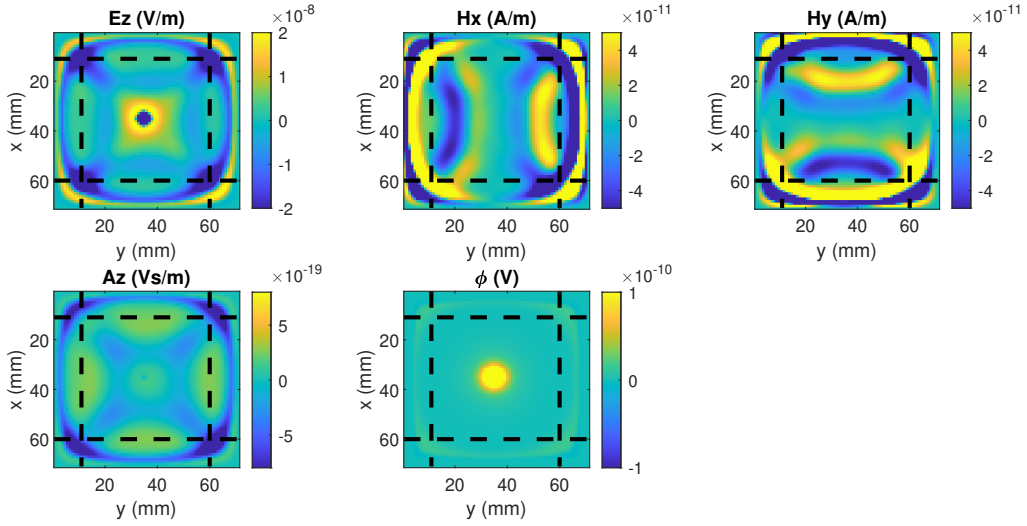

(b) FiPo Hybrid

Figure 6.9: Spatial profile of (top row) E_x, H_x, and H_y, as well as (bottom row) A_z and ϕ for a differentiated Gaussian current source from Eq. (5.17) in soil at time $t = 0.61$ ns ($350\Delta_t$ or $11.4t_w$) after start of the simulation. Dashed black line represents CPML boundary.

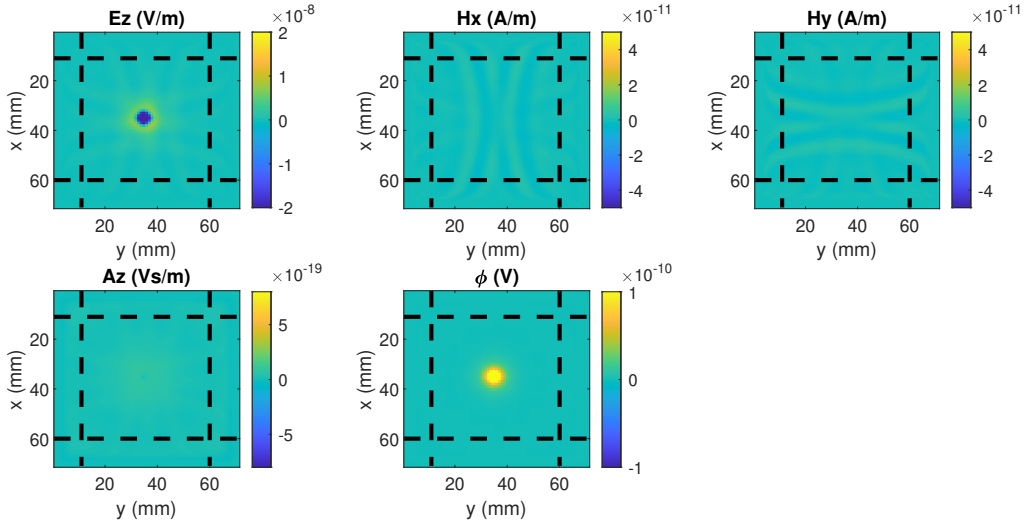

(a) FiPo Basic

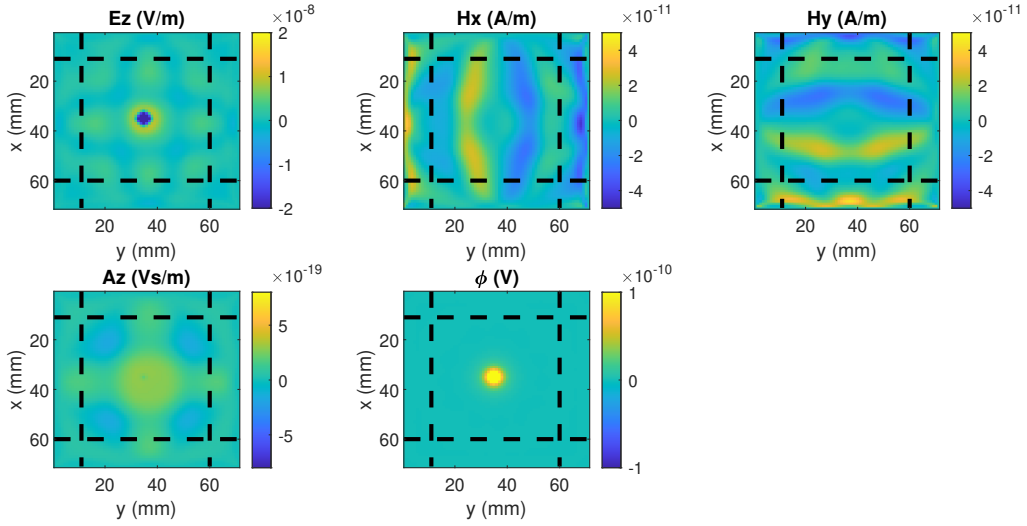

(b) FiPo Hybrid

Figure 6.10: Spatial profile of (top row) E_x, H_x, and H_y, as well as (bottom row) A_z and ϕ for a differentiated Gaussian current source from Eq. (5.17) in soil at time $t = 0.87$ ns ($500\Delta_t$ or $16.3355t_w$) after start of the simulation. Dashed black line represents CPML boundary.

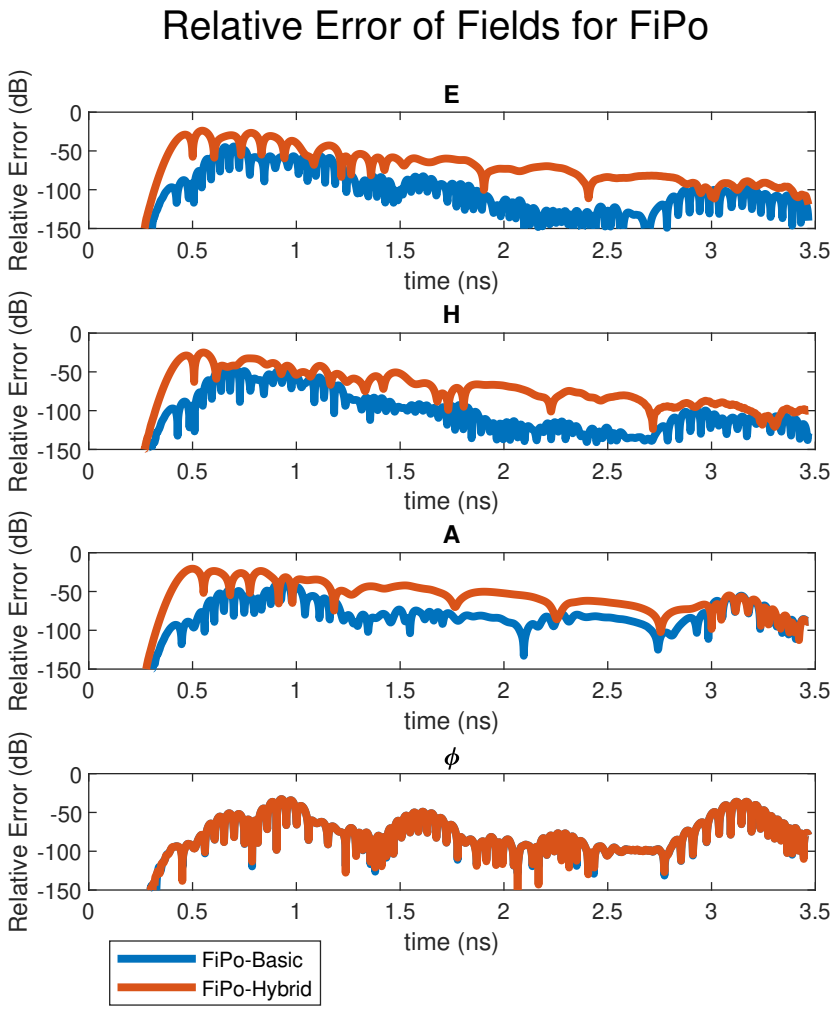

Figure 6.11: Relative error of fields and potentials for FiPo Basic and FiPo Hybrid simulations for a wave propagating in soil.

6.5.2.2 PEC Scatterer in Soil

The PEC in this simulation is defined from $x \in 30\ [\mathrm{mm}, 40\ \mathrm{mm}]$ and $y \in [30\ \mathrm{mm}, 40\ \mathrm{mm}]$, where z is at the center of the simulation.

Wave propagation is identical for FiPo Basic and FiPo Hybrid as it emanates from the source at $t = 200\Delta_t$ in Figure 6.12. At $t = 500\Delta_t$ in Figure 6.13, the wave enters the PML. ϕ appears identical in both FiPo Basic and FiPo Hybrid, but $\mathbf{H}$ has waves penetrating farther into the PML. The difference in $\mathbf{E}$ and $\mathbf{A}$ between the two algorithms is visible, but not pronounced. By $t = 1000\Delta_t$ in Figure 6.14, both FiPo Basic and FiPo Hybrid look identical without waves propagating in the background medium; however, values of $\mathbf{H}$ are present in the PEC. Relative error for a simulation of a PEC in soil is shown in Figure 6.15. The relative error between FiPo Basic and FiPo Hybrid is larger for FiPo Hybrid initially but begins to become more comparable to FiPo Basic over time. FiPo Hybrid peaks at above -50 dB while FiPo peaks at about -50 dB. Both FiPo Basic and FiPo Hybrid's error decreases from the peak over time to levels between -50 dB and -100 dB. The relative error for ϕ is about the same in both FiPo Basic and FiPo Hybrid. The added loss of soil and the addition on the PEC plate have resulted in reflection error for FiPo Basic and FiPo Hybrid being closer in magnitude for simulations in soil than in free-space simulations.

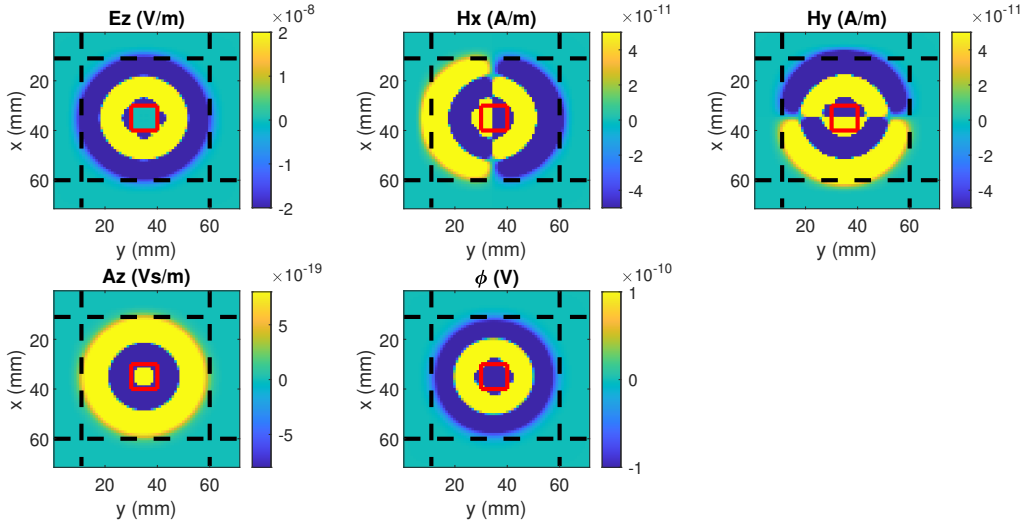

(a) FiPo Basic

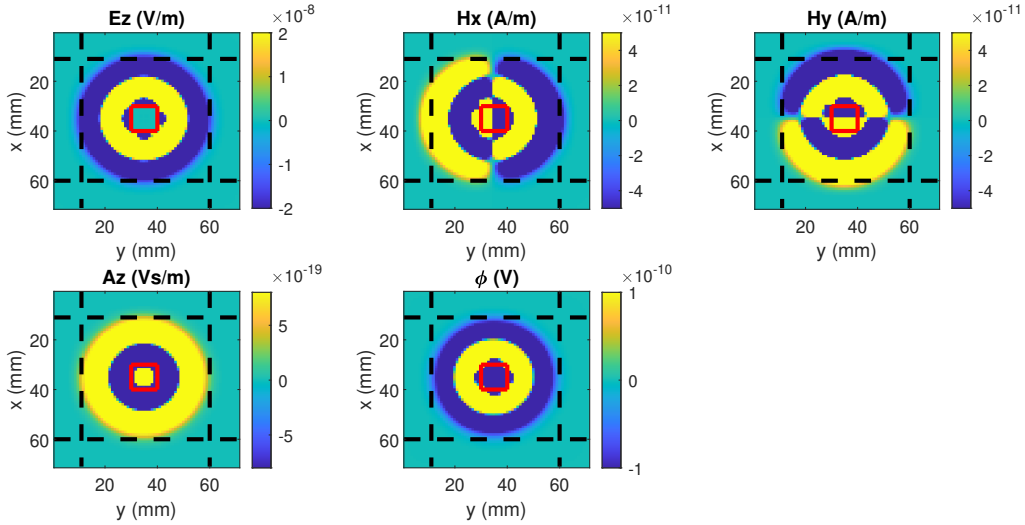

(b) FiPo Hybrid

Figure 6.12: Spatial profile of (top row) E_x, H_x, and H_y, as well as (bottom row) A_z and ϕ for a differentiated Gaussian current source from Eq. (5.17) in soil at time $t = 0.35$ ns ($200\Delta_t$ or $6.5t_w$) after start of the simulation. Dashed black line represents CPML boundary. Solid red line outlines the region defined as a PEC.

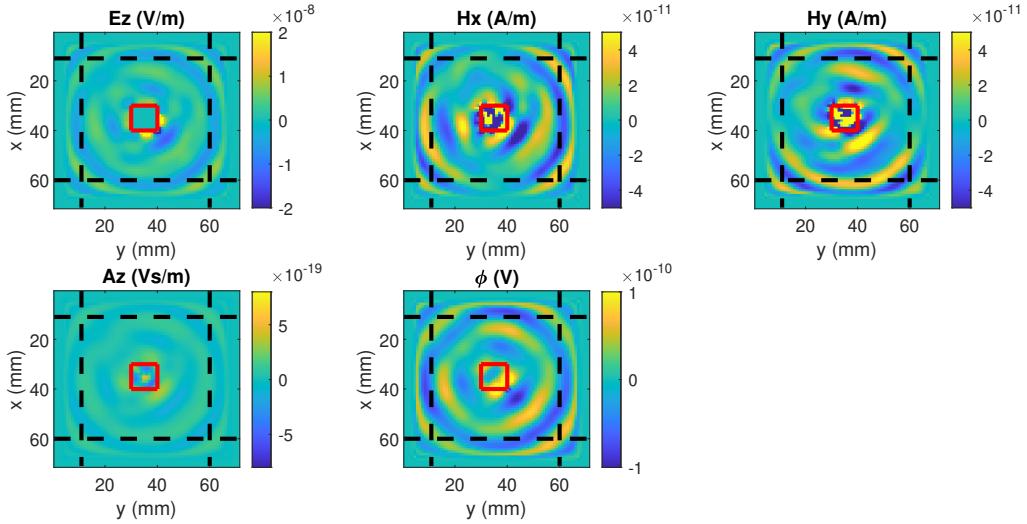

(a) FiPo Basic

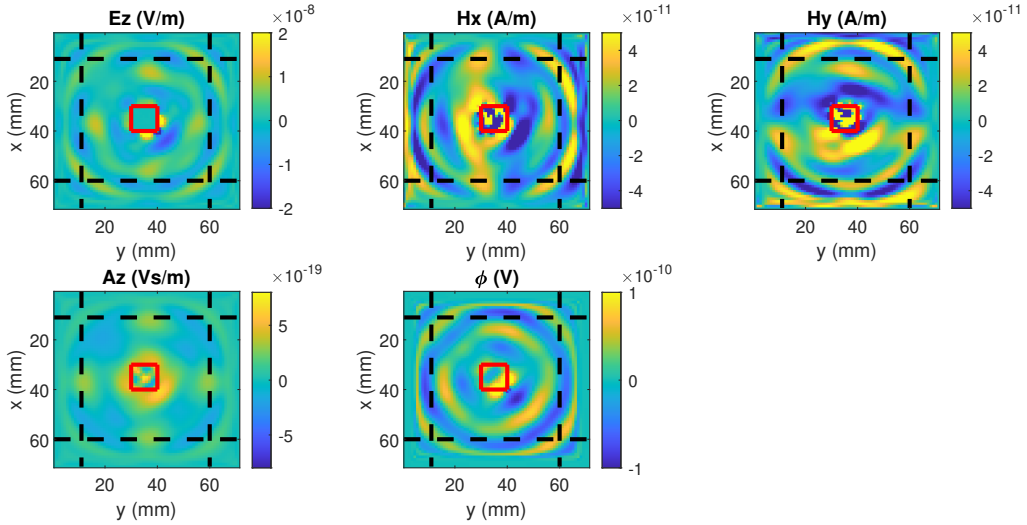

(b) FiPo Hybrid

Figure 6.13: Spatial profile of (top row) E_x, H_x, and H_y, as well as (bottom row) A_z and ϕ for a differentiated Gaussian current source from Eq. (5.17) in soil at time $t = 0.87$ ns ($500\Delta_t$ or $16.3t_w$) after start of the simulation. Dashed black line represents CPML boundary. Solid red line outlines the region defined as a PEC.

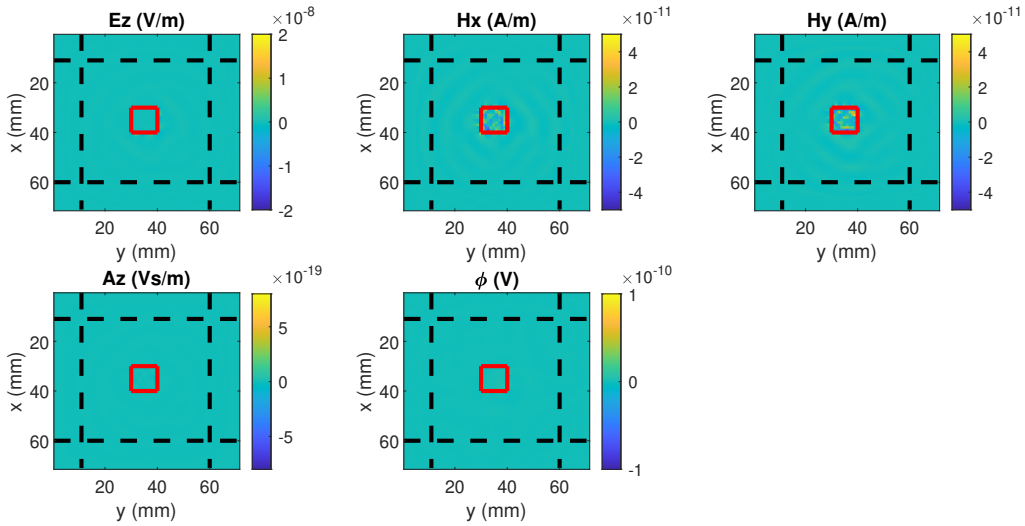

(a) FiPo Basic

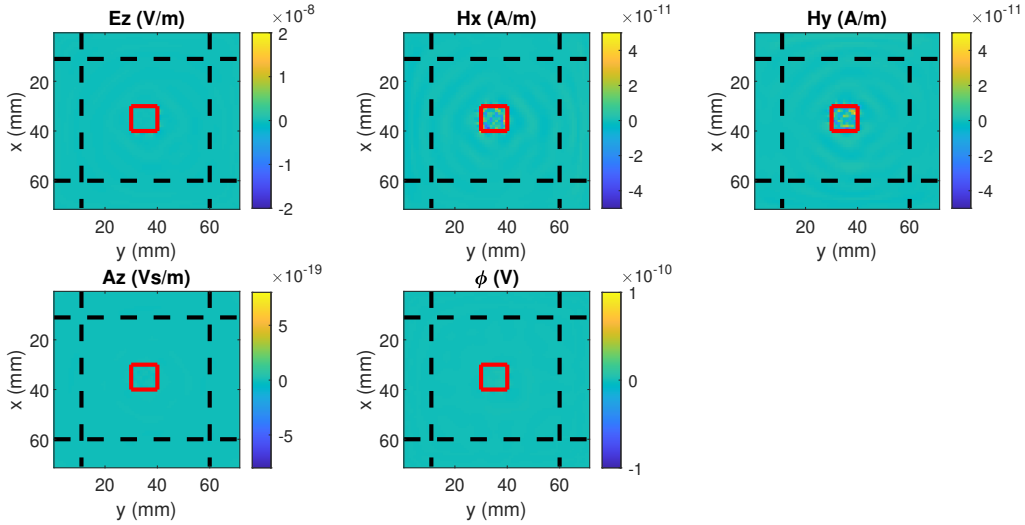

(b) FiPo Hybrid

Figure 6.14: Spatial profile of (top row) E_x, H_x, and H_y, as well as (bottom row) A_z and ϕ for a differentiated Gaussian current source from Eq. (5.17) in soil at time $t = 1.73$ ns ($1000\Delta_t$ or $32.7t_w$) after start of the simulation. Dashed black line represents CPML boundary. Solid red line outlines the region defined as a PEC.

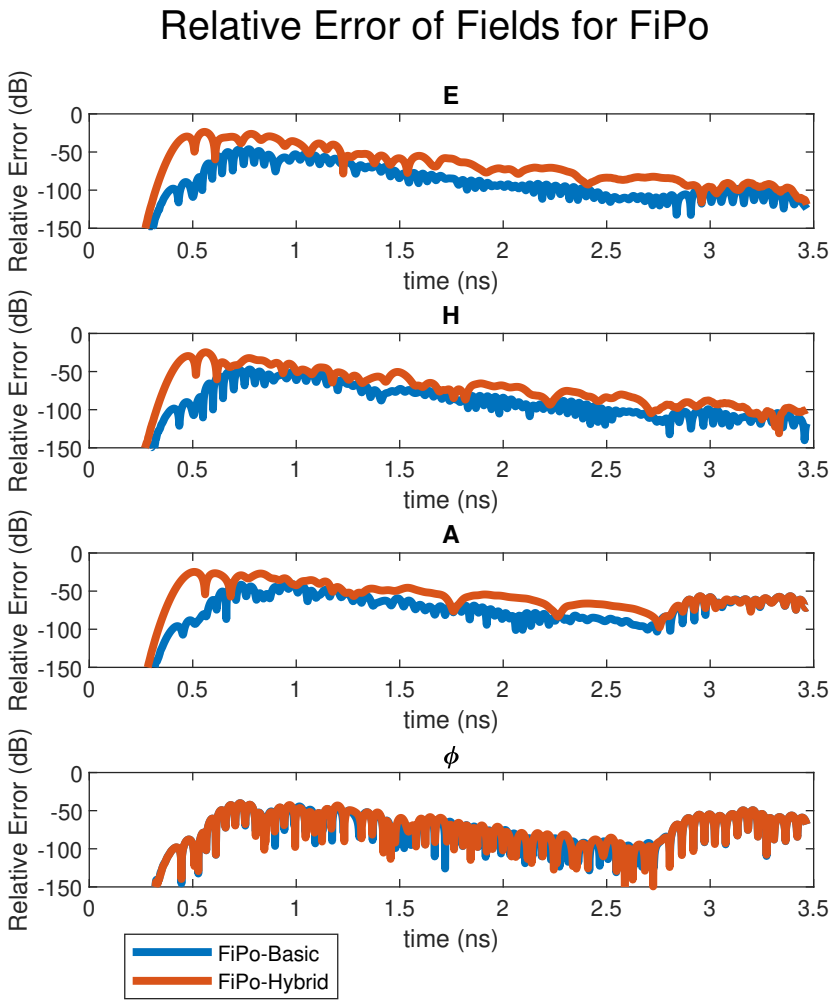

Figure 6.15: Relative error of fields and potentials for FiPo Basic and FiPo Hybrid simulations for a wave propagating around a PEC in soil.

Chapter 7

Conclusion

In order to tackle the challenge of coupling quantum transport to electrodymanics, we have developed FiPo FDTD, a first-order solver for Maxwell's equations for both fields and potentials. These potentials are able to couple to quantum transport via the electromagnetic Hamiltonian for a single particle, and a quantum transport solver can output charge and current density that can be input into FDTD. The development of FiPo may prove to be a cornerstone of conquering this challenge by tackling the electromagnetic modeling of potentials in an approachable way, as an extension of conventional FDTD.

To introduce the techniques needed to deveop FiPo, Chapter 2 covers theoretical electromagnetic background for electromagnetic fields and potentials. Evaluating electromagnetic equations on a discrete lattice is covered in Chapter 3, where conventional FDTD is explained, including the Yee grid and formalism for discretizing equations. We discuss the second-order FDTD developed by Ryu *et al.* [14] in Chapter 4. This method solves for the magnetic vector potential and the electric scalar potential using second-order Maxwell's equations coupled by the continuity equation. We have implemented this method without a PML absorbing boundary layer. The PML for this method is computationally expensive and storage intensive, meaning it is not practical for use in coupling to quantum transport. Exploration into this method drove us to develop a first-order solver.

FiPo FDTD, our first-order solver for Maxwell's equations is introduced in Chapter 5. Two different algorithms for FiPo FDTD have been developed, FiPo Basic and FiPo Hybrid. FiPo Basic is identical to conventional FDTD in its updating for the electric and magnetic fields, but introduces updates for the magnetic vector potential and electric scalar potential. FiPo Hybrid is a

self-consistent method to solve for fields and potentials, allowing information from the potentials to pass into the electric and magnetic fields. Absorbing boundary conditions, developed in Chapter 6, allow for the truncation of the simulation grid while minimizing reflection error from the outer boundary. A CPML boundary layer has been formulated for both FiPo Basic and FiPo Hybrid. The CPML for FiPo Hybrid has auxiliary variables, the mechanism for absorption, removed from its update equations for $\mathbf{H}$ due to the nature of FiPo Hybrid's algorithm. The removal of these variables causes absorption of the CPML in FiPo Hybrid to be less effective than that of FiPo Basic. However, this work has developed a framework for CPML for a self-consistent method for modeling fields and potentials and can utilize the existing work from CPML for conventional FDTD to improve its performance. The CPML for FiPo Basic performs as well as the CPML for conventional FDTD for both fields and potentials.

LIST OF REFERENCES

[1] Paolo Biagioni, Jer-Shing Huang, and Bert Hecht. Nanoantennas for visible and infrared radiation. *Reports Prog. Phys.*, 75(2):24402, 2012.

[2] Mark L Brongersma. Engineering optical nanoantennas. *Nat. Photonics*, 2(5):270–272, 2008.

[3] F. Karimi, S. Soleimanikahnoj, and I. Knezevic. Tunable plasmon-enhanced second-order optical nonlinearity in transition metal dichalcogenide nanotriangles. *Phys. Rev. B*, 103:L161401, Apr 2021.

[4] Rico Gutzler, Manish Garg, Christian R Ast, Klaus Kuhnke, and Klaus Kern. Light–matter interaction at atomic scales. *Nat. Rev. Phys.*, 3(6):441–453, 2021.

[5] Nicholas Rivera and Ido Kaminer. Light–matter interactions with photonic quasiparticles. *Nat. Rev. Phys.*, 2(10):538–561, 2020.

[6] Parinda Vasa and Christoph Lienau. Strong light–matter interaction in quantum emitter/metal hybrid nanostructures. *ACS Photonics*, 5(1):2–23, 2018.

[7] Mohsen Rahmani and Chennupati Jagadish. Light–matter interactions on the nanoscale. *Beilstein Journal of Nanotechnology*, 9:2125–2127, 2018.

[8] Robert W. Boyd, editor. Academic Press, San Diego, second edition edition, 2003.

[9] Shobhit K. Patel and Christos Argyropoulos. Plasmonic nanoantennas: enhancing light-matter interactions at the nanoscale. *EPJ Applied Metamaterials*, 2:4, 2015.

[10] Pai-Yen Chen. Semiclassical modeling of individual and arrayed nanoantennas in the quantum plasmonic regime. In *2016 URSI International Symposium on Electromagnetic Theory (EMTS)*, pages 686–689, 2016.

[11] Kevin J Savage, Matthew M Hawkeye, Rubén Esteban, Andrei G Borisov, Javier Aizpurua, and Jeremy J Baumberg. Revealing the quantum regime in tunnelling plasmonics. *Nature*, 491:574, nov 2012.

[12] Jorge Zuloaga, Emil Prodan, and Peter Nordlander. Quantum Description of the Plasmon Resonances of a Nanoparticle Dimer. *Nano Lett.*, 9(2):887–891, 2009.

[13] Ke Wang, Jilin Zheng, Hao Huang, Yunxiang Chen, Yufeng Song, Jianhua Ji, and Han Zhang. All-optical signal processing in few-layer bismuthene coated microfiber: towards applications in optical fiber systems. *Opt. Express*, 27(12):16798–16811, Jun 2019.

[14] Christopher Jayun Ryu, Aiyin Y Liu, Wei E I Sha, and Weng Cho Chew. Finite-Difference Time-Domain Simulation of the Maxwell–Schrödinger System. *IEEE Journal on Multiscale and Multiphysics Computational Techniques*, 1:40–47, 2016.

[15] Fahri Alkan and Christine M Aikens. TD-DFT and TD-DFTB Investigation of the Optical Properties and Electronic Structure of Silver Nanorods and Nanorod Dimers. *J. Phys. Chem. C*, 122(41):23639–23650, oct 2018.

[16] Antton Babaze, Ruben Esteban, Javier Aizpurua, and Andrei G Borisov. Second-Harmonic Generation from a Quantum Emitter Coupled to a Metallic Nanoantenna. *ACS Photonics*, 7(3):701–713, mar 2020.

[17] Nicolas Tancogne-Dejean, Micael J. T. Oliveira, Xavier Andrade, Heiko Appel, Carlos H. Borca, Guillaume Le Breton, Florian Buchholz, Alberto Castro, Stefano Corni, Alfredo A. Correa, Umberto De Giovannini, Alain Delgado, Florian G. Eich, Johannes Flick, Gabriel Gil, Adrián Gomez, Nicole Helbig, Hannes Hübener, René Jestädt, Joaquim Jornet-Somoza, Ask H. Larsen, Irina V. Lebedeva, Martin Lüders, Miguel A. L. Marques, Sebastian T. Ohlmann, Silvio Pipolo, Markus Rampp, Carlo A. Rozzi, David A. Strubbe, Shunsuke A. Sato, Christian Schäfer, Iris Theophilou, Alicia Welden, and Angel Rubio. Octopus, a computational framework for exploring light-driven phenomena and quantum dynamics in extended and finite systems. *The Journal of Chemical Physics*, 152(12):124119, 2020.

[18] Xavier Andrade, David Strubbe, Umberto De Giovannini, Ask Hjorth Larsen, Micael J. T. Oliveira, Joseba Alberdi-Rodriguez, Alejandro Varas, Iris Theophilou, Nicole Helbig, Matthieu J. Verstraete, Lorenzo Stella, Fernando Nogueira, Alán Aspuru-Guzik, Alberto Castro, Miguel A. L. Marques, and Angel Rubio. Real-space grids and the octopus code as tools for the development of new simulation approaches for electronic systems. *Phys. Chem. Chem. Phys.*, 17:31371–31396, 2015.

[19] Alberto Castro, Heiko Appel, Micael Oliveira, Carlo A. Rozzi, Xavier Andrade, Florian Lorenzen, M. A. L. Marques, E. K. U. Gross, and Angel Rubio. octopus: a tool for the application of time-dependent density functional theory. *physica status solidi (b)*, 243(11):2465–2488, 2006.

[20] Yi Gao and Daniel Neuhauser. Communication: Dynamical embedding: Correct quantum response from coupling tddft for a small cluster with classical near-field electrodynamics for an extended region. *The Journal of Chemical Physics*, 138(18):181105, 2013.

[21] O Jonasson, F Karimi, and I Knezevic. Partially coherent electron transport in terahertz quantum cascade lasers based on a Markovian master equation for the density matrix. *J. Comput. Electron.*, 15(4):1192–1205, 2016.

[22] M. Lindskog, J. M. Wolf, V. Trinite, V. Liverini, J. Faist, G. Maisons, M. Carras, R. Aidam, R. Ostendorf, and A. Wacker. Comparative analysis of quantum cascade laser modeling based on density matrices and non-equilibrium green's functions. *Applied Physics Letters*, 105(10):103106, 2014.

[23] Andrzej Kolek. Light-matter interaction in negf simulations of intersubband-emitting devices. In *2018 International Conference on Numerical Simulation of Optoelectronic Devices (NUSOD)*, pages 51–52, 2018.

[24] Massimo V. Fischetti and William G. Vandenberghe. *Overview of Quantum-Transport Formalisms*, pages 361–380. Springer International Publishing, Cham, 2016.

[25] David J Griffiths. *Introduction to electrodynamics; 4th ed.* Pearson, Boston, MA, 2013. Re-published by Cambridge University Press in 2017.

[26] John David Jackson. *Classical electrodynamics*. John Wiley & Sons, third edit edition, 1999.

[27] James Clerk Maxwell. Viii. a dynamical theory of the electromagnetic field. *Philosophical Transactions of the Royal Society of London*, 155:459–512, 1865.

[28] W C Chew, D Y. Na, P Bermel, T E Roth, C J Ryu, and E Kudeki. Quantum Maxwell's Equations Made Simple: Employing Scalar and Vector Potential Formulation. *IEEE Antennas Propag. Mag.*, 63(1):14–26, 2021.

[29] Christopher J. Ryu. *Finite-Difference Time-Domain Simulation of the Maxwell-Schrödinger System*. PhD thesis, University of Illinois at Urbana-Champaign, 2015.

[30] W. C. Chew, A. Y. Liu, C. Salazar-Lazaro, and W. E.I. Sha. Quantum electromagnetics: A new look - Part I. *IEEE Journal on Multiscale and Multiphysics Computational Techniques*, 1:73–84, 2016.

[31] W. C. Chew, A. Y. Liu, C. Salazar-Lazaro, and W. E.I. Sha. Quantum electromagnetics: A new look - Part II. *IEEE Journal on Multiscale and Multiphysics Computational Techniques*, 1:85–97, 2016.

[32] Weng Cho Chew. Vector Potential Electromagnetics with Generalized Gauge for Inhomogeneous Media: Formulation. *Progress In Electromagnetics Research*, 149(August):69–84, 2014.

[33] Yan-Lin Li, Sheng Sun, Qi I. Dai, and Weng Cho Chew. Finite element implementation of the generalized-lorenz gauged a- ϕ formulation for low-frequency circuit modeling. *IEEE Transactions on Antennas and Propagation*, 64(10):4355–4364, 2016.

[34] Zahra Shaterian, Thomas Kaufmann, and Christophe Fumeaux. Hybrid staggered perfectly matched layers in non-staggered meshless time-domain vector potential technique. *2014 International Workshop on Antenna Technology: Small Antennas, Novel EM Structures and Materials, and Applications, iWAT 2014*, pages 375–378, 2014.

[35] Zhipeng Liu, Guoda Xie, Bo Wu, Xingang Ren, Ming Fang, and Zhixiang Huang. A novel fdtd algorithm based on the vector and scalar potentials equations. In *2019 IEEE International Conference on Computational Electromagnetics (ICCEM)*, pages 1–3, 2019.

[36] David J Griffiths. *Introduction to quantum mechanics*. Pearson Prentice Hall, Upper Saddle River, NJ, 2005.

[37] Charles. Kittel. *Quantum theory of solids*. Wiley, New York, 1963.

[38] Albert. Messiah and G M Temmer. *Quantum mechanics*. North-Holland Pub. Co. ; Interscience Publishers, Amsterdam; New York, 1961.

[39] J. J. Sakurai and Jim Napolitano. *Modern Quantum Mechanics*. Cambridge University Press, 2 edition, 2017.

[40] Leonard I Schiff. *Quantum mechanics*. McGraw-Hill, New York, 1968.

[41] Ramamurti Shankar. *Principles of quantum mechanics*. Plenum, New York, NY, 1980.

[42] J. D. Jackson. From lorenz to coulomb and other explicit gauge transformations. *American Journal of Physics*, 70(9):917–928, Sep 2002.

[43] Umran S. Inan and Robert A. Marshall. *Numerical Electromagnetics: The FDTD Method*. Cambridge University Press, 2011.

[44] Allen Taflove and Susan C. Hagness. *Computational electrodynamics: the finite-difference time-domain method*. Artech House, Norwood, 3rd edition, 2005.

[45] Allen Taflove, Susan C. Hagness, and Melinda Piket-May. 9 - computational electromagnetics: The finite-difference time-domain method. In Wai-Kao Chen, editor, *The Electrical Engineering Handbook*, pages 629–670. Academic Press, Burlington, 2005.

[46] Lumerical Inc. Lumerical fdtd.

[47] Ardavan F. Oskooi, David Roundy, Mihai Ibanescu, Peter Bermel, J.D. Joannopoulos, and Steven G. Johnson. Meep: A flexible free-software package for electromagnetic simulations by the fdtd method. *Computer Physics Communications*, 181(3):687–702, 2010.

[48] K. J. Willis, S. C. Hagness, and I. Knezevic. Terahertz conductivity of doped silicon calculated using the ensemble monte carlo/finite-difference time-domain simulation technique. *Applied Physics Letters*, 96(6):062106, 2010.

[49] K. J. Willis, S. C. Hagness, and I. Knezevic. Multiphysics simulation of high-frequency carrier dynamics in conductive materials. *Journal of Applied Physics*, 110(6):063714, 2011.

[50] K. J. Willis, S. C. Hagness, and I. Knezevic. A generalized drude model for doped silicon at terahertz frequencies derived from microscopic transport simulation. *Applied Physics Letters*, 102(12):122113, 2013.

[51] Furrukh S. Khan, John H. Davies, and John W. Wilkins. Quantum transport equations for high electric fields. *Phys. Rev. B*, 36:2578–2597, Aug 1987.

[52] Pratik B. Vyas, Maarten L. Van de Put, and Massimo V. Fischetti. Master-equation study of quantum transport in realistic semiconductor devices including electron-phonon and surface-roughness scattering. *Phys. Rev. Applied*, 13:014067, Jan 2020.

[53] Franco De Flaviis, Massimo G. Noro, Rodolfo E. Diaz, G. Franceschetti, and Nicolaos G. Alexopoulos. A Time-Domain Vector Potential Formulation for the Solution of Electromagnetic Problems. *IEEE Microwave and Guided Wave Letters*, 8(9):310–312, 1998.

[54] Kane S. Yee. Numerical solution of initial boundary value problems involving maxwell's equations in isotropic media. *IEEE Transactions on Antennas and Propagation*, 14(3):302–307, 1966.

[55] W. C. Chew. Electromagnetic theory on a lattice. *Journal of Applied Physics*, 75(10):4843–4850, 1994.

[56] J. Alan Roden and Stephen D. Gedney. Convolution pml (cpml): An efficient fdtd implementation of the cfs–pml for arbitrary media. *Microwave and Optical Technology Letters*, 27(5):334–339, 2000.

[57] Jean-Pierre Berenger. Perfectly matched layer for the FDTD solution of wave-structure interaction problems. *IEEE Transactions on Antennas and Propagation*, 44(1):110–117, 1996.

[58] Jean Pierre Berenger. A perfectly matched layer for free-space simulation in finite-difference computer codes. *Annales des Telecommunications/Annals of Telecommunications*, 51(1-2):39–46, 1996.

[59] Jean-Pierre Berenger. Three-Dimensional Perfectly Matched Layer for the Absorption of Electromagnetic Waves. *Journal of Computational Physics*, 127(2):363–379, 1996.

[60] Jean-Pierre Berenger. Numerical reflection from fdtd-pmls: a comparison of the split pml with the unsplit and cfs pmls. *IEEE Transactions on Antennas and Propagation*, 50(3):258–265, 2002.

[61] Weng Cho Chew and William H. Weedon. A 3D perfectly matched medium from modified maxwell's equations with stretched coordinates. *Microwave and Optical Technology Letters*, 7(13):599–604, 1994.

[62] S.D. Gedney. An anisotropic perfectly matched layer-absorbing medium for the truncation of fdtd lattices. *IEEE Transactions on Antennas and Propagation*, 44(12):1630–1639, 1996.

[63] Jacques R. Ernst, Klaus Holliger, Hansruedi Maurer, and Alan G. Green. Realistic fdtd modelling of borehole georadar antenna radiation: methodolgy and application. *Near Surface Geophysics*, 4(1):19–30, 2006.

[64] S.D. Gedney. An anisotropic perfectly matched layer-absorbing medium for the truncation of fdtd lattices. *IEEE Transactions on Antennas and Propagation*, 44(12):1630–1639, 1996.

[65] J. Alan Roden and Stephen D. Gedney. Convolution PML (CPML): An efficient FDTD implementation of the CFS-PML for arbitrary media. *Microwave and Optical Technology Letters*, 27(5):334–339, 2000.

[66] Stephen D Gedney and Bo Zhao. An Auxiliary Differential Equation Formulation for the Complex-Frequency Shifted {PML}. {*IEEE*} *Transactions on Antennas and Propagation*, 58(3):838–847, mar 2010.

[67] Naixing Feng and Jianxiong Li. Novel and efficient fdtd implementation of higher-order perfectly matched layer based on ade method. *Journal of Computational Physics*, 232(1):318–326, 2013.

[68] David F. Kelley and Raymond I. Luebbers. Piecewise linear recursive convolution for dispersive media using FDTD. *IEEE Transactions on Antennas and Propagation*, 44(6 PART 1):792–797, 1996.

[69] Hossein Mosallaei. Fdtd-plrc technique for modeling of anisotropic-dispersive media and metamaterial devices. *IEEE Transactions on Electromagnetic Compatibility*, 49(3):649–660, 2007.

[70] Antonios Giannopoulos. Higher-order convolution pml (cpml) for fdtd electromagnetic modeling. *IEEE Transactions on Antennas and Propagation*, 68(8):6226–6231, 2020.

[71] W. C. Chew, J. M. Jin, and E. Michielssen. Complex coordinate stretching as a generalized absorbing boundary condition. *Microwave and Optical Technology Letters*, 15(6):363–369, 1997.

[72] Mustafa Kuzuoglu and Raj Mittra. Frequency dependence of the constitutive parameters of causal perfectly matched anisotropic absorbers. *IEEE Microwave and Guided Wave Letters*, 6(12):447–449, 1996.

[73] Jean-Pierre Berenger. Numerical reflection of evanescent waves from perfectly matched layers. In {*IEEE*} *Antennas and Propagation Society International Symposium 1997. Digest*. IEEE, 1997.

[74] Raymond Luebbers, Forrest R. Hunsberger, Karl S. Kunz, Ronald B. Standler, and Michael Schneider. A Frequency-Dependent Finite-Difference Time-Domain Formulation for Dispersive Materials. *IEEE Transactions on Electromagnetic Compatibility*, 32(3):222–227, 1990.

[75] Raymond J. Luebbers and Forrest Hunsberger. FDTD for Nth-Order Dispersive Media. *IEEE Transactions on Antennas and Propagation*, 40(11):1297–1301, 1992.

[76] Raymond Luebbers and Karl Kunz. FDTD Calculation of Scattering from Frequency-Dependent Materials. *IEEE Transactions on Antennas and Propagation*, 41(9):1249–1257, 1993.

[77] J.-P. Berenger. Improved pml for the fdtd solution of wave-structure interaction problems. *IEEE Transactions on Antennas and Propagation*, 45(3):466–473, 1997.

[78] Zhonghua Wu and Jiayuan Fang. High-performance pml algorithms. *IEEE Microwave and Guided Wave Letters*, 6(9):335–337, 1996.